PALMITOYLATION AND MEMBRANE INTERACTIONS OF CYSTEINE STRING PROTEIN

JENNIFER GREAVES

A thesis presented to the University of Glasgow for the degree of Doctor of Philosophy

Division of Biochemistry and Molecular Biology

Faculty of Biomedical and Life Sciences

UNIVERSITY OF GLASGOW

July 2008

University of Glasgow

VIA VERITAS VITA

ABSTRACT

S-palmitoylation is the reversible post-translational attachment of the 16-carbon saturated fatty acid palmitate to the sulphydryl group of cysteine residues through a thioester linkage. The primary function of palmitoylation has often been regarded as simply a means to increase the hydrophobicity and membrane affinity of modified proteins, allowing them to become stably membrane-associated. However, recent evidence has demonstrated additional roles for palmitoylation in regulating protein trafficking, the membrane micro-localisation of proteins, protein stability, and protein-protein interactions. A family of twenty-three mammalian proteins containing a conserved DHHC cysteine-rich domain have recently been identified, and several of these proteins have been shown to palmitoylate specific substrate proteins. The DHHC family of palmitoyl transferases are polytopic membrane proteins containing 4-6 membrane-spanning domains that are localised to distinct intracellular membranes, including the endoplasmic reticulum, Golgi apparatus, endosomes, and the plasma membrane. Since palmitoyl transferases are integral membrane proteins, substrate proteins must contain additional membrane targeting signals that mediate membrane association prior to palmitate transfer. For many proteins, the mechanism that mediates initial membrane binding prior to palmitoylation is clear; for example, initial membrane binding can be mediated by transmembrane domains or other lipid modifications such as prenyl or myristoyl groups, which are added to proteins in the cytosol. However, a number of palmitoylated proteins lack any obvious membrane targeting motifs and it is unclear how this class of proteins associate with membranes to allow palmitoylation to occur. The vesicle-associated, exocytotic chaperone Cysteine String Protein (CSP) is an example of such a protein. CSP is extensively palmitoylated on a "string' of fourteen cysteine residues present within its signature cysteine string domain. Palmitoylation of CSP is essential for its intracellular sorting and function, and thus it is important to understand how this essential modification of CSP is regulated. In this study, a detailed mutagenesis approach has been employed to elucidate the mechanisms governing the initial membrane targeting of CSP, and the enzymes that palmitoylate CSP have been identified. As well as providing important information on CSP palmitoylation and membrane interactions, it is hoped that this analysis will also serve as a paradigm to understand the mechanisms by which other proteins become palmitoylated.

As a first step to characterising CSP membrane interactions, a hydrophobic 31 amino acid domain of CSP was identified as the minimal membrane binding domain present within the protein. This domain includes the cysteine string domain, and indeed cysteine residues within this domain are proposed to play an essential role in membrane interaction prior to

palmitoylation. Membrane association of the minimal membrane binding domain is not sufficient to trigger palmitoylation, which requires additional residues downstream of the cysteine string domain. Intriguingly one role of these downstream residues in CSP appears to be to weaken membrane affinity and indeed, in contrast to the minimal membrane binding domain, full-length CSP was cytosolic in the absence of palmitoylation. The family of 23 DHHC proteins were screened for activity against CSP, showing that palmitoylation is specifically enhanced by co-expression of the Golgi-localised palmitoyl transferases DHHC3, DHHC7, DHHC15 or DHHC17; co-expression of these enzymes is sufficient to promote the stable membrane attachment of CSP. CSP mutants with an increased membrane affinity were localised to the ER, and thus physically separated from the Golgi-localised partner DHHC proteins of CSP, offering an explanation of why these mutants are not palmitoylated. Interestingly, palmitoylation of an ER-localised mutant could be rescued by Brefeldin A (BFA) treatment, which promotes the mixing of ER and Golgi membranes, supporting the view that mutants with an increased membrane affinity are not palmitoylated because they associate with 'inappropriate' membranes. In addition, the palmitoylated mutant remained at the ER following BFA washout and did not traffic to more distal membrane compartments, suggesting that palmitoylation of CSP may have a specific requirement to take place at Golgi membranes to facilitate subsequent intracellular sorting.

A model is proposed whereby CSP utilises a weak membrane affinity to "sample" intracellular membranes for DHHC protein content. As partner DHHC proteins of CSP are restricted to the Golgi, palmitoylation and stable membrane attachment only occurs at this intracellular compartment. Mutations that enhance initial membrane affinity prevent sampling and lead to accumulation of CSP on abundant cellular membranes such as the ER. As a palmitoylated CSP mutant did not traffic from the ER, the coupling of CSP palmitoylation to Golgi membranes may therefore be an important requirement for subsequent sorting. These findings suggest that membrane "sampling" through specialised protein domains might be a common mechanism employed by substrate proteins to locate their specific DHHC partner proteins.

TABLE OF CONTENTS

LIST OF TABLES

LIST OF FIGURES

CHAPTER ONE:

CHAPTER SIX:

CHAPTER SEVEN:

ACKNOWLEDGEMENTS

There are many people to whom I'm grateful, but I would like to extend special thanks to the following folk:

First and foremost, my supervisor Luke Chamberlain: it's a pleasure to work for you, and I'm sincerely grateful for the opportunity you've given me.

The "usual suspects" of Lab241, especially Christine Salaün, Fiona Brandie, Rebecca McCann, Mairi Clarke and "Uncle" Ian Salt; for your scientific assistance, good laughs and the obligatory and frequent booze-fuelled evenings.

Thanks to David, for your willingness to head west and dish out encouragement and helpful suggestions in the 3J's.

Finally, I'd like to acknowledge the support I've received from my parents, Erica and Michael; my brilliant sister, Rachael; my good friend, Kathryn; and most importantly, Daniel - you deserve a medal!

AUTHOR'S DECLARATION

The contents of this thesis and the investigations presented herein, unless otherwise stated, were conducted by the author. No part of this work has been, or is being, submitted for any other degree or qualification at the University of Glasgow or at any other institution.

Jennifer Greaves

July 2008

ABBREVIATIONS

A	adenine
A	adenosine
A	alanine
ACBP	acyl-coenzyme A binding protein
APT	acyl-protein thioesterase
ATP	adenosine triphosphate
BFA	Brefeldin A
Bq	Becquerels
BSA	bovine serum albumin
C	cysteine
C	cytosine
C-	carboxy-(terminus)
cDNA	complementary DNA
C. Elegans	*Caenorhabditis elegans*
CFTR	cystic fibrosis transmembrane conductance regulator
CHO	Chinese hamster ovary cell line
CO_2	carbon dioxide gas
COS 1	African green monkey kidney fibroblast cell line
CSP	Cysteine string protein
°C	degrees Celcius
D	aspartate
DEPC	diethyl pyrocarbonate
dH_2O	distilled water
DHHC-CRD	Aspartate-Histidine-Histidine-Cysteine Cysteine-Rich Domain
DMEM	Dulbecco's modified Eagle's medium
DMSO	dimethyl sulphoxide
DNA	deoxyribonucleic acid
Drosophila	*Drosophila melanogaster*
dNTP	2'-deoxynucleoside 5'-triphosphate
DTT	dithio-1,4-threitol
E	glutamic acid
E. coli	*Eschericia coli*
ECL	enhanced chemiluminescence
EDTA	ethylenediamine tetra-acetic acid
EGFP	enhanced green fluorescent protein
EGTA	ethylene glycol bis(β-aminoethyl ether)-N,N,N',N'-tetraacetate)
eNOS	endothelial nitric oxide synthase
ER	endoplasmic reticulum
F	phenylalanine
FBS	foetal bovine serum
FITC	fluorescein isothiocyanate-conjugated
FTase	farnesyltransferase
g	gram
g	gravitational force
G	glycine
G	guanine
GAP-43	growth associated protein of 43 kDa
GDP	guanosine diphosphate
GEF	guanine nucleotide exchange factor
GGTase	geranylgeranyltransferase
GRASP55	Golgi reassembly stacking protein of 55 kDa

GTP	guanosine triphosphate
h	hours
H	histidine
H_2O	water
HA	haemagglutinin
HA	hydroxylamine
HCl	hydrochloric acid
HEK-293	human embryonic kidney cell line
HEPES	4-(2-hydroxyethyl)-1-piperazineethanesulphonic acid
HRP	horseradish peroxidase
HSC70	heat shock cognate protein of 70 kDa
Hsp40	heat shock protein of 40 kDa
I	isoleucine
IgG	immunoglobulin G
K	lysine
K_2HPO_4	dipotassium hydrogen orthophosphate
kb	kilobase-pair(s)
KCl	potassium chloride
K_d	dissociation constant
kDa	kiloDaltons
KH_2PO_4	potassium dihydrogen orthophosphate
l	litre
L	leucine
M	molar
mA	milliamp
MES	2-(N-morpholino) ethane sulphonic acid
mg	milligram
mins	minutes
ml	millilitre
mM	millimolar
MOPS	3-(N-morpholino) propane sulphonic acid
µg	microgram
µl	microlitre
µm	micron
µM	micromolar
N	asparagine
N-	amino-(terminus)
N_2	nitrogen gas
NaCl	sodium chloride
Na_2CO_3	sodium carbonate
ng	nanogram
nm	nanometre
nM	nanomolar
NMT	*N*-myristoyl transferase
NSF	soluble-N-ethyl-maleimide sensitive factor
P	proline
PAGE	polyacrylamide gel electrophoresis
PAT	palmitoyl transferase
PBS	phosphate-buffered saline solution
PC12	pheochromocytoma cells
PCR	polymerase chain reaction
Pfu	*Pyrococcus furiosis*
PKC	protein kinase C

PM	plasma membrane
PPT	palmitoyl thioesterase
PSD-95	postsynaptic density-95 protein
Q	glutamine
R	arginine
RNA	ribonucleic acid
RNAi	RNA interference
Rnase	ribonuclease
s	second(s)
S	serine
S. cervevisiae	*Saccharmocyces cervevisiae*
SDS	sodium dodecyl sulphate
SDS-PAGE	sodium dodecyl sulphate polyacrylamide gel electrophoreses
S.E.M.	standard error of mean
SGT	small glutamine-rich tetratricopeptide repeat domain protein
SH	sulph-hydryl
siRNA	short interference RNA
αSNAP	alpha-soluble NSF attachment protein
SNAP25	synaptosomal-associated protein of 25 kDa
SNARE	soluble N-ethylmaleimide-sensitive fusion protein-attachment protein receptor
T	threonine
T	thymine
TAE	Tris-Acetic acid-EDTA
Taq	*Thermus aquaticus*
TEMED	N,N,N',N'-tetramethyl-ethane-1,2-diamine
Thesit	2-dodecoxyethanol
Torpedo	*Torpedo californica*
Tris	Tri (hydroxymethyl)-aminomethane
V	valine
VAMP	vesicle-associated membrane protein
v/v	volume per volume
w/v	weight per volume
Xenopus	*Xenopus laevis*
Y	tyrosine

CHAPTER ONE: INTRODUCTION

1.1 INTRODUCTION

Eukaryotic cells are compartmentalised into discrete membrane-bounded organelles, each possessing specialised functions that are fundamental to cellular viability. To maintain their specificity and function, the identity of each organelle is defined by a unique composition of proteins and lipids. During membrane trafficking, membrane constituents and cargo are transported from one compartment to another, reaching their correct subcellular localisation without compromising this membrane integrity. In order to achieve this, proteins and lipids must be faithfully targeted to their specific resident subcellular membranes, or else cells risk the scrambling of membrane compartments and subsequent loss of organelle and cellular identity.

Membrane proteins potentially face a myriad of lipid bilayer-enclosed intracellular compartments with which to associate; therefore, mechanisms that regulate the trafficking of these proteins, from their synthesis until the deposition at their correct final destination, must exist. The mechanisms that target a membrane protein to its correct intracellular compartment are thus fundamental to cellular organisation and function.

1.2 MEMBRANE PROTEINS

A classic example of a membrane-associated protein is one that transverses the lipid bilayer through one (bitopic) or more (polytopic) hydrophobic membrane-spanning domains. During synthesis, many integral (also called intrinsic) membrane proteins are co-translationally inserted into the endoplasmic reticulum (ER) membrane, where they are transported through the secretory pathway (See Chapter 1.7) until they reach their resident organelle membrane. Transmembrane proteins interact extensively with the hydrocarbon chains of membrane lipids through hydrophobic interactions and can only be released from membranes through the action of detergents, which disrupt the hydrophobic core of the phospholipid bilayer. Bitopic membrane proteins can be categorised as Type I-IV according to the way that they are inserted into the membrane and the resultant topology (Blobel, 1980; von Heijne and Gavel, 1988). Type I membrane proteins have an amino terminal (N-terminal) cleavable signal peptide and an apolar stop-transfer sequence resulting in a luminal N-terminus and a cytoplasmic carboxyl (C-) terminus. Type II membrane proteins have the reverse topology to Type I membrane proteins, due to the presence of an uncleaved signal peptide either internally or at the N-terminus. Type III membrane proteins are topologically identical to Type I membrane proteins, but possesses an N-terminal stop transfer sequence (von Heijne and Gavel, 1988). Another class of intrinsic membrane proteins, C-tail anchored proteins (or Type IV membrane proteins), are topologically

similar to Type II membrane proteins, yet do not encode a signal sequence and hence become membrane inserted post-translationally (Kutay *et al.*, 1993). C-tail anchored proteins possess a hydrophobic segment near to their C-terminus, which is inserted into the lipid bilayer, leaving the N-terminus orientated cytosolically (Kutay *et al.*, 1993; Kutay *et al.*, 1995). Polytopic membrane proteins may have their N- and C-termini on the same or opposite sides of the lipid bilayer.

In contrast to intrinsic membrane proteins, peripherally associated membrane proteins are traditionally viewed as ones that are synthesised on free ribosomes and interact relatively weakly with membranes. Peripheral membrane proteins are able to associate with membranes either directly, through electrostatic interactions involving charged amino acids and phospholipid headgroups, and/or indirectly via interactions with integral membrane proteins. Due to their weak ionic membrane interactions, peripheral membrane proteins are able to be solubilised in solutions of high ionic strength (*e.g.* 1M NaCl) or high pH (*e.g.* 0.1M Na_2CO_3, pH 11), and are classically distinguished from integral membrane proteins based on this difference in membrane release. However, some membrane proteins share elements with both integral and peripheral membrane proteins. These membrane proteins are synthesised as soluble proteins but become modified by the attachment of hydrophobic lipid groups, allowing them to interact extensively with the hydrophobic core of the bilayer, and requiring detergent for solubilisation. The post-translational attachment of lipid groups is not specific to soluble proteins but also occurs with some integral membrane proteins. Examples of the different types of membrane-associated protein are illustrated in Figure 1.1.

1.3 LIPID MODIFICATION OF PROTEINS

Proteins may be modified by the covalent attachment of lipid groups containing long (C_{14}-C_{20}) hydrocarbon chains, which, due to their hydrophobic nature, are able to embed in the phospholipid bilayer of intracellular membranes. Lipid anchors often enable otherwise soluble proteins to become membrane-associated; however, since both soluble and integral membrane proteins can be modified in this way, and more than one type of lipid modification may be present on an individual protein, the attachment of lipid anchors are likely to serve functions other than simply membrane-tethering. Indeed, recent studies have highlighted roles for lipid anchors in targeting proteins to specific subcellular membranes or specific microdomains present within the same membrane (El-Husseini *et al.*, 2001; Goodwin *et al.*, 2005; Rocks *et al.*, 2005; Roy *et al.*, 2005). Lipid-modified proteins can be divided into four subgroups based on
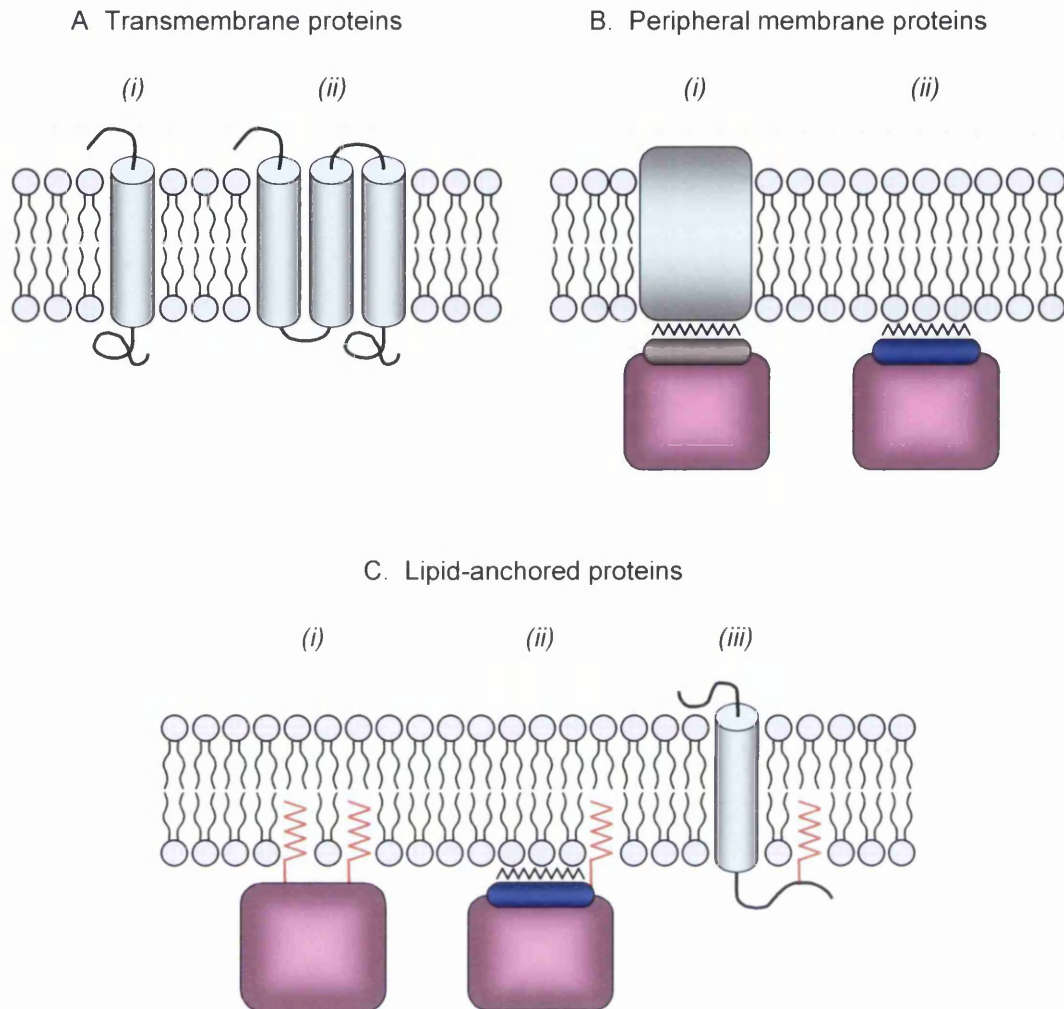
Figure 1.1 Classes of membrane proteins. *A*. Transmembrane (TM) proteins interact extensively with the hydrocarbon core of the phospholipid bilayer, through one or more membrane-spanning domains. Proteins containing a single-pass membrane-spanning domain are known as bitopic proteins (i), whereas proteins that have more than one membrane-spanning domain are termed polytopic membrane proteins (ii). The N- and C-termini may be present on either or both sides of the bilayer. *B*. Peripheral membrane proteins (purple) interact with the surface of membranes. This interaction is either indirect through binding to another membrane protein (i; light blue) or direct through electrostatic interactions involving charged amino acids (dark blue) and the phospholipid headgroups on the inner leaflet of the membrane. *C*. Soluble proteins can become membrane-associated by the addition of one or more lipid-anchor(s) (i). Peripherally associated membrane proteins and TM proteins containing one (shown) or more membrane-spanning domains may also be post-translationally modified with lipid anchor(s) (ii-iii).

the nature of the attached lipid: fatty acylated, prenylated, glypiated and cholesteroylated (Figure 1.2).

In eukaryotic cells, two types of membrane anchor, prenyl and acyl groups, allow proteins to associate with the cytosolic face of intracellular membranes. In contrast to prenylation and acylation, glypiation and cholesteroylation serve to tether proteins to the extracellular leaflet of the plasma membrane: both of these processes occur post-translationally and luminally (Englund, 1993; Mann and Beachy, 2004).

Glypiation is one of the most-studied lipid modifications, involving the modification of numerous functionally diverse proteins with a glycosylphosphatidyl inositol (GPI) anchor (Englund, 1993). The GPI anchor consists of a phosphatidylinositol group embedded in the outer leaflet of the plasma membrane, connected by glycerophosphate to a complex oligosaccharide linker, which in turn is connected to the C-terminus of the protein through phosphoethanolamine (Englund, 1993).

Cholesteroylation refers to the modifcation of proteins with cholesterol, and is exemplified by the secreted tissue patterning factor Hedgehog (Mann and Beachy, 2004; Porter et al., 1996b). The addition of cholesterol to Hedgehog is essential for its normal cellular location, thereby preventing inappropriate signaling activity (Porter et al., 1996a).

1.3.1 PRENYLATION

The covalent attachment of isoprenyl groups, such as farnesyl (C_{15}) or geranylgeranyl (C_{20}), occurs via a stable thioether linkage to one or more cysteine residues at or near the C-terminus of proteins. The donors for farnesylation and geranylgeranylation are farnesyl pyrophosphate and geranylgeranyl pyrophosphate, respectively, and the enzymes responsible have been identified and characterised at the molecular level (Casey and Seabra, 1996). The three isoprenyltransferases, farnesyltransferase (FTase), geranylgeranyltransferase I (GGTase I), and geranylgeranyl transferase II (GGTase II) can be divided into two groups depending on the consensus sequence they recognise (Zhang and Casey, 1996). Candidate proteins for FTase and GGTase I are those with cysteine residues at a C-terminal CaaX motif, where the cysteine residue (C) is followed by two aliphatic amino acids (a), and X is the carboxyl-terminal residue (Clarke, 1992; Zhang and Casey, 1996). Conversely, GGTase II specifically acts on Rab proteins that have two cysteine residues at or near the C-terminus (Farnsworth et al., 1994; Seabra et al., 1992). Following protein isoprenylation, the terminal three amino acids are

A Fatty Acylation

(i) *S*-Palmitoylation
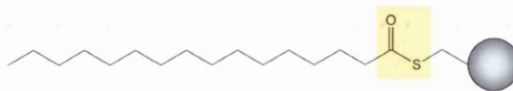
(ii) *N*-Palmitoylation
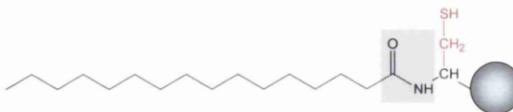
(iii) *N*-Myristoylation
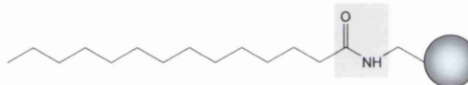
B Prenylation

(i) Farnesylation
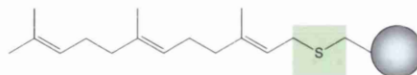
(ii) Geranylgeranylation
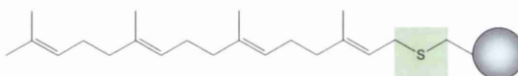
C Glypiation
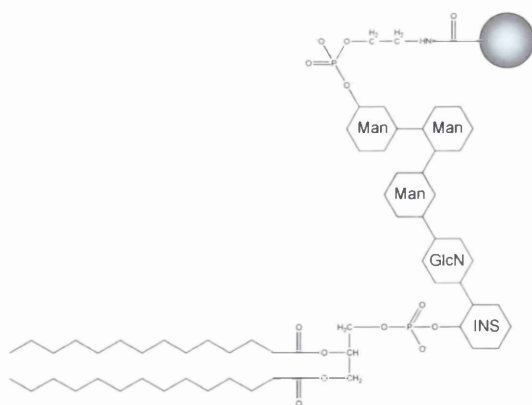
D Cholesteroylation
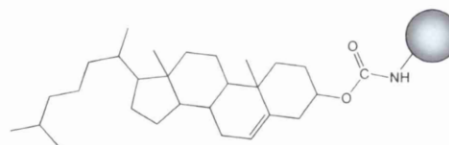
Figure 1.2 Hydrophobic lipid modifications.

Figure 1.2 Hydrophobic lipid modifications. The structures of lipid anchors that are covalently attached to eukaryotic proteins via post-translational modifications are shown. *A.* Fatty acylated proteins may be *S*-palmitoylated (i) through the attachment of a 16-carbon saturated fatty acid, palmitate, via a labile thioester bond to the thiol group of cysteine residues. Alternatively, proteins may be *N*-palmitoylated (ii) via a stable amide bond to an N-terminal glycine. Occasionally, *N*-palmitoylation occurs as the result of a spontaneous bond rearrangement following the addition of palmitate to an N-terminal cysteine (red side-chain). Proteins modified by the addition of a 14-carbon saturated fatty acid, myristate, to an N-terminal glycine residue via a stable amide linkage are known to be *N*-myristoylated (iii). *B.* Prenylation involves the addition of branched unsaturated prenyl groups, such as farnesyl (C:15; i) or geranylgeranyl (C:20; ii), to one or more cysteines at or near the C-terminus via a stable thioether linkage. The addition of glycophosphitidylinositol (GPI; *C*) and cholesterol (*D*) occurs in the ER and results in the deposition of proteins on the exoplasmic face of the PM. A simplified structure of a GPI anchor is shown; proteins are linked at their C-terminus through a phosphodiester linkage to a phosphoethanolamine unit of GPI. The phosphoethanolamine unit is linked to trimannosyl-non-acetylated glucosamine (Man3-GlcN) core, with the reducing end of GlcN linked to phosphatidylinositol (PI). The covalent bond generated as a result of the modification are shaded: thioester, yellow; amide, grey; thioether, green. A blue sphere represents the modified protein. Chemical structures were generated using ChemBioDraw® Ultra 11.0 software (CambridgeSoft®, Cambridge, Massachusetts, U.S.A.).

proteolytically cleaved, and the new terminal carboxylate group is methyl esterified, creating a C-terminal *S*-isoprenyl cysteine α-methyl ester (Clarke *et al.*, 1988; Gutierrez *et al.*, 1989). The majority of Ras and Rho small GTPase family proteins terminate with a CaaX motif and undergo sequential isoprenylation by FTase or GGTase I, proteolysis and carboxyl methylation (Pechlivanis and Kuhlmann, 2006). Farnesylation of H- (Harvey-), K- (Kirsten-) and N- (Neuroblastoma-) Ras is essential for membrane association and Ras signalling (Magee and Marshall, 1999). The Rab family of GTPases are geranylgeranylated on one or both cysteines by GGTase II, at C-terminal CC, CXC or CCX(XX) motifs (Farnsworth *et al.*, 1994; Zhang and Casey, 1996). Rab family proteins modified by GGTase II require a helper protein, Rab escort protein (REP), to be efficiently prenylated (Pereira-Leal *et al.*, 2001).

1.3.2 FATTY ACYLATION

Fatty acylation refers to the covalent attachment of fatty acids to proteins. Three classes of fatty acylation in eukaryotes have been described: *N*-myristoylation, *N*-palmitoylation and *S*-palmitoylation.

N-myristoylation is the irreversible addition of the 14-carbon saturated fatty acid myristate to the N-terminal glycine of proteins by an amide bond. Proteins that become myristoylated usually begin with the sequence Met-Gly, and often contain a serine or threonine at position 6. *N*-myristoylation usually occurs co-translationally, whereby the initiating methionine is cleaved by cellular methionylaminopeptidases, followed by the addition of myristate to the N-terminal glycine by the enzyme *N*-myristoyl transferase (NMT) using myristoyl CoA as its substrate (Farazi *et al.*, 2001; Towler *et al.*, 1987). Less frequently a protein may be *N*-myristoylated post-translationally, for example following proteolytic cleavage which reveals an otherwise hidden myristoylation motif (Zha *et al.*, 2000). Of all eukaryotic proteins, approximately 0.5% are *N*-myristoylated (Resh, 2006), including many signalling proteins, such as members of the Src family of non-receptor tyrosine kinases, guanine nucleotide binding (G-) protein α subunits of heterotrimeric G proteins, and proteins involved in membrane fusion events, for example Arf proteins (Resh, 1999). In addition to the role myrisoylation plays in membrane binding, X-Ray crystallography has revealed how myristoylation contributes towards the structural stability of proteins, such as the catalytic subunit of protein kinase A (PKA) (Zheng *et al.*, 1993), and the protein shell of poliovirus (Chow *et al.*, 1987).

Some myristoylated proteins are able adopt two conformations: one in which the myristate is available for bilayer interactions, and one in which it is sequestered inside a hydrophobic pocket

within the protein. The transition between these two conformations is known as a 'myristoyl switch' (McLaughlin and Aderem, 1995) and often allows membrane binding to be dynamically regulated. The triggers for the switch include ligand binding, electrostatic interactions and proteolysis (Resh, 1999). For example, guanine nucleotide exchange from the guanine diphosphate (GDP-) bound form of Arf to the guanine triphosphate (GTP-) bound generates a conformational change in Arf that exposes its myristoylated N-terminus allowing for membrane binding (Goldberg, 1998).

In addition to protein acylation with myristoyl groups, many proteins are modified by attachment of the fatty acid palmitate. This occurs by distinct mechanisms to *N*-myristoylation, and will be discussed in detail in Chapter 1.4.

1.3.3 MEMBRANE AFFINITY OF LIPID ANCHORS

The effects that various lipid anchors exert on the affinity of proteins for intracellular membranes can be estimated by measuring the rate of association/dissociation of model acylated and prenylated peptides for artificial phospholipid vesicles (Peitzsch and McLaughlin, 1993; Shahinian and Silvius, 1995; Silvius and l'Heureux, 1994). Such studies have consistently implied that neither farnesylation nor myrisoylation alone provide sufficient hydrophobicity to stably anchor modified proteins to intracellular membranes. Accordingly, a peptide modified by a single farnesyl group dissociates from liposomes within 1-2 minutes (Silvius and l'Heureux, 1994). Analysis of myristoylated peptide binding to phospholipids bilayers revealed a K_d of approximately 10^{-4} M: this dissociation constant provides barely enough energy to incorporate into the plasma membrane (Peitzsch and McLaughlin, 1993). Fatty acids with longer hydrocarbon chains, and therefore greater hydrophobicity, confer stronger membrane association than fatty acids with shorter and less hydrophobic chains, and the strength of membrane binding of acylated peptides has been shown to be directly proportional to the number of carbon atoms in the hydrocarbon chain (Peitzsch and McLaughlin, 1993). Thus, a C_{16} palmitoyl group has a higher membrane affinity than a C_{14} myristoyl group, but nevertheless a single palmitate still does not allow stable membrane binding of peptides (Peitzsch and McLaughlin, 1993).

The stable membrane binding of both farnesylated and myristoylated proteins requires additional signals to enhance membrane affinity, which can include hydrophobic residues or a polybasic domain, which interacts electrostatically with acidic phospholipids. For example, the prenylated protein K-ras has six lysines at its C-terminus, which act synergistically with an

adjacent farnesyl group to enhance stable plasma membrane binding (Hancock *et al.*, 1990). Similarly, the myrisoylated N-terminal domain of Src contains basic amino acids, which enhance membrane binding through electrostatic interactions with acidic phospholipid headgroups (Sigal *et al.*, 1994). Alternatively, a second lipid anchor, such as palmitate can promote stable membrane binding of both farnesylated and myristoylated proteins. Indeed, tandem lipid modifications have been shown to be sufficient at promoting high affinity interactions with lipid bilayers (Peitzsch and McLaughlin, 1993; Shahinian and Silvius, 1995).

1.4 PALMITOYLATION

Palmitoylation refers to the post-translational addition of the 16-carbon saturated fatty acid palmitate to proteins in one of two ways: by a cleavable thioester linkage to the sulphydryl group of cysteine residues (known as *S*-palmitoylation), or, less frequently, by an amide linkage (known as *N*-palmitoylation).

The amide bond in *N*-palmitoylation (palmitoylamide) is non-cleavable, and has only been described for a few proteins, the first being the secreted signalling protein sonic hedgehog (Pepinsky *et al.*, 1998), where palmitate is attached to a N-terminal cysteine. In this case, palmitate is thought to initially attach to the cysteine residue through a thioester bond, after which spontaneous bond rearrangement generates the amide linkage. Palmitate has also been shown to be attached to an N-terminal glycine residue by an amide bond, as is the case for the $G_{\alpha s}$ subunit of heterotrimeric G proteins (Kleuss and Krause, 2003).

Nearly all palmitoylated proteins are *S*-palmitoylated. It is important to note that labelling a protein as being 'palmitoylated' is historically based on the observed incorporation of [^{3}H] palmitic acid into proteins. However, when the lipid profile of palmitoylated proteins has been examined using techniques such as mass spectrometry, it is clear that other medium- and long-chain fatty acids are also attached to proteins through thioester linkages, such as the saturated fatty acids myristate and stearate (Liang *et al.*, 2002; Nadler *et al.*, 1994), and the unsaturated fatty acids oleate or arachidonate (Hallak *et al.*, 1994). Therefore, the term *S*-acylation is more appropriate; however, since the majority of *S*-acylated proteins incorporate palmitate, the term palmitoylation is generally used, and will be used synonymously with acylation hereafter.

A key difference between palmitoylation and myristoylation/farnesylation is that *S*-palmitoylation is a reversible modification, and thus the membrane binding of palmitoylated proteins can be under regulation. Indeed, the membrane localisation and activity of Ras

proteins are regulated by cycles of palmitoylation and depalmitoylation (See Chapter 1.4.2) (Rocks *et al.*, 2005).

1.4.1 PROTEIN FEATURES ASSOCIATED WITH PALMITOYLATION

In contrast to other forms of lipid modification, such as prenylation or myristoylation, which have well-defined consensus sequences for modification (See Chapters 1.3.1-2), there is no general consensus that specifies whether a protein becomes palmitoylated or not. In fact, the only sequence requirement for palmitoylated proteins appears to be the presence of a cysteine residue. Palmitoylated cysteine residues are, however, frequently located close to the regions within a protein that are primarily associated with membrane binding: for example, cysteines adjacent to membrane-spanning, hydrophobic or polybasic domains, or close to the site of a different lipid anchor, such as a prenyl or myristoyl group. The synaptic vesicle protein synaptotagmin I is palmitoylated on a cluster of five cysteine residues adjacent to the transmembrane anchor (Chapman *et al.*, 1996); it is predicted that one of the cysteines is located in the cytoplasmic tail region, while the remaining four are in the transmembrane region (Heindel *et al.*, 2003). Indeed, for most palmitoylated transmembrane proteins, the palmitoylated cysteines are located within the ten amino acids flanking the transmembrane domain/cytoplasmic domain boundary (Bijlmakers and Marsh, 2003). Ras proteins are dually modified by prenylation and palmitoylation in their C-terminus, and the site modified by palmitate is only 4-5 amino acids upstream of the farnesyl anchor (Hancock *et al.*, 1989; Hancock *et al.*, 1990). Similarly, in nearly all proteins having dual palmitate and myristate modifications at their N-terminal, the palmitoylated cysteine is localised immediately after the myristoylated glycine (Resh, 1999). However, since some otherwise cytosolic proteins (*i.e.* those not in possession of membrane-spanning domains or additional lipid anchors) have cysteine residues that may become palmitoylated, the factors that determine whether a cysteine in a protein gets palmitoylated are more complex than simply just being close to a membrane-binding domain.

1.4.2 FUNCTIONS OF PALMITOYLATION

Protein palmitoylation has a primary function in allowing otherwise soluble proteins, including both exclusively palmitoylated and dually lipidated proteins, to become stably membrane-bound by increasing the affinity of the modified protein for the lipid bilayer through the insertion of the hydrophobic C_{16} lipid anchor. However, despite the important role that palmitoylation plays in membrane binding, it is becoming clear that palmitoylation does not always function as a

simple membrane anchor. This point is emphasised by the demonstrated palmitoylation of a number of transmembrane proteins, which clearly do not require palmitoylation for membrane anchoring. Furthermore, palmitoylation of extracellular proteins has also been documented (Pepinsky *et al.*, 1998). Indeed, palmitoylation has now been shown to play diverse roles in addition to membrane tethering: in the targeting of both soluble and transmembrane proteins to distinct membrane compartments and membrane microdomains (El-Husseini *et al.*, 2001; Roy *et al.*, 2005); in the trafficking of proteins between various intracellular membranes (Goodwin *et al.*, 2005; Kang *et al.*, 2004; Kinlough *et al.*, 2006; Rocks *et al.*, 2005); in promoting protein stability, for example by regulating protein degradation or ensuring correct protein folding (Lam *et al.*, 2006; Valdez-Taubas and Pelham, 2005); and in regulating protein-protein interaction (Hayashi *et al.*, 2005). Examples of just a few of the multiple functions that palmitoylation plays are given below.

Palmitoylation is required for efficient biosynthetic delivery of some polytopic membrane proteins to the plasma membrane, such as members of the G-protein coupled receptor (GPCR) family. This is the case for the human δ opiod receptor (Petaja-Repo *et al.*, 2006) and the canine histamine H2 receptor (Fukushima *et al.*, 2001). Furthermore, palmitoylation has been shown to influence the localisation of proteins within plasma membrane microdomains. H-ras is dually palmitoylated at cys181 and cys184, and monopalmitoylation of H-ras at each of these cysteines alters the lateral segregation of H-ras between plasma membrane cholesterol-dependent and cholesterol-independent microdomains (Roy *et al.*, 2005). Palmitoylation-dependent effects on protein microlocalisation within membranes have also been highlighted for growth associated protein (GAP-) 43 and postsynaptic density (PSD-) 95 (El-Husseini *et al.*, 2001).

The trafficking of many transmembrane proteins between the plasma membrane and various intracellular membranes can also be regulated by palmitoylation.

Palmitoylation-dependent trafficking between the plasma membrane and the Golgi is exemplified by the postsynaptic receptor trafficking of AMPA (α-amino-3-hydroxy-5-methyl-4-isoxazole propionic acid) receptors. AMPA receptors have four subunits, GluR1-GluR4, which are palmitoylated at two sites: site one is at the end of transmembrane domain two, and site two is within the C-terminal domain. The stable cell surface expression of AMPA receptors depends on its interaction with protein 4.1N, since disrupting this interaction leads to a decrease in cell surface expression (Shen *et al.*, 2000). Palmitoylation at the C-terminal site inhibits the interaction with protein 4.1N, resulting in the agonist-induced regulated endocytosis of the

AMPA receptor (Hayashi *et al.*, 2005). In contrast, palmitoylation at site one appears to be more important in regulating the biosynthetic delivery of AMPA receptors to the plasma membrane, as palmitoylation of this site by the Golgi-localised PAT DHHC3/GODZ suppresses the sorting of the receptor from the Golgi (Hayashi *et al.*, 2005; Uemura *et al.*, 2002). Furthermore, the activation of AMPA receptors by glutamate addition promotes depalmitoylation (Hayashi *et al.*, 2005).

MUC1 is a mucin-like transmembrane protein normally expressed on the apical membrane of epithelial cells, where it has a protective function. Palmitoylation of MUC1 has been shown to regulate its trafficking between the plasma membrane and endosomes. MUC1 is dually palmitoylated on cysteines located at the boundary of the transmembrane domain and the C-terminal tail. Blocking palmitoylation by mutating these cysteine residues inhibits the recycling of MUC1 from endosomes back to the cell surface, resulting in the accumulation of MUC1 in endosomal compartments (Kinlough *et al.*, 2006).

Palmitoylation is also involved in the sorting of synaptotagmin 1 from the plasma membrane to an intracellular vesicle pool. Synaptotagmin 1 is palmitoyated on five cysteine residues in the boundary between the transmembrane and cytoplasmic region (Heindel *et al.*, 2003). Mutating these cysteine residues prevents palmitoylation of synaptotagmin 1, leading to an increase in cell surface expression in both PC12 cells and primary hippocampal neurons. Palmitoylation is thus required for internalisation and sorting of synaptotagmin 1 to the presynaptic vesicle pool (Kang *et al.*, 2004).

The role of palmitoylation in the trafficking of otherwise cystosolic proteins is best illustrated by the small GTPase Ras. A dynamic palmitoylation-depalmitoylation cycle drives the distribution of Ras between the plasma membrane and Golgi membranes. Palmitoylation of farnesylated Ras at the Golgi leads to stable membrane-binding and onward transport to the plasma membrane, where it is able to participate in signalling events. Depalmitoylation of Ras at the plasma membrane releases Ras into the cytosol where it transiently interacts with membranes by virtue of a farnesyl anchor until it becomes palmitoylated, and hence stably membrane-associated, once again, at the Golgi (Goodwin *et al.*, 2005; Rocks *et al.*, 2005).

Finally, the functions of palmitoylation are not just restricted to membrane targeting or membrane trafficking: palmitoylation presents more diverse roles, as exemplified by two yeast proteins, the yeast chitin synthase Chs3p, and the yeast homologue of syntaxin 6, Tlg1p. In these cases although palmitoylation still influences protein trafficking it also has effects on

protein aggregation and protein stability. Chs3p is a transmembrane protein containing 6-8 predicted membrane-spanning domains and is involved in cell wall growth. Preventing Chs3p palmitoylation leads to its aggregation and blocks the trafficking of Chs3p out of the ER (Lam *et al.*, 2006). This suggests that palmitoylation of Chs3 may be required, and serves as a marker, for the proper folding of the protein. Tlg1p mediates fusion between endosomes and the *trans* Golgi network, and is palmitoylated by Swf1p on two cysteine residues neighbouring the transmembrane domain (Valdez-Taubas and Pelham, 2005). Palmitoylation prevents the ubiquitination of Tlg1p by the E3 ubiquitin ligase, Tul1p, which would result in Tlg1p being targeted to the vacuole for degradation (Valdez-Taubas and Pelham, 2005). Here, palmitoylation protects Tlg1p from degradation and ensures that it is retained in its correct subcellular localisation. Interestingly, interplay between protein palmitoylation and unbiquitination has also been observed for mammalian proteins. The co-receptor for Wnt, LRP6 (lipoprotein receptor-related protein 6), is palmitoylated on two cysteines adjacent to its transmembrane domain: mutating these cysteines leads to the ubiquitination of LRP6 and its retention in the endoplasmic reticulum (Abrami *et al.*, 2008).

1.4.3 MECHANISM OF PALMITOYLATION

Whether palmitoylation *in vivo* is a spontaneous occurrence or enzyme-mediated has been much debated in recent years. The lack of readily identifiable palmitoylation consensus motifs, the difficulty in purifying putative active palmitoylation enzymes, and the high reactivity of acyl-coenzyme A donors with substrate protein thiols *in vitro*, which permits *in vitro* palmitoylation in the absence of a catalyst, all contributed to the belief that palmitoylation may not be a catalytic event *in vivo* (Dietrich and Ungermann, 2004). For spontaneous palmitoylation to occur, the sulphydryl group on the cysteine residue would require deprotonation to form a thiolate. Thiolate is a reactive nucleophile, and so nucleophilic attack of the highly reactive α-carbon of the thioester bond between the coenzyme A and the palmitoyl group could occur. The pKa of cysteine ionisation to form a thiolate is ~8.5 and so thiolate formation in the cell cytosol (pH 7.3-7.4) would be predicted to be a rare event (Dietrich and Ungermann, 2004). However, the amino acids that surround a cysteine could promote thiolate formation *in vivo*, perhaps allowing spontaneous palmitoylation to occur. The pKa of cysteine-containing peptide sequences was decreased following the addition of charged (lysine/arginine) or aromatic amino acids to the peptide sequence (Bizzozero *et al.*, 2001), suggesting that by lowering the pKa these residues could increase the ionisation of the neighbouring cysteine and thus promote thiolate formation.

1.4.3.1 SPONTANEOUS PALMITOYLATION

In agreement with palmitoylation being a spontaneous event, many proteins and peptides have been shown to be palmitoylated on cysteine residues *in vitro* in the absence of a specific acyltransferase, using palmitoyl-coenzyme A as the acyl donor. Furthermore, several similarities between *in vitro* palmitoylation, and cellular palmitoylation have been observed. Such similarities include palmitoylation on specific cysteine residues, the requirement for prior *N*-myristoylation, and the need for other proteins or cofactors.

Peptide fragments derived from *in vivo* palmitoylated proteins were palmitoylated *in vitro*, while other cysteine-containing peptides were not (Bharadwaj and Bizzozero, 1995), suggesting that spontaneous palmitoylation can be a specific event, as would be expected for a process that needs to be regulated *in vivo*. This non-enzymic reaction is not just restricted to peptides: the G_α subunit of heterotrimeric G proteins became autopalmitoylated *in vitro* on the same cysteine residue that is palmitoylated *in vivo* (Duncan and Gilman, 1996). In addition, palmitoylation only occured after G_α had first been myristoylated on an N-terminal glycine. Furthermore, palmitoylation of G_α *in vitro* was greatly enhanced by inclusion of $G_{\beta\gamma}$ subunits in the palmitoylation reaction (Duncan and Gilman, 1996). Similarly, the SNARE (soluble *N*-ethylmaleimide-sensitive factor attachment protein receptor) SNAP25 (25 kDa synaptosome-associated protein) was also palmitoylated *in vitro*, and this was shown to be dramatically enhanced by the presence of its binding partner, the SNARE syntaxin 1A (Veit, 2000).

Finally, the conditions used for palmitoylation of peptides *in vitro*, specifically the dependence on time, pH, temperature and the concentration of the substrate, suggests that the reaction could occur spontaneously *in vivo* (Bano *et al.*, 1998). If palmitoylation were to occur spontaneously *in vivo*, then this process would need to be regulated. Such regulation may be accomplished by protein palmitoyl thioesterases, which deacylate palmitoylated proteins (see Chapter 1.6), and/or by specific binding partners of the palmitoylation substrate.

Despite the ability of some proteins and peptides to undergo palmitoylation on specific cysteines and in the absence of an enzyme *in vitro*, several factors argue against spontaneous palmitoylation occurring *in vivo*.

First, non-selective palmitoylation of proteins also occurs *in vitro*. For example, the cytoskeletal protein actin has five cysteine residues that are not palmitoylated *in vivo*, however, conditions that favour palmitoylation of peptide fragments *in vitro* also non-specifically palmitoylate actin (Bano *et al.*, 1998). Conversely, not all palmitoylated proteins could be

palmitoylated *in vitro* (*e.g.* Fyn kinase) or palmitoylation was inefficient (*e.g.* for GAP-43, SNAP25 and some G$_\alpha$ subunits) (Duncan and Gilman, 1996).

Second, palmitoylation in cells is dependent on the sequence surrounding the palmitoylation site, which would be difficult to regulate if cysteine residues were able to undergo spontaneous palmitoylation *in vivo*. Mutation of residues surrounding the palmitoylated cysteine residue in the tyrosine kinase Fyn abolishes its palmitoylation *in vivo* but the mutant protein is still able to undergo spontaneous palmitoylation *in vitro* (Resh, 1999). However, a caveat to these points, as discussed in Chapter 1.4.3, is that thiolate formation *in vivo* may be critically dependent upon surrounding amino acids: this requirement could be bypassed *in vitro*, for example, through manipulation of the pH and salt concentration.

It is also noteworthy to mention that most of the free cytosolic fatty acyl-coenzyme A within a cell is thought to be sequestered by acyl-coenzyme A binding proteins (ACBPs), ubiquitously expressed cytosolic proteins of ~ 10 kDa, which bind medium- and long-chain acyl-coenzyme A esters with very high affinities (Faergeman *et al.*, 1996; Faergeman and Knudsen, 1997; Frolov and Schroeder, 1998; Rosendal *et al.*, 1993). In this way, physiological concentrations of acyl-coenzyme A are predicted to be much lower than the concentrations required for spontaneous palmitoylation *in vitro*, although, the actual free cytosolic concentration of long-chain acyl-coenzyme A esters is not known (Faergeman and Knudsen, 1997). Indeed, the addition of physiological concentrations of ACBPs to *in vitro* palmitoylation reaction mixtures results in a concentration-dependent inhibition of the otherwise spontaneous palmitoylation of both proteins and peptides (Dunphy *et al.*, 2000; Leventis *et al.*, 1997). By taking into consideration the existence of cytosolic ACBPs, it is predicted that in the absence of a catalyst the rate of palmitoylation of membrane-associated proteins in cells would be extremely slow (days) (Leventis *et al.*, 1997), and therefore not physiologically relevant, given the short palmitoylation half lives of some proteins *in vivo*. For example, the half-life of palmitate turnover on N-Ras was predicted to be around twenty minutes (Magee *et al.*, 1987), and indeed more recent experiments have suggested a far more rapid rate of turnover (Goodwin *et al.*, 2005; Rocks *et al.*, 2005).

Finally, even in the absence of ACBPs, the rates at which *in vitro* palmitoylation reactions proceed vary greatly, and in most cases have been relatively slow. Given that many palmitoylated proteins are subject to dynamic cycles of acylation and deacylation *in vivo*, the spontaneous acylation of proteins in cells seems unlikely to be a widespread event.

1.4.3.2 PROTEIN ACYLTRANSFERASES

The enzymes that catalyse the thioesterification of cysteines in substrate proteins with palmitate have only relatively recently been reported. The identification of protein acyltranferases (PATs) was previously hindered in part by the difficulties in preserving enzyme activity of putative PATs following purification or membrane solubilisation. Furthermore, previous attempts to purify PAT activity have been misleading; for example, one PAT that was purified to apparent homogeneity and shown to have activity towards Ras proteins was later identified as thiolase A, a peroxisomal enzyme (Liu *et al.*, 1996).

The first enzyme possessing PAT activity towards cytosolic proteins was identified and isolated from *Saccharomyces cerevisiae* in 2002 (Lobo *et al.*, 2002). Ras proteins and their post-translational processing are conserved from yeast to man. Wild-type mature Ras is localised primarily to the cytoplasmic face of the plasma membrane (Magee and Marshall, 1999). Plasma membrane targeting of most Ras proteins is dependent on a series of post-translational modifications, specifically farnesylation of a C-terminal *CaaX* box cysteine, –*aaX* proteolysis and methyl esterification of the newly exposed cysteinyl α-carboxyl, prior to palmitoylation of one or more neighbouring cysteines (Hancock *et al.*, 1990). To identify the genes responsible for palmitoylation of yeast Ras2, a previously characterised prenylation-deficient Ras2 mutant protein was exploited. Replacing the C-terminal *CaaX* box of yeast Ras2 (CCIIS) with a basic extension sequence (CSIIKLIKRK) generated a mutant Ras2 protein, which could be palmitoylated on the equivalent cysteine to wild-type protein and targeted correctly, while bypassing the requirement for farnesylation (Mitchell *et al.*, 1994). A genetic screen of a Ras2 palmitoylation-dependent yeast strain was employed to identify mutations that diminished Ras2 palmitoylation, as determined by loss of viability. Two legitimate complementation groups that disrupted modified Ras2 palmitoylation were identified; one was designated ERF2 (for *effector of Ras function*), and the other was recognized as ERF4 (also called SHR5; *suppressor of hyperactive Ras*) (Bartels *et al.*, 1999). An *in vitro* palmitoylation assay was used to confirm that the Erf2p/Erf4p complex directly catalysed *S*-palmitoylation of yeast Ras. By incubating partially purified Erf2p/Erf4p with prenylated Ras in the presence of tritiated palmitoyl coenzyme A as the palmitate donor, the rate of Ras2 palmitoylation was 160-fold greater than the rate in the absence of the Erf2p/Erf4p complex (Lobo *et al.*, 2002). The catalytic activity of the yeast Ras PAT requires a heterodimeric complex of both Erf2p and Erf4p, since neither protein is capable of carrying out palmitoylation reactions individually (Lobo *et al.*, 2002). Concurrent with the discovery of the Erf2p/Erf4p complex as a palmitoyl transferase, a second yeast protein, Akr1p (Ankyryn repeat-containing protein), was shown to catalyse the *S*-palmitoylation of the yeast type I casein kinase Yck2p *in vitro* (Roth *et al.*, 2002). Unlike the

PAT for the yeast Ras2, Akr1p does not require to be part of a complex for catalytic activity, as it is able to work independently without accessory subunits (Roth *et al.*, 2002). Sequence analysis of Erf2p, Erf4p and Akr1p reveals that there is a single region of sequence homology between Efr2p and Akr1p: both Efr2p and Akr1p share a conserved 51-residue-long zinc-finger like domain, known as a DHHC (aspartate-histidine-histidine-cysteine) cysteine-rich domain (CRD), which is not present in Erf4p.

In addition to the DHHC-CRD family of PATs, a second class of palmitoylating enzymes has been identified. These PATs modify N-terminal cysteines on proteins that are located exclusively in the lumen of organelles. These PATs were first identified in *Drosophila melanogaster* and were shown to palmitoylate N-terminal cysteines of the secreted morphogens Hedgehog and Wnt (Chamoun *et al.*, 2001; Zhai *et al.*, 2004). The *N*-palmitoyltransferase Skinny hedgehog (*Ski*; also known as Rasp, Central missing, and Sightless), was first shown to be required for the palmitoylation of Hedgehog (Chamoun *et al.*, 2001) and subsequently, Spitz (Miura *et al.*, 2006). Wnt requires a different *N*-palmitoyltransferase, Porcupine (*Porc*), for palmitoylation (Zhai *et al.*, 2004). Skinny hedgehog and Porcupine do not possess the conserved DHHC domain as seen for the yeast PATs, but share limited sequence homology with certain *O*-acyltransferases that add acyl groups onto hydroxyl groups of membrane-anchored substrates (Hofmann, 2000).

1.5 THE DHHC FAMILY OF PALMITOYL ACYLTRANSFERASES

The finding that the two PATs in yeast, Erf2p and Akr1p, share a conserved DHHC domain, and that mutations within this domain abolish catalytic activity (Lobo *et al.*, 2002; Roth *et al.*, 2002), suggested that the DHHC domain may be a palmitoyl transferase motif. Similarly, it was proposed that proteins containing the DHHC-CRD may represent a family of PATs (Roth *et al.*, 2002). Subsequent analysis of the yeast and mammalian genomes has identified a family of seven proteins in yeast; Akr1p, Akr2p, Erf2p, Pfa3p, Pfa4p, Pfa5p and Swf1p; and twenty-three in mammals; DHHC1-DHHC23 (Fukata *et al.*, 2004), all containing a conserved DHHC-CRD (Figure 1.3). Genetic and biochemical analyses have demonstrated the palmitoyl transferase activity of several of these DHHC-CRD containing proteins, and accordingly, many substrates have been identified.

Five yeast DHHC-containing proteins have been shown to catalyse *S*-palmitoylation so far and several enzyme-substrate pairs have been identified. As mentioned above, *in vitro* and *in vivo* palmitoylation assays have shown that Erf2p palmitoylates Ras (Lobo *et al.*, 2002), and Akr1p

A

N-Variable   C-Variable

B   DHHC Cysteine Rich Domain

Figure 1.3 The DHHC family of palmitoyl acyltransferases. *A.* Members of the DHHC family of palmitoyl transferases are polytopic integral membrane proteins encoding 4-6 predicted membrane-spanning domains with the DHHC Cysteine Rich Domain and both N- and C-termini oriented cytosolically. *B.* Alignment of the twenty-three mouse DHHC proteins; conserved residues are shaded in grey.

palmitoylates Yck2p (Roth *et al.*, 2002). In addition to Yck2p, Akr1p also palmitoylates the sphingoid long-chain base kinase, Lcb4 (Kihara *et al.*, 2005). Swf1p is likely to be the enzyme responsible for palmitoylation of the yeast SNAREs Snc1p, Tlg1p and Syn8p (Valdez-Taubas and Pelham, 2005). Pfa3p (Protein fatty acyltransferase 3) has been shown to palmitoylate Vac8p, a protein involved in yeast vacuolar inheritance, *in vitro* and *in vivo* (Hou *et al.*, 2005; Smotrys *et al.*, 2005), while palmitoylation of the yeast chitin synthase, Chs3p, is dependent on Pfa4p (Lam *et al.*, 2006). Substrates for the remaining two yeast DHHC-CRD proteins, Akr2p and Pfa5p, have yet to be determined.

Palmitoyl transferase activity has been reported for nine of the twenty-three mammalian DHHC-CRD proteins to date and, for the majority of these PATs, palmitate can be incorporated into multiple substrates. The first mammalian DHHC-CRD protein shown to have PAT activity was DHHC3, also known as GODZ (Keller *et al.*, 2004; Uemura *et al.*, 2002). The $\gamma2$ subunit of the $GABA_A$ (γ-aminobutyric acid) receptor is essential for postsynaptic clustering of $GABA_A$ receptor subtypes (Essrich *et al.*, 1998), and palmitoylation of the $\gamma2$ subunit in a non-neuronal cell line was dependent on co-expression of DHHC3 (Keller *et al.*, 2004). Subsequently, Fukata *et al* screened all twenty-three mammalian DHHC-CRD proteins for their ability to increase radiolabelled palmitate incorporation into the neuronal scaffolding protein, PSD-95, in non-neuronal cells (Fukata *et al.*, 2004). Palmitoylation of PSD-95 was increased after co-expression of DHHCs -2, -3, -7 and -15 in COS7 cells, however, DHHC15 produced the greatest incorporation of palmitate (Fukata *et al.*, 2004). To date, PAT activity has been confirmed for DHHCs -2, -3, -7, -8, -9, -15, -17, -18 and -21 (Fernandez-Hernando *et al.*, 2006; Fukata *et al.*, 2004; Hayashi *et al.*, 2005; Huang *et al.*, 2004; Keller *et al.*, 2004; Ohyama *et al.*, 2007; Swarthout *et al.*, 2005). Substrate proteins ascribed to these DHHC proteins are listed in Table 1.

The finding that some proteins are palmitoylated by multiple PATs implies a certain level of redundancy for enzyme substrates. However, not all PATs were able to palmitoylate every protein tested, and thus PATs do display a certain level of substrate specificity. Finally, not every DHHC-CRD protein has been shown to possess palmitoylation activity. This may be because their substrate proteins have yet to be determined, or because some of the DHHC proteins require accessory proteins. For example, the DHHC proteins that palmitoylate yeast and mammalian Ras, Erf2p and DHHC9, require Er4p and GCP16, respectively, for stable expression and transferase activity (Lobo *et al.*, 2002; Swarthout *et al.*, 2005). Finally, it may be that not all DHHC-CRD containing proteins harbour palmitoyl transferase activity.

TABLE 1: DHHC PROTEIN SUBSTRATES IDENTIFIED

DHHC	Substrates
DHHC2	eNOS (Fernandez-Hernando *et al.*, 2006) PSD-95 (Fukata *et al.*, 2004)
DHHC3	AMPA receptor subunits (Hayashi *et al.*, 2005) G$_{\alpha s}$(Fukata *et al.*, 2004) GABA$_A$ receptor subunits (Keller *et al.*, 2004) PSD-95 (Fukata *et al.*, 2004) SNAP-25 (Fukata *et al.*, 2004)
DHHC7	eNOS (Fernandez-Hernando *et al.*, 2006) G$_{\alpha s}$(Fukata *et al.*, 2004) GAP-43 (Fukata *et al.*, 2004) PSD-95 (Fukata *et al.*, 2004) SNAP-25 (Fukata *et al.*, 2004)
DHHC8	eNOS (Fernandez-Hernando *et al.*, 2006)
DHHC9	H-/N-Ras (Swarthout *et al.*, 2005)
DHHC15	GAP-43 (Fukata *et al.*, 2004) PSD-95 (Fukata *et al.*, 2004)
DHHC17	CSP (Ohyama *et al.*, 2007) GAD-65 (Huang *et al.*, 2004) htt (Huang *et al.*, 2004) Lck (Fukata *et al.*, 2004) PSD-95 (Fukata *et al.*, 2004; Huang *et al.*, 2004) SNAP25 (Fukata *et al.*, 2004; Huang *et al.*, 2004) Synaptotagmin 1 (Huang *et al.*, 2004)
DHHC18	Lck (Fukata *et al.*, 2004)
DHHC21	eNOS (Fernandez-Hernando *et al.*, 2006)

Abbreviations: AMPA, α-amino-3-hydroxy-5-methyl-4-isoxazole propionic acid; CSP, cysteine string protein; eNOS, endothelial nitric oxide synthase; GAD, Glutamate decarboxylase 65; GAP-43, Growth-associated protein 43; htt, huntingtin; PSD-95, Post-synaptic density protein of 96 kDa; SNAP25, synaptosomal-associated protein of 25 kDa.

Recently, an acyl biotin exhange method was employed that identified thirty-five novel palmitoylated proteins in yeast, including eight SNARE proteins (Drisdel and Green, 2004; Roth *et al.*, 2006). Yeast strains deficient in multiple DHHC-CRD-containing proteins revealed several potential enzyme-substrate pairs and demonstrated that the DHHC-CRD family of proteins account for the majority of cellular palmitoylation reactions in yeast (Roth *et al.*, 2006).

1.5.1 THE DHHC DOMAIN AND CATALYTIC ACTIVITY

The DHHC-CRD was first reported when a unique clone was isolated from a human pancreatic cDNA library (Putilina *et al.*, 1999). Sequence analysis revealed a cysteine-rich domain which

includes a C_2H_2 zinc finger-like region upstream of a complex Cys-His region (Putilina *et al.*, 1999). Accordingly, the approximately 50-residue long DHHC-CRD is classed as a variant of the C_2H_2 zinc finger motif (Bohm *et al.*, 1997), and is defined by the core asp-his-his-cys tetrapeptide sequence (Figure 1.3).

The first clue that the conserved DHHC-CRD domain was linked to PAT activity was established when a yeast genetic screen of palmitoylation-dead mutants revealed point mutations within the ERF2 DHHC-CRD (Bartels *et al.*, 1999). Subsequently, site-directed mutations introduced into the DHHC signature motif of the yeast PATs, Erf2p (H201A and C203S) and Akr1p (D543A, H544A and C546A), abolished the *in vivo* labelling of their substrate proteins, confirming the requirement of the DHHC motif for catalytic activity (Lobo *et al.*, 2002; Roth *et al.*, 2002). Furthermore, a similar loss of palmitoylating activity has been reported whenever cysteine mutations have been introduced into the DHHC domain of any of the DHHC-CRD family of proteins studied (Ducker *et al.*, 2004; Fernandez-Hernando *et al.*, 2006; Fukata *et al.*, 2004; Hayashi *et al.*, 2005; Huang *et al.*, 2004; Lam *et al.*, 2006; Lobo *et al.*, 2002; Roth *et al.*, 2002; Smotrys *et al.*, 2005; Swarthout *et al.*, 2005; Valdez-Taubas and Pelham, 2005). Mutational analysis revealed that Erf2p and Akr1p form an acyl-enzyme intermediate when incubated with palmitoyl-coenzyme A, likely becoming palmitoylated on the conserved cysteine within the DHHC motif (Lobo *et al.*, 2002; Roth *et al.*, 2002). Similar autopalmitoylation has been observed for all of the DHHCs in which analysis has been carried out (Ducker *et al.*, 2004; Fukata *et al.*, 2004; Hayashi *et al.*, 2005; Keller *et al.*, 2004; Lobo *et al.*, 2002; Roth *et al.*, 2002; Smotrys *et al.*, 2005; Swarthout *et al.*, 2005). These observations have led to suggestions that palmitate transfer from enzyme to substrate may be required for palmitoylation, however the exact mechanism has not yet been determined. Interestingly, mutation of the conserved histidine residue in the DHHC motif of Erf2p preserved autopalmitoylation of Erf2p, but led to a loss of PAT activity, suggesting that the histidine may be involved somehow in palmitate transfer from enzyme to substrate (Lobo *et al.*, 2002).

1.5.2 MEMBRANE TOPOLOGY AND SUBCELLULAR LOCALISATION OF DHHC-CRD PROTEINS

The DHHC-family of PATs are a family of polytopic integral membrane proteins that share little or no homology out-with their DHHC-CRD (Figure 1.3). DHHC proteins and/or PAT activities have been identified on diverse intracellular membranes; examples include the Golgi, ER, plasma membrane, endosomes/vesicular compartments and the yeast vacuole (Dunphy *et al.*, 1996; Fukata *et al.*, 2004; Huang *et al.*, 2004; Keller *et al.*, 2004; Roth *et al.*, 2002;

Schroeder *et al.*, 1996; Singaraja *et al.*, 2002; Swarthout *et al.*, 2005; Uemura *et al.*, 2002; Valdez-Taubas and Pelham, 2005; Veit *et al.*, 2001).

The transmembrane topology of Akr1p has been investigated experimentally by constructing several Akr1p mutants with the coding sequence for the yeast secretory protein invertase introduced into each of the putative hydrophilic loop domains (as revealed by hydropathy analysis) (Politis *et al.*, 2005). In *S. cerevisiae*, invertase is glycosylated at 10 sites, and since glycosyltransferase activity is present only in the lumen of intracellular organelles, the transmembrane topology and orientation can be determined biochemically. This analysis revealed that Akr1p has 6 membrane-spanning domains, with both the N- and C-termini and the DHHC-CRD located cytoplasmically. The DHHC-CRD is present on an intracellular loop between the fourth and fifth membrane-spanning domains (Politis *et al.*, 2005). Hydropathy sequence analysis predicts that a similar topology holds for all of the DHHC-CRD containing proteins, having between four and six transmembrane domains, with the DHHC-CRD located on the second or third cytoplasmic loop and with both the N-and C-terminal domains cytosolically exposed (Figure 1.3) (Mitchell *et al.*, 2006).

1.6 PROTEIN THIOESTERASES

The dynamic palmitoylation of some proteins, for example H-and N-Ras (Rocks *et al.*, 2005), suggests that mechanisms must exist to remove palmitate groups from proteins in a regulated manner. Such regulation is achieved by the action of palmitoyl thioesterases, enzymes that selectively cleave the thioester linkage of palmitoylated proteins (Figure 1.4).

Three such palmitoyl thioesterases have been identified and characterized: the lysosomal hydrolase, protein palmitoyl thioesterase 1 (PPT1) and its homologue PPT2, and the cytoplasmic enzyme, acyl-protein thioesterase (APT1) (Bellizzi *et al.*, 2000; Camp and Hofmann, 1993; Devedjiev *et al.*, 2000; Duncan and Gilman, 1998; Soyombo and Hofmann, 1997).

PPT1 was originally purified from bovine brain cytosol, and the palmitoyl thioesterase activity of PPT1 was demonstrated by its ability to remove radiolabelled palmitate from H-ras and G_α subunits (Camp and Hofmann, 1993). Subsequent cloning of the rat and bovine cDNA identified PPT1 as a classical lysosomal hydrolase, which is targeted to the lumen of lysosomes by mannose-6-phosphate modification of *N*-linked oligosaccharides (Camp *et al.*, 1994; Hellsten *et al.*, 1996; Sleat *et al.*, 1996; Verkruyse and Hofmann, 1996). The lysosomal

Palmitoyl transferase

HS-CoA   Pal-CoA

palmitoylation

depalmitoylation

H₂O   Pal-OH
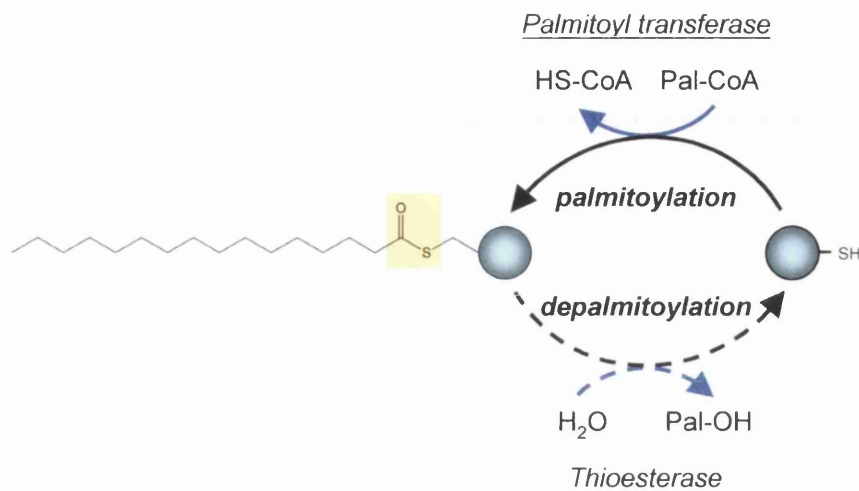
Thioesterase

Figure 1.4 Regulation of palmitoylation. Palmitoyl transferases catalyse the addition of palmitate moieties from palmitoyl-coenzyme A (Pal-CoA) to the sulphydryl group of cysteine residues through a thioester linkage (yellow). The thioester bond is cleavable and so allows protein palmitoylation to be a reversible modification, and proteins may be depalmitoylated *in vivo* through the action of thioesterases. A blue sphere represents the modified protein. The chemical structure was generated using ChemBioDraw® Ultra 11.0 software (CambridgeSoft®).

localisation of PPT1 argues against a role in the regulated depalmitoylation of substrates, and instead points towards a role for PPT1 in the degradation of palmitoylated proteins.

Later studies isolated palmitoyl protein thioesterase activity from rat liver cytosol, which was termed APT1 (Duncan and Gilman, 1998). Subsequent sequence analysis revealed that APT1 had been previously described as a lysophospholipase (Sugimoto *et al.*, 1996; Wang *et al.*, 1997a; Wang *et al.*, 1997b). APT1 is a cytosolic protein showing substrate preference for acylated proteins over other lipidated substrates, and cleaves thioesters in both acyl-coenzyme A and acylated proteins (Duncan and Gilman, 1998). APT1 has been demonstrated to have thioestarase activity towards Ras proteins, G$_\alpha$ subunits, eNOS and viral glycoproteins (Duncan and Gilman, 1998; Duncan and Gilman, 2002; Veit and Schmidt, 2001; Yeh *et al.*, 1999). The expression of APT1 increases the rate of palmitate turnover on G$_\alpha$ subunits (Duncan and Gilman, 1998), and disruption of the *APT1* gene in *S. cerevisiae* leads to a significant reduction in acyl protein thioesterase activity and prevents the depalmitoylation of the yeast G$_\alpha$ subunit homologue, Gpa1p (Duncan and Gilman, 2002). Similarly, APT1 regulates the depalmitoylation of eNOS since overexpression of APT1 and eNOS in a heterologous cell line leads to an increased turnover of ³H palmitic acid on eNOS (Yeh *et al.*, 1999). A second lysophospholipase sharing sequence homology to APT1 has been identified (Toyoda *et al.*, 1999), though thioesterase activity and substrate specificity have not been determined. It is

suspected that many protein palmitoyl thioesterases exist, each having substrate specificity to regulate depalmitoylation cycles *in vivo*. However, many proteins are stably palmitoylated, for example SNAP25 and synaptotagmin I (Heindel *et al.*, 2003; Kang *et al.*, 2004), therefore an interesting possibility is that sensitivity to APT1 or similar enzymes dictates whether or not a protein undergoes dynamic palmitoylation.

1.7 THE SECRETORY PATHWAY

The concept of a secretory pathway was introduced with the advent of electron microscopy in the 1960s and 1970s and by biochemical experiments, which showed that proteins to be secreted are synthesised in the endoplasmic reticulum and move to and through the Golgi complex, from where they are packaged into secretory vesicles (Palade, 1975). Movement of proteins through the compartments of the secretory pathway is mediated by transport vesicles, which bud from donor membranes and are targeted to specific acceptor compartments. Fusion of the vesicles with the acceptor membrane then transfers lipid and protein to that compartment. Membrane fusion is a fundamental event in a wide variety of cellular processes including cell growth and division, vesicular traffic along the secretory pathway, organelle inheritance, and neurotransmitter and hormone release. Most research has supported the general belief that all types of cells, from yeast to man, share a universal core membrane fusion mechanism with specialised features in different pathways. Furthermore, these underlying mechanisms appear to be conserved among all eukaryotic cells and also between constitutive and regulated secretory pathways (Katagiri *et al.*, 1995).

1.7.1 CONSTITUTIVE AND REGULATED SECRETION

Exocytosis is the fusion of intracellular vesicles with the plasma membrane and takes place through two separate pathways: constitutive and regulated. The former occurs in all eukaryotic cells and functions in the continual maintenance of plasma membrane lipids and proteins and the extracellular environment. Regulated exocytosis is a more specialised pathway limited to cells carrying out specific functions, and where secretion occurs only in response to particular stimuli. In most cases an increase in intracellular calcium ion concentration is the major trigger for regulated exocytosis (Lin and Scheller, 2000). Regulated exocytosis underlies diverse processes such as enzyme and cytokine release, neurotransmitter release and endocrine hormone secretion. Regulated exocytosis therefore forms the basis of co-ordinated responses such as movement and behaviour (Knight, 1999). It is also crucial in controlling the levels of different lipids, receptors, and transporters in the plasma membrane, so altering the cell's limiting

membrane. For example, the insertion of Glut4 glucose transporters into the plasma membrane of fat and muscle cells in response to insulin stimulation occurs via regulated exocytosis (Rea and James, 1997).

Regulated secretory vesicles undergo a series of maturation steps before they become fusion competent; these maturation steps include vesicle tethering prior to docking at the plasma membrane, followed by vesicle priming (Klenchin and Martin, 2000; Sudhof, 2004). Following vesicle priming, the vesicle is able to respond to the increase in intracellular calcium concentration and undergo fusion with the plasma membrane in a regulated manner. Biochemical and genetic studies have identified a vast array of proteins involved in the intracellular transport of secretory vesicles and their subsequent fusion with the plasma membrane. At least three protein families appear to be universally involved in all intracellular fusion reactions: the SNAREs (SNAP receptors) and associated proteins (N-ethylmaleimide-sensitive factor [NSF] and soluble NSF attachment proteins [SNAPs]), the Sec1/Munc18 homologs (SM proteins), and small GTPases known as Rabs and their effector proteins (Jahn et al., 2003). It is thought that the function of SNARE proteins is to mediate vesicle docking and lipid bilayer fusion (Weber et al., 1998), while the Sec1 and Rab/Rab effector proteins assist by regulating SNARE complex association and vesicle targeting (Grosshans et al., 2006; Jahn, 2000). Following fusion, the SNAREs are disassembled in a process dependent on the ATPase NSF, releasing them for another round of membrane fusion (Littleton et al., 2001). This basic fusion machinery appears to be conserved between different transport steps and amongst all eukaryotes (Bonifacino and Glick, 2004).

1.8 THE SNARE PROTEINS

At the heart of intracellular trafficking lie the SNARE proteins, a conserved family of small and integral membrane proteins that play a crucial role in mediating intracellular fusion in eukaryotic cells of numerous organisms (Bruns and Jahn, 2002; Jahn and Sudhof, 1999; Jahn et al., 2003). SNARE proteins were originally discovered in independent studies of yeast and mammalian cells (Bennett and Scheller, 1993), and on the basis of their localisation and overall structure, SNAREs were divided into two categories: v-(vesicle) SNAREs and t-(target membrane) SNAREs. In neuronal synaptic vesicle exocytosis, the v-SNAREs are VAMP1/2 (also known as synaptobrevin), and the t-SNAREs are syntaxin 1A/B and SNAP25A/B (Jahn et al., 2003). The v-SNAREs are located on the membrane of the trafficking vesicle, and the t-SNAREs are present on target membranes. However, since this classification is not appropriate for all membrane fusion events, for example, in homotypic membrane fusion where the two

membranes are functionally and structurally equivalent, SNARE proteins have been re-classified as Q- and R-SNAREs (see Chapter 1.8.1) (Fasshauer *et al.*, 1998b). Two different biochemical approaches, immunoprecipitation and sucrose-gradient centrifugation, yielded evidence of complex formation between the SNAREs and two proteins previously discovered as essential for secretion in yeast and intra-Golgi transport in mammalian cells: α-SNAP (Sec17p) and NSF (Sec18p) (Sollner *et al.*, 1993b). The fundamental importance of the SNARE proteins in neurosecretion is highlighted by the ability of tetanus and botulinum neurotoxins, which specifically cleave these proteins, to abolish neurotransmission (Schiavo *et al.*, 1992a; Schiavo *et al.*, 1993a). The defining feature of all SNAREs is a homologous domain of ~60 amino acids referred to as the SNARE motif (Weimbs *et al.*, 1997).

1.8.1 SNARE PROTEINS AND MEMBRANE FUSION

SNARE proteins on opposing membranes interact to form a highly stable trimeric SNARE (or core) complex (Sollner *et al.*, 1993a; Sollner *et al.*, 1993b). The intrinsic stability of the SNARE complex is supported by data showing that it resists denaturation by the ionic detergent sodium dodecyl sulphate (SDS) (Hayashi *et al* 1994), has a melting temperature of more than 90 °C (Fasshauer *et al.*, 1998a; Yang *et al.*, 1999), and that SNAREs assembled into a complex can resist proteolysis by the botulinum and tetanus toxins (Hayashi *et al* 1994).

Formation of the SNARE core complex is tightly coupled to membrane fusion as it brings the two opposing membranes into close proximity (Hayashi *et al.*, 1994). During SNARE complex assembly, the individual coiled-coil (helical) SNARE motifs present in the SNARE proteins interact to form a parallel four-helix bundle (Poirier *et al.*, 1998). X-ray crystallography of the core complex involved in neuronal exocytosis revealed that one helix is provided by VAMP, one by syntaxin 1A, and the other two by SNAP25 (Sutton *et al.*, 1998). There are several layers of hydrophobic interactions between the different helices (designated as -7 through to +8), with a central (or 'zero' layer) ionic interaction formed between three glutamines and one arginine residue (Sutton *et al.*, 1998). Shortly after the structure of the neuronal SNARE complex was presented, it was noted that essentially all SNARE proteins contained either a conserved arginine (R) or glutamine (Q) residue that would contribute to zero layer interactions (Fasshauer *et al.*, 1998b). In light of this, it was proposed that SNAREs be reclassified as R- or Q-SNAREs (Fasshauer *et al.*, 1998b). R-SNAREs comprise the VAMPs, Qa-SNAREs include the syntaxins, and Qb- and Qc-SNAREs are the homologues of the N- and C-terminal SNARE motif, respectively, of SNAP25 (Bock *et al.*, 2001; Fasshauer *et al.*, 1998b). All functional cellular

SNARE complexes appear to contain one copy of R-, Qa-, Qb-, and Qc-SNARE motifs (Jahn *et al.*, 2003).

It is generally (though not universally) believed that formation of a trans-SNARE complex is sufficient to pull the opposing membranes together, overcoming the energy barrier opposing fusion of the two lipid bilayers. Indeed, the introduction of cognate SNAREs into different populations of liposomes generated SNARE interactions that facilitated a slow rate of liposome fusion (Weber *et al.*, 1998). The fusion of these proteoliposomes has been demonstrated with specific combinations of the cognate Q-and R-SNAREs only (McNew *et al.*, 2000; Parlati *et al.*, 2000), suggesting that complementary SNAREs on opposing membranes are necessary and sufficient to determine their compatibility for fusion. Although SNAREs are sufficient to catalyse fusion *in vitro*, this occurs at a slow rate and it is likely that other factors facilitate fusion *in vivo*. Indeed, the addition of SM proteins into SNARE reconstituted liposomes has been shown to stimulate *in vitro* fusion activity by several-fold (Shen *et al.*, 2007), and factors that regulate the formation of a 1:1 stoichiometric syntaxin/SNAP25 acceptor complex have also been proposed to greatly enhance fusion efficiency (Pobbati *et al.*, 2006; Weninger *et al.*, 2008). Consistent with the ability of SNAREs to enhance fusion *in vitro*, studies using the botulinum and tetanus toxins in the squid giant axon have shown that SNARE action occurs downstream of vesicle docking, with toxin cleavage of SNAREs preventing vesicular fusion but leaving docking unaffected (Hunt *et al.*, 1994; O'Connor *et al.*, 1997). More recent work, however, has suggested an important role for syntaxin in the docking of secretory granules in neuroendocrine cells (Gulyas-Kovacs *et al.*, 2007).

After membrane fusion, the *cis*-SNARE complex is dissociated through the action of α-SNAP and the ATPase NSF (Littleton *et al.*, 2001; Sollner *et al.*, 1993a). α-SNAP binds to the core complex, in turn recruiting NSF and simultaneously enhancing and harnessing its ATPase activity for complex disassembly (Barnard *et al.*, 1997), allowing the free SNAREs to be released for subsequent rounds of fusion.

At least 35 SNARE proteins have been identified in mammals, with the majority specifically localised to distinct membrane compartments; the creation of particular SNARE complexes may contribute to the specificity of membrane fusion fundamental to membrane compartment organisation (Bock *et al.*, 2001).

Despite the general agreement that the SNARE complex plays an important role in synaptic membrane fusion, evidence from other systems has indicated that core complex assembly does

not coincide with fusion pore opening. The SNARE complexes mediating sea urchin egg cortical vesicle fusion are disrupted prior to membrane fusion in the presence of free Ca^{2+} concentrations that trigger maximal membrane fusion (Tahara *et al.*, 1998). Similarly, in this same system, fusion is unaffected by proteolytic removal of membrane proteins, including the SNAREs (Szule *et al.*, 2003). In yeast vacuolar fusion, blocking SNAREs with anti-SNARE antibodies after complex dissociation by NSF prevents complex reformation but vesicular fusion remains uninhibited (Ungermann *et al.*, 1998). Furthermore, it has been proposed that the V_0 subunits of the vacuolar protein pump form *trans*-complexes across otherwise opposing vacuolar membranes that may create a proteolipid-lined channel spanning both membranes. The suggestion is that the *trans*-SNARE pairing on opposing membranes serves to assemble the V_0 subunits into these *trans*-complexes (Peters *et al.*, 2001). Following this, the *trans*-SNARE pairs may go on to help stabilise the opposing membranes, or may simply become dispensable. However, mutations in the V_0 subunit only delay fusion, whereas mutations in SNAREs can block fusion. Thus SNARE-mediated fusion remains to be the most popular model.

1.8.2 SYNTAXIN

Syntaxin was originally described as an antigen for a monoclonal antibody, HPC-1, that labels ~ 35 kDa proteins localised to the plasma membrane in neurons, and subsequently, as a protein that interacts with the synaptic vesicle membrane protein, synaptotagmin, and N-type Ca^{2+}-channels (Barnstable *et al.*, 1985; Bennett *et al.*, 1992; Inoue *et al.*, 1992; Yoshida *et al.*, 1992). There are 15 members of the syntaxin family in the human genome, each localised to various intracellular organelles and essential for multiple distinct intracellular fusion events (Teng *et al.*, 2001). The specific syntaxin isoforms each mediate specific membrane fusion events: syntaxin 1A is almost exclusively found in neuronal and neuroendocrine cells and functions in regulated exocytosis at the plasma membrane. The importance of this protein in exocytosis was demonstrated in PC12 cells, where microinjection of anti-syntaxin 1A antibodies inhibited calcium-dependant secretion (Bennett *et al.*, 1993). Syntaxin 1A forms complexes with SNAP25 (Pevsner *et al.*, 1994a), VAMP (Calakos *et al.*, 1994; Pevsner *et al.*, 1994a), and synaptotagmin (Bennett *et al.*, 1992; Sollner *et al.*, 1993a), and binds to at least 10 other neuronal proteins, including Munc18 (Hata *et al.*, 1993; Pevsner *et al.*, 1994a; Pevsner *et al.*, 1994b), complexins (McMahon *et al.*, 1995), α-SNAP, rsec6/rsec8 (Hsu *et al.*, 1996), CIRL/latrophilin (Krasnoperov *et al.*, 1997), tomosyn (Fujita *et al.*, 1998), Munc13 (Betz *et al.*, 1997) and cysteine string protein (Evans *et al.*, 2001; Nie *et al.*, 1999). Syntaxin 1A also directly interacts with and functionally regulates Ca^{2+} channels (Bezprozvanny *et al.*, 1995;

Sheng *et al.*, 1994; Sutton *et al.*, 1999; Wiser *et al.*, 1996), cystic fibrosis Cl⁻ channels (Naren *et al.*, 1997), K⁺ channels (Fili *et al.*, 2001) and epithelial Na⁺ channels (Qi *et al.*, 1999).

Syntaxin is a C-tailed membrane-anchored protein: it is membrane-associated by virtue of a single stretch of hydrophobic amino acids close to its C-terminus. Nuclear magnetic resonance (NMR) spectroscopy has revealed that the N-terminus of syntaxin 1A consists of a short unstructured N-terminal sequence followed by an autonomous H_{abc} regulatory domain consisting of three alpha helices (Fernandez *et al.*, 1998). A linker domain separates the H_{abc} domain and the SNARE motif. Syntaxin exists in at least two conformations: one being an open conformation, in which the SNARE motif is exposed and thus available for core complex formation, and another being a closed conformation, where the H_{abc} domain folds back onto the SNARE motif, preventing syntaxin assembly into the SNARE complex (Dulubova *et al.*, 1999). As these conformational states of syntaxin differ in their ability to promote core complex formation, it appears likely that circumstances controlling membrane fusion will regulate transformations between these two conformations.

1.8.3 SNAP25

SNAP25 is a plasma membrane-attached SNARE that binds to synaptobrevin/VAMP and syntaxin. SNAP25 was first isolated as a 25 kDa neuronal protein localised exclusively to presynaptic terminals (Oyler *et al.*, 1989). Subsequently, two highly homologous isoforms, SNAP25A and SNAP25B, were isolated and found to differ by only nine amino acids (Bark and Wilson, 1994). The expression of SNAP25A/B exclusively in neuronal and neuroendocrine cells relates to their requirement for fast regulated exocytosis pathways, for example, in synaptic vesicle exocytosis. SNAP23 is another member of the SNAP25 protein family, sharing ~60% amino acid identity with SNAP25 (Ravichandran *et al.*, 1996; Wang *et al.*, 1997c). SNAP23 is ubiquitously expressed and functions in both constitutive and regulated exocytosis in non-neuronal cells (Leung *et al.*, 1998; Rea *et al.*, 1998).

In the core complex, syntaxin binds to SNAP25, inducing a conformational change in SNAP25 necessary for the formation of the core SNARE complex (Fasshauer *et al.*, 1997). SNAP25 contributes two of its α-helices to the core SNARE complex, one SNARE motif from its N-terminal domain and the other from its C-terminal domain (Sutton *et al.*, 1998). The essential role of SNAP25 in exocytosis is demonstrated by the action of botulinum neurotoxins (BoNTs) of serotypes 'A' and 'E', which selectively cleave SNAP25 near the C terminus resulting in the inhibition of exocytosis (Blasi *et al.*, 1993; Schiavo *et al.*, 1993a; Schiavo *et al.*, 1993b).

1.8.3.1 SNAP25 AND MEMBRANE BINDING

SNAP25 is synthesised as a soluble protein, yet it is bound to the cytoplasmic face of the plasma membrane. Membrane association of SNAP25 is dependent on palmitoylation of up to four cysteine residues present within a cysteine-rich linker domain located between the two SNARE motifs: deletion of a twelve amino acid region containing the four cysteines, or mutation of the cysteines within the cysteine-rich domain of SNAP25, both render the protein cytosolic (Gonelle-Gispert *et al.*, 2000; Lane and Liu, 1997; Veit *et al.*, 1996). Since palmitoylation of proteins occurs on membranes, mechanisms that target SNAP25 to its site of palmitoylation must exist. The minimum membrane-binding domain of SNAP25 has been mapped to amino acids 85-120: this domain includes the palmitoylated cysteine-rich domain plus the twenty-eight amino acids immediately downstream of this region (Gonzalo *et al.*, 1999). Interestingly, SNAP25 remains membrane-bound even after chemical depalmitoylation, suggesting that in the absence of palmitoylation, other factors exist to allow continued association of SNAP25 with the plasma membrane (Gonzalo *et al.*, 1999). The SNARE protein syntaxin 1 has been implicated in the trafficking of SNAP25 to the plasma membrane, by acting as a chaperone protein for SNAP25 (Vogel *et al.*, 2000; Washbourne *et al.*, 2001); by analogy, the interaction of syntaxin with SNAP25 at the plasma membrane may persist in the absence of SNAP25 palmitoylation, thus allowing SNAP25 to remain membrane-bound following de-palmitoylation. Several data have supported these hypotheses in both neuronal and non-neuronal cells. Removal of the C-terminus of SNAP25 by BoNT/E in chromaffin cells disrupts the interaction of SNAP25 with syntaxin, leading to the partial redistribution of SNAP25 into the cytosol (Rickman *et al.*, 2004). In non-neuronal cells, newly synthesised exogenously expressed SNAP25 is effectively localised to the cytosolic fraction: on co-expression of syntaxin, there was a dramatic increase in the proportion of SNAP25 localised to the membrane fraction (Vogel *et al.*, 2000). Furthermore, co-expression of a mutant syntaxin that is lacking its transmembrane domain resulted in both syntaxin and SNAP25 remaining in the cytosolic fraction (Vogel *et al.*, 2000). Finally, a mutant SNAP25 that is missing its cysteine-rich domain was efficiently targeted to membranes when co-expressed with syntaxin (Gonelle-Gispert *et al.*, 2000; Vogel *et al.*, 2000).

Despite these findings, several lines of evidence have argued against a role for syntaxin in the trafficking and stable membrane binding of SNAP25, at least in neuroendocrine cells. In PC12 cells, the majority of SNAP25 is not found in a complex with syntaxin (Xiao *et al.*, 2004). Additionally, the minimum membrane binding domain of SNAP25, amino acids 85-120, traffics to the plasma membrane in PC12 cells, despite lacking the binding site for syntaxin (Gonzalo *et al.*, 1999). Similarly, a mutation generated within the N-terminal domain of SNAP25 (glycine

43 to aspartate) that abolishes its interactions with syntaxin does not perturb the correct plasma membrane targeting and palmitoylation of SNAP25 in PC12 cells (Loranger and Linder, 2002). Finally, in neuroendocrine cells, downregulation of the SM protein Munc18 prevents plasma membrane delivery of syntaxin, however the trafficking of SNAP25 is unaffected (Arunachalam et al., 2007). Thus, it appears that initial membrane targeting and palmitoylation of SNAP25 may occur independently of syntaxin in neuronal/neuroendocrine cells. The inefficient membrane binding of SNAP25 in non-neuronal cells, however, suggests that these cell types may lack a specific factor required for SNAP25 membrane targeting and palmitoylation.

Recently three DHHC proteins, DHHC-3, -7 and -17 were shown to increase incorporation of radiolabelled palmitate into SNAP25 (Fukata et al., 2004).

1.8.4 VAMP

The final member of the neuronal ternary SNARE complex is the vesicle-associated membrane protein (VAMP; also called synaptobrevin) family of small conserved C-tail anchored proteins, first identified as a neuronal specific protein isolated from a cDNA expression library of *Torpedo californica* electromotor nucleus mRNA (Sudhof et al., 1989; Trimble et al., 1988). Sequence homology has identified several different VAMP isoforms, each localised to distinct subcellular compartments where they function as R-SNAREs in membrane fusion events (Advani et al., 1998; Galli et al., 1998; Wong et al., 1998; Zeng et al., 1998). VAMP1 and VAMP2 are the two isoforms involved in Ca^{2+}-dependent regulated exocytosis in neuronal and neuroendocrine cells (Baumert et al., 1989; Trimble et al., 1988), whereas cellubrevin is a ubiquitously expressed VAMP isoform involved in constitutive exocytosis pathways in non-neuronal cells (McMahon et al., 1993). VAMPs contain four functional domains: a transmembrane domain flanked by a variable C-terminal intravesicular tail and a conserved coil-coil region containing a SNARE motif, and an N-terminal proline-rich region (Elferink et al., 1989; Sudhof et al., 1989; Trimble et al., 1988). The VAMPs contribute directly to membrane fusion by providing one helix to the core complex (Sutton et al., 1998), and mice lacking the gene for VAMP2 have dramatically reduced Ca^{2+}-dependent exocytosis (Schoch et al., 2001). VAMPs are essential for membrane fusion events and are susceptible to cleavage by TeNT and BoNT serotypes 'B', 'D', 'F' and 'G' (Schiavo et al., 1992a; Schiavo et al., 1992b; Schiavo et al., 1993a; Schiavo et al., 1993c; Schiavo et al., 1994; Yamasaki et al., 1994a; Yamasaki et al., 1994b). VAMP2 has also been shown to be required for synaptic vesicle endocytosis (Deak et al., 2004).

1.9 SNARE REGULATORS

The finding that membrane fusion can be recreated *in vitro* by reconstituting SNARE proteins into lipid bilayer vesicles suggests that the SNARE proteins comprise the minimal machinery required for membrane fusion reactions (Weber *et al.*, 1998). However, this *in vitro* fusion process is very slow compared to the extremely rapid membrane fusion reactions that can take place *in vivo* (for example, synaptic vesicle fusion can occur in less than one millisecond following a rise in intracellular Ca^{2+} concentration (Sabatini and Regehr, 1996)). This discrepancy may reflect suboptimal conditions used in the *in vitro* fusion reactions, for example, aggregation of SNARE proteins (Liu *et al.*, 2005); alternatively, it is possible that other factors may assist in the membrane fusion reaction *in vivo*. Indeed, membrane fusion must be tightly regulated, both temporally and spatially, ensuring that non-specific and inappropriate fusion reactions are prevented, and that (in the case of regulated exocytosis) membrane fusion is closely coupled to the stimulus. Such regulation is carried out by SNARE regulators, which include (but are not limited to) the SM proteins, the Rab proteins, members of the synaptotagmin family and many other membrane-associated proteins, such as cysteine string protein.

1.9.1 THE MAMMALIAN *UNC* HOMOLOGUES

A group of *Caenorhabditis elegans* mutants that exhibit an uncoordinated (*unc*) phenotype, and which are wholly or partially paralysed were identified (Brenner, 1974). A subset of these *unc* mutants exhibited characteristics suggestive of defects in presynaptic neurotransmitter release (Hosono *et al.*, 1987), and several genes in this *unc* subgroup were identified. Mammalian homologues of two of these *C. elegans unc* genes include *Munc-13* (Brose *et al.*, 1995; Varoqueaux *et al.*, 2002) and *Munc-18* (Hata *et al.*, 1993; Pevsner *et al.*, 1994b).

1.9.1.1 MUNC13

The mammalian homologues of the *C. elegans unc-13* were cloned and named Munc13-1, 13-2, and 13-3 (Brose *et al.*, 1995). Munc 13-1 and 13-3 are specific to neurons and neuroendocrine cells, while Munc13-2 is expressed only in brain. These proteins have a molecular weight of ~200 kDa and contain a C-terminal C1 domain that binds diacylglycerol and phorbol ester, and two or three C2 domains that serve as Ca^{2+}/phospholipid-binding or protein interaction domains. Munc-13 is known to interact with at least 7 exocytotic proteins; RIM1, syntaxin, calmodulin, DOC2α (double C2 protein, α isoform), msec7-1, a brain-specific spectrin, and Munc-18 (Brose *et al.*, 2000). Munc13 is essential for regulated exocytosis, since evoked

neurotransmitter release is blocked in neurons lacking Munc13, the consequence of a dramatic decrease in the number of mature (fusion competent) vesicles (Augustin *et al.*, 1999; Varoqueaux *et al.*, 2002). Furthermore, overexpression of Munc13 in neuroendocrine cells has no apparent effect on the number of vesicles docked at the plasma membrane yet still leads to a threefold increase in Ca^{2+}-dependent exocytosis (Ashery *et al.*, 2000). Both of these findings point to a role for Munc13 in promoting the priming step of vesicle maturation in regulated exocytosis, which is likely to involve SNARE complex formation. The C-terminal domain of Munc13 binds directly to the autoinhibitory N-terminal domain of syntaxin, and Munc13 mutants that are unable to bind syntaxin are unable to promote vesicle priming in neuroendocrine cells, as assessed by rescue experiments in a null background (Stevens *et al.*, 2005). Furthermore, loss of secretion in *C. elegans unc13* mutants was partially restored on overexpression of a constitutively "open" form of syntaxin (Richmond *et al.*, 2001). Thus, a current model for the function of Munc13 in regulated exocytosis is based on the hypothesis that Munc13 promotes vesicle priming by regulating the conformational state of syntaxin, through stabilising or promoting its open conformation thus making it available for SNARE complex formation (Richmond *et al.*, 2001).

1.9.1.2 MUNC18

Munc18-1 was first characterised in brain as a protein that binds to syntaxin with high affinity (Hata and Sudhof, 1995), and was later cloned by homology screening based on its similarity to *Drosophila* Rop (Ras opposite) and *C. elegans* Unc18 (Halachmi and Lev, 1996). Three isoforms of Munc18 have been described (Munc18-1, Munc18-2 and Munc18-3) all of which are involved in exocytosis at the plasma membrane. Munc18-1 is the predominantly expressed isoform in neuronal and neuroendocrine cells, whereas Munc18-2 and −3 are ubiquitously expressed (Hata *et al.*, 1993; Hata and Sudhof, 1995; Katagiri *et al.*, 1995; Pevsner *et al.*, 1994b; Tellam *et al.*, 1995). All SNARE-mediated intracellular membrane fusion processes studied to date involve a Munc18 homologue (Dulubova *et al.*, 1999), highlighting its central role in these fusion pathways. Munc18 is a soluble hydrophilic protein and its membrane localisation is largely dependent on its interaction with the SNARE syntaxin (Rickman *et al.*, 2007).

Munc18 proteins are required for exocytosis: secretion is blocked in *S. cerevisae* Sec1p mutants and in *Drosophila* Rop null mutants, and synaptic transmission is inhibited in murine Munc18-1 null mutants (Harrison *et al.*, 1994; Novick *et al.*, 1980; Verhage *et al.*, 2000). The finding that overexpression of *Drosophila* Rop led to a decrease in neurotransmitter release (Schulze *et al.*,

1994), suggested a negative role for Munc18 in secretion; however, no inhibitory role was observed on overexpression of Munc18-1 in neuroendocrine cells (Graham *et al.*, 1997). The inhibitory effect caused by Rop overexpression most likely reflects a perturbation in the balance of exocytotic protein expression, rather than highlighting an inhibitory role of Munc18 in membrane fusion. The roles Munc18 has in secretion are likely exerted through its interaction with syntaxin, and indeed syntaxin 1A becomes unstable in the absence of Munc18-1 expression (Voets *et al.*, 2001). Furthermore, there is evidence that plasma membrane delivery of syntaxin requires Munc18, as syntaxin is unable to exit from the ER/Golgi in the absence of Munc18 in non-neuronal cells (Medine *et al.*, 2007; Rowe *et al.*, 2001) and after downregulation of Munc18 in PC12 cells (Arunachalam *et al.*, 2007). These findings suggest that Munc18 chaperones newly synthesised syntaxin to the plasma membrane.

1.9.1.3 MUNC18 AND SYNTAXIN 1A BINDING

SNARE complex formation is regulated in part by the conformational status of syntaxin. In the open conformation, the SNARE motif is exposed and thus available for core complex formation, whereas in the closed conformation, the H_{abc} domain folds back onto the SNARE motif, preventing SNARE complex assembly (Dulubova *et al.*, 1999). Interestingly, Munc18 has recently been shown to bind the N-terminus of syntaxin in both the open and closed conformations (Khvotchev *et al.*, 2007; Rickman *et al.*, 2007). In the early secretory pathway, Munc18 is exclusively bound to the closed conformation of syntaxin, thus preventing SNARE complex formation prior to plasma membrane delivery (Medine *et al.*, 2007; Rickman *et al.*, 2007). At the plasma membrane, a conformational change allows syntaxin to adopt the open conformation, and participates in SNARE complex assembly (Medine *et al.*, 2007; Rickman *et al.*, 2007). It will be interesting to identify factors that regulate the conversion of syntaxin from a closed to an open form; one interesting candidate in this regard is Munc13, however membrane lipid composition may also have a role (Darios and Davletov, 2006).

1.9.2 THE RAB GTPASES

The Rab proteins are members of the Ras superfamily of small, monomeric GTPases, whose primary function is in marking the site of attachment between donor and acceptor membranes, thereby providing spatial specificity to fusion reactions (Grosshans *et al.*, 2006). Rab proteins function in vesicular trafficking throughout the secretory and endocytic pathways, with each Rab protein regulating a distinct transport step (Collins, 2003).

The Rabs were first identified in genetic screens in yeast as proteins essential for vesicular trafficking (Salminen and Novick, 1987; Segev *et al.*, 1988). Subsequently, eleven yeast Rab proteins have since been identified, and more than sixty have been discovered in mammals, each localised to specific membrane compartments where they regulate multiple and discrete intracellular trafficking events, including vesicle budding, motility, docking and fusion (Novick and Zerial, 1997; Pereira-Leal and Seabra, 2000; Pereira-Leal and Seabra, 2001; Pfeffer, 2001). Rab proteins do not contain a transmembrane domain, but are instead tethered to membranes via a dual C-terminal geranylgeranyl anchor, which contributes to the reversible membrane binding of Rab that is fundamental to its function.

The function of the Rab proteins lies in their ability to act as molecular switches, cycling between an inactive GDP-bound form in the cytosol, and an active GTP-bound form that is membrane-bound (Grosshans *et al.*, 2006). At steady-state, most Rab proteins are in their active GTP-bound form, in which they are thought to initiate membrane attachment by interacting with specific effector proteins on the target membrane, thus tethering the two membranes together (Pfeffer, 2001). Following membrane fusion, a GTPase activating protein (GAP) inactivates Rab by triggering the hydrolysis of Rab-GTP to Rab-GDP (Grosshans *et al.*, 2006). GDI (GDP dissociation inhibitor) recognises GDP-bound Rab, binding it tightly and removing it from the membrane by enveloping the hydrophobic geranylgeranyl anchors (Araki *et al.*, 1990; Wu *et al.*, 1996). Specific membrane-bound GEFs (guanine nucleotide exchange factors) recognise GDP-Rab and catalyze the exchange of GDP and GDI for GTP, thereby allowing Rab to rebind to its specific intracellular membrane in order to participate in another round of fusion (Grosshans *et al.*, 2006).

Rab3 is the most highly expressed member of the Rab family in brain and endocrine tissues (Fischer von Mollard *et al.*, 1991). Rab3 has four isoforms, Rab3A, Rab3B, Rab3C and Rab3D, which are all functionally redundant (Schluter *et al.*, 2004; Touchot *et al.*, 1987). Although the Rab3 proteins are expressed at highest levels in neuronal and neuroendocrine cells, they have also been found in exocrine glands and adipocytes (Baldini *et al.*, 1995; Schluter *et al.*, 2002). All isoforms of Rab3 appear to be localised to exocytotic vesicles, from which they dissociate following exocytosis (Fischer von Mollard *et al.*, 1991; Fischer von Mollard *et al.*, 1994). Rab3 has been implicated in various steps of the exocytotic pathway, including vesicle docking, fusion and biogenesis (Darchen and Goud, 2000), however the precise function remains unclear.

1.9.3 THE SYNAPTOTAGMINS

The final stages of neurotransmitter release depend upon a rise in intracellular free Ca^{2+} concentration, triggering the opening of a 'fusion pore', with the subsequent release of vesicular contents. Much work has therefore focussed on the idea of a Ca^{2+} 'sensor', which functions to detect and respond to this localised rise in intracellular Ca^{2+}, resulting in neurotransmitter release. In 1981, a 65-kDa antigen (then called p65) was found to be present on the surface of synaptic vesicles and large dense-core vesicles (LDCVs) (Matthew *et al.*, 1981). The cDNA encoding this protein was cloned and its sequence determined and subsequently renamed synaptotagmin 1 (Perin *et al.*, 1990). The synaptotagmins are type I transmembrane proteins with a single membrane-spanning domain. The intra-luminal N-terminal domain is glycosylated, and the C-terminal domain is composed of tandem Ca^{2+}-binding motifs called C2 domains, which are homologous to the Ca^{2+}-binding domain of protein kinase C (PKC) (Perin *et al.*, 1990; Perin *et al.*, 1991). In addition to being glycosylated, synaptotagmin is palmitoylated on cysteines adjacent to its transmembrane domain; both these modifications are required for the correct vesicle targeting of synaptotagmin (Chapman *et al.*, 1996; Haigh *et al.*, 1989; Kang *et al.*, 2004; Kanno and Fukuda, 2007). Since synaptotagmin was originally cloned, twelve additional isoforms have been discovered (Craxton, 2001), each characterised by an N-terminal transmembrane domain, a variable linker, and two tandem C-terminal C2-domains (C2A- and C2B-domains) (Perin *et al.*, 1991).

The balance of evidence suggests that the synaptotagmins function as key Ca^{2+} sensors for exocytotic vesicle fusion (Chapman, 2002; Fernandez-Chacon *et al.*, 2001; Geppert *et al.*, 1994; Rhee *et al.*, 2005; Sudhof, 2004). As would be expected for a putative Ca^{2+} sensor, synaptotagmin binds three and two calcium ions via its C2A- and C2B-domains, respectively (Fernandez *et al.*, 2001; Ubach *et al.*, 1998), which facilitates the interaction of these domains with membranes (Davletov and Sudhof, 1993). In addition to calcium binding, synaptotagmin has been shown to interact with several neuronal proteins, including the SNAREs syntaxin and SNAP25, and the exocytotic chaperone protein cysteine string protein (CSP) (Bennett *et al.*, 1992; Evans and Morgan, 2002; Schiavo *et al.*, 1997; Shao *et al.*, 1997). Through the C2A-domain, synaptotagmin binds to syntaxin and phospholipids in a calcium-dependent manner (Bennett *et al.*, 1992; Davletov and Sudhof, 1993; Shao *et al.*, 1997), and through the C2B-domain it interacts with SNAP25 (Schiavo *et al.*, 1997). Evidence that synaptotagmin functions as a Ca^{2+}-sensor for neurotransmitter release was obtained when expression of a synaptotagmin mutant, with reduced affinity for Ca^{2+}, in a null background, led to a decrease in the Ca^{2+}-sensitivity of neurotransmitter release (Fernandez-Chacon *et al.*, 2001). Mutations created in SNAP25 that reduced its affinity for synaptotagmin diminished exocytosis in PC12 cells (Zhang

et al., 2002b), and inhibitors preventing synaptotagmin from binding to syntaxin or SNAP25 abruptly blocked release from cracked PC12 cells (Earles *et al.*, 2001), suggesting that synaptotagmin binding to SNAREs is necessary for fusion to proceed. It has been proposed that synaptotagmin simultaneously binds both the SNARE complex and membranes (Davis *et al.*, 1999); this would place it in an ideal position to regulate SNARE function. Recently, it has been demonstrated that following calcium binding, synaptotagmin induces membrane curvature through insertion of its C2A- and C2B-domains into the phospholipid bilayer of the plasma membrane, which effectively "pulls" the plasma membrane towards the vesicle membrane and reduces the energy barrier between the opposing membranes, thus promoting vesicle fusion (Martens *et al.*, 2007; Shahin *et al.*, 2008).

1.10 CYSTEINE STRING PROTEIN

Cysteine string proteins (CSPs) are predominantly vesicle-associated proteins that are essential for regulated exocytosis in neuronal and neuroendocrine cells (Chamberlain and Burgoyne, 1998a; Chamberlain and Burgoyne, 1998b; Graham and Burgoyne, 2000; Umbach *et al.*, 1994). The importance of CSP for viability is demonstrated in *Drosophila csp* null mutants and CSP knockout mice, with both exhibiting progressive uncoordinated motor behaviour prior to premature death (Fernandez-Chacon *et al.*, 2004; Zinsmaier *et al.*, 1994). *Drosophila csp* null mutant larvae have a decreased number of nerve terminals (Bronk *et al.*, 2005; Dawson-Scully *et al.*, 2007). Furthermore, these mutant larvae show a decrease in synchronous transmitter release and an increase in both asynchronous release and paired-pulse facilitation, suggesting that CSP helps to couple Ca^{2+}-influx to exocytosis (Heckmann *et al.*, 1997). Finally, CSP knockout mice have a decrease in synaptic transmission and enhanced synaptic depression, suggesting that CSP has a neuroprotective function (Fernandez-Chacon *et al.*, 2004).

1.10.1 DISCOVERY OF CSP

In 1990, a hybridoma library screening of antigens against the *Drosophila* nervous system was used to identify novel synaptic proteins. Immunohistochemical staining of *Drosophila* heads by one of the monoclonal antibodies was localised exclusively to synaptic nerve terminals, and the resultant cDNAs were recovered and sequenced. Two novel proteins, generated by alternative splicing, were found to contain a continuous string of eleven cysteine residues, and as a result, were named the cysteine string proteins (Zinsmaier *et al.*, 1990). The localisation of CSP to synaptic nerve terminals suggested an involvement for CSP in synaptic transmission, however its role was yet to be determined.

1.10.2 CSP ISOFORMS

Since the discovery of CSP in *Drosophila* (Gundersen and Umbach, 1992; Zinsmaier *et al.*, 1990; Zinsmaier *et al.*, 1994), CSP has been identified in *Torpedo* (Gundersen and Umbach, 1992), *Xenopus laevis* (Mastrogiacomo *et al.*, 1998b), *C. elegans* (GenBank Accession Number AAK39254) and several mammalian species, including rat (Mastrogiacomo and Gundersen, 1995), mouse (GenBank Accession Number AF032115), bovine (Chamberlain and Burgoyne, 1996) and human (Coppola and Gundersen, 1996). There is no CSP homologue in yeast. Sequence analysis of the mammalian CSPs reveals high homology, with 98-100% identity at the amino acid level. Homology between mammalian CSPs and CSPs from other classes vary: *Torpedo* and *Xenopus* CSP share 85-86% homology to mammalian CSPs, *Drosophila* is 50-60% identical, while the *C. elegans* CSP is the most divergent, with only 37-38% sequence similarity.

In addition to the two isoforms of CSP originally identified in *Drosophila* (CSP1 and 3) (Zinsmaier *et al.*, 1990), a third isoform (CSP2) has been identified (Zinsmaier *et al.*, 1994). The three *Drosophila* isoforms are encoded by the same gene localised on chromosome 3 at position 79E1-2 and are generated by alternative splicing (Zinsmaier *et al.*, 1994). A fourth *Drosophila* splice variant has been postulated (Arnold *et al.*, 2004). Two mammalian isoforms, CSP1 and CSP2, have since been identified in rat (Mastrogiacomo and Gundersen, 1995), bovine (Chamberlain and Burgoyne, 1996) and human (Coppola and Gundersen, 1996) tissue. CSP1 is the mammalian homologue to *Torpedo* CSP (Gundersen and Umbach, 1992), while CSP2 is identical to CSP1 with the exception of the C-terminus. CSP2 is generated by the retention of a seventy-two nucleotide exon insert which introduces premature stop codons, resulting in a C-terminally truncated CSP isoform (Chamberlain and Burgoyne, 1996; Coppola and Gundersen, 1996). Finally, the mRNA sequences of two further mammalian isoforms, CSPβ and γ, have been described: the full mRNA sequence of the CSPβ isoform has been isolated from human testis and a mouse testis cDNA library, while only a partial mRNA sequence of the human CSPγ, and predicted coding sequences of the human CSPγ and mouse CSPγ isoforms, have been obtained (Evans *et al.*, 2003). A summary of the various mammalian CSP isoforms can be found in Table 2.

1.10.3 TISSUE DISTRIBUTION AND SUBCELLULAR LOCALISATION OF CSP

Despite having been first identified in brain, CSP is expressed in a wide range of non-neuronal tissues, including the adrenal medulla of the adrenal gland (Chamberlain and Burgoyne, 1996; Kohan *et al.*, 1995), pancreas (Braun and Scheller, 1995; Chamberlain and Burgoyne, 1996),

TABLE 2: THE MAMMALIAN CSP ISOFORMS

Isoform	Tissue Distribution	Subcellular localisation	Comments
CSP1/α	Adrenal gland; Brain; Kidney; Lung; Liver; Muscle; Pancreas; Retina; Spleen; Testis.	Secretory vesicles; Secretory granules; Plasma membrane.	198 amino acids; Highly enriched in brain; multiply palmitoylated.
CSP2	Kidney, Spleen.	Unknown.	A C-terminally truncated isoform encoding amino acids 1-167 of CSP1
CSPβ	Testis.	*Trans*-Golgi Network.	199 amino acids; Non-palmitoylated
CSPγ	Testis.	Unknown.	189 amino acids.

References: Boal *et al.*, 2007; Braun and Scheller, 1995; Brown *et al.*, 1998; Chamberlain and Burgoyne, 1996; Chamberlain *et al.*, 2001; Fernandez-Chacon *et al.*, 2004; Pupier *et al.*, 1997; Redecker *et al.*, 1998; Schmitz *et al.*, 2006; Zhang *et al.*, 1998.

kidney, liver, spleen, lung and testis (Chamberlain and Burgoyne, 1996). CSP mRNA was detected in all human tissues examined (Coppola and Gundersen, 1996).

Consistent with its widespread expression, CSP is not restricted to synaptic vesicles, but has been found associated with secretory vesicles in several non-neuronal cells, including chromaffin granules of the adrenal medulla (Chamberlain *et al.*, 1996), pancreatic zymogen granules (Braun and Scheller, 1995), insulin-containing granules (Brown *et al.*, 1998; Zhang *et al.*, 1998), secretory granules of neurosecretory neurons in the neurohypophysis (Pupier *et al.*, 1997), cortical granules of *Xenopus* oocytes (Gundersen *et al.*, 2001), and synaptic-like microvesicles of pinealocytes (Redecker *et al.*, 1998). Furthermore, CSP has been shown to be localised to the plasma membrane in adipocytes (Chamberlain *et al.*, 2001) and in Calu-3 lung epithelial cells (Zhang *et al.*, 2002a). Finally, CSP has also been localised at the ER in Calu-3 cells (Zhang *et al.*, 2002a).

1.10.4 CSP DOMAINS

Analysis of the amino acid sequence reveals that CSP has five domains; an N-terminal domain, a J-domain, a linker domain, a hydrophobic cysteine string domain and a C-terminal domain: the relative location of these domains is outlined in Figure 1.5.
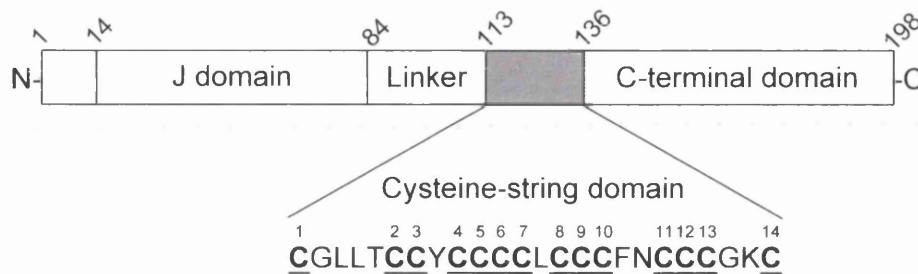
Figure 1.5 Domain structure of Cysteine String Protein. CSP has five domains: an N-terminal domain, a J domain, a linker domain, the signature cysteine string domain (shaded), and a variable C-terminal domain. The relative positioning of these domains are illustrated, and residues lying at the boundaries of the domains in bovine CSP are numbered above. The cysteine string domain contains fourteen cysteine residues (numbered 1-14), and the majority of these cysteines are believed to palmitoylated *in vivo*.

Between all species, the J-domain, the linker domain and the cysteine string domain are all highly conserved, whereas the extreme N-terminal and the C-terminal domains are variable. The N-terminal domain of CSP is phosphorylated by protein kinase A on a serine at position 10 (Evans *et al.*, 2001; Evans and Morgan, 2005), and this phosphorylation reduces the affinity of CSP for syntaxin 1A (Evans *et al.*, 2001) and synaptotagmin 1 (Evans and Morgan, 2002). The J-domain is a conserved region of approximately seventy amino acids that is homologous to the bacterial DnaJ proteins, and is the defining domain of the DnaJ/Hsp40 (Heat shock protein of 40 kDa) family of molecular chaperones. Through its J domain, CSP functions as a molecular chaperone by binding to and activating the ATPase activity of the ubiquitous chaperone Hsc70 (Braun *et al.*, 1996; Chamberlain and Burgoyne, 1997a; Chamberlain and Burgoyne, 1997b). The conserved linker domain, flanked by the J domain and the cysteine string domain, has been proposed to have a functional role in regulated exocytosis (Zhang *et al.*, 1999). However, the putative functional role of the linker domain of CSP is based upon a single mutation (E93V) within the linker region, which reversed the inhibitory effects of CSP2 (but not CSP) overexpression on exocytosis (Zhang *et al.*, 1999). Thus, it is not easy to assess exactly what role the linker domain plays in exocytosis. In addition, both the J domain and (to a lesser extent) the linker domain have been shown to be involved in maintaining normal intracellular Ca^{2+} levels prior to neurotransmitter release (Bronk *et al.*, 2005). Furthermore, the linker domain, together with the cysteine string domain, has been shown to be important for CSP self-association (Boal *et al.*, 2004; Swayne *et al.*, 2003). The cysteine string domain is the defining domain of CSP and contains fourteen cysteines within twenty-four amino acids (in vertebrates), the majority of which are palmitoylated (Gundersen *et al.*, 1994). The intrinsic hydrophobicity

of the cysteine string domain, and the ability of its many cysteines to become palmitoylated, suggests that this domain is fundamentally important for CSP membrane binding.

1.10.5 MEMBRANE ASSOCIATION AND PALMITOYLATION OF CSP

In 1994, an antiserum was raised against CSP from the marine ray *Torpedo*. This CSP antiserum labelled *Torpedo* cholinergic synaptic vesicles and revealed that endogenous *Torpedo* CSP is a predominantly membrane-associated protein of approximately 34 kDa (Mastrogiacomo *et al.*, 1994a). Unexpectedly, immunoblot analysis using the CSP antiserum revealed that the molecular weight of CSP in *Torpedo* was 6-7 kDa greater than the product of *in vitro* translated CSP, leading to the proposal that CSP is post-translationally modified *in vivo* (Mastrogiacomo *et al.*, 1994a). Furthermore, the differential solubility of *in vitro* translated CSP and endogenous CSP in detergents demonstrated that the increase in molecular mass of native CSP correlated to an increase in its hydrophobicity (Mastrogiacomo *et al.*, 1994a).

Several complementary approaches were used to demonstrate for the first time that CSP is palmitoylated (Gundersen *et al.*, 1994). First, following microinjection into *Xenopus* oocytes, the molecular mass of a pool of *in-vitro* translated CSP is increased by 7 kDa, and this higher molecular weight form was labelled with ^{3}H palmitic acid. Second, both endogenous CSP and the higher molecular mass variant of exogenously expressed CSP recovered from *Torpedo* electric organ were sensitive to treatment with methanolic potassium hydroxide and hydroxylamine, reagents that selectively cleave the fatty acyl thioesters of proteins. Interestingly, while the 34 kDa form of CSP recovered from the micro-injected oocytes was membrane-associated, the 27 kDa fraction of CSP was only recovered in the cytosolic pool. Finally, gas chromatography-mass spectrometry was used to determine that the predominant fatty acid attached to CSP is palmitic acid, though a small amount of stearic acid was also detected. In *Torpedo* CSP, as many as eleven of the thirteen cysteine residues were found to be fatty acylated, though the number of cysteines palmitoylated in CSPs from other species has yet to be determined (Gundersen *et al.*, 1994). CSP is stably palmitoylated, and palmitoylation of CSP is thought to take place fairly quickly following its synthesis, since very little of the lower molecular weight (hence unpalmitoylated) form of CSP is detected in tissues (Gundersen *et al.*, 1996). Antibodies specific for the N- and C-terminal domains of CSP were both able to precipitate CSP from intact synaptic vesicles in *Torpedo* (Mastrogiacomo *et al.*, 1994b). Since CSP is fatty acylated, it was suggested that CSP is tethered to the cytoplasmic surface of vesicles by a palmitoylated cysteine string domain, with both the N-and C-termini located cytoplasmically (Mastrogiacomo *et al.*, 1994b).

Several studies have demonstrated that chemical depalmitoylation of CSP does not disrupt CSP membrane association (Chamberlain and Burgoyne, 1998a; Mastrogiacomo *et al.*, 1998a; van de Goor and Kelly, 1996); furthermore, chemically-depalmitoylated CSP can only be released from membranes by treating with detergent (Mastrogiacomo *et al.*, 1998a). These results indicate that the membrane association of depalmitoylated CSP is mediated by the ability of hydrophobic amino acids within the cysteine string domain to interact with the lipid bilayer: following deacylation, the cysteines within the cysteine string domain remain in a hydrophobic environment (Mastrogiacomo *et al.*, 1998a). Interestingly, when a CSP mutant in which the 7 central cysteine amino acids were mutated to the less hydrophobic amino acid serine (7CS) and was expressed in PC12 and HeLa cells, it was found to be cytosolic and unpalmitoylated (Chamberlain and Burgoyne, 1998a).

Finally, the importance of an intact palmitoylated cysteine string domain for the function of CSP, in addition to membrane binding, was demonstrated when cysteine deletions were introduced into the cysteine string domain of *Drosophila*. Deletion of some of the cysteine residues in the cysteine string domain resulted in a protein that was correctly targeted to membranes, but was not able to rescue the null mutant phenotype (Arnold *et al.*, 2004).

1.10.6 LETHALITY OF CSP INACTIVATION IN *DROSOPHILA*

The functional importance of CSP for *Drosophila* viability was determined soon after its discovery, through analysis of the phenotype of null (csp^{R1}) and partial (csp^{X1}) csp gene deletions (Zinsmaier *et al.*, 1994). Ninety-six percent of flies that lacked the entire *csp* gene died embryonically, and those that hatched died prematurely in a temperature-sensitive manner: flies lived for only 4-5 days at 22 °C, while at 25 °C death occurred rapidly (hours). Preceding death, the flies displayed progressively uncoordinated motor behaviour finally leading to paralysis. These temperature-sensitive phenotypes prompted investigations into the physiological defects resulting from *csp* deletions. Electroretinography performed on adult survivors suffering from a partial loss of the *csp* gene (csp^{X1}) identified a loss of "on" and "off" transients at higher temperatures, correlating to a temperature-sensitive loss of neurotransmission (Zinsmaier *et al.*, 1994).

To determine the cellular basis for the temperature-sensitive loss of neurotransmission in *Drosophila* csp^{R1} and csp^{X1} gene deletions, electrophysiological recordings at the neuromuscular junction of *Drosophila* csp^{X1} mutant larvae were measured. The recordings revealed that a partial loss of the *csp* gene results in nerve impulses that are unable to trigger neurotransmitter

release at non-permissive temperatures: there was a reduction by 50% of depolarization-secretion coupling at 22 °C, and a complete loss at 30 °C, which was overcome by restoring the temperature back to 22 °C (Umbach *et al.*, 1994). These were the first results to implicate CSP in regulated exocytosis; no temperature-sensitive effect on spontaneous release was observed (Umbach *et al.*, 1994). The effects of loss of the *csp* gene in *Drosophila* were strongly reminiscent of *dnaJ* deletion mutants observed in *Escherichia coli*: growth of *E. coli* was blocked at high temperatures, but permitted at lower temperatures (Ohki *et al.*, 1992), suggesting that CSP may have a chaperone-like activity. These early observations provided the foundation of a working hypothesis for CSP function: that CSP may act as an exocytotic chaperone, by helping to stabilise components of the neurotransmitter release machinery.

1.10.7 CSP AND REGULATED EXOCYTOSIS

Following the observed effects in transmitter release in *Drosophila csp* null mutants, much work has focussed on identifying the role of CSP in regulated exocytosis, and in particular, the precise steps during vesicle fusion at which CSP functions. Shortly after the cloning of *Drosophila* CSP, a putative functional role for CSP was proposed following attempts to identify potential subunits of presynaptic calcium channels in vertebrates (Gundersen and Umbach, 1992). Injection of *Torpedo* electric lobe mRNAs into *Xenopus* oocytes resulted in the ectopic expression of functional voltage-sensitive N-type calcium channels, and the activity of these calcium channels was abolished by the co-expression of specific antisense RNA transcripts (Gundersen and Umbach, 1992). Consequently, the resultant cDNA isolated from the *Torpedo* inhibitory antisense RNA was found to encode CSP, and thus CSP was proposed to be a potential calcium channel subunit or modulator (Gundersen and Umbach, 1992). The proposal that CSP was an essential component of calcium channels was only briefly held however, since CSP was subsequently shown to be localised not to the plasma membrane (where N-type calcium channels reside), but to synaptic vesicles in *Torpedo* electric organ (Mastrogiacomo *et al.*, 1994b). CSP has since been found localised to many types of secretory vesicles (see Chapter 1.10.3). It was subsequently proposed that CSP, present on docked vesicles, might be able to activate nearby calcium channels, thus forming an important link between synaptic vesicles and calcium channels. This hypothesis was attractive as it implied that calcium entry would be greatest through channels that were physically linked to synaptic vesicles. In support of this model, *in vitro* translated CSP has been shown to specifically bind a recombinant fusion protein containing a domain that encodes a cytoplasmic loop of the $\alpha_1 A$ subunit of P/Q-type calcium channels (Leveque *et al.*, 1998).

Later studies suggested that the temperature-sensitive loss of neurotransmission in *csp* mutants at the *Drosophila* neuromuscular junction involved either a defect in Ca^{2+} entry or in the ability of Ca^{2+} to trigger exocytosis (Umbach and Gundersen, 1997; Umbach *et al.*, 1998). First, the temperature-sensitive loss of neurotransmission could be overcome by stimulating mutant neuromuscular junctions with secretagogues that bypass presynaptic Ca^{2+} channel opening, such as α-latrotoxin and ionomycin, at non-permissive temperatures (32 °C) (Umbach and Gundersen, 1997). Second, Ca^{2+} crimson fluorescence was used to measure cytosolic calcium influx into mutant nerve terminals following stimulation. At 22 °C, there was an increase in the fluorescence intensity after stimulation, indicating normal Ca^{2+} entry. However, when the temperature was raised to 32 °C, no increase in the fluorescent intensity was observed, suggesting that at elevated temperatures Ca^{2+} entry is inhibited in *csp* mutants (Umbach *et al.*, 1998). Collectively, these results implied that CSP acts upstream of, or within, the calcium signalling cascade mediating evoked exocytosis.

Despite the data supporting a role for CSP in Ca^{2+} channel regulation, several studies are inconsistent with this notion. In particular, subsequent studies revealed that calcium entry was not impaired in *Drosophila csp* mutants (Dawson-Scully *et al.*, 2000; Morales *et al.*, 1999). Work utilising the fluorescent calcium indicator fura-2 AM revealed that, despite having a huge reduction in neurotransmitter release, *Drosophila csp* null mutant nerve terminals retain a robust increase in presynaptic Ca^{2+} signals at elevated temperatures, but indeed exhibit an increased rate of Ca^{2+} clearance (Dawson-Scully *et al.*, 2000). Furthermore, it was shown that the reduction in neurotransmitter release in *Drosophila csp* null mutant nerve terminals could be restored at non-permissive temperatures by raising the extracellular Ca^{2+} concentration. These findings suggest that *Drosophila csp* null mutants have a decreased efficiency in the ability of Ca^{2+} to trigger neurotransmitter release, and are indicative of a direct function for CSP in exocytosis, downstream of Ca^{2+} entry. In addition to these analyses of Ca^{2+} channel activity in *csp* null mutants, many studies have failed to demonstrate the binding of CSP to native Ca^{2+} channels (Leveque *et al.*, 1998; Martin-Moutot *et al.*, 1996; Pupier *et al.*, 1997). Furthermore, calcium channel activity is not detectably modified by either overexpression of CSP in PC12 and insulinoma cells or by deletion of *csp* in *Drosophila* (Brown *et al.*, 1998; Chamberlain and Burgoyne, 1998b; Dawson-Scully *et al.*, 2000).

The cloning of the mammalian CSPs enabled further analysis of the effects CSP had on regulated exocytosis. There have been contradictory reports of the effects on regulated exocytosis following the overexpression of CSP in neuroendocrine cells. PC12 cells stably overexpressing CSP showed a ~50% increase in dopamine release, suggesting that CSP exerts a

positive function on exocytosis (Chamberlain and Burgoyne, 1998b). However, in contrast, transient overexpression of CSP in pancreatic β-cell lines or chromaffin cells significantly reduced secretion (Boal *et al.*, 2004; Brown *et al.*, 1998; Graham and Burgoyne, 2000; Zhang *et al.*, 1998). This inhibitory effect of CSP transient overexpression likely reflects perturbation of the exocytotic machinery caused by excess CSP titrating other essential components. Indeed, CSP knockdown in pancreatic β cells reduced insulin secretion (Zhang *et al.*, 1998), supporting the notion that CSP has a positive role in exocytosis. These combined studies highlight an important role for CSP in regulated exocytosis in non-neuronal cells in addition to neurons. Furthermore, the effects of CSP overexpression or knockdown in exocytosis in these cells were preserved in permeabilised cells; exocytosis from permeabilised cells is independent of calcium channel activity, further demonstrating that CSP has calcium channel-independent functions in exocytosis. Interestingly, more thorough investigation of CSP function in exocytosis using carbon fibre amperometry found that the overexpression of CSP in adrenal chromaffin cells resulted in a 82% decrease in the number of fusion events, and the release events that did occur were much slower (Graham and Burgoyne, 2000). This implicated CSP in the control of either fusion pore formation or opening. Other proteins that exhibit effects on fusion kinetics are those that modulate exocytosis through interaction with the SNARE complex or its components, for example the putative calcium sensor synaptotagmin (Wang *et al.*, 2001), complexin (Archer *et al.*, 2002) and Munc18 (Barclay *et al.*, 2003; Fisher *et al.*, 2001). Thus, the functions of CSP in regulated exocytosis may be through the interactions of CSP with members of the SNARE complex or SNARE regulators; interestingly, mice lacking the CSP gene have a decrease in SNARE complex formation (Chandra *et al.*, 2005). Consistent with this theory, CSP and VAMP have been found in a complex following immunoprecipitation of rat brain homogenate (Leveque *et al.*, 1998) and a direct interaction between CSP and VAMP2 has been reported (Boal *et al.*, 2004). The t-SNARE syntaxin has been shown to bind CSP *in vitro* in *Drosophila*, and the defect in neurotransmission caused by overexpression of syntaxin is overcome by overexpressing CSP (Nie *et al.*, 1999). Similarly in neuroendocrine cells, syntaxin forms a complex with CSP *in vitro*, which is dependent on the phosphorylation state of CSP (Evans *et al.*, 2001). Finally, synaptotagmin has been shown to bind CSP both *in vitro* and *in vivo* and, as in the interaction of CSP with syntaxin, has a reduced affinity for CSP when phosphorylated (Evans and Morgan, 2002); this interaction may explain how CSP affects the Ca^{2+}-sensitivity of exocytosis (see previous section). When an unphosphorylatable mutant of CSP was overexpressed in chromaffin cells, the inhibition of exocytosis was still observed (as in the overexpression of wild-type CSP), but the release kinetics and the total vesicle content that was released per fusion event were no different to those in control cells (Evans *et al.*, 2001). Since the only difference in these experiments was the phosphorylation state of CSP, it was suggested

that the phosphorylation of CSP plays a role at a late stage of exocytosis. Finally, it has been hypothesized that phophorylated CSP may act through an unidentified protein to slow the kinetics of release, while unphosphorylated CSP may chaperone the interaction of syntaxin and/or VAMP for faster release (Evans *et al.*, 2003).

1.10.8 PROPOSED FUNCTION OF CSP AS AN EXOCYTOTIC CHAPERONE PROTEIN

The molecular cloning of CSP and the deduced amino acid sequence revealed that CSP contains a J domain, a 70 amino acid domain present within a number of eukaryotic Hsp40 proteins, which is homologous to a region of the bacterial protein DnaJ and other unrelated eukaryotic proteins. DnaJ interacts with the chaperone protein DnaK, and, as part of a complex with the nucleotide exchange factor, GrpE, stimulates the ATPase activity of DnaK, allowing it to function in many cellular processes, such as protein folding and replication of bacteriophage lambda (Liberek *et al.*, 1988; Liberek *et al.*, 1991; Yochem *et al.*, 1978). The eukaryotic homologue of the bacterial DnaK proteins is the Hsp70 (Heat shock protein of 70 kDa) protein family, an abundant and ubiquitous family of chaperone proteins involved in many protein folding reactions, such as the folding of newly-synthesised proteins, the refolding of misfolded and aggregated proteins, and providing protein stability during translation and translocation (Mayer and Bukau, 2005). Hsc70 (Heat shock cognate protein of 70 kDa) is constitutively expressed, whereas Hsp70 expression can be regulated by heat-shock. The functions of Hsp70 depend on its ability to selectively bind short hydrophobic stretches of substrate polypeptides, a process that is regulated by a cycle of ATP binding, hydrolysis and nucleotide exchange (Minami *et al.*, 1996). The ATP-regulated association of Hsp70 with substrate proteins is brought about by a conformational change in the C-terminal peptide binding domain of Hsp70 upon ATP binding, in which the substrate binding pocket is in an open conformation and Hsp70 has a low affinity for substrates and fast association and dissociation rates (Bukau and Horwich, 1998). Following ATP hydrolysis, the substrate binding pocket of Hsp70 adopts a closed conformation, which has a high affinity for substrates and slow exchange rates (Bukau and Horwich, 1998).

The interactions of CSP with Hsp70 proteins are likely central to its function. Recombinant CSP can interact with both recombinant and purified Hsc70, and this interaction is ATP-dependent (Chamberlain and Burgoyne, 1997b). Furthermore, this binding of CSP to Hsp70/Hsc70 increases the ATPase activity of these proteins by as much as 14-fold (Braun *et al.*, 1996; Chamberlain and Burgoyne, 1997b). Importantly, there is also genetic evidence for the interaction of *Csp* and *hsc70-4* in *Drosophila* (Bronk *et al.*, 2001). The J domain of CSP is

necessary and sufficient to stimulate ATPase activity: a truncation mutant containing the J domain alone was able to stimulate the ATPase activity of Hsc70 (Braun *et al.*, 1996); conversely, a truncation mutant lacking the J domain was not (Chamberlain and Burgoyne, 1997b). The functional importance of the ability of CSP to stimulate the ATPase activity of Hsc70 was shown when CSP, in a complex with Hsc70, prevented the aggregation of a model unfolded substrate (Braun *et al.*, 1996; Chamberlain and Burgoyne, 1997a). This observation suggests that CSP/Hsc70 might regulate the folding of specific exocytotic proteins.

The J domain of DnaJ/Hsp40 proteins consists of four alpha helices containing a highly conserved tripeptide histidine-proline-aspartic acid (HPD) motif located within a loop region between helices II and III (Qian *et al.*, 1996). The HPD motif is required for ATPase stimulation, as mutations within the HPD motif (H43Q or D45A) of CSP abolished binding to Hsc70 and thus prevented the stimulation of its ATPase activity (Chamberlain and Burgoyne, 1997a).

The anticipated function of CSP as a chaperone is thus proposed to centre on its ability to interact with and stimulate the ATPase activity of Hsc70. CSP has been shown to interact with the SNARE proteins syntaxin and VAMP, and synaptotagmin, and it is possible that the exocytotic chaperone activity of CSP may be exerted during these interactions (Boal *et al.*, 2004; Evans *et al.*, 2001; Evans and Morgan, 2002; Leveque *et al.*, 1998; Nie *et al.*, 1999). It would be interesting to determine whether CSP regulates the folding of these proteins, or is involved in the assembly/disassembly of protein complexes associated with the exocytotic fusion machinery. In support of this theory is the observation that CSP null mice have a decrease in SNARE complex formation (Chandra *et al.*, 2005); this perhaps reflects a chaperone role of CSP in promoting SNARE complex assembly. Consistent with the hypothesis that CSP acts as an exocytotic chaperone, CSP has been found on synaptic vesicles in a complex with Hsc70 and several vesicular proteins. For example, as part of a complex with Hsc70, CSP has been implicated in vesicle filling, through interactions with the enzyme glutamate decarboxylase (GAD) (Hsu *et al.*, 2000). GABA is the major inhibitory neurotransmitter in brain (Roberts and Kuriyama, 1968), and is synthesised by GAD: the activity of GAD is dependent on phosphorylation by a kinase located on the synaptic vesicle membrane (Hsu *et al.*, 1999). Hsc70 and CSP binding to GAD are thought to aid GAD targeting to synaptic vesicle membranes, thereby facilitating GABA synthesis (Hsu *et al.*, 2000). In addition, CSP has been found as part of a chaperone complex containing αGDI, Hsp90 and Hsc70 (Sakisaka *et al.*, 2002). As outlined in Chapter 1.9.2, Rab3A is the major Rab GTPase in neurons, and Rab cycling depends on its dissociation from vesicles through the action of αGDI (Luan *et al.*,

1999). Following vesicle fusion, the CSP-Hsp90-Hsc70 chaperone complex is thought to target αGDI to vesicle membranes, thereby indirectly functioning in vesicle trafficking by promoting Rab3A recycling (Sakisaka *et al.*, 2002).

CSP has also been implicated as a regulator of G protein signalling at the plasma membrane (Natochin *et al.*, 2005). Heterotrimeric G proteins are composed of α, β and γ subunits, which, when activated, dissociate into G_α and $G_{\beta\gamma}$ subunits that interact with downstream effectors. Activation of G proteins involves the exchange of GDP bound to G_α for GTP, catalysed by a guanine nucleotide exchange factor (GEF). CSP has been shown to interact with $G_{\alpha s}$ and act as a GEF, by promoting GDP/GTP exchange. Furthermore, the interaction of CSP with Hsc70 and SGT (small glutamine-rich tetratricopeptide) was found to regulate the GEF activity of CSP (Natochin *et al.*, 2005).

In addition to functions related to secretory vesicle dynamics, CSP may also have a chaperone function at early compartments in the secretory pathway. For example, CSP has been proposed to function in the maturation, biogenesis and trafficking of the cystic fibrosis transmembrane conductance regulator (CFTR), a cAMP-regulated chloride channel located on the apical membrane of epithelial cells that functions in salt secretion and absorption (Zhang *et al.*, 2002a; Zhang *et al.*, 2006). CFTR exists in two forms, an immature, core glycosylated form, and a mature, fully glycosylated form; CSP interacts predominantly with the immature form (Zhang *et al.*, 2002a). Overexpression of CSP in HEK293 cells blocks the formation of mature CFTR, leading to the accumulation of the immature form in the ER, and hence preventing CFTR trafficking to the plasma membrane (Zhang *et al.*, 2002a). The regulation of CFTR trafficking is dependent on CSP possessing a functional J domain, since overexpression of the CSP(H43Q) mutant, which is unable to bind to Hsc70 or stimulate its ATPase activity (Chamberlain and Burgoyne, 1997a), restored the maturation and export of CFTR (Zhang *et al.*, 2006). Although these results are of significant interest, one possibility is that CSP overexpression has effects on the folding of newly synthesised proteins such as CFTR by sequestering Hsc70. A similar caveat also applies to other studies utilising CSP overexpression.

1.11 MEMBRANE TARGETING AND TRAFFICKING OF PALMITOYLATED PROTEINS

As the enzymes that transfer palmitate onto substrate proteins are membrane-associated, substrate proteins require being membrane proximal in order to be palmitoylated. Thus, it is essential that palmitoylated proteins have a mechanism to target them to the specific membrane compartment that houses their partner PAT. The mechanisms that govern the initial membrane

targeting and subsequent trafficking of palmitoylated proteins are dependent on the type of membrane protein involved and its final subcellular localisation.

For the majority of palmitoylated transmembrane proteins (with the exception of Type IV membrane proteins: see Chapter 1.2, and below), the route of primary membrane interaction is obvious: these proteins are co-translationally inserted into the ER membrane by a signal-peptide-mediated process. From the ER these proteins can traffic through the secretory pathway until they reach the compartment where their partner PAT is localised; if this is prior to reaching their resident membrane, the protein is subsequently sorted to its target membrane. This is true for the palmitoylated vesicle membrane protein synaptotagmin, a palmitoylated Type I membrane protein that associates with vesicle membranes through an N-terminal transmembrane domain. Synaptotagmin traffics through the secretory pathway to the plasma membrane; the internalisation and subsequent sorting of synaptotagmin to the intracellular vesicle pool is dependent on both glycosylation at an N-terminal intralumenal domain and palmitoylation of cysteines adjacent to the transmembrane domain (Han *et al.*, 2004; Kang *et al.*, 2004).

C-terminal anchor proteins (Type IV membrane proteins) are post-translationally inserted into the ER and subsequently sorted into budding vesicles for transport through the secretory pathway until they reach their resident membrane (Kutay *et al.*, 1995). The vesicle-associated SNARE protein VAMP2 is a Type IV membrane protein that can be palmitoylated *in vitro* (Veit *et al.*, 2000). The two yeast VAMP2 homologues, Snc-1p and Snc-2p (Suppressor of the null allele of CAP), are palmitoylated on a single cysteine *in vivo*. Whilst this palmitoylation is not essential for the exocytotic function of these proteins, it was suggested to be involved in protein stability (Couve *et al.*, 1995). Insertion of VAMP2 into the ER membrane requires ATP and is dependent upon a tail of 15-22 hydrophobic amino acids (Kutay *et al.*, 1995; Whitley *et al.*, 1996); in fact, a stretch of 12 hydrophobic amino acids is sufficient to integrate VAMP2 into microsomal membranes (Whitley *et al.*, 1996). Targeting of VAMP2 to ER membranes requires 4 positively charged amino acids within an amphipathic helix, located to the N-terminus of the insertion sequence (Kim *et al.*, 1999). Sorting determinants for the trafficking of C-tail anchored proteins out of the ER include the length of the tail anchor, though other factors are likely to exist. For example, the trafficking of VAMP2 to synaptic vesicle membranes following membrane insertion in the ER requires co-expression of another protein, synaptophysin 1 (Honsho *et al.*, 1998; Pennuto *et al.*, 2003), and specific amino acids within the SNARE domain (Grote *et al.*, 1995; Hao *et al.*, 1997).

How are palmitoylated proteins that lack membrane-spanning domains targeted to their membrane-associated partner PAT? These proteins are synthesised on free ribosomes yet must be targeted to membranes in order to be palmitoylated. Many soluble proteins undergo modification with different lipids prior to palmitoylation. For example the Ras- and Rho-GTPases, which have tandem isoprenyl and palmitoyl anchors, are synthesised on free ribosomes and become farnesylated in the cytoplasm by a farnesyltransferase prior to palmitoylation (Adamson *et al.*, 1992; Hancock *et al.*, 1989). Similarly, members of the Src family of tyrosine kinases, certain G_α subunits, and eNOS, all have tandem myristoyl and palmitoyl anchors, and myrisoylation is a prerequisite for subsequent palmitoylation (Koegl *et al.*, 1994; Morales *et al.*, 1998; Robinson *et al.*, 1995). Thus, for these proteins, a different lipid modification attached to the proteins in the cytoplasm serves as their primary membrane-targeting signal. The finding that these dual-modified proteins require modification with either a prenyl or a myristoyl group prior to palmitoylation, and that long-lived membrane association of these proteins depends on palmitoylation (See Chapter 1.3.3), both contributed to the kinetic membrane trapping model (Shahinian and Silvius, 1995). In this model, proteins that are modified with a single myristoyl or farnesyl anchor (and thus have weak membrane affinity) will cycle on and off membranes, thereby "sampling" the different intracellular membranes, until they eventually encounter a membrane housing their partner PAT. Palmitoylation by the membrane-resident PAT yields a dually-lipidated protein that has a stronger membrane affinity, resulting in a much longer-lived association with the membrane; hence the protein becomes membrane "trapped". This stronger membrane affinity might now ensure that the protein does not dissociate from the membrane during vesicle budding and trafficking, resulting in efficient intracellular sorting. In this way, the primary lipid modification serves to target the protein to membranes in order for it to be palmitoylated; once palmitoylated, the protein can be sorted to its correct final destination. Release of the palmitoylated protein from the membrane can also be regulated through depalmitoylation by a protein acylthioesterase (e.g H/N-Ras; see Chapter 1.4.2 and (Rocks *et al.*, 2005). The kinetic trapping model is exemplified by the Ras proteins; furthermore, it is supported by biophysical studies that have measured the varied membrane affinities of lipidated peptides for model membranes, and fluorescence bleaching techniques applied to dually lipidated proteins in live cells (Goodwin *et al.*, 2005; Peitzsch and McLaughlin, 1993; Rocks *et al.*, 2005; Shahinian and Silvius, 1995; Silvius and l'Heureux, 1994).

Finally, some palmitoylated soluble proteins lack consensus sites for modification with prenyl or myristoyl anchors, yet are still able to become stably associated with membranes via palmitoylated cysteines. These proteins, which include the secretory vesicle proteins CSP and

GAD-65, and the plasma membrane SNARE SNAP25, must possess mechanisms that allow initial membrane targeting prior to palmitoylation. The exact mechanism that underlies the initial membrane targeting, palmitoylation, and subsequent trafficking of such proteins to their target membranes is limited. Perhaps the best characterised example is for GAD-65, which is synthesised as a soluble hydrophilic protein, yet is stably associated with vesicle membranes through the palmitoylation of two cysteines within the N-terminus (Christgau *et al.*, 1991; Christgau *et al.*, 1992). The extreme N-terminus of GAD-65 is required for GAD-65 association with Golgi membranes, and this region is sufficient to target other soluble proteins to Golgi membranes (Solimena *et al.*, 1993; Solimena *et al.*, 1994). Furthermore, only once GAD-65 is palmitoylated on cysteines at positions 30 and 45, is it able to be moved out of the Golgi and sorted into the desired carrier vesicle (Huang *et al.*, 2004; Kanaani *et al.*, 2002). However, the molecular mechanisms that govern initial membrane interactions of other non-myristoylated/prenylated proteins remain unknown. In particular, it is not clear whether these proteins utilise a similar mechanism for initial membrane targeting or whether more protein-specific mechanisms are employed. An additional area of interest is the role that palmitoylation plays in specifying the sorting of these proteins to defined intracellular locations such as the plasma membrane or secretory vesicles.

1.12 AIMS AND HYPOTHESIS

The mechanisms that govern initial membrane targeting, palmitoylation, and subsequent trafficking of solely palmitoylated proteins to their target membranes are ambiguous. Following synthesis, these proteins somehow need to be presented to their membrane-resident partner PAT for palmitate transfer to take place. In most cases, palmitoylation is a prerequisite for the subcellular trafficking of these proteins to their resident membrane compartment. Thus, the initial membrane targeting of these proteins is thereby essential for their localisation, and hence their function. It is possible that a common mechanism governs the initial membrane targeting of these proteins. One hypothesis is an extension of the kinetic membrane-trapping model proposed for dual-lipidated proteins, outlined in Chapter 1.11 (Shahinian and Silvius, 1995). This hypothesis states that in the absence of a primary lipid anchor, other mechanisms that provide initial affinity for membranes, and hence target the protein to its resident PATs, could substitute. Examples of such membrane affinity could include clusters of basic amino acids or hydrophobic domains. Palmitoylation would then regulate the subsequent sorting of these proteins to their correct subcellular membrane. This model would explain how some proteins, in particular palmitoylated proteins that have no obvious membrane-targeting motifs, are presented to their membrane-resident partner PAT in order for palmitate transfer to occur.

Following palmitoylation, the protein is now stably membrane-bound, and can be sorted to its final subcellular membrane. The exocytotic chaperone protein, CSP, is an excellent model protein with which to test this hypothesis. CSP is synthesised as a soluble protein, yet is stably and permanently associated with vesicle membranes through a palmitoylated cysteine string domain. Furthermore, the recent cloning of 23 mammalian palmitoyl transferases allows for the cellular site of CSP palmitoylation to be examined *in vivo*. The aims of this study are to determine the mechanisms that govern the initial membrane binding of CSP, its palmitoylation and subsequent trafficking routes to vesicle membranes. The above hypothesis will be tested, and a model for the initial membrane binding, palmitoylation and subsequent trafficking of this class of otherwise soluble, yet palmitoylated membrane proteins, will be proposed.

CHAPTER TWO: MATERIALS AND METHODS

2.1 MATERIALS AND SUPPLIERS

2.1.1 CHEMICALS

All chemicals were supplied by the Sigma-Aldrich Company Ltd (Dorset, U.K.), except where otherwise stated, and were of the highest grade available.

2.1.2 MOLECULAR BIOLOGY REAGENTS

Oligonucleotide primers were synthesised by Sigma™-Proligo® (Dorset, U.K.). DNA polymerases and dNTPs were obtained from Promega Corporation U.K (Southampton, Hampshire, U.K.). XL1-Blue Supercompetent Cells (strain *recA1 endA1 gyrA96 thi-1 hsdR17 supE44 relA1 lac* [F'*proAB lacIqZDM15 Tn10* (Tetr)]) were purchased from Stratagene (La Jolla, U.S.A). One Shot® TOP10 Competent Cells (Strain F- *mcrA* (*mrr-hsd*RMS-*mcr*BC) 80*lac*ZM15 *lac*X74 *rec*A1 *ara*139 (*ara-leu*)7697 *gal*U *gal*K *rps*L (StrR) *end*A1 *nup*G) were obtained from Invitrogen Ltd (Paisley, U.K.). QIAfilter® Plasmid Maxi Kit, QIAprep® Spin Miniprep Kit and QIAquick® Gel Extraction Kit were acquired from Qiagen Ltd (Crawley, West Sussex, U.K.). DNA ladders (100 bp and 1 kB) were purchased from New England Biolabs (U.K.) Ltd (Hitchin, Hertfordshire, U.K.).

2.1.3 CELL CULTURE MEDIA AND PLASTICS

All cell culture plastics were purchased from Corning B.V, (Schiphol-Rijk, The Netherlands) unless otherwise specified. Thirteen millimetre coverslips and 24-well plates, pre-coated with poly-D-lysine, were purchased from Biotrace International (Bridgend, U.K.). RPMI Media 1640, Dulbecco's Modified Eagle Medium (D-MEM), OPTI-MEM, Horse Serum, Foetal Calf Serum, F-10 Nutrient Mixture (Ham), L-Glutamine, Trypsin-EDTA and Lipofectamine™ 2000 Reagent were all purchased from Invitrogen Ltd. Six-well plates were coated with 1 ml Poly-D-Lysine (100 ng/ml, in sterile distilled (d) H_2O) for 1 hour at room temperature, then washed twice with RPMI 1640 and stored at 4°C until required.

2.1.4 ANTIBODIES

2.1.4.1 PRIMARY ANTIBODIES

The anti-calreticulin antibody was from Abcam plc (Cambridge, U.K.). Recombinant human calreticulin was produced in the Baculovirus insect cell system and raised in rabbit polyclonal

whole antiserum IgG. Dilutions were 1:1000 for immunoblotting and 1:200 for immunofluorescence.

The anti-Cysteine string protein polyclonal antibody was purchased from StressGen Biotechnologies Corporation (Victoria, B.C., Canada). This immunoaffinity purified rabbit antibody was raised against a synthetic peptide corresponding to the extreme C-terminus of rat cysteine string protein (residues 182-198) conjugated to KLH and raised in rabbit. Dilutions were 1:10000 for immunoblotting and 1:100 for immunofluorescence.

Clontech laboratories, Inc (Mountain View, CA, U.S.A) supplied the Living Colors® A.v. anti-GFP (JL-8) affinity purified monoclonal IgG2a antibody. This antibody was produced by hybridoma cells against full-length *Aequoria victoria* green fluorescent protein and was used at a dilution of 1:5000 for immunoblotting.

The sheep anti-Grasp55 antibody was a gift from Dr Francis Barr (Shorter *et al.*, 1999) and was used at a dilution of 1:50 for immunofluorescence.

The anti-HA and Rhodamine-conjugated anti-HA antibodies were from Roche (Welwyn Garden City, Hertfordshire, U.K.). Both antibodies are specifically raised to the peptide epitope YPYDVPDYA, derived from the human influenza haemagglutinin (HA) protein. The monoclonal rat anti-HA (clone 3F10) was used at a dilution of 1:1000 for immunoblotting. The Rhodamine-conjugated mouse monoclonal antibody (clone 12CA5) was used at 1:100 for immunofluorescence. A fluorescein isothiocyanate-conjugated (FITC) anti-HA mouse monoclonal IgG2a was supplied by Santa Cruz Biotechnology Inc (Heidelberg, Germany) and used for immunofluorescence at a dilution of 1:50.

A mouse monoclonal α-SNAP antibody (Clone 77.1) was purchased from Synaptic Systems (Göttingen, Germany). The antibody was raised against recombinant full length rat αSNAP and was used at a dilution of 1:5000 for immunoblotting.

An anti-munc18 antibody was supplied by Becton Dickinson (Oxford, UK). Purified monoclonal mouse IgG1 antibody was raised against the C-terminus of rat Munc-18-1 and was used at a dilution of 1:250 for immunoblotting.

A mouse anti-transferrin receptor monoclonal antibody (clone H68.4) was purchased from Zymed Laboratories Inc (Cambridge, UK). Affinity purified mouse IgG1 antibody was raised

against the N-terminus of recombinant human transferrin receptor. A dilution of 1:1000 was used for immunoblotting.

2.1.4.2 SECONDARY ANTIBODIES

Alexa Fluor® 594 goat anti-rabbit, Alexa Fluor® 488 goat anti-rabbit, Alexa Fluor® 568 donkey anti-sheep affinity purified antibodies were from Invitrogen Ltd and used at a dilution of 1:400 for immunofluorescence.

Horse-radish peroxidase (HRP)-conjugated donkey anti-rabbit, goat anti-rat and sheep anti-mouse antibodies were from GE Healthcare UK Ltd (Little Chalfont, Buckinghamshire, U.K.) and used for immunoblotting at a dilution of 1:2000. An ImmunoPure HRP-conjugated rabbit anti-sheep antibody was supplied by Pierce Biotechnology (Rockford, IL, U.S.A) and used for immunoblotting at a dilution of 1:2000.

2.1.5 RADIOACTIVE MATERIALS

[9,10(n)-^{3}H]Palmitic acid was obtained from PerkinElmer (Beaconsfield, Buckinghamshire, U.K.). Pro-mix L-[^{35}S] *in vitro* cell labelling mix was purchased from Amersham plc (Little Chalfont, Buckinghamshire, U.K.).

2.1.6 PLASMIDS

Living Colors® pEGFP-C2 and dsRed2-ER fluorescent vectors were purchased from Clontech laboratories, Inc. A pCR2.1-TOPO vector was purchased from Invitrogen Ltd. To generate the EGFP-CSP plasmid, full-length bovine CSP (lacking the initiating methionine) was PCR amplified and inserted in frame into pEGFP-C2 as a *Hind*III/*Bam*HI fragment containing a linker sequence as part of the multiple cloning site encoding the following amino acids: SGRTQISSSSL. This plasmid was constructed by Dr. Luke Chamberlain (Zhang *et al.*, 1998) and was used as a template for generating all of the CSP mutants used in this study. The following CSP mutants were constructed by Dr. Luke Chamberlain: CSP(C1-3S), CSP(C4-7S), CSP(C8-10S), CSP(C11-14S), CSP$_{1-136}$ and CSP$_{113-198}$. A plasmid containing human SNAP25B fused to an N-terminal GFP tag was provided by Dr. Maureen Linder (Gonzalo et al., 1999). pEFBOS-HA vectors containing each of the twenty-three mouse DHHC-containing palmitoyl transferases were gifts from Professor Masaki Fukata (Fukata et al., 2004). DHHC3(C157S), DHHC7(C160S) and DHHC17(C457S) site-directed mutants were constructed by Dr. Christine

Salaün (INSERM U845, Faculte de Medecine Paris Descartes, Paris, France). The DHHC17-EGFP plasmid was provided by Dr Alaa El-Husseini (Huang *et al.*, 2004).

2.2 STANDARD MOLECULAR BIOLOGY PROTOCOLS

E.coli were cultured in sterile 2 x YT culture media (16 g/l bacto-tryptone, 10 g/l yeast extract, 5 g/l NaCl; pH 7.0) containing 100 µg/ml ampicillin or 30 µg/ml kanamycin according to standard protocols (Sambrook et al., 1989). 2 x YT agar plates were prepared by supplementing 2 x YT culture media with 1.5% (w/v) bacto-agar (Melford Laboratories Ltd) prior to autoclaving. On cooling to approximately 60 °C, the appropriate concentration of antibiotic was added and, following gentle mixing, approximately 25 ml was poured into 10 cm^2 diameter Petri dishes. Plates were allowed to set at room temperature before storage at 4 °C for up to four weeks.

For diethyl pyrocarbonate (DEPC) -treated water, 500 µl DEPC was added to 1 l of 0.22 µm-sterile-filtered distilled water for 16 hours, then autoclaved and left to cool.

2.2.1 AMPLIFICATION OF DNA BY PCR

The polymerase chain reaction (PCR) was used to amplify and introduce mutations into segments of DNA of a known sequence. Standard PCR (Chapter 2.2.1.1) was used to amplify fragments of DNA used for subcloning, and site-directed mutagenesis (Chapter 2.2.1.2) was used to introduce nucleotide substitutions into double-stranded plasmid DNA.

2.2.1.1 STANDARD PCR

Two oligonucleotide primers were designed, each having different sequences which were complementary to opposite strands of a known section of template DNA. A reaction mix consisting of 50 ng of template DNA, 5 µl of 10 x reaction buffer, 125 ng of each sense and antisense oligonucleotide primer, 1 µl of a 10 mM dNTP mix (10 mM of each dATP, dCTP, dGTP and dTTP in DEPC-treated dH$_2$0) and 0.75 µl of *Pfu* DNA polymerase, made to a final volume of 50 µl with DEPC-treated dH$_2$0 was constructed. Initially, template DNA was heat-denatured by heating the reaction mixture to 95 °C for 1 minute prior to thermal cycling reactions. Typically, template DNA was heat-denatured at 95 °C for 30 seconds, primers were allowed to anneal for 30 seconds at 55 °C and DNA synthesis was promoted for 1 minute at 72

°C for a total of 30 cycles. A final incubation at 72 °C for 7 minutes terminated DNA synthesis. PCR products were stored at 4 °C until required.

2.2.1.2 SITE-DIRECTED MUTAGENESIS

Two complementary primers were designed to anneal to the same sequence on opposite strands of the plasmid with the desired mutation flanked with 15-20 nucleotides. Where possible, primers were designed to have a melting temperature (T_m) of at least 78 °C, to contain a minimum GC content of 40%, and to terminate with one or more C or G bases. The T_m of primers was calculated using the following formula: $T_m = 81.5 + 0.41$ (%GC) - (675/N) - % mismatch, where N = primer length in bases, and the % GC and % mismatch are whole numbers. A reaction mixture was assembled, containing 50 ng of template DNA, 5 µl of 10 x reaction buffer, 125 ng of each sense and antisense primer, 1 µl of a 10 mM dNTP mix, 1 µl of *Pfu* polymerase and made to a final volume of 50 µl with DEPC-treated dH$_2$0. DNA was heat denatured at 95 °C for one minute. Thermal cycling parameters were as followed; DNA was heat denatured at 95 °C for 30 seconds, primer annealing took place at 55 °C for 30 seconds, and DNA synthesis proceeded at 68 °C: the time allowed for DNA synthesis varied depending on the template used - generally, an extension time of one minute for every kb of plasmid length was sufficient. The number of cycles depended on the number of nucleotide substitutions created; generally twelve cycles were required for a single nucleotide substitution, sixteen cycles for up to three nucleotide substitutions, and eighteen cycles for more than three nucleotide substitutions. To select for mutation-containing synthesised DNA, 1 µl of *Dpn* I was added to the PCR reaction and incubated at 37 °C for 1 h. *Dpn* I cleaves dam methylated DNA isolated from *E. coli*, and hence specifically digests the non-mutated parental plasmid (*i.e.* template cDNA). Ten percent (v/v) of the *Dpn* I-treated PCR reaction was subjected to agarose gel electrophoresis (Chapter 2.2.2) to verify amplification of mutated DNA. Two microlitres of the PCR product was used to transform XL1-Blue supercompetent cells (Stratagene; Chapter 2.2.7), and, typically, plasmid DNA from three separate colonies was isolated (Chapter 2.2.9). Sequencing of both strands of the plasmid DNA was used to verify the desired mutations were incorporated and to ensure any additional unwanted mutations were absent (Chapter 2.2.13).

2.2.2 AGAROSE GEL ELECTROPHORESIS

DNA fragments generated by PCR (Chapter 2.2.1) and restriction endonuclease digestion (Chapter 2.2.5) were resolved electrophoretically through agarose gels (1% (w/v)) in tris-acetate (TAE) buffer (40 mM Tris-acetate, 1 mM EDTA) supplemented with 2.5 µg/ml ethidium

bromide (Severn Biotech Ltd, Kidderminster, Worcestershire, U.K.). Typically, 10% (v/v) of a PCR or restriction digest product, or 1 µg plasmid DNA, was added to a 6 x stock of DNA Loading Buffer (10% (w/v) Ficoll 400 (Pharmacia Biotech, Uppsala, Sweden), 0.25% (w/v) Bromophenol Blue, in dH_2O) and made up to a final volume of 12 µl in DEPC-treated dH_2O, prior to loading. Samples were subjected to a potential difference of 120 V for approximately 30 minutes prior to visualisation by UV irradiation. To estimate the concentration and size of the DNA to be analysed, samples were routinely electrophoresed against 5 µl of a 100 bp or 1 kB DNA ladder (New England Biolabs).

2.2.3 PURIFICATION OF DNA FROM AGAROSE GELS

DNA fragments generated by PCR (Chapter 2.2.1) and restriction endonuclease digestion (Chapter 2.2.5) and subjected to agarose gel electrophoresis (Chapter 2.2.2) were purified using the QIAquick® extraction kit (Qiagen Ltd) according to the manufacturer's protocol. A band corresponding to the DNA fragment required was visualised by UV irradiation and excised. Three volumes of Buffer QG were added to the gel slice and the mixture was heated to 50 °C for 10 minutes with occasional mixing to solubilise the agarose. One gel volume of isopropanol was added to the mix, and after briefly mixing, the contents were decanted into a QIAquick® spin column and centrifuged at 17 500 x g for 1 minute, and the flow-through was discarded. The column was washed once with 500 µl Buffer QG to remove any residual agarose, followed by a further wash with 750 µl of Buffer PE. After discarding the flow-through the column was centrifuged for a further minute at 17 500 x g to eliminate any residual buffer in the column. Finally, 30 µl of DEPC-treated dH_2O was added to the column, and after a minute, the column was centrifuged at 17 500 x g for 1 minute, and the eluted DNA was collected into a sterile 1.5 ml tube. Successful recovery of DNA was determined by subjecting 10% (v/v) of the sample to agarose gel electrophoresis (See Chapter 2.2.2).

2.2.4 TA CLONING

DNA fragments generated by standard PCR (Chapter 2.2.1.1) were cloned into a pCR2.1-TOPO vector (Invitrogen Ltd). pCR2.1-TOPO vectors are supplied linearized containing single overhanging 3'-deoxythymidine (T) residues. *Taq*-amplified PCR products contain a single deoxyadenosine (A) overhang at the 3' end, allowing Topoisomerase I from *Vaccinia* virus to ligate the PCR product directly into the TOPO vector. For this purpose, *Pfu*-amplified PCR products were *Taq*-treated prior to TA cloning. A cocktail containing 20 µl of gel-purified PCR product (Chapter 2.2.5), 2 µl of 10 x Mg^{2+}-free buffer, 1.2 µl of 25 mM Mg^{2+}, 0.4 µl of a10 mM

dNTP mix and 0.4 μl of *Taq* polymerase was incubated at 72 °C for 20 minutes. To ligate the *Taq*-treated PCR product to the TOPO vector, two microlitres of the *Taq*-treated PCR product were added to 0.5 μl of pCR2.1 TOPO vector and incubated at room temperature for 5 minutes. Half a microlitre of salt solution (1.2 M NaCl, 0.06 M $MgCl_2$) was added prior to the transformation of TOP10 competent cells (Promega Corporation U.K.; Chapter 2.2.7).

2.2.5 RESTRICTION ENDONUCLEASE DIGESTION OF DNA

Most plasmid vectors contain polycloning sites that consist of recognition sequences for various restriction enzymes. Digestion of DNA with the appropriate restriction endonucleases was performed in order to generate compatible ends for sub-cloning and to confirm successful ligation of a construct. Directional cloning was achieved by using two restriction enzymes lacking complementarity between the two protruding ends to ensure that re-circularisation of the vector was inefficient. If both of the restriction enzymes work well in the same buffer, the digestion was carried out simultaneously; otherwise, sequential reactions were performed, with the enzyme that works best in the buffer containing the lowest ionic strength being used first, followed by the second enzyme. In most cases, 1-5 μg of vector DNA were digested in a 20 μl reaction mixture containing 1 μl of the restriction enzyme and 2 μl of 10 x enzyme buffer by incubating at 37 °C for approximately 1 hour. The restriction digestions were terminated by incubation at 70 °C for 10 minutes and confirmation of successful digestion was sought by subjecting the DNA to agarose gel electrophoresis (Chapter 2.2.2).

2.2.6 LIGATION OF PLASMID VECTOR AND INSERT DNA

Ligation of a fragment of foreign DNA to a linearised plasmid vector involves the formation of phosphodiester bonds between adjacent 5'-phosphate and 3'-hydroxy residues at the termini of double-stranded DNA. This reaction can be catalysed *in vitro* by using *bacteriophage* T4 DNA ligase (Promega Corporation U.K.). The efficiency of producing monomeric circular recombinant genomes is affected by the relative concentrations of the termini of both the plasmid and the foreign DNA. Concentrations of vector and insert DNA were estimated by agarose gel electrophoresis (Chapter 2.2.2) and comparison with DNA molecular weight markers of known concentration. Various vector:insert ratios were tested to find the optimum ratio for each particular vector and insert. In most cases, a molar mass ratio of 1:1 or 1:3 vector:insert was found to work well. The molar mass ratio for DNA molecules was estimated using the following formula: [ng vector x insert size (kb) / vector size (kb)] x molar ratio of insert = ng of insert required. Individual ligation reactions were set up using the appropriate

vector:insert ratios, 1 μl of T4 DNA ligase, and 2 μl of 10 x enzyme buffer in a final volume of 10 μl. The ligation reactions were incubated at 16 °C overnight, and terminated by incubation at 70 °C for 10 minutes.

2.2.7 TRANSFORMATION OF COMPETENT CELLS

Commercially available XL1-Blue supercompetent cells (Stratagene) and TOP10 competent cells (Promega Corporation U.K.) were used as bacterial host to amplify cloned plasmid DNA; the method used is described by Hanahan (Hanahan, 1983) and was the same for each competent cell type. XL1-Blue supercompetent cells were specifically used for plasmid DNA synthesised by site-directed mutagenesis (Chapter 2.2.1.2), while TOP10 competent cells were used for routine transformations. Cells stored at –80 °C were allowed to thaw on ice, and a 50 μl aliquot of bacterial suspension was gently transferred to a thin-walled tube. One microgram of DNA (or 2 μl of the PCR product from a site-directed mutagenesis reaction) was added to the competent cells, mixed gently and incubated on ice for 30 minutes. Competent cells were heat-shocked at 42 °C for 45 seconds to encourage DNA uptake, and allowed to recover by incubating on ice for 2 minutes. Two hundred microlitres of 2 x YT culture media was added to the cells before incubation at 37 °C for one hour with shaking (~150 rpm). The transformation reactions were plated onto sterile 2 x YT agar plates (Chapter 2.2) pre-warmed to 37 °C and supplemented with the appropriate antibiotic (100 μg/ml ampicillin or 30 μg/ml kanamycin). Plates were inverted and incubated at 37 °C for approximately 16 hours.

2.2.8 SMALL-SCALE PLASMID PREPARATION: "MINIPREPS"

Transformants were analysed by purifying plasmid DNA from individual clones and identifying the insert in the recombinant plasmid by restriction enzyme digest and agarose gel electrophoresis. The "miniprep" protocol used in this study was a modified alkaline lysis method of Birnboim and Doly (Birnboim and Doly, 1979) using a QIAprep® Miniprep Kit (Qiagen Ltd) according to manufacturer's guidelines, with modification. Briefly, individual bacterial colonies were picked from the agar plates and used to inoculate 3.5 ml 2 x YT culture media containing the appropriate antibiotic. Bacterial colonies were grown up for approximately 16 hours at 37°C with vigorous shaking (~150 rpm). One-and-a-half millilitres of the culture was transferred to 1.5 ml microfuge tubes and centrifuged at 17 500 x g for 1 minute to pellet bacterial cells, the supernatant was discarded. Cells were resuspended in 250 μl Buffer P1 (50 mM Tris-Cl, pH 8.0; 10 mM EDTA, 100 μg/ml Rnase A) by vortexing. To lyse, an equal volume of Buffer P2 (200 mM NaOH, 1% (w/v) SDS) was added to the cells followed

by gentle mixing. Three hundred and fifty microlitres of buffer N3 was added to neutralise the alkaline solutions, the contents gently mixed, followed by centrifugation at 17 500 x *g* for 10 minutes to pellet cell debris. The supernatant containing plasmid DNA was transferred to a QIAprep® Spin Column, which consists of a silica matrix that selectively adsorbs plasmid DNA when present in a high salt buffer. The column was centrifuged at 17 500 x *g* for one minute, washed once with 500 μl of Buffer PB and once with 750 μl Buffer PE followed by a final centrifugation at 17 500 x *g* for 1 minute. Purified plasmid DNA was eluted from the column into a sterile 1.5 ml tube by adding 50 μl Buffer EB (10 mM Tris-Hcl, pH 8.5), and after 1 minute, centrifuging for 1 minute at 17 500 x *g*. The restriction enzyme(s) used to prepare the vector and insert DNA for ligation were used to digest the purified plasmid DNA (as before; Chapter 2.2.5). Where this was not possible (for example, if digestion had resulted in obliteration of the restriction site), restriction enzymes that cleave flanking polycloning sequences were used. Identification of DNA "inserts" was achieved by electrophoresing 10% (v/v) of the digested plasmid alongside 10% (v/v) of the undigested plasmid "miniprep" on a 1% (v/v) agarose gel (Chapter 2.2.2).

2.2.9 LARGE-SCALE PREPARATION OF PLASMID DNA: "MAXIPREPS"

Purified plasmid DNA was isolated from bacterial cultures following a modified alkaline lysis system (Birnboim and Doly, 1979) using a QIAGEN® Plasmid Maxi Kit (Qiagen Ltd) according to manufacturer's guidelines, with modification. Briefly, single colonies picked from agar plates were cultured in 100 ml of 2 x YT culture media containing the appropriate antibiotic overnight at 37 °C, with vigorous shaking (~150 rpm). Bacterial cells were harvested by centrifugation at 4 300 x *g* for 20 minutes at 4 °C and resuspended in 10 mls of cold Buffer P1 (50 mM Tris-Cl, pH 8.0; 10 mM EDTA, 100 μg/ml Rnase A). Lysis of bacterial cells was achieved by the addition of 10 mls of Buffer P2 (200 mM NaOH, 1% (w/v) SDS) with gentle mixing followed by an incubation period of 5 minutes. Following this, the alkaline solution was neutralised and cellular components precipitated using 10 mls of chilled potassium acetate solution (3.0 M; pH 5.5), with gentle mixing. Immediately, the lysate was transferred to a QIAfilter® Cartridge and incubated at room temperature. After 10 minutes, the cleared lysate was filtered into a QIAGEN-tip column that had been previously equilibriated with 10 mls of Buffer QBT (750 mM NaCl, 50 mM MOPS, pH 7.0; 15% (v/v) isopropanol). After the cleared lysate had passed through the resin, the QIAGEN-tip was washed twice with 30 mls Buffer QC (1.0 M NaCl, 50 mM MOPS, pH 7.0; 15% (v/v) isopropanol) to remove RNA, proteins and other impurities. The plasmid DNA was eluted into a 50 ml centrifuge tube by adding 15 mls of Buffer QF (1.25 M NaCl, 50 mM Tris-Cl, pH 8.5; 15% (v/v) isopropanol) to the QIAGEN-

tip. Eluted DNA was concentrated, desalted and precipitated by mixing with 10.5 mls of isopropanol and centrifuging at 4 300 x g for 1 hour at 4 °C. Further purification was achieved by washing the pellet with 5 mls of 70% (v/v) ethanol. Following centrifugation at 4 300 x g for 15 minutes at 4 °C, the supernatant was decanted and the pellet was allowed to air dry for 10 minutes. Finally, the purified plasmid DNA was dissolved in 200-500 μl DEPC-treated H_2O and the concentration determined spectrophotometrically (Chapter 2.2.11). Plasmid DNA was stored at –20 °C.

2.2.10 GLYCEROL STOCKS

For long-term storage of plasmids, stocks containing a bacterial broth suspended in 40% (v/v; final concentration) sterile glycerol were prepared for storage at – 80 °C. Five hundred microlitres of overnight culture was added to 500 μl sterile 80% (v/v) glycerol in a sterile 1.5 ml tube. The sample was vortexed to promote mixing and frozen at – 80 °C. When a new stock of plasmid DNA was required, a small amount of the glycerol stock was transferred on a sterile tip to 100 ml of fresh 2 x YT culture media for overnight growth and large-scale plasmid isolation (Chapter 2.2.9).

2.2.11 QUANTITATION OF DNA

To measure the amount of nucleic acid in a relatively pure preparation, spectrophotomeric measurement of the amount of ultraviolet irradiation absorbed by the DNA bases was used. Double-stranded DNA was diluted 1:200 in DEPC-treated H_2O and the absorbance was measured at 260 nm. The concentration of nucleic acid in the sample can now be calculated, since an absorbance of one at 260 nm corresponds to approximately 50 μg/ml for double-stranded DNA. A ratio between readings at 260 nm and 280 nm (A260/A280) provides an estimate of the relative purity of the nucleic acid: pure DNA has an A260/A280 value of 1.8, and this value is lower if there is contamination with protein or phenol (Sambrook *et al.*, 1989).

2.2.12 NUCLEIC ACID PRECIPITATION

Nucleic acid precipitation with ethanol was used for concentrating nucleic acids. Sodium acetate (3M, pH 5.2) was added to the nucleic acid solution to a final concentration of 300 mM. To this, 2.5 volumes of absolute ethanol (stored at –20 °C) was added, and the solution was chilled at –20 °C for approximately 20 minutes. The precipitate of nucleic acid was then

recovered by centrifugation at 17 500 x g for 30 minutes, the supernatant aspirated and the purified DNA pellet resuspended in DEPC-treated H_2O at the desired concentration.

2.2.13 DNA SEQUENCING

To verify the mutants generated, sequencing of all constructs on both strands was performed by The Sequencing Service, University of Dundee, Dundee, U.K.

2.3 GENERATION OF MUTANT CONSTRUCTS

For generating the CSP N-terminal truncation mutants, oligonucleotide primers incorporating restriction sites flanking the cDNA region of interest were designed (Appendix one; mutated nucleotides are underlined and in bold). CSP cDNA was amplified using standard PCR practices (Chapter 2.2.1.1) and the resultant amplified product was ligated into a pCR2.1-TOPO vector (Invitrogen Ltd; Chapter 2.2.6). These constructs were *Hind*III/*Bam*HI digested and ligated in frame into a Living Colors® pEGFP-C2 vector (Invitrogen Ltd).

For CSP C-terminal truncations, a premature stop codon was introduced into the EGFP-CSP template by site-directed mutagenesis (Chapter 2.2.1.2) using primers described in Appendix two; mutated nucleotides are underlined and in bold.

Amino acid substitution(s) introduced into EGFP-CSP and HA-DHHC15 were performed by site-directed mutagenesis (Chapter 2.2.1.2) and the oligonucleotide primers used are listed in Appendices three and four; mutated nucleotides are underlined and in bold.

2.4 MAMMALIAN CELL CULTURE

Rat pheochromocytoma-12 (PC12) cells were cultured in suspension in 150 cm² flasks in Complete Media (RPMI-1640 supplemented with 10% (v/v) horse serum, 5% (v/v) Foetal Calf Serum (FCS) and 1% (v/v) penicillin-streptomycin (all Invitrogen Ltd). Human Embryonic Kidney (HEK) -293 cells, HeLa cells and COS 1 cells were all cultured in 75 cm² flasks in DMEM (Invitrogen Ltd) supplemented with 10% (v/v) FCS and 1% (v/v) penicillin-streptomycin. Chinese Hamster Ovary (CHO) cells were cultured in 75 cm² flasks in F-10 Nutrient Mixture (Ham) (Invitrogen Ltd) supplemented with 10% (v/v) FCS, 1 % L-Glutamine (Invtrogen) and 1% (v/v) penicillin-streptomycin. All cells were cultured at 37 °C in a

humidified atmosphere containing 95% (v/v) air and 5% (v/v) CO_2, according to standard procedures (Doyle et al., 1994).

To passage, PC12 cells were harvested by centrifugation at 500 x g for 3 minutes, the supernatant discarded, and the cell pellet resuspended in 10 ml Trypsin-EDTA (0.05% Trypsin, 0.53 mM EDTA•4Na; Invitrogen Ltd) and incubated for 5 minutes at 37 °C. Following collection of cell pellets by centrifugation at 500 x g for 3 minutes, the cells were washed once in Complete Media and reseeded into flasks at a ratio of 1:5 or onto 6 or 24 well plates for microscopic or assay purposes. All other cell lines were harvested by applying 5 ml/75 cm^2 Trypsin-EDTA to the cell layer with incubation times ranging from 1 minute to 5 minutes depending on the cell type. The cells were washed off the flask surface with the appropriate medium and resuspended, before being reseeded into flasks, typically by a dilution factor of 1:10. For microscopic or assay purposes, cells were resuspended in the appropriate medium at a density of approximately 10^6 cells/ml before being seeded onto 6- or 24-well plates.

2.4.1 STORAGE AND RESUSCITATION OF MAMMALIAN CELLS

For long-term storage, 1 ml aliquots of approximately 10^6 cells suspended in media supplemented with 10% (v/v) dimethylsulfoxide (DMSO) were transferred to sterile cryotubes and stored in an insulated polystyrene box at −70 °C overnight. The tubes were then transferred to a liquid nitrogen storage facility indefinitely. To resuscitate the cells, cryotubes were thawed at room temperature before transferring the contents to 10 ml of the cell-type specific media, pre-warmed to 37 °C. The cells were resuspended in media by gentle pipetting prior to seeding in a 25cm^2 flask and incubating overnight at 37 °C in a humidified atmosphere containing 95% (v/v) air and 5% (v/v) CO_2. Cell media was replaced to remove traces of DMSO and the cells cultured as normal.

2.4.2 TRANSIENT TRANSFECTION OF PLASMID DNA INTO MAMMALIAN CELLS

To introduce exogenous cDNA into mammalian cells, the cationic lipid Lipofectamine™ 2000 reagent (Invitrogen Ltd) was used. Lipofectamine™ 2000 reagent utilises liposomes (which are able to fuse with phospholipids bilayers) that associate with the negatively charged nucleic acids, resulting in a net positively charged or neutral lipid/nucleic acid complex, thereby allowing exogenous cDNA to be introduced into a cell. Approximately 10^6 cells/ml of media were seeded onto 6-well or 24-well lysine-coated plates, or into flasks, 24 hours prior to transfection. Plasmid cDNA of known concentration was mixed with 50 µl of OPTIMEM in a

sterile 1.5 ml tube. Lipofectamine™ 2000 reagent, at a ratio of 2 μl of reagent for every μg of plasmid to be transfected, was mixed with 50 μl of OPTIMEM in a sterile 1.5 ml tube and left to incubate at room temperature for 5 minutes. Following the incubation period, the contents of the two tubes were mixed, and incubation was allowed to proceed for 20-30 minutes at room temperature. The cDNA:Lipofectamine™ 2000 reagent complex was transferred directly onto the media maintaining the cells, before returning the cells to the incubator for up to 48 h prior to harvesting.

2.5 PROTEIN BIOCHEMISTRY

2.5.1 SDS-PAGE

Proteins were resolved electrophoretically in vertical discontinuous sodium dodecyl sulphate polyacrylamide gels according to the Laemmli method (Laemmli, 1970) using two systems; the Bio-Rad mini-PROTEAN® 3 electrophoresis system (Bio-Rad) using 1 mm spacers for hand-cast gels, or the Invitrogen Ltd NuPAGE® Novex® Bis-Tris mini gel system employing pre-cast gels. Prior to loading, protein samples were denatured for 5 min at 100 °C in SDS sample buffer (50 mM Tris-Hcl, pH 6.8; 10% (v/v) glycerol, 2% (w/v) SDS, 0.1% (w/v) Bromophenol Blue) supplemented with 25 mM DTT. Typically, between five and twenty microlitres of the protein samples were loaded into each well of the gel for analysis by SDS-PAGE.

2.5.1.1 BIO-RAD MINI-PROTEAN® 3 ELECTROPHORESIS SYSTEM

For hand-cast gels, clean glass plates were assembled into the casting stand according to the manufacturer's guidelines. A gel cassette sandwich was constructed, which comprised of a resolving gel monomer (8-15% acrylamide-bisacrylamide in Resolving Buffer; 0.75 M Tris-HCl, pH 8.8; 0.2% (w/v) SDS) overlaid with a stacking gel monomer (5% acrylamide-bisacrylamide in Stacking Buffer; 0.25M Tris-HCl, pH 6.8; 0.2% (w/v) SDS). A 30% stock acrylamide-bisacrylamide (37.5:1) (Anachem Ltd, Luton, Bedfordshire, U.K.) was used and its polymerization was accelerated using 0.1% (v/v) N,N,N',N'-tetramethyl-ethane-1,2-diamine (TEMED), with ammonium persulphate as the catalyst. The electrode assembly holding the gel cassette sandwich was held in place with a clamping frame to form an inner chamber, and was submerged in a Mini Tank containing tris-glycine electrophoresis buffer (25 mM Tris-Hcl, 250 mM glycine, 0.1% (w/v) SDS). Denatured proteins were concentrated in the stacking gel by applying a constant current of 80 V for approximately 20 minutes, prior to being resolved at a constant potential of 150 V for approximately 90 minutes.

2.5.1.2 INVITROGEN LTD NuPAGE® NOVEX® BIS-TRIS MINI GEL SYSTEM

Ten percent and 4-12% Novex® Bis-tris pre-cast NuPAGE gradient gels (Invitrogen Ltd) were assembled into an Xcell *SureLock* Mini-Cell (Invitrogen Ltd) according to the manufacturer's instructions. The inner and outer chambers were filled with 1 x MES (50 mM MES, 50 mM Tris-Base, 1 mM EDTA, 0.1% (w/v) SDS; pH 7.3) or 1 x MOPS (50 mM MOPS, 50 mM Tris-Base, 1 mM EDTA, 0.1% (w/v) SDS; pH 7.7) running buffer. Electrophoresis was performed at a constant potential of 180 V for approximately 1 h.

2.5.2 IMMUNOBLOTTING

Following electrophoresis, separated proteins in polyacrylamide gels were transferred onto nitrocellulose membranes (Protran® nitrocellulose membrane, 0.45 um pore size; Whatman plc, Brentford, Middlesex, U.K.) in order to make them accessible to antibody detection. Polyacrylamide gels, overlaid with nitrocellulose membranes, were sandwiched between 2 pieces of Whatman 3mm blotting paper (Whatman Plc), all pre-soaked in Transfer Buffer (48 mM Tris-Base, 39 mM Glycine, 0.037% (w/v) SDS, 20% (v/v) methanol) and placed gel side towards the cathode into the transfer cassette of a Bio-Rad Trans-Blot Cell. To transfer proteins, a constant current of 90 mA was applied overnight. Successful transfer was confirmed by incubating membranes in a solution of Ponceau S (0.1% (w/v) Ponceau S, 3% (v/v) trichloroacetic acid) for one minute, followed by washing in dH_2O to remove excess stain. To block non-specific interactions between antibody and nitrocellulose, membranes were incubated in 5% (w/v) non-fat dried milk (Marvel, Premier Foods, St Albans, U.K.) in PBS-T (Phosphate-Buffered saline (137 mM NaCl, 10 mM Phosphate, 2.7 mM KCl, pH 7.4) containing 0.02% (v/v) Tween® 20) for 45 minutes at room temperature with agitation. Membranes were probed with appropriate primary antibody concentration (Chapter 2.1.41) in PBS-T for between 1 hour at room temperature to 4 °C overnight (depending on the antibody used), with shaking. Unbound antibody was removed from membranes by washing 5 x 5 minutes in PBS-T. To detect sites bound by primary antibody, the membrane was exposed to appropriate horseradish-peroxidase conjugated secondary antibody concentration (Chapter 2.1.4.2) raised against the species used for the primary antibody in PBS-T supplemented with 1% (w/v) non-fat dried milk (Marvel) for 45 minutes with gentle agitation at room temperature. Membranes were washed for a further 5 x 5 minutes in PBS-T to eliminate unbound secondary antibody, followed by a final wash in PBS. Protein bands were visualised using enhanced chemiluminescence (ECL) detection methods (GE Healthcare UK Ltd) according to manufacturer's protocol. The membrane was exposed to light sensitive film (Kodak) in an X-ray cassette for between 1 second and 20 minutes and the film developed using an automatic X-ray developer (X-OMAT).

The film was scanned using Adobe Photoshop 7.0 (Adobe Systems, CA, U.S.A.) software on an Apple Macintosh.

2.5.3 FIXING AND DRYING OF POLYACRYLAMIDE GELS

Proteins separated by SDS-PAGE were fixed by incubating the gel in fixing solution (25% (v/v) isopropanol, 65% (v/v) dH_2O, 10% (v/v) acetic acid) for 30 minutes at room temperature with gentle agitation. The gel was washed briefly in dH_2O before being sandwiched between two sheets of cellulose, pre-soaked in dH_2O, and clamped into a frame. Gels were dried at room temperature for between 24 and 48 hours.

2.5.4 PREPARATION OF CELL LYSATES

For detection of proteins expressed in cell populations, approximately 10^6 transfected PC12 cells growing on poly-D-lysine coated 24-well plates were washed once in ice-cold PBS and incubated in 150 µl of ice-cold lysis buffer (1% (v/v) Nonidet P-40, 1% (v/v) n-Octyl-β-D-glucopyranoside, 1% (v/v) Thesit, 0.5% (w/v) saponin in PBS, containing a protease inhibitor cocktail; cOmplete, Mini, Roche) for 30 minutes on ice. Lysed cells were transferred to 1.5 ml tubes, vortexed briefly and centrifuged at 17 500 x g for 15 minutes at 4 °C to pellet cellular debris. The supernatant containing the cell lysate was decanted into a separate tube containing 50 µl of 4 x SDS sample buffer (containing 100 mM DTT; 25 mM final concentration) and incubated at 100 °C for 5 minutes. Cellular proteins were detected by subjecting the samples to SDS-PAGE and immunoblotting (Chapters 2.5.1-2).

2.5.5 PREPARATION OF POSTNUCLEAR SUPERNATANTS

Transiently transfected cells were harvested and centrifuged at 900 x g for 5 minutes at 4 °C, and the supernatant discarded. The cells were washed twice in 10 ml of ice-cold PBS by resuspension and centrifugation at 900 x g for 5 minutes at 4 °C. Next, the cells were resuspended in 500 µl HES homogenisation buffer (0.32 M sucrose, 20 mM HEPES, 1 mM EDTA, pH 7.4, plus protease inhibitors) and homogenised with 20 strokes of a Dounce homogeniser. The homogenised cells were centrifuged at 500 x g for 5 minutes at 4 °C and supernatant containing the postnuclear supernatant (PNS) was recovered.

2.5.6 SUBCELLULAR FRACTIONATION

Cells were separated into cytosolic and membrane fractions using a ProteoExtract® Subcellular Proteome Extraction Kit (Calbiochem). This approach was easier and more efficient than standard fractionation techniques, which often require extensive centrifugation steps. The ProteoExtract® Subcellular Proteome Extraction Kit relies on the differential solubility of specific subcellular compartments (and hence their associated proteins) in the reagent mixtures provided (composition not specified).

For PC12 cell fractionations, approximately 3×10^6 cells were seeded onto each well of a 6-well plate, pre-coated with poly-D-Lysine, and transfected with 1-3 μg plasmid DNA. Forty-eight hours post-transfection, adherent cells were separated into cytosolic and membrane fractions following the manufacturer's protocol, with modifications. All steps were carried out at 4 °C, and a protease inhibitor cocktail was included in all buffers. Briefly, cells were washed twice for 5 minutes with 800 μl Wash Buffer followed by incubation in 400 μl Extraction Buffer I, with gentle agitation. After 10 minutes, the buffer was harvested, centrifuged at 500 x *g* for 10 minutes to remove whole cell contaminants, and the supernatant containing the cytosolic protein fraction was transferred to fresh tubes. The cells were then washed for 5 minutes at 4 °C with Wash Buffer to remove any residual cytosolic proteins. Finally, the cells were incubated with 400 μl Extraction Buffer II for 30 minutes, and the buffer containing membrane-bound proteins was removed, centrifuged at 17 500 x *g* for 10 minutes each, and the supernatants containing membrane-bound proteins isolated. To each recovered cell fraction, 167 μl of 4x SDS sample buffer with 25 mM DTT (final concentration) was added. For detection of proteins in each fraction, equal volumes of the samples were subjected to SDS-PAGE and immunoblotting (Chapter 2.5.1-2).

For fractionation of all other cells types, approximately 10^6 cells/ml of media were seeded onto poly-D-lysine-coated 24-well plates. Cells were transiently transfected with 0.8-3 μg plasmid DNA and incubated for 24-48 hours. Separation of cellular proteins into cytosolic and membrane fractions was performed as described above with the following modifications to the buffer volumes: in each case cells were washed with 400 μl Wash Buffer and fractionation was accomplished with 150 μl of each Extraction Buffer I and II. To each recovered cell fraction, 50 μl of 4 x SDS sample buffer with 25 mM DTT (final concentration) was added and the samples were processed as before.

2.5.7 CHEMICAL DEPALMITOYLATION OF CELL MEMBRANES

Cell membranes were isolated by centrifuging postnuclear supernatants at 196 000 x g for 30 minutes at 4 °C in a Beckman TLX ultracentrifuge (Beckman Coulter Ltd, High Wycombe, Buckinghamshire, U.K.), using a TLA100.4 rotor (Beckman Coulter Ltd). The pellet containing the membrane fraction was resuspended in 500 μl of 1 M hydroxylamine (pH 7; containing protease inhibitors) or 1 M Tris (pH 7; containing protease inhibitors) and incubated for up to 20 hours at room temperature. The treated membranes were recovered by centrifugation at 196 000 x g for 30 minutes and resuspended in 500 μl SDS sample buffer containing 25 mM DTT. For detection of proteins in each fraction, equal volumes of the samples were subjected to SDS-PAGE and immunoblotting (Chapter 2.5.1-2).

2.5.8 IMMUNOPRECIPITATION

GFP and myc-tagged proteins were isolated from protein populations using a μMACS™ Epitiope Tag Protein Isolation Kit (Miltenyi Biotec Ltd, Bisley, Surrey, U.K.). This technique employs a colloidal suspension of small (50 nm in diameter) super-paramagnetic MicroBeads conjugated to anti-GFP or anti-myc antibodies, which specifically bind the tagged proteins. The magnetically labelled proteins are retained on a column in a magnetic field where non-specific interacting molecules can be washed away, allowing the isolation of highly purified target molecules. Isolated cytosolic and membrane fractions or cell lysates, from transiently transfected cells (Chapter 2.5.6) containing epitope-tagged target proteins, were magnetically labelled by incubating with 20 μl of Anti-Tag MicroBeads (raised against the epitope tag) for 30 minutes on ice. A μ Column, placed in the magnetic field of the μMACS Seperator, was prepared by applying 200 μl of Lysis Buffer (150 mM NaCl, 1% (v/v) Triton® X-100, 50 mM Tris-Hcl, pH 8.0; containing protease inhibitor cocktail). Magnetically labelled cell constituents were applied to the column, and unlabelled proteins were allowed to run through. The column was rinsed with 4 x 200 μl Lysis Buffer and 1 x 100 μl Wash Buffer 2 (20 mM Tris-Hcl, pH 7.5; plus protease inhibitor cocktail). Twenty microlitres of SDS sample buffer (containing 25 mM DTT), preheated to 95 °C, was added to the column and allowed to incubate for 5 minutes. Finally, 50 μl of hot (95 °C) SDS sample buffer (containing 25 mM DTT) was added to the column and the eluate containing isolated GFP or myc-tagged proteins was collected. The immunoprecipitate was analysed by SDS-PAGE and immunoblotting and/or autoradiography.

2.5.9 [³H] PALMITIC ACID LABELLING

Transfected PC12 cells (~ 3x10⁶) were cultured for 48 hours and then incubated in serum-free RPMI1640 medium containing 10mg/ml BSA for 30 minutes at 37 °C. Following this, the cells were incubated in RPMI1640/BSA containing 37 MBq/ml [³H] palmitic acid for 4 hours at 37 °C. Radiolabelled cells were separated into cytosolic and membrane fractions using a ProteoExtract® Subcellular Proteome Extraction Kit (Chapter 2.5.6). Following fractionation, GFP-tagged constructs were isolated using a μMACS™ Epitope Tag Protein Isolation Kit (Chapter 2.5.8). Immunoprecipitated samples were separated by SDS-PAGE (Chapter 2.5.1) and transferred to duplicate nitrocellulose membranes (Chapter 2.5.2). One membrane was processed for immunoblotting analysis using a monoclonal GFP antibody (Chapter 2.5.2). The duplicate membrane was allowed to air-dry, and was sprayed three times with KODAK™ EN³HANCE™ Spray Surface Autoradiography Enhancer (PerkinElmer) according to the manufacturer's instructions to enhance detection of radiolabel incorporation. Nitrocellulose membranes were exposed to light-sensitive film for 10-14 days at –80 °C.

2.5.10 [³⁵S] METABOLIC LABELLING

Approximately 3 x 10⁶ cells were seeded onto each well of a 6-well plate, pre-coated with poly-D-Lysine, and were transfected with 1-3 μg plasmid DNA. Forty-eight hours post-transfection, adherent cells were incubated in serum-free RPMI1640 (without cysteine/methionine) medium containing 10% (v/v) dialysed FBS for 45 minutes at 37 °C. Following this, the cells were incubated in RPMI1640(-cys/met)/dialysed FBS containing 4-11 MBq/ml [³⁵S] cysteine/methionine (Pro-mix L-[³⁵S] *in vitro* cell labeling mix; Amersham plc) for 15 minutes at 37 °C. The labelled cells were 'chased' by incubating in normal cell culture media for various time points (ranging from 0 minutes to 4 hours) at 37 °C and separated into cytosolic and membrane fractions as before (Chapter 2.5.6). GFP-tagged constructs were isolated using magnetic separation following incubation of cytosolic and membrane fractions with magnetic microbeads coupled to GFP antibody (Miltenyi Biotec; Chapter 2.5.8). Immunoprecipitated samples were separated by SDS-PAGE in duplicate. Proteins on one polyacrylamide gel were transferred to nitrocellulose membrane and processed for immunoblotting analysis (Chapter 2.5.2) using a monoclonal GFP antibody, whereas proteins on the duplicate polyacrylamide gel were fixed in fixing solution (Chapter 2.5.3). To enhance detection of radiolabel incorporation, the polyacrylamide gel was incubated in Amplify™ Fluorographic Reagent (Amersham plc) for 30 minutes at room temperature with gentle agitation prior to drying (Chapter 2.5.3). Dried gels were exposed to light-sensitive film for 1-10 days at –80 °C.

2.5.11 ANALYSIS OF PROTEIN-MEMBRANE INTERACTIONS

Approximately 10 x 10^6 PC12 cells were transiently transfected with 10 μg cDNA. Forty-eight hours post-transfection, the cells were washed in PBS and resuspended in HES buffer (containing protease inhibitor cocktail). The cells were homogenised with twenty stokes of a Dounce homogeniser and membranes recovered by centrifugation at 196 000 x g for 30 minutes. The recovered membranes were incubated in 500 μl of HES buffer, 1 M NaCl (in PBS), 0.1 M sodium carbonate (pH 11.5), or 1% (v/v) Triton® X-100 (in PBS; all containing protease inhibitor cocktail) for 30 minutes at 4 °C, followed by centrifugation at 196 000 x g for 30 minutes. The supernatant containing proteins released from membranes was recovered, and the membrane pellet was resuspended in 500 μl of HES buffer. To each sample, 167 μl of 4 x SDS sample buffer containing 25 mM DTT (final concentration) was added. For detection of proteins in each sample, equal volumes of the samples were subjected to SDS-PAGE and immunoblotting (Chapter 2.5.1-2).

2.6 INDIRECT IMMUNOFLUORESCENCE

Transfected PC12 and HEK293 cells growing on poly-D-Lysine coated coverslips in 6-well plates were washed three times with 2 ml of PBS and fixed in 2 mls of PBS containing 4% formaldehyde for 30 minutes at room temperature. The cells were washed twice in PBS and incubated for 5 minutes in PBTA (0.3% (w/v) BSA, 0.1% (v/v) Triton® X-100 in PBS) to permeabilise the plasma membrane; BSA was included to block non-specific binding sites. Primary antibody binding was achieved by inverting the coverslips, cell-side down, on parafilm spotted with 50 μl of the appropriate concentration of primary antibody (Chapter 2.1.4.1) in PBS containing 0.3% (w/v) BSA and incubating for 1-2 hours at room temperature. Coverslips were returned to a 6-well plate, cell side up, and unbound antibody was removed by washing the cells three times in 2 ml of PBS containing 0.3% (w/v) BSA. Following this, coverslips were incubated cell-side down on 50 μl of the appropriate concentration of Alexa Fluor® conjugated secondary antibody (Chapter 2.1.4.2) raised against the species used for the primary antibody in PBS containing 0.3% (w/v) BSA spotted onto parafilm, for 1 hour at room temperature in darkness. The cells were then returned cell-side up to a 6-well plate and washed three times in 2 ml of PBS containing 0.3% (w/v) BSA and once in 2ml of PBS. Coverslips were mounted onto slides, cell-side down, using Mowiol® 4-88 Reagent (Calbiochem) and allowed to dry in darkness at room temperature for 24 hours. Slides were stored in darkness at room temperature until required.

For analysis of the CSP(C4-7L) mutant (See chapter four), cells were washed and incubated in PBS containing 20 μM digitonin for 20 minutes at room temperature prior to fixing. The permeabilised cells were then washed three times in 2 ml of PBS prior to fixation and processing as described above.

2.7 CONFOCAL MICROSCOPY

Image acquisition was obtained using a Zeiss LSM 5 Pascal laser scanning confocal microscope (Carl Zeiss, Oberkochen, Germany) with a PlanApochromat 63x/1.4 Oil DIC objective. Fluorophores were scanned with an excitation double dichroic beam splitter (488 FITC/568 TRITC). Emission wavelengths corresponding to 488 nm excitation were collected through a reflection short pass (RSP) filter at 580 nm followed by a Band Pass 525/50 nm filter. Emission wavelengths at 568 nm were collected through a Long Pass 590 nm filter. The pinhole was set to 1 Airy Unit and scan speed to maximum. Images were acquired at 8 bit per pixel depth and sequentially tracked for each channel with a minimum average of 8 passes to reduce noise.

2.8 QUANTITATIVE DENSITOMETRY

Quantitative densitometry values were derived using a ScanAnalysis program (Biosoft, Cambridge, U.K.), and were corrected for background.

2.9 DATA ANALYSIS

Values measured by densitometry (Chapter 2.8) were described as the mean ± standard error of the mean. The standard error was calculated by dividing the standard deviation by the square root of n-1, where n is the number of individual experiments. Statistical significance was determined using a two-sample unequal variance Student's t-test using Microsoft Excel software. Graphs were generated using Microsoft Excel software.

CHAPTER THREE: THE MINIMUM MEMBRANE BINDING DOMAIN OF CSP

3.1 INTRODUCTION

Protein palmitoylation not only provides stable membrane binding to certain substrate proteins, it can also regulate the intracellular localisation of proteins and target them to distinct membrane microdomains (El-Husseini *et al.*, 2001; Goodwin *et al.*, 2005; Hayashi *et al.*, 2005; Kang *et al.*, 2004; Kinlough *et al.*, 2006; Rocks *et al.*, 2005; Roy *et al.*, 2005; Uemura *et al.*, 2002). The enzymes that catalyse the addition of palmitic acid onto cysteine(s) of mammalian proteins have recently been identified (Fukata *et al.*, 2004), and are characterised by the presence of a signature DHHC-containing cysteine-rich domain (Roth *et al.*, 2002). These DHHC-CRD palmitoyl transferases (PATs) are polytopic integral membrane proteins (Politis *et al.*, 2005), which are associated with various intracellular membranes throughout the cell, including the Golgi apparatus, ER, the plasma membrane, endosomal and vesicular compartments, and the yeast vacuole (Dunphy *et al.*, 1996; Huang *et al.*, 2004; Keller *et al.*, 2004; Roth *et al.*, 2002; Schroeder *et al.*, 1996; Singaraja *et al.*, 2002; Swarthout *et al.*, 2005; Uemura *et al.*, 2002; Valdez-Taubas and Pelham, 2005; Veit *et al.*, 2001).

Since palmitoylating enzymes are membrane-anchored, substrate proteins must have a mechanism to associate with the specific subcellular membrane at which their partner PAT resides, prior to palmitate transfer. For many palmitoylated proteins, the mechanism(s) that govern their initial membrane binding prior to palmitoylation are obvious. Palmitoylated polytopic membrane proteins, such as members of the GPCR family, including the human δ opiod receptor (Petaja-Repo *et al.*, 2006) and the canine histamine H2 receptor (Fukushima *et al.*, 2001), integrate into membranes during synthesis. Other palmitoylated proteins, in particular those that lack membrane-spanning domains, often become modified by a different lipid anchor, such as a prenyl or a myristoyl group, which facilitates membrane association prior to palmitoylation. This is the case for the Ras- and Rho-GTPases, whose primary membrane targeting signal is a farnesyl anchor (Adamson *et al.*, 1992; Hancock *et al.*, 1989), and members of the Src family of tyrosine kinases, G_α subunits and eNOS, for which myristoylation serves as the primary membrane targeting signal (Koegl *et al.*, 1994; Morales *et al.*, 1998; Robinson *et al.*, 1995). However, for a subset of palmitoylated proteins that are synthesised as soluble proteins and do not undergo lipid modification prior to palmitoylation, the primary membrane targeting mechanism is poorly understood. This group of proteins include molecules such as PSD-95 (Craven *et al.*, 1999), an essential scaffolding protein of the post-synaptic density; the enzyme GAD-65, which catalyses the decarboxylation of glutamate to the inhibitory neurotransmitter GABA (Solimena *et al.*, 1993; Solimena *et al.*, 1994); SNAP25, an important regulator of exocytotic membrane fusion (Lane and Liu, 1997); and cysteine string protein

(CSP), a molecular chaperone of the Hsp40 protein family that has a range of cellular functions (Gundersen *et al.*, 1994).

In neuronal and neuroendocrine cells, CSP is found predominantly localised to the membrane of secretory vesicles, and has also been shown to localise to the plasma membrane and ER in some cells types (Braun and Scheller, 1995; Chamberlain *et al.*, 1996; Chamberlain *et al.*, 2001; Gundersen *et al.*, 2001; Pupier *et al.*, 1997; Redecker *et al.*, 1998; Zhang *et al.*, 1998; Zhang *et al.*, 2002). The stable membrane association of CSP is due to the palmitoylation of a "string" of cysteine amino acids present within its signature cysteine string domain (Gundersen *et al.*, 1994; Gundersen *et al.*, 1996; Mastrogiacomo *et al.*, 1994). CSP is synthesised as a soluble protein and does not undergo any other known lipid modification prior to being palmitoylated. Thus, the primary mechanisms that target CSP to intracellular membranes are unknown. In this chapter, detailed mutagenesis has been used to identify the domains and amino acids required for the membrane targeting and palmitoylation of CSP.

3.2 MEMBRANE BINDING, PALMITOYLATION AND LOCALISATION OF FLUORESCENTLY-TAGGED CSP

CSP is extensively palmitoylated within its cysteine string domain, a twenty-four amino acid region containing fourteen cysteines, the majority of which are thought to be palmitoylated *in vivo* (Gundersen *et al.*, 1994). Rat phaeochromocytoma-12 cells (PC12 cells) are a tumour cell derivative of neuroendocrine adrenal medullary chromaffin cells that have been extensively used as a neuronal cell model (Morgan and Burgoyne, 1997). PC12 cells express CSP endogenously, where it is localised to large dense core secretory granules (Chamberlain and Burgoyne, 1998b). Hydroxylamine cleaves the thioester linkage between palmitate groups and cysteines, and has been used extensively as a tool to study protein palmitoylation (Chamberlain and Burgoyne, 1998a; Gundersen *et al.*, 1994; Mastrogiacomo and Gundersen, 1995; Mastrogiacomo *et al.*, 1998; van de Goor and Kelly, 1996). Treatment of PC12 cell membranes with 1M hydroxylamine to induce the depalmitoylation of CSP results in a large (~8 kDa) shift in CSP mobility by SDS-PAGE (Chamberlain and Burgoyne, 1998a; Gundersen *et al.*, 1994; Mastrogiacomo and Gundersen, 1995; Mastrogiacomo *et al.*, 1998; van de Goor and Kelly, 1996). To gauge the extent to which individual CSP molecules are palmitoylated in PC12 cells, a time-course of CSP depalmitoylation was carried out by treating isolated membranes with 1 M hydroxylamine, pH 7.0 (or 1 M Tris, pH 7.0, as a control) for a range of times. A similar approach has previously been used to estimate the level of acylation of *Torpedo* CSP (Gundersen *et al.*, 1994). After recovery by centrifugation, proteins present within the cell

membranes were resolved by SDS-PAGE and transferred to nitrocellulose membranes, and endogenous CSP was detected by immunoblotting using a polyclonal anti-CSP antibody. Figure 3.1A reveals that following chemical depalmitoylation, several immunoreactive bands corresponding to endogenous CSP are present, and the speed that CSP migrates by SDS-PAGE increases with the incubation period with hydroxylamine. These results suggest that hydroxylamine treatment promotes the depalmitoylation of CSP in a time-dependent manner, in agreement with previous results obtained for *Torpedo* CSP (Gundersen *et al.*, 1994). The presence of several immunoreactive bands and the large decrease in mass of CSP following depalmitoylation are consistent with the notion that endogenous CSP is multiply palmitoylated in PC12 cells.

The fusion of enhanced green fluorescent protein (EGFP) cDNA, a variant of the autoflourescent green fluorescent protein isolated from the jellyfish *Aequoria victoria*, to cDNA encoding a protein of interest, has long been a valuable tool for studying the localisation and trafficking of proteins *in vivo* (Chalfie *et al.*, 1994; Cubitt *et al.*, 1995). An EGFP tag was thus fused to the N-terminus of CSP (EGFP-CSP) by PCR amplification of full-length bovine CSP (lacking the initiating methionine; (Zhang *et al.*, 1998) followed by in-frame insertion into a pEGFP-C2 vector as a *Hind*III/*Bam*HI fragment by Dr. Luke Chamberlain; the N-terminal EGFP fusion of CSP is still functional (Zhang *et al.*, 1998). To ensure that EGFP-CSP is efficiently palmitoylated, PC12 cells transfected with EGFP-CSP for 48 hours were metabolically labelled with ^{3}H palmitic acid for 4 hours, followed by immunoprecipitation of EGFP-CSP, SDS-PAGE and analysis by immunoblotting and fluorography. The left panel of Figure 3.1B shows that immunoprecipitated EGFP-CSP from transfected PC12 cell lysates is present in two distinct forms, a lower molecular weight band (indicated by an *arrowhead*) and an upper band (indicated by an *asterisk*). Fluorography (right panel) reveals that the higher molecular weight form of CSP strongly incorporates radiolabel (indicated by an *asterisk*), whereas the lower molecular weight band of CSP is unlabelled. These results demonstrate that EGFP-CSP is palmitoylated when expressed in PC12 cells, and confirms that the differences in migration of CSP on SDS gels can be used as a measure of CSP palmitoylation.

To investigate the relationship between membrane binding and palmitoylation of CSP, PC12 cells transfected with EGFP-CSP for 48 hours were either fractionated into cytosolic (C) and membrane (M) fractions, or the cell membranes were isolated and membrane proteins were chemically depalmitoylated by incubation in 1 M hydroxylamine, pH 7.0 (HA) for 20 hours at room temperature (1 M Tris, pH 7.0 (T) was used as a control). Immunoblotting using an anti-GFP monoclonal antibody revealed that the majority of EGFP-CSP expressed in PC12 cells is
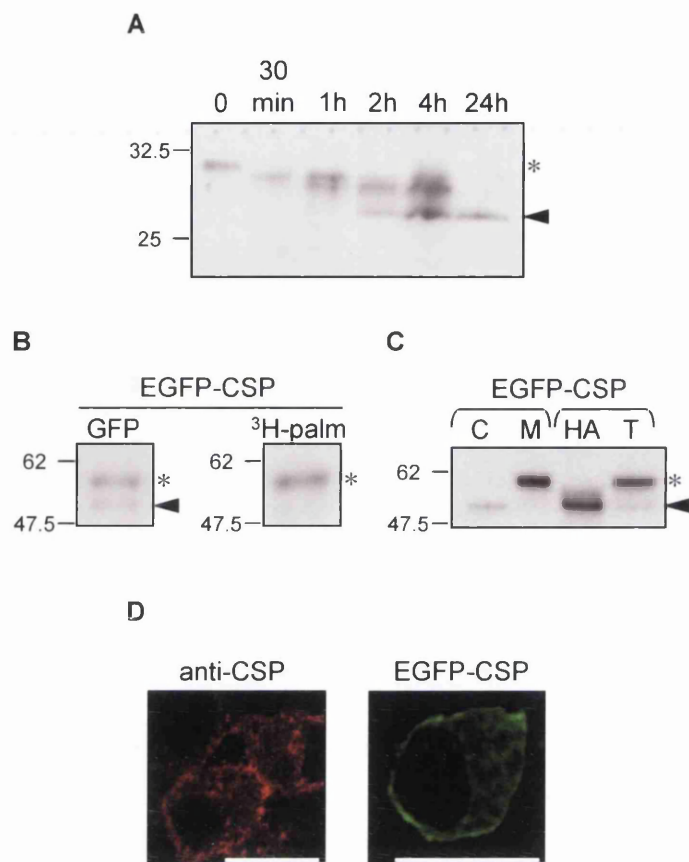
Figure 3.1 CSP is multiply palmitoylated. *A*. Isolated PC12 cell membranes were incubated in 1M Tris, pH 7.0, for 20 hours (0) or 1M hydroxylamine, pH 7.0, for various time points (30 minutes, 1 hour, 2 hours, 4 hours or 24 hours) at room temperature. The treated membranes were recovered by centrifugation at 196 000 x *g* for 30 minutes and depalmitoylation of endogenous CSP was analysed following SDS-PAGE and transfer to nitrocellulose membranes by immunoblotting using an anti-CSP polyclonal antibody. *B*. PC12 cells were transfected with EGFP-CSP for 48 h followed by incubation in ^{3}H palmitate for 4 hours. EGFP-CSP was immunoprecipitated from cell lysates and subjected to SDS-PAGE and transfer to nitrocellulose membranes, in duplicate. One membrane was analysed by probing with a monoclonal anti-GFP antibody (*left panel*; "GFP"), the other was processed for fluorographic detection of incorporated radiolabel (*right panel*; "^{3}H-palm"). *C*. PC12 cells transfected with EGFP-CSP for 48 h were fractionated into cytosolic (C) and membrane (M) fractions. An aliquot of membranes was incubated in 1 M Tris, pH 7.0 (T) or 1 M hydroxylamine, pH 7.0 (HA) for 20 hours. Samples were separated by SDS-PAGE, transferred to nitrocellulose and probed using a monoclonal anti-GFP antibody. The position of molecular weight standards (in kDa) is shown on the left side of all panels; *asterisks* identify palmitoylated CSP and *arrowheads* indicate unpalmitoylated CSP. Representative blots are shown (n = 3). *D*. Untransfected PC12 cells and PC12 cells transfected with EGFP-CSP for 48 h growing on glass coverslips were fixed in 4% (v/v) formaldehyde. Untransfected PC12 cells were permeabilised and probed with a polyclonal anti-CSP antibody to label endogenous CSP. CSP labelling was detected by probing with a rhodamine-conjugated anti-rabbit IgG (red). Localisation of the labelled proteins was determined by confocal microscopy. Images are representative of a single 0.13 μm thick confocal section. Scale bar = 10 μm.

present in the membrane fraction, with only a small percentage of the total EGFP-CSP present in the cytosolic fraction (Figure 3.1C). Furthermore, EGFP-CSP recovered from the membrane fraction of PC12 cells migrates at the same size as palmitoylated EGFP-CSP (as indicated by an *asterisk*), whereas EGFP-CSP present in the cytosolic fraction migrates at the same size as hydroxylamine treated EGFP-CSP (as indicated by an *arrowhead*). These results are consistent with the concept that, *in vivo*, the majority of EGFP-CSP overexpressed in PC12 cells is both membrane-bound and fully palmitoylated. The small percentage of cytosolic EGFP-CSP isolated from PC12 cells most likely represents an unpalmitoylated pool of CSP.

The results presented in Figure 3.1A, *B* and *C* reveals that there is a large difference in migration of CSP by SDS-PAGE depending on the palmitoylation status: fully palmitoylated CSP migrates approximately 8 kDa slower than unpalmitoylated CSP. This band-shift of CSP allows fully palmitoylated, partially palmitoylated and unpalmitoylated variants of CSP to be distinguished from each other based on their migration by SDS-PAGE alone. This assay has distinct advantages over metabolically labelling cells with ^{3}H palmitic acid: it allows for the direct analysis of the percentage of CSP molecules that are palmitoylated and the level of palmitoylation of CSP, as partially palmitoylated CSP variants can be detected as intermediate bands between fully palmitoylated (higher molecular weight) and unpalmitoylated (lower molecular weight) bands (See Figure 3.1A).

To examine the intracellular localisation of EGFP-CSP, transfected PC12 cells were fixed and the localisation of EGFP-CSP was compared to the localisation of endogenous CSP by confocal microscopy. The left panel of Figure 3.1D illustrates that, in PC12 cells, endogenous CSP primarily has a punctate (vesicular) distribution, with some enrichment at the plasma membrane, consistent with previous findings that CSP is localised to secretory vesicles in PC12 cells and several other non-neuronal cell types (Braun and Scheller, 1995; Brown *et al.*, 1998; Chamberlain *et al.*, 1996; Chamberlain and Burgoyne, 1998b; Gundersen *et al.*, 2001; Pupier *et al.*, 1997; Redecker *et al.*, 1998; Zhang *et al.*, 1998). EGFP-CSP expressed in PC12 cells (Figure 3.1D; *Right panel*) is also localised to punctate intracellular structures but with greater enrichment at the plasma membrane. It has previously been shown that CSP overexpressed in PC12 cells displays a more prominent plasma membrane localisation than endogenous CSP (Chamberlain and Burgoyne, 1998b). This is not a consequence of the EGFP tag, and is also seen for untagged CSP (Chamberlain and Burgoyne, 1998b).

3.3 THE MINIMUM MEMBRANE-BINDING DOMAIN OF CSP

CSP can be divided into five domains: an N-terminal domain, a J-domain, a linker domain, a hydrophobic cysteine string domain and a C-terminal domain (See Figure 1.5). It is not known which of these domains are required for the initial membrane binding of CSP, prior to palmitoylation. To identify which domains of CSP are required for its membrane association, a series of N- and C-terminal truncation mutants fused to EGFP were constructed. PC12 cells were transfected with either full-length EGFP-CSP, a C-terminal truncation mutant lacking the cysteine string and C-terminal domains (EGFP-CSP$_{1-112}$), a C-terminal mutant including the cysteine string domain but lacking the C-terminal domain (EGFP-CSP$_{1-136}$), or a truncation mutant encoding the cysteine string domain alone (EGFP-CSP$_{113-136}$). Forty-eight hours post-transfection, cells were separated into cytosolic and membrane fractions to measure the extent of membrane association of the transfected constructs. Equal volumes of the isolated cytosolic and membrane fractions were subjected to SDS-PAGE, transfer to nitrocellulose and immunoblotting using a monoclonal antibody against GFP. The upper panel of Figure 3.2 illustrates that, whereas full-length EGFP-CSP and the mutant lacking the C-terminal domain (EGFP-CSP$_{1-136}$) are enriched in the membrane fraction, the CSP mutant lacking both the cysteine string and the C-terminal domains (EGFP-CSP$_{1-112}$), and the CSP mutant encoding the cysteine string domain alone (EGFP-CSP$_{113-136}$), are not able to target EGFP efficiently to membranes. These results demonstrate that the cysteine string domain alone is not sufficient for membrane binding, and since EGFP-CSP$_{1-136}$ is correctly targeted to membranes, indicates that amino acids upstream of the cysteine string domain are required for membrane targeting. As a control for the fractionation procedure, duplicate nitrocellulose membranes were also probed using antibodies against membrane-associated and cytosolic proteins (Figure 3.2; *Middle* and *Lower panels*, respectively). The transferrin receptor is an integral membrane protein, whereas protein kinase B (PKB) is predominantly a cytosolic protein in PC12 cells (Salaun *et al.*, 2005).

To further analyse the membrane targeting of CSP, a mutant that was lacking the J domain and N-terminal region of CSP (EGFP-CSP$_{(84-136)}$) was constructed (See Figure 1.5). This mutant was expressed in PC12 cells for 48 hours, and it's partitioning into cytosolic and membrane fractions was determined. EGFP-CSP$_{84-136}$ was found highly enriched in the membrane fraction (Figure 3.3A), demonstrating that amino acids 1-83 (the extreme N-terminus and the J-domain) are not required for membrane association of CSP (in agreement with Boal *et al.*, 2004).

To determine the *minimum* region of CSP required for membrane targeting, further N-terminal deletions were made. CSP truncation mutants containing amino acids 93-136 and 103-136 of CSP and expressed in PC12 cells were also recovered in the membrane fraction (Figure 3.3A)
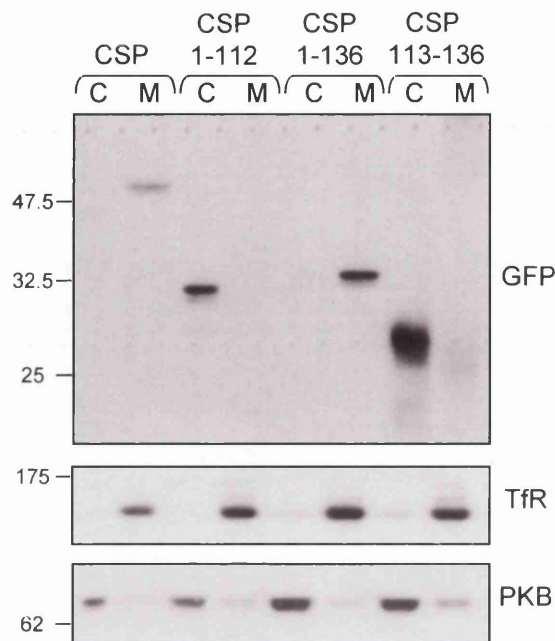
Figure 3.2 The cysteine string domain of CSP is not sufficient for membrane association *in vivo*. PC12 cells were transfected with wild-type EGFP-CSP, EGFP-CSP$_{(1-112)}$, EGFP-CSP$_{(1-136)}$ or EGFP-CSP$_{(113-136)}$. Forty-eight hours post-transfection, the cells were fractionated into cytosolic (C) and membrane (M) fractions and analysed following SDS-PAGE and transfer to nitrocellulose membranes by immunoblotting using an anti-GFP monoclonal antibody (*Upper panel*). To confirm the faithful partition of proteins into cytosolic and membrane fractions, duplicate nitrocellulose membranes were probed to analyse the distribution of the transferrin receptor (TfR, membrane protein; *Middle panel*) and protein kinase B (PKB, cytosolic protein; *Lower panel*). The position of molecular weight standards (in kDa) is shown on the left side of the panel. Representative blots are shown (n = 3).

Figure 3.3 Analysis of the minimal membrane-binding domain of CSP. PC12 cells transfected with wild-type EGFP-CSP or EGFP-CSP truncation mutants for 48 h were fractionated into cytosolic (C) and membrane (M) fractions and analysed following SDS-PAGE and transfer to nitrocellulose membranes by immunoblotting using an anti-GFP monoclonal antibody. *A*. Distribution of CSP truncation mutants encoding the linker domain and cysteine string domain only (EGFP-CSP$_{(84-136)}$), EGFP-CSP$_{(93-136)}$, EGFP-CSP$_{(103-136)}$, or the cysteine string domain alone (EGFP-CSP$_{(113-136)}$). *B*. Distribution of CSP truncation mutants encoding EGFP-CSP$_{(103-136)}$, EGFP-CSP$_{(106-136)}$, EGFP-CSP$_{(109-136)}$, and EGFP-CSP$_{(112-136)}$. *C*. Distribution of CSP truncation mutants encoding EGFP-CSP$_{(106-136)}$, EGFP-CSP$_{(107-136)}$, EGFP-CSP$_{(108-136)}$, and EGFP-CSP$_{(109-136)}$. The position of molecular weight standards (in kDa) is shown on the left side of panels *A*, *B* and *C* and the results shown in panels *A*, *B* and *C* are representative blots. *D*. The percentage CSP membrane association +/- SEM was determined by quantification of immunoblots by densitometry (n=4 from 3 separate experiments). Statistical significance was determined by a Student's *t*-test, whereby * represents a p value of < 0.0016 and ** represents a p value equal to 0.0005 compared to EGFP-CSP$_{(106-136)}$. *E*. Alignment of the amino acid sequence of the minimum membrane-binding domain of CSP (amino acids 106-136) from various species. Conserved amino acids are shaded; cysteines are shown in bold. Numbering of amino acids is shown; the cysteine string domain encompasses amino acids 113-136.

revealing that the entire linker domain is not required for membrane targeting. Further N-terminal deletions in the linker domain between amino acids 103 and 113 were constructed and, as shown in Figure 3.3*B*, whereas a mutant containing amino acids 106-136 was recovered in the membrane fraction of PC12 cells, a mutant having amino acids 109-136 was entirely cytosolic. Further mutational analysis showed that the shortest truncation that consistently supported robust membrane association included amino acids 106-136 of CSP (Figure 3.3*C* and *D*).

Alignment of this minimum membrane-binding region of CSP from different species reveals many conserved amino acids (Figure 3.3*E*). Most importantly, this region of CSP is predominantly hydrophobic, a property that may be required for membrane binding.

3.4 CSP MUTANTS LACKING THE C-TERMINAL DOMAIN ARE UNPALMITOYLATED AND MISLOCALISED

To investigate whether the membrane-associated truncated mutants of CSP are correctly palmitoylated, membranes prepared from PC12 cells expressing EGFP-CSP$_{(1-136)}$ and EGFP-CSP$_{(106-136)}$ for 48 hours were treated with 1 M Hydroxylamine, pH 7.0 (or 1 M Tris, pH 7.0 as a control) for 20 hours at room temperature. Previous results have shown that the chemical depalmitoylation of PC12 cell membranes results in a dramatic molecular mass shift between palmitoylated (Figure 3.1*C*; *asterisk*) and unpalmitoylated (Figure 3.1*C*; *arrowhead*) forms of CSP. Although both EGFP-CSP$_{(1-136)}$ and EGFP-CSP$_{(106-136)}$ are localised to the membrane fraction (Figures 3.2 *(Upper panel)* and 3.3*C*, respectively), there was no detectable molecular mass shift between Tris- and hydroxylamine-treated samples (Figure 3.4*A*; *arrowhead*). These results suggest that, in contrast to full-length EGFP-CSP, EGFP-CSP$_{(1-136)}$ and EGFP-CSP$_{(106-136)}$ are either unpalmitoylated or their level of palmitoylation is dramatically reduced. To examine the extent of palmitoylation of these membrane-associated CSP mutants further, cells expressing full length EGFP-CSP or EGFP-CSP$_{(1-136)}$ were metabolically labelled with ^{3}H palmitic acid for 4 hours, followed by immunoprecipitation of EGFP-tagged proteins, SDS-PAGE and analysis by immunoblotting and fluorography. As shown previously (Figure 3.1*B*), full-length EGFP-CSP immunoprecipitated from PC12 cell lysates migrates by SDS-PAGE as two bands, with the higher molecular weight band incorporating ^{3}H palmitate (Figure 3.4*B*; *asterisk*). In contrast to full length EGFP-CSP, EGFP-CSP$_{(1-136)}$ immunoprecipitated from PC12 cell lysates migrates as a single species by SDS-PAGE (Figure 3.4*B*; *arrowhead*) and does not incorporate detectable ^{3}H palmitate (Figure 3.4*B*), demonstrating that palmitoylation of EGFP-CSP$_{(1-136)}$ is greatly decreased relative to full-length protein, despite being membrane-associated.
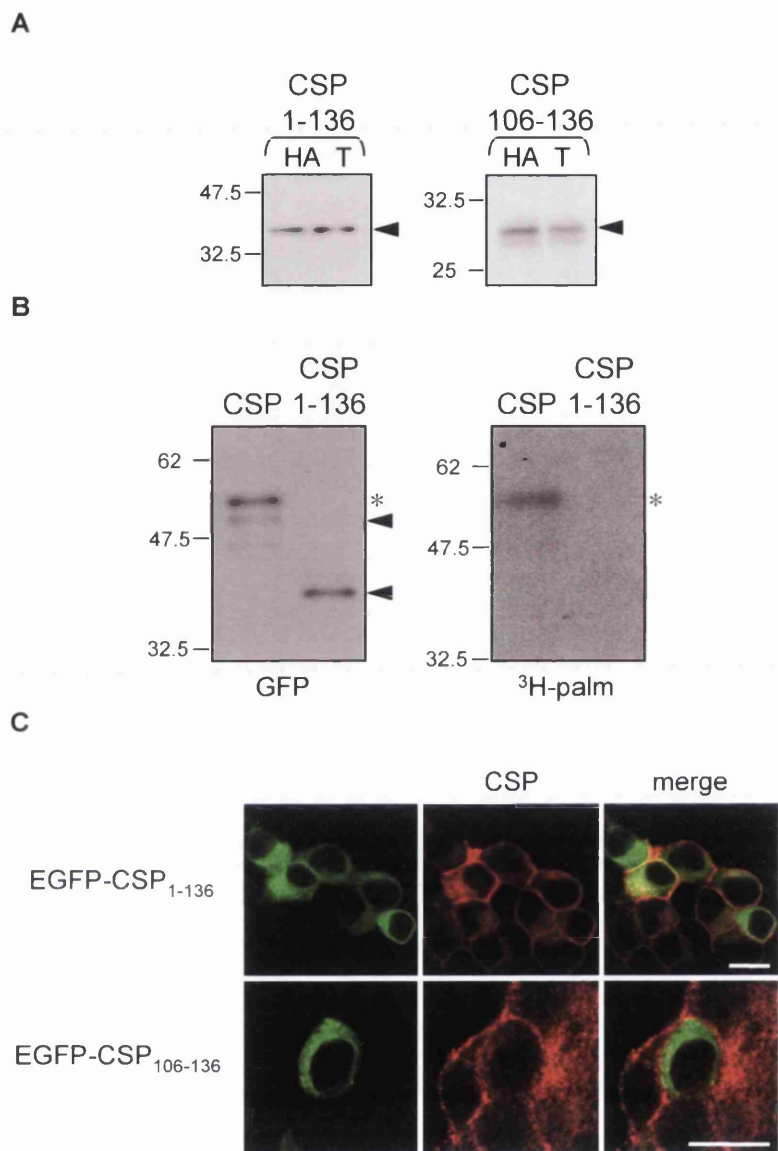
Figure 3.4 CSP C-terminal truncation mutants are unpalmitoylated and mislocalised

Figure 3.4 CSP C-terminal truncation mutants are unpalmitoylated and mislocalised. *A.* PC12 cells were transfected with EGFP-CSP$_{(1-136)}$ or EGFP-CSP$_{(106-136)}$ for 48 h and isolated cell membranes were incubated in 1M Tris, pH 7.0 (T) or 1M hydroxylamine, pH 7.0 (HA) for 20 hours at room temperature. The treated membranes were recovered by centrifugation at 196 000 x *g* for 30 minutes and analysed following SDS-PAGE and transfer to nitrocellulose membranes by immunoblotting using an anti-GFP monoclonal antibody. *B.* PC12 cells were transfected with EGFP-CSP or EGFP-CSP$_{(1-136)}$ for 48 h followed by incubation in ^{3}H palmitate for 4 hours. EGFP-CSP and EGFP-CSP$_{(1-136)}$ were immunoprecipitated from cell lysates and subjected to SDS-PAGE and transfer to nitrocellulose membranes, in duplicate. One membrane was analysed by probing with a monoclonal anti-GFP antibody (left; "GFP"), the other was processed for fluorographic detection of incorporated radiolabel (right; "^{3}H-palm"). The position of molecular weight standards (in kDa) is shown on the left side of panels *A* and *B*; *asterisks* identify palmitoylated CSP and *arrowheads* indicate unpalmitoylated CSP. The results shown in panels *A* and *B* are representative of a single experiment from three separate experiments. *C.* PC12 cells growing on glass coverslips and transfected with EGFP-CSP$_{(1-136)}$ or EGFP-CSP$_{(106-136)}$ for 48 h were fixed in 4% (v/v) formaldehyde, permeabilised and probed with a polyclonal anti-CSP antibody to label endogenous CSP. CSP labelling was detected by incubating with a rhodamine-conjugated anti-rabbit IgG (red) and compared with the GFP signal (green). Localisation of the labelled proteins was determined by confocal microscopy and images are representative of a single 0.13 μm thick confocal section. Scale bar = 10 μm.

Since EGFP-CSP$_{(1-136)}$ and EGFP-CSP$_{(106-136)}$ are membrane-bound but not efficiently palmitoylated *in vivo*, the subcellular membrane localisation of these mutants was determined to investigate whether they target EGFP to the same membranes as endogenous CSP. As protocols for subcellular fractionation of PC12 cells do not adequately separate internal membranes (Gonzalo and Linder, 1998), protein distribution was examined by transfecting PC12 cells with EGFP-CSP$_{(1-136)}$ or EGFP-CSP$_{(106-136)}$ for 48 hours, fixing and permabilising the cells, and comparing the localisation of EGFP-CSP$_{(1-136)}$ or EGFP-CSP$_{(106-136)}$ to that of endogenous CSP by confocal microscopy. To label endogenous CSP distribution, transfected cells were probed using an antibody that recognises the extreme C-terminus of CSP, thus preventing the cross-recognition of the ectopically expressed EGFP-tagged C-terminally truncated CSP mutants. Detection of antibody-labelled endogenous CSP was determined by probing cells with a rhodamine-conjugated anti-rabbit IgG antibody prior to visualisation by confocal microscopy. Figure 3.4C illustrates that, whereas endogenous CSP in PC12 cells has a punctuate distribution with partial enrichment at the plasma membrane (red), EGFP-CSP$_{(1-136)}$ (Figure 3.4C; *Upper panel*; green) and EGFP-CSP$_{(106-136)}$ (Figure 3.4C; *Lower panel*; green) have a clearly distinct localisation to endogenous CSP. Similarly, the distribution of these mutants is distinct from full-length EGFP-CSP (Figure 3.1D; *Right panel*), implying that these unpalmitoylated mutants are incorrectly sorted in PC12 cells.

The distribution of EGFP-CSP$_{(1-136)}$ and EGFP-CSP$_{(106-136)}$ was reminiscent of an ER localisation (Rocks *et al.*, 2005; Swarthout *et al.*, 2005). Thus, to determine the membrane compartment that the unpalmitoylated CSP C-terminal truncation mutants associate with, PC12 cells were transfected with full-length EGFP-CSP, EGFP-CSP$_{(1-136)}$ or EGFP-CSP$_{(106-136)}$ for 48 hours, the cells were fixed, permabilised and incubated with a polyclonal antibody recognising the ER resident protein calreticulin. Detection of antibody labelled calreticulin was determined by probing cells with a rhodamine-conjugated anti-rabbit IgG antibody prior to visualisation by confocal microscopy. As shown in Figure 3.5A, full-length EGFP-CSP (*Upper panel*) showed little overlap with the calreticulin staining. In contrast, EGFP-CSP$_{(1-136)}$ and EGFP-CSP$_{(106-136)}$ were both found to share significant overlap with calreticulin (Figure 3.5A; *middle* and *lower panels*). The presence of EGFP-CSP$_{(1-136)}$ and EGFP-CSP$_{(106-136)}$ at the ER was further confirmed by co-transfecting EGFP-CSP, EGFP-CSP$_{(1-136)}$ and EGFP-CSP$_{(106-136)}$ with DsRed2-ER, a red fluorescent protein fused to an ER targeting sequence (Figure 3.5B). Consistent with results presented in Figure 3.5A, EGFP-CSP$_{(1-136)}$ and EGFP-CSP$_{(106-136)}$ both showed marked overlap with DsRed-ER (Figure 3.5B, *middle* and *lower panels*), whereas transfected EGFP-CSP showed little overlap with the ER marker (Figure 3.5B; *Upper panel*). The results presented in this section show that although EGFP-CSP$_{(1-136)}$ and EGFP-CSP$_{(106-136)}$ are predominantly

A

B
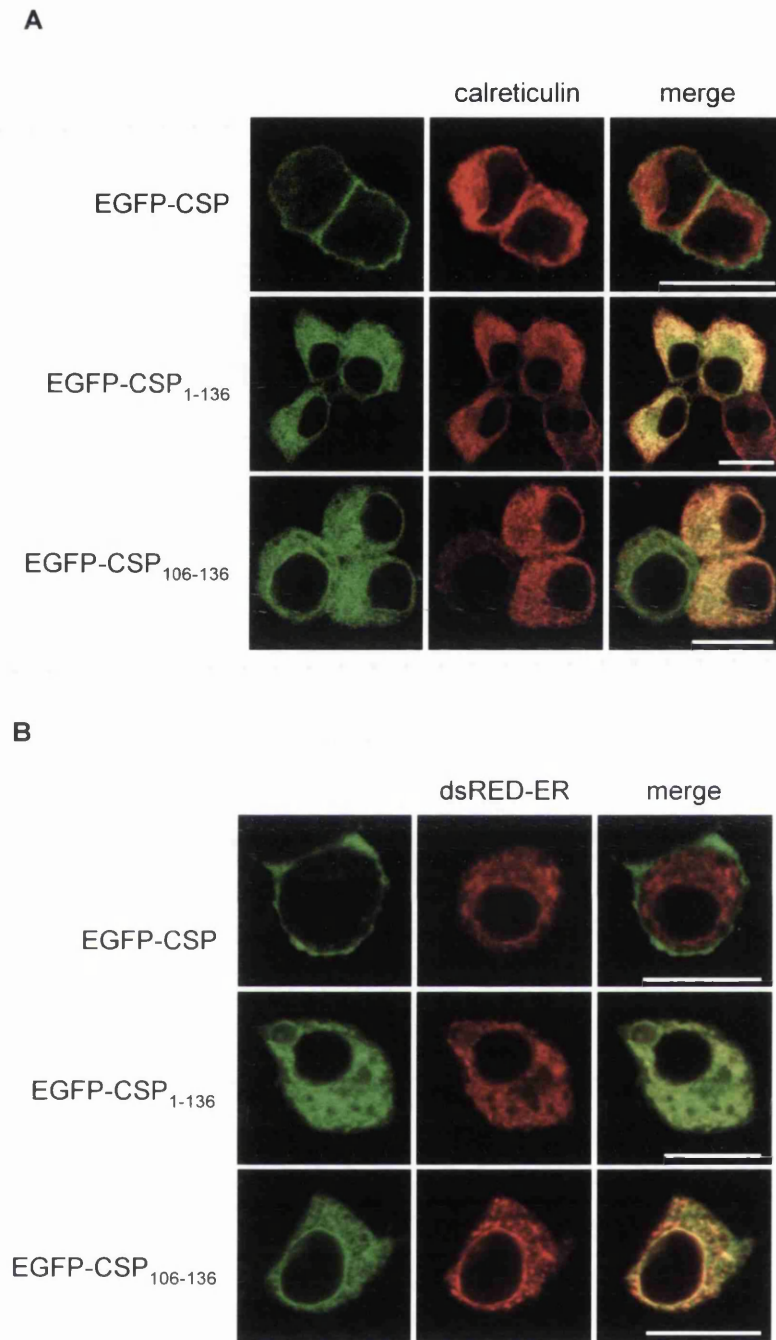
Figure 3.5 Localisation of CSP C-terminal truncation mutants in PC12 cells. *A*. PC12 cells growing on glass coverslips and transfected with EGFP-CSP, EGFP-CSP$_{(1-136)}$ or EGFP-CSP$_{(106-136)}$ for 48 h were fixed, permeabilised and probed with a polyclonal anti-calreticulin antibody. Calreticulin labelling was detected by probing with a rhodamine-conjugated anti-rabbit IgG (red) and compared with the GFP signal (green). *B*. PC12 cells growing on glass coverslips were cotransfected with dsRED-ER and EGFP-CSP, EGFP-CSP$_{(1-136)}$ or EGFP-CSP$_{(106-136)}$. Forty-eight hours post-transfection, the cells were fixed in 4% (v/v) formaldehyde and the localisation of the transfected proteins, dsRED-ER (red) and EGFP-CSP, EGFP-CSP$_{(1-136)}$ or EGFP-CSP$_{(106-136)}$ (green) was determined by confocal microscopy. Images are representative of a single 0.13 μm thick confocal section through PC12 cells. Scale bar = 10 μm.

associated with membranes, these mutant proteins are not palmitoylated and are mislocalised, showing noticeable overlap with ER marker proteins.

3.5 HYDROPHOBIC INTERACTIONS MEDIATE MEMBRANE BINDING OF NON-PALMITOYLATED CSP

Peripheral membrane proteins interact weakly with membranes through ionic interactions, and so they can be solubilised in solutions of high ionic strength or high pH, such as 1 M sodium chloride or 0.1 M sodium carbonate, pH 11.5, respectively. In contrast, integral membrane proteins that are embedded in the phospholipid bilayer, such as transmembrane proteins, interact strongly with membranes through hydrophobic interactions and can only be solubilised from membranes in solutions containing detergent, for example the non-ionic detergent Triton$^®$ X-100. Based on this difference in solubility, it is possible to determine whether a protein is a peripheral or integral membrane protein by incubating membranes in solutions containing 1 M sodium chloride, 0.1 M sodium carbonate, pH 11.5, or 1% (v/v) Triton$^®$ X-100 and measuring the extent of the release of proteins from the membranes. To examine the type of interactions that mediate EGFP-CSP$_{(1-136)}$ membrane association, membranes isolated from PC12 cells expressing EGFP-CSP and EGFP-CSP$_{(1-136)}$ were incubated in HES buffer (as a control), 1 M sodium chloride (NaCl), 0.1 M sodium carbonate, pH 11.5 (Na_2CO_3), or HES buffer containing 1% (v/v) Triton$^®$ X-100 for 30 minutes. Treated membranes were then centrifuged, and the extent of protein release from membranes under the various incubation conditions was determined by immunoblotting the recovered pellet (P) and supernatant (S) fractions. Figure 3.6 shows that the peripheral membrane proteins munc18-1 and αSNAP were released to different extents from membranes treated with sodium chloride or sodium carbonate. In contrast, full-length EGFP-CSP and EGFP-CSP$_{(1-136)}$ are both tightly associated with membranes, since their release into the supernatant only occurred following treatment with Triton X-100$^®$. This result is consistent with the idea that the initial membrane association of CSP (prior to palmitoylation) is mediated by hydrophobic interactions between the cysteine string domain and the membrane, and reveals that non-palmitoylated mutants of CSP can associate tightly with membranes in the absence of palmitoylation.

3.6 AMINO ACIDS DOWNSTREAM OF THE CYSTEINE STRING DOMAIN ARE REQUIRED FOR THE PALMITOYLATION AND CORRECT SORTING OF CSP

The major pool of the C-terminally truncated CSP mutant, EGFP-CSP$_{(1-136)}$, is membrane-bound but not palmitoylated (Figure 3.2 and 3.4A and B). To investigate whether regions downstream
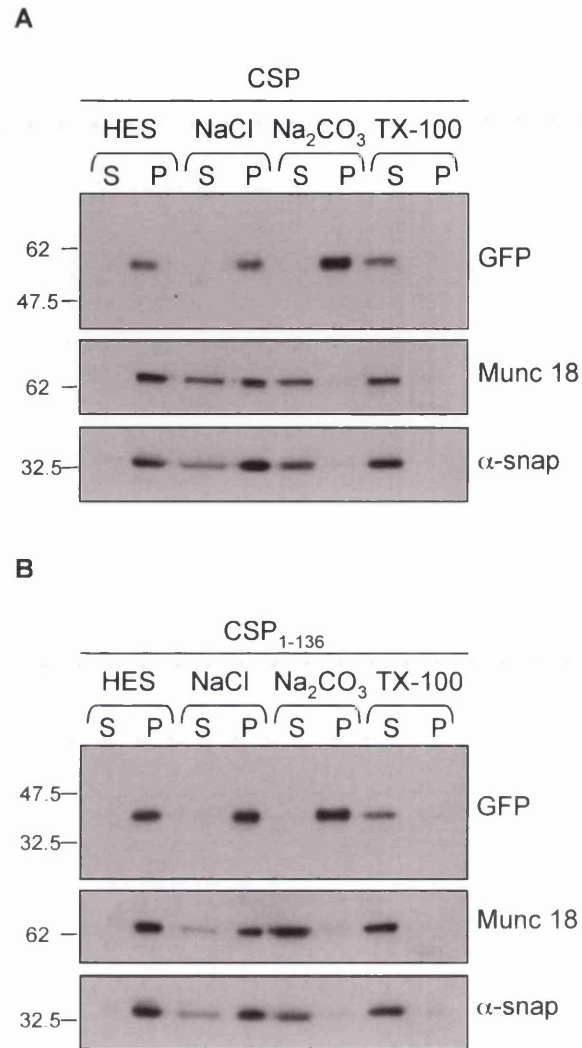
Figure 3.6 Analysis of membrane binding of EGFP-CSP and EGFP-CSP$_{(1-136)}$. PC12 cells were transfected with EGFP-CSP (*A*) or EGFP-CSP$_{(1-136)}$ (*B*) for 48 h and isolated cell membranes were incubated in HES Buffer, 1M NaCl, 0.1 M Na$_2$CO$_3$, pH 11.5, or HES Buffer supplemented with 1% (v/v) Triton® X-100 for 30 minutes at 4 °C. Supernatant (S) and pelleted membrane (P) fractions were recovered by centrifugation at 196 000 x *g* for 30 minutes and analysed following SDS-PAGE and transfer to nitrocellulose membranes by immunoblotting using an anti-GFP monoclonal antibody (*Upper panels*). To examine the partition of peripheral membrane proteins into supernatant and pelleted membrane fractions, nitrocellulose membranes were also probed using mouse monoclonal antibodies against Munc 18 (*Middle panels*) and α-SNAP (*Lower panels*). The position of molecular weight standards (in kDa) is shown on the left side of panels *A* and *B*, and the results shown are representative blots from the same experiment.

from the cysteine string domain are required for palmitoylation of CSP, several additional C-terminal CSP truncation mutants were constructed. PC12 cells were transfected with full-length EGFP-CSP, EGFP-CSP$_{(1-136)}$, EGFP-CSP$_{(1-146)}$, EGFP-CSP$_{(1-156)}$, or EGFP-CSP$_{(1-166)}$ for 48 hours. Cells were then fractionated into membrane and cytosolic fractions, and the protein distribution was determined by SDS-PAGE and immunoblotting. Efficient palmitoylation of the mutant proteins was indicated by a change in mobility (as shown in Figure 3.1). By this criterion EGFP-CSP$_{(1-146)}$, EGFP-CSP$_{(1-156)}$, and EFP-CSP$_{(1-166)}$ were all found to be efficiently palmitoylated due to the presence of a higher molecular weight band present in the membrane fraction, compared to the cytosolic fraction (Figure 3.7A; *upper panel*). These results are in contrast to EGFP-CSP$_{(1-136)}$ which migrates at the same position in both the cytosolic and membrane fractions (Figure 3.7A; *upper panel*). To confirm the faithful partition of proteins into cytosolic and membrane fractions, duplicate nitrocellulose membranes were probed to analyse the distribution of the transferrin receptor (TfR; Figure 3.7A, *Middle panel*) and protein kinase B (PKB; Figure 3.7A, *Lower panel*). Figure 3.7B shows that the palmitoylation of EGFP-CSP$_{(1-146)}$, but not EGFP-CSP$_{(1-136)}$, was efficient in PC12 cells, and not statistically different from full-length EGFP-CSP. Interestingly, despite being efficiently palmitoylated, EGFP-CSP$_{(1-146)}$, EGFP-CSP$_{(1-156)}$, and EFP-CSP$_{(1-166)}$ displayed a modest reduction in membrane binding (significant only for EGFP-CSP$_{(1-156)}$, and EFP-CSP$_{(1-166)}$). Thus, residues between amino acids 136-146 of CSP are clearly required for efficient palmitoylation of the cysteine string domain.

To identify the exact sequence of amino acids downstream from the cysteine string domain that are required for palmitoylation of CSP, EGFP-CSP$_{(1-137)}$, EGFP-CSP$_{(1-138)}$, EGFP-CSP$_{(1-139)}$, EGFP-CSP$_{(1-140)}$, EGFP-CSP$_{(1-141)}$, EGFP-CSP$_{(1-142)}$, EGFP-CSP$_{(1-143)}$, EGFP-CSP$_{(1-144)}$, and EGFP-CSP$_{(1-145)}$ truncation mutants were constructed and transfected into PC12 cells for 48 hours. Transfected cells were separated into membrane and cytosolic fractions, and protein distribution was determined by SDS-PAGE and immunoblotting using a monoclonal anti-GFP antibody. Efficient palmitoylation of the mutant proteins was determined by the band-shift assay as outlined in Chapter 3.2.1. An immunoblot showing the profile of these mutant proteins in cytosol and membrane fractions prepared from PC12 cells is shown in Figure 3.8A (*Upper panels*). To confirm the faithful partition of proteins into cytosolic and membrane fractions, duplicate nitrocellulose membranes were probed to analyse the distribution of the transferrin receptor (TfR; Figure 3.8A, *Middle panel*) and protein kinase B (PKB; Figure 3.8A, *Lower panel*). The immunoblot reveals that there is a gradual increase in the level of palmitoylation (*asterisk*) as the number of residues downstream from the cysteine string domain is increased, with the membrane-bound fraction of CSP showing an almost complete shift to a slower migrating, fully-palmitoylated band in the EGFP-CSP$_{(1-145)}$ mutant. The percentage
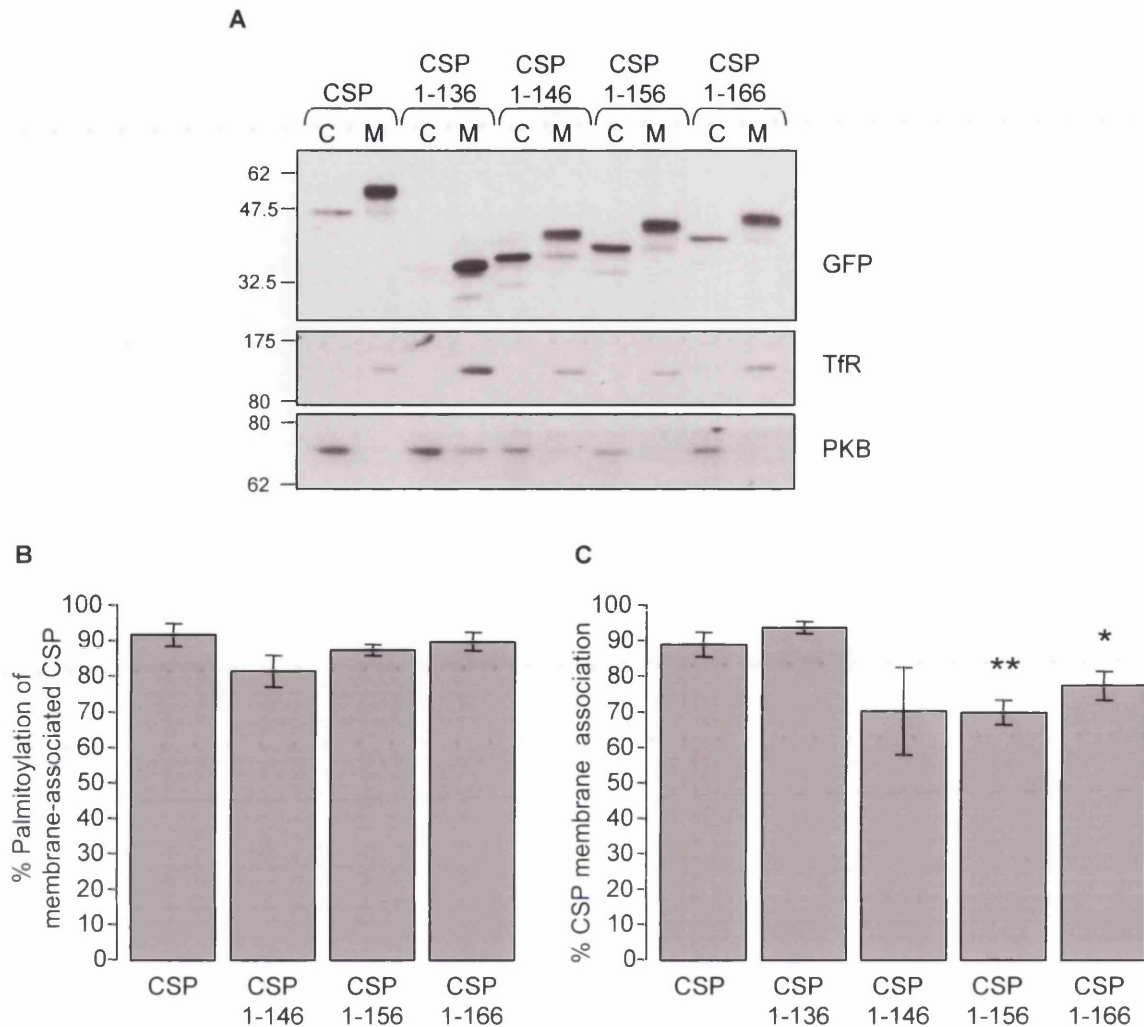
Figure 3.7 Amino acids downstream from the cysteine string domain are required for palmitoylation of CSP. *A*. PC12 cells transfected with wild-type EGFP-CSP, EGFP-CSP$_{(1-136)}$, EGFP-CSP$_{(1-146)}$, EGFP-CSP$_{(1-156)}$, or EGFP-CSP$_{(1-166)}$, for 48 h were fractionated into cytosolic (C) and membrane (M) fractions and analysed following SDS-PAGE and transfer to nitrocellulose membranes by immunoblotting using an anti-GFP monoclonal antibody (*Upper panel*). To confirm the faithful partition of proteins into cytosolic and membrane fractions, duplicate nitrocellulose membranes were probed to analyse the distribution the transferrin receptor (TfR, membrane protein; *Middle panel*) and protein kinase B (PKB, cytosolic protein; *Lower panel*). The position of molecular weight standards (in kDa) is shown on the left side of the panel. Representative blots are shown. *B*. The percentage CSP palmitoylation +/- SEM was determined by quantification of immunoblots by densitometry as a percentage of the total membrane-associated pool (n = 5 from 4 separate experiments). *C*. The percentage CSP membrane association +/- SEM was determined by quantification of immunoblots by densitometry (n = 5 from 4 separate experiments). Statistical significance was determined by a Student's *t*-test, whereby * represents a p value of < 0.05 and ** represents a p value of < 0.003, compared to wild-type EGFP-CSP.

A

B

C
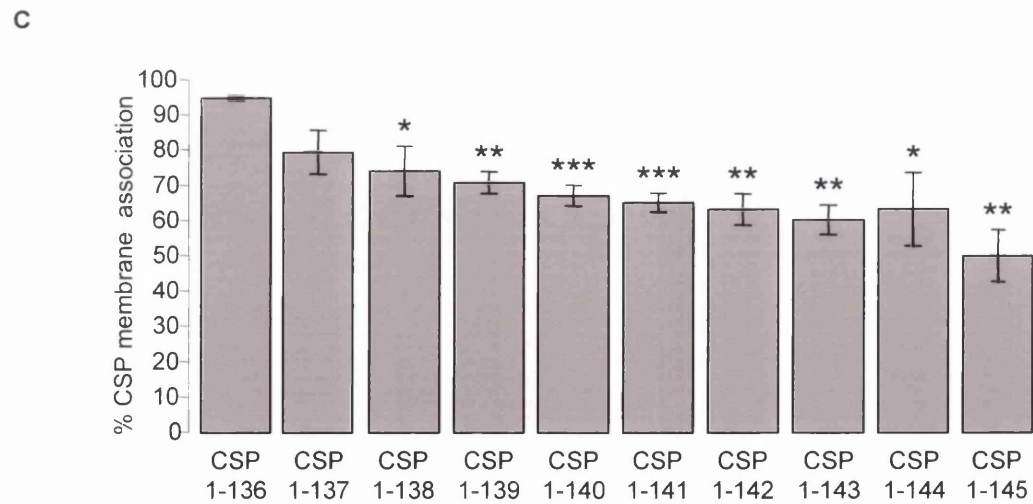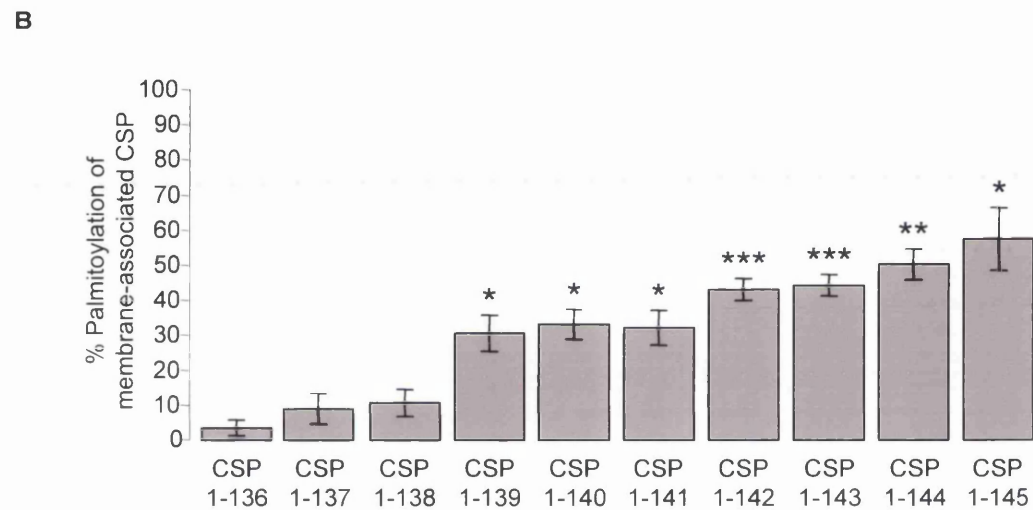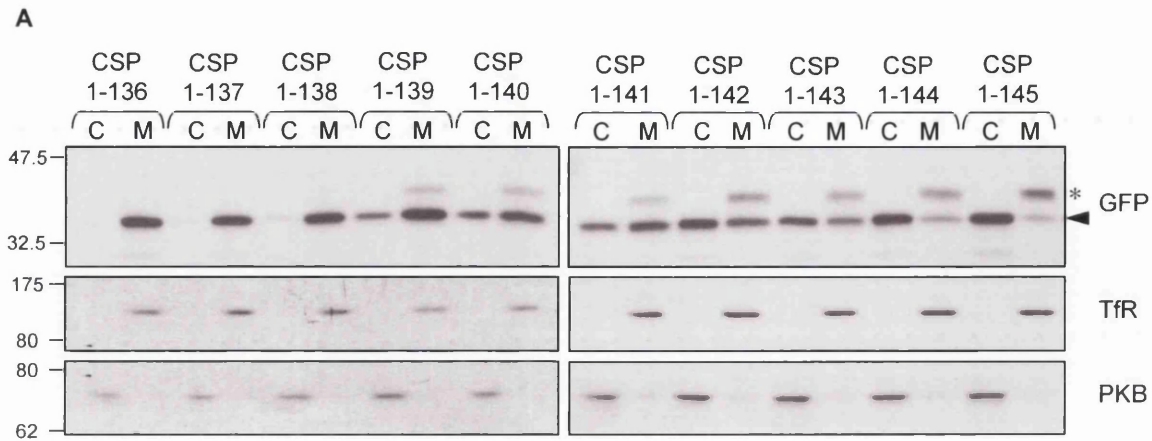
Figure 3.8 Amino acids downstream from the cysteine string domain are required for efficient palmitoylation and correct intracellular sorting of CSP *(continued overleaf)*.

D

E

calreticulin   merge

EGFP-CSP$_{1-146}$
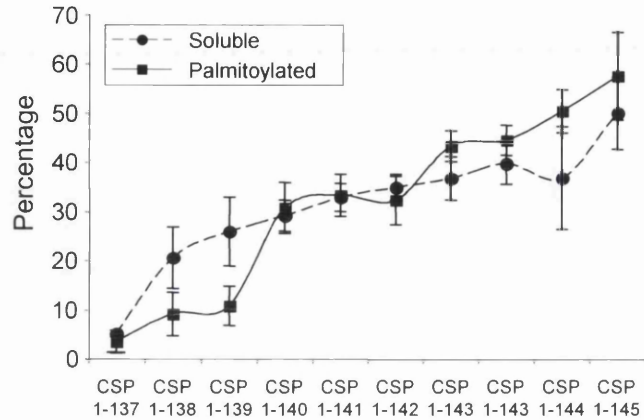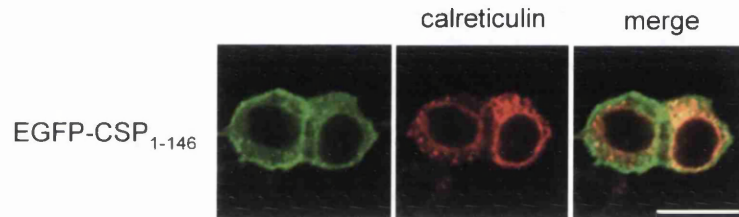
Figure 3.8 *(continued)* **Amino acids downstream from the cysteine string domain are required for efficient palmitoylation and correct intracellular sorting of CSP**. *A.* PC12 cells transfected with the indicated EGFP-CSP C-terminal truncation mutants for 48 h were fractionated into cytosolic (C) and membrane (M) fractions and analysed following SDS-PAGE and transfer to nitrocellulose membranes by immunoblotting using an anti-GFP monoclonal antibody (*Upper panel*). To confirm the faithful partition of proteins into cytosolic and membrane fractions, nitrocellulose membranes were probed to analyse the distribution of control proteins in the fractions, the transferrin receptor (TfR, membrane protein; *Middle panel*) and protein kinase B (PKB, cytosolic protein; *Lower panel*). The position of molecular weight standards (in kDa) is shown on the left side of the panel; *asterisks* identify palmitoylated CSP and *arrowheads* indicate unpalmitoylated CSP. Representative blots are shown. *B.* The percentage CSP palmitoylation +/- SEM was determined by quantification of immunoblots by densitometry as a percentage of the total membrane-associated pool (n = 4 from 2 separate experiments). Statistical significance was determined by a Student's *t*-test, whereby * represents a p value of < 5 x 10^{-3}, ** represents a p value of < 2 x 10^{-4} and *** represents a p value of < 4 x 10^{-5} compared to EGFP-CSP$_{(1-136)}$. *C.* The percentage CSP membrane association +/- SEM was determined by quantification of immunoblots by densitometry (n = 4 from 2 separate experiments). Statistical significance was determined by a Student's *t*-test, whereby * represents a p value of < 0.05, ** represents a p value of < 6 x 10^{-3} and *** represents a p value of < 10^{-3} compared to EGFP-CSP$_{(1-136)}$. *D.* The percentage palmitoylation of membrane-associated CSP +/- SEM plotted against the percentage of CSP recovered from the soluble fraction +/- SEM of the indicated EGFP-CSP C-terminal truncation mutants. *E.* PC12 cells growing on glass coverslips and transfected with EGFP-CSP$_{(1-146)}$ for 48 h were fixed in 4% (v/v) formaldehyde, permeabilised and probed with a polyclonal anti-calreticulin antibody. Calreticulin labelling was detected by probing with a rhodamine-conjugated anti-rabbit IgG (red) and compared with the GFP signal (green). Images are representative of a single 0.13 μm thick confocal section through PC12 cells. Scale bar = 10 μm.

palmitoylation of the truncation mutants was significantly increased after the addition of three amino acids downstream from the cysteine string domain (K137A, P138A, K139A) compared to EGFP-CSP$_{(1\text{-}136)}$ (Figure 3.8*B*). In addition to enhancing palmitoylation of CSP, the addition of extra amino acids to the C-terminus of the cysteine string domain also appeared to increase the soluble pool of the protein (Figure 3.8*A*, *Upper panel*; "C"), and became significant after the addition of two extra amino acids following the cysteine string domain (Figure 3.8*C*). Thus, amino acids immediately downstream from the cysteine string domain are required for the efficient palmitoylation of CSP.

Interestingly, and as mentioned above, there is an increase in solubility (decrease in membrane association) of the C-terminal truncation mutants as the number of amino acids downstream from the cysteine string domain increases (See Figure 3.8*A* and *B*). To explore the possibility that the decrease in membrane affinity of the C-terminal truncation mutants is associated with the increase in their palmitoylation status, the percentage of protein recovered from the soluble fraction of PC12 cells expressing the C-terminal truncation mutants was plotted against the percentage palmitoylation of the membrane-associated pool. As can be seen from Figure 3.8*D*, there is a direct correlation between the differential solubility of the C-terminal truncation mutants and their ability to become palmitoylated. The correlation between CSP membrane affinity and the palmitoylation status of CSP indicates that the strength of membrane binding of CSP may be regulating the ability of CSP to get palmitoylated. However, other experiments will be needed to determine whether these effects are merely correlative or causal.

To explore the possibility that efficient palmitoylation of CSP corresponds to a change in intracellular localisation, the distribution of EGFP-CSP$_{(1\text{-}146)}$ in PC12 cells was examined by confocal imaging; cells were transfected with EGFP-CSP$_{(1\text{-}146)}$ for 48 hours, fixed, permabilised and incubated with a polyclonal anti-calreticulin antibody to label the ER. Detection of antibody labelled calreticulin was determined by probing cells with a rhodamine-conjugated anti-rabbit IgG antibody prior to visualisation by confocal microscopy. As shown in Figure 3.8*D*, EGFP-CSP$_{(1\text{-}146)}$ has a subcellular distribution similar to that of full-length EGFP-CSP (See Figure 3.5*A*; *Upper panel*) and does not show the same ER overlap as EGFP-CSP$_{(1\text{-}136)}$ (Figure 3.5*A*: *Middle panel*). Thus, these results point to a model whereby efficient palmitoylation of the CSP C-terminal truncation mutants correlates with their correct intracellular sorting.

To investigate the mechanism whereby addition of downstream residues facilitates palmitoylation of the cysteine string domain, a series of point mutations were created in the amino acids directly downstream from the cysteine string domain, in *full-length* EGFP-CSP;

K137A, P138A, K139A, A140L, P141A, E142A and G143A. This analysis is particularly important in order to test whether residues downstream of the cysteine string domain, which regulate the palmitoylation of CSP truncation mutants, also regulate the palmitoylation of full-length CSP. PC12 cells were transfected with these mutant constructs for 48 hours. Expressed proteins were separated into membrane and cytosolic fractions, and protein distribution was determined by SDS-PAGE and immunoblotting. Efficient palmitoylation of the mutant proteins was determined by the band-shift assay as discussed in Chapter 3.2.1. An immunoblot showing the profile of these mutant proteins in cytosol and membrane fractions prepared from PC12 cells is shown in Figure 3.9A (*Upper panel*). The middle and lower panels compares the distribution of the transferrin receptor (TfR; Figure 3.9A, *Middle panel*) and protein kinase B (PKB; Figure 3.9A, *Lower panel*). Interestingly, as shown in the upper panel of Figure 3.9A, mutation of lysine 137 to alanine (K137A) was found to significantly reduce membrane binding and palmitoylation of CSP (Figure 3.9A-C), implying that this residue is important for efficient membrane binding and/or palmitoylation of the cysteine string domain. In contrast, mutation of any other residue in the domain had no effect on either the level of membrane association or palmitoylation of EGFP-CSP (Figure 3.9A-C). Thus, lysine 137 has a critical role in both the membrane association and palmitoylation of full-length CSP, in agreement with the required role for this residue in the palmioylation of CSP truncation mutants (Figure 3.8).

To further investigate the role of lysine 137 in membrane binding and palmitoylation, alternative point mutations were constructed at this site. A conservative substitution of lysine-to-arginine (K137R), or the introduction of an oppositely charged glutamic acid residue (K137E), were assessed for effects on membrane binding and palmitoylation (Figure 3.10A (*upper panel*), B-C). As before, the faithful partition of proteins into cytosolic and membrane fractions was confirmed by probing duplicate nitrocellulose membranes for the transferrin receptor (TfR; Figure 3.10A, *Middle panel*) and protein kinase B (PKB; Figure 3.10A, *Lower panel*). Interestingly, as determined by the band shift assay, both K137R and K137E mutations were tolerated far better than the K137A mutation, and displayed membrane binding and palmitoylation (*asterisk*) at similar to wild-type levels (Figure 3.10A; compare with wild-type EGFP-CSP in Figure 3.9A). This is in contrast to the K137A mutant, which had significantly reduced membrane binding compared to wild-type EGFP-CSP (See above). Similarly, the percentage palmitoylation of the membrane-associated pool of both the K137E and the K137R mutants was not significantly different to that of wild-type EGFP-CSP. These results suggest that lysine 137 may be important in maintaining the correct membrane orientation of the cysteine string domain, rather than specifying interaction with a PAT. This region of the protein may require to be localised at the surface of the membrane to allow efficient palmitoylation of

A
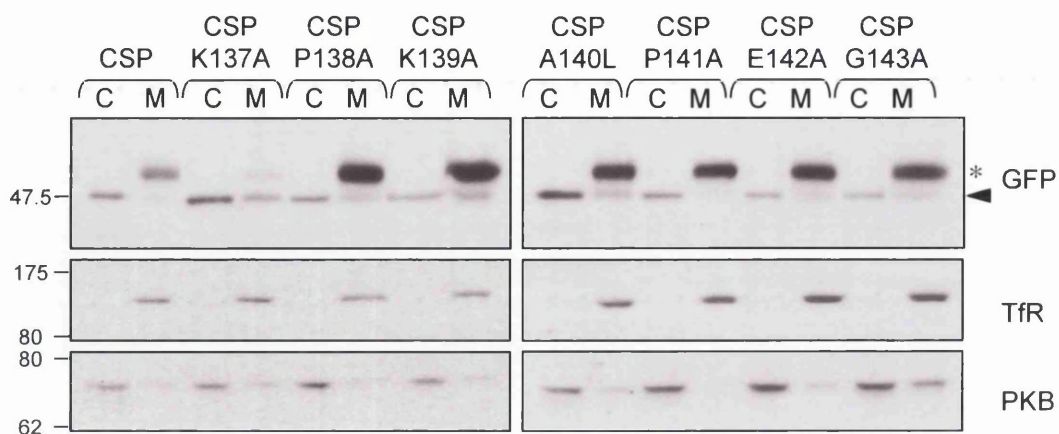
B
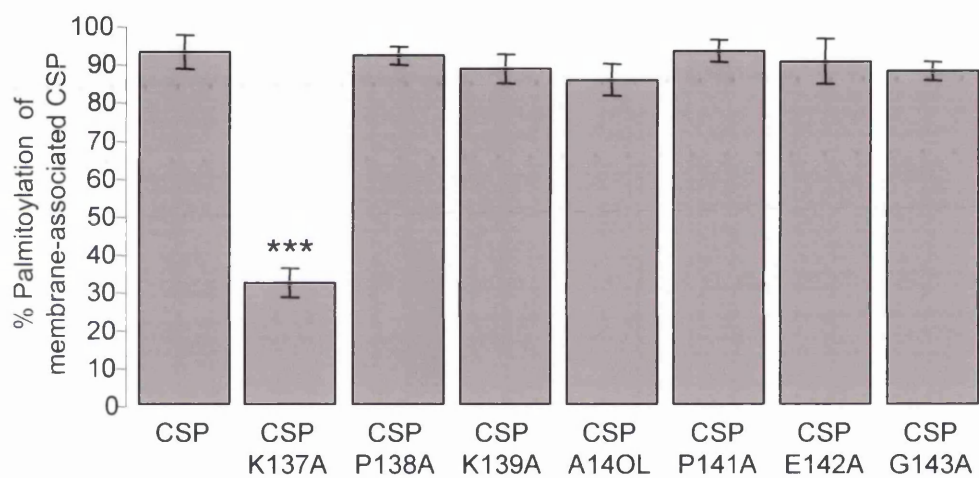
C
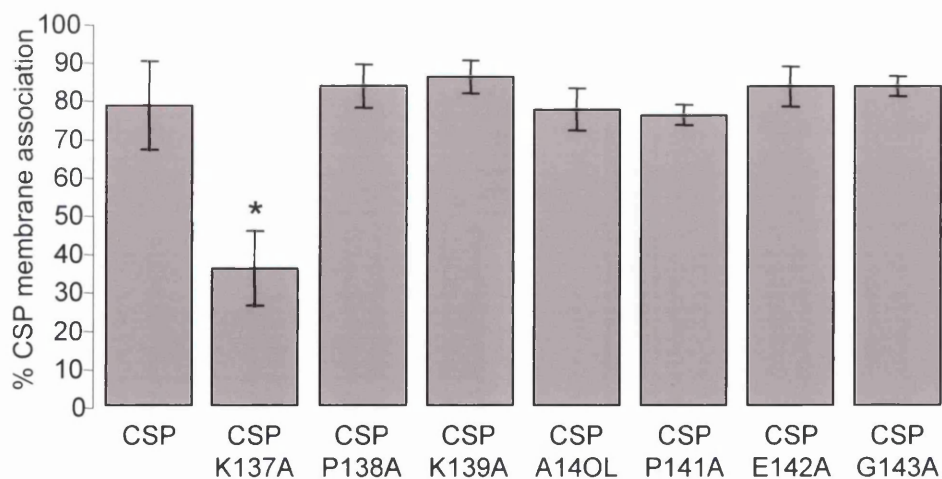
Figure 3.9 Requirement for a specific amino acid downstream from the cysteine string domain for efficient membrane association and palmitoylation of full-length CSP.

Figure 3.9 Requirement for a specific amino acid downstream from the cysteine string domain for efficient membrane association and palmitoylation of full-length CSP. *A.* PC12 cells transfected with wild-type EGFP-CSP or EGFP-CSP point mutants (K137A, P138A, K139A, A140L, P141A, E142A or G143A) for 48 h were fractionated into cytosolic (C) and membrane (M) fractions and analysed following SDS-PAGE and transfer to nitrocellulose membranes by immunoblotting using an anti-GFP monoclonal antibody (*Upper panel*). To confirm the faithful partition of proteins into cytosolic and membrane fractions, duplicate nitrocellulose membranes were probed to analyse the distribution of the transferrin receptor (TfR, membrane protein; *Middle panel*) and protein kinase B (PKB, cytosolic protein; *Lower panel*). The position of molecular weight standards (in kDa) is shown on the left side of the panel; *asterisks* identify palmitoylated CSP and *arrowheads* indicate unpalmitoylated CSP. Representative blots are shown. *B.* The percentage CSP palmitoylation +/- SEM was determined by quantification of immunoblots by densitometry as a percentage of the total membrane-associated pool (n=3 from 3 separate experiments). Statistical significance was determined by a Student's *t*-test, whereby *** represents a p value of <0.0003 compared to wild-type EGFP-CSP. *C.* The percentage CSP membrane association +/- SEM was determined by quantification of immunoblots by densitometry (n=3 from 3 separate experiments). Statistical significance was determined by a Student's *t*-test, whereby * represents a p value of <0.03 compared to wild-type EGFP-CSP.
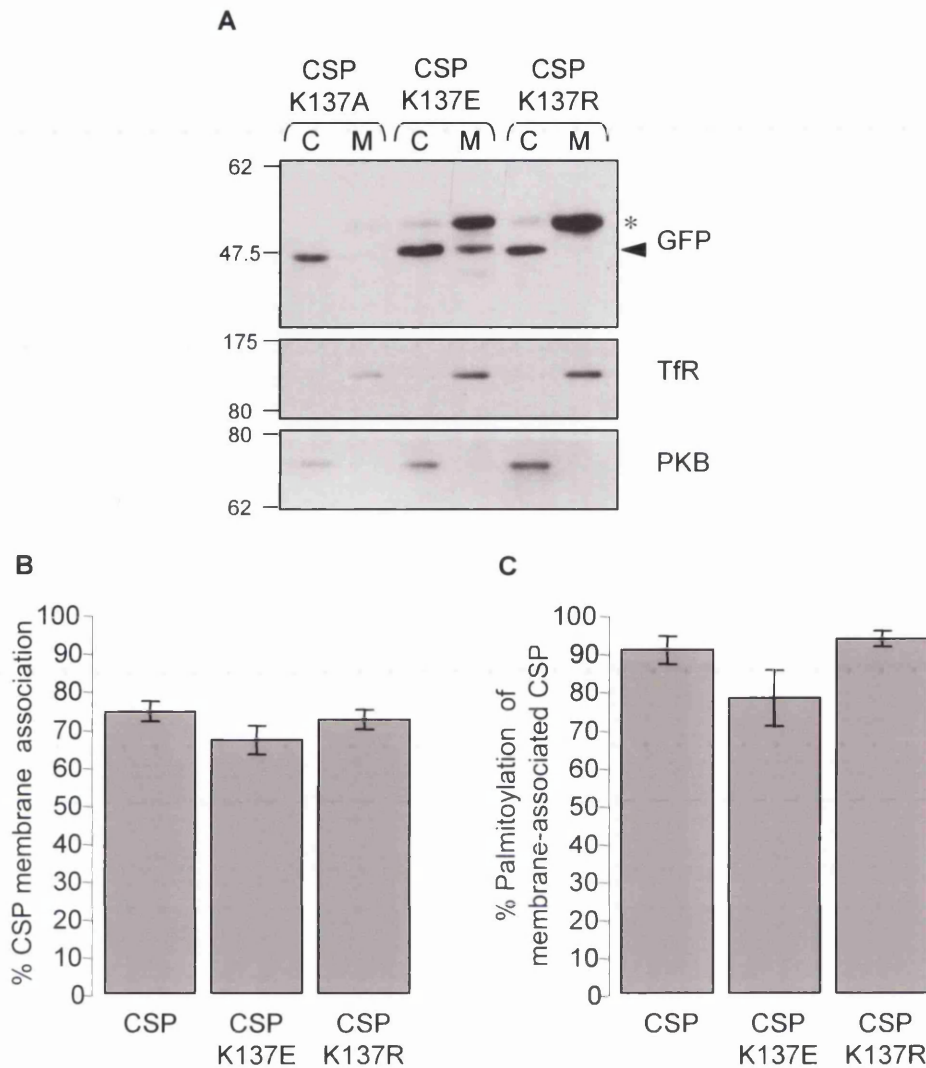
Figure 3.10 Differential effects of K137 substitutions on the membrane binding and palmitoylation of CSP. *A*. PC12 cells transfected with EGFP-CSP(K137) point mutants (K137A, K137E or K137R) for 48 h were fractionated into cytosolic (C) and membrane (M) fractions and analysed following SDS-PAGE and transfer to nitrocellulose membranes by immunoblotting using an anti-GFP monoclonal antibody (*Upper panel*). To confirm the faithful partition of proteins into cytosolic and membrane fractions, duplicate nitrocellulose membranes were probed to analyse the distribution of the transferrin receptor (TfR, membrane protein; *Middle panel*) and protein kinase B (PKB, cytosolic protein; *Lower panel*). The position of molecular weight standards (in kDa) is shown on the left side of the panel; *asterisks* identify palmitoylated CSP and *arrowheads* indicate unpalmitoylated CSP. The results shown are representative blots from the same experiment. *B*. The percentage CSP membrane association +/- SEM was determined by quantification of immunoblots by densitometry (n=3 from 2 separate experiments). *C*. The percentage CSP palmitoylation +/- SEM was determined by quantification of immunoblots by densitometry as a percentage of the total membrane-associated pool (n=3 from 2 separate experiments).

the cysteine string domain; this extra-membrane position would presumably be satisfied by the charged lysine, arginine or glutamic acid residues, whereas alanine may be more embedded in the lipid bilayer.

3.7 CONSERVED AMINO ACIDS UPSTREAM OF THE CYSTEINE STRING DOMAIN ARE IMPORTANT FOR CSP MEMBRANE BINDING

Finally, the primary sequence of the minimal membrane-binding domain of CSP (amino acids 106-136) from various species was examined to identify conserved amino acids upstream from the cysteine string domain that may be important for CSP membrane binding. As illustrated in Figure 3.3*E*, there are several conserved amino acids immediately upstream of the cysteine string domain, within the minimal membrane-binding domain. Point and double mutations of the conserved lysine at position 107 and the conserved leucine at point 109 were constructed in full-length EGFP-CSP, and these mutants were transfected into PC12 cells for 48 hours. Expressed proteins were separated into membrane and cytosolic fractions, and protein distribution was determined by SDS-PAGE and immunoblotting. Efficient palmitoylation of the mutant proteins was determined by the band-shift assay as detailed in Chapter 3.2.1. An immunoblot showing the profile of these mutant proteins in cytosol and membrane fractions prepared from PC12 cells is shown in Figure 3.11*A*. Figure 3.11*A* reveals that the proportion of the K107R, L109A and L109E mutants partitioning in the membrane fraction is similar to that of wild-type EGFP-CSP. The K107A and K107E point mutants, and the K107A/L109A and K107E/L109E double mutants, however, appear to have increased solubility compared to wild-type EGFP-CSP.

To confirm the reduction in membrane binding of the K107A and K107E point mutants, and the K107A/L109A and K107E/L109E double mutants statistically, immunoblots were quantified by densitometry and the percentage membrane binding is illustrated in Figure 3.11*B*. Indeed, compared to wild-type EGFP-CSP, the membrane binding of the K107A and K107E point mutants, and the K107A/L109A and K107E/L109E double mutants were significantly reduced. In contrast, the percentage membrane association of the K107R, L109A and L109E mutants was not statistically different to that of wild-type EGFP-CSP. Overall, this mutational analysis highlights an important role of the residues upstream of the cysteine string domain for membrane recognition and palmitoylation of full-length CSP, and supports the truncation analysis, which found a role for residues 106-136 in membrane binding.
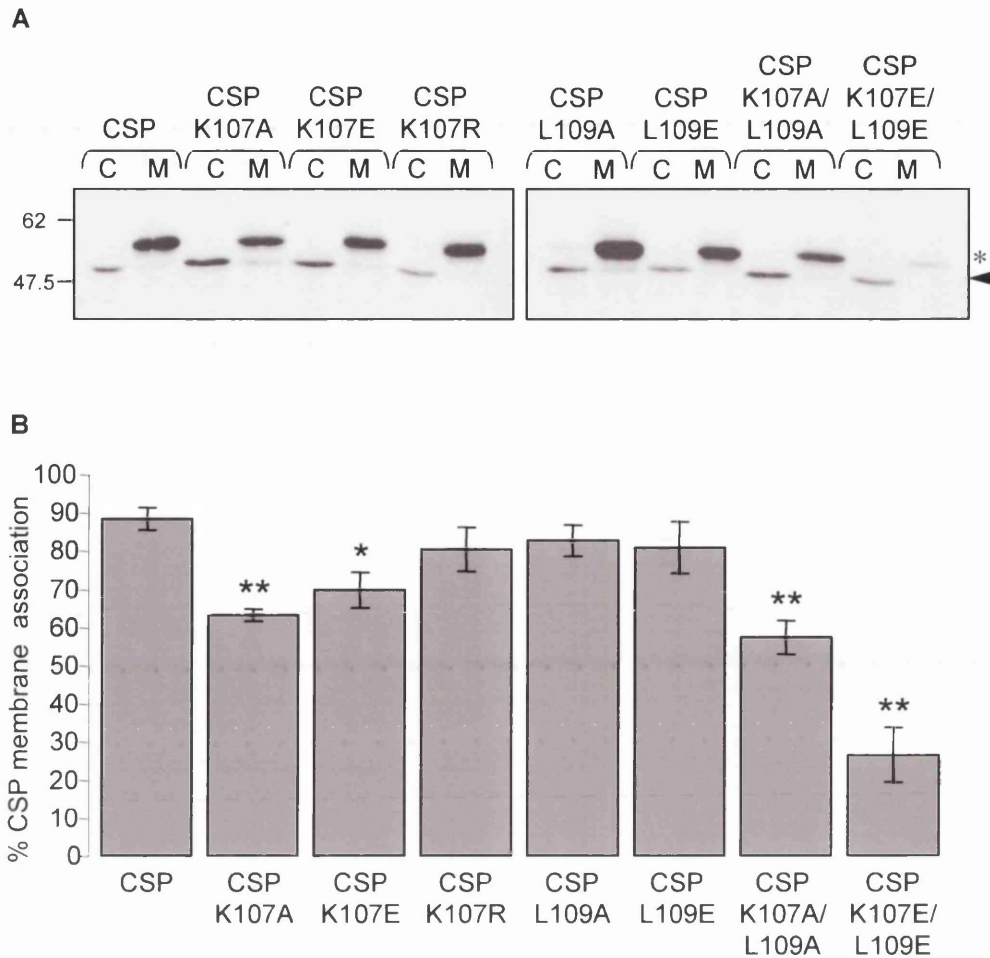
Figure 3.11 **Amino acids upstream from the cysteine string domain are required for efficient membrane binding of full-length CSP**. *A*. PC12 cells transfected with wild-type EGFP-CSP, EGFP-CSP(K107) point mutants (K107A, K107E or K107R), EGFP-CSP(L109) point mutants (L109A or L109E) or EGFP-CSP(K107/L109) double mutants (K107A/L109A or K107E/L109E) for 48 h were fractionated into cytosolic (C) and membrane (M) fractions and analysed following SDS-PAGE and transfer to nitrocellulose membranes by immunoblotting using an anti-GFP monoclonal antibody. The position of molecular weight standards (in kDa) is shown on the left side of the panel; *asterisks* identify palmitoylated CSP and *arrowheads* indicate unpalmitoylated CSP. Representative blots are shown. *B*. The percentage CSP membrane association +/- SEM was determined by quantification of immunoblots by densitometry (n=3 from 3 separate experiments). Statistical significance was determined by a Student's *t*-test, whereby * represents a p value < 0.03 and ** represents a p value < 0.004 compared to wild-type EGFP-CSP.

3.8 DISCUSSION

The mechanisms that control the initial membrane attachment of some soluble palmitoylated proteins are poorly understood. CSP is synthesized as a soluble protein and does not undergo any other known lipid modification prior to palmitoylation. Since palmitoyl transferases are integral membrane proteins, CSP must have a mechanism to associate with the membrane that houses the appropriate PAT for palmitate transfer to occur. The results in this chapter have demonstrated that the minimum membrane-binding domain of CSP maps to amino acids 106-136. This membrane targeting domain includes the cysteine string domain (amino acids 113-136) and a short stretch of amino acids immediately upstream in the linker domain. An interesting question is whether this domain associates directly with membranes or if another protein is required to present newly synthesized CSP to membranes. If this were the case, then the minimum membrane binding domain of CSP would presumably serve as the minimum binding site for these molecules. None of the known CSP binding partners interact specifically with residues 106-136, and thus if CSP is targeted to membranes by a "chaperone" then the identity of this molecule is unknown. The interaction of the minimal membrane binding domain of CSP with other molecules could be tested directly, for example by using purified recombinant protein encoding this domain as bait against cell lysates, followed by mass spectrometry analysis of putative interacting proteins.

Interestingly, the membrane binding of CSP truncation mutants (EGFP-CSP$_{(1-136)}$ and EGFP-CSP$_{(106-136)}$) occurs in the absence of CSP palmitoylation. This finding implies that membrane binding alone is not sufficient to initiate palmitoylation. The observation that truncated CSP mutants bind to membranes in the absence of palmitoylation also suggests that the minimum membrane binding domain is sufficiently hydrophobic to associate tightly with membranes. Indeed, these mutants remain associated with membranes after treatment with solutions of high ionic strength or high pH, and are only released from membranes following treatment with Triton® X-100. Therefore, the initial interaction of CSP with membranes is likely to involve direct hydrophobic interactions with membrane lipids. The interaction of the minimal membrane binding domain of CSP with lipids could be tested directly by examining the interaction of this domain with liposomes *in vitro*. Furthermore, by preparing liposomes with different lipid compositions, it would be possible to assess whether this domain of CSP has a specific lipid preference.

The finding that CSP truncation mutants are able to bind membranes tightly in the absence of palmitoylation raises the possibility that palmitoylation of CSP has functions independent of

membrane anchoring. One possibility is that extensive palmitoylation is somehow required for the function of CSP. The known functions of palmitoylation, in addition to promoting stable membrane binding, include: mediating protein-protein interactions (Hayashi *et al.*, 2005; Washbourne *et al.*, 2001), regulating protein folding or promoting protein stability (Lam *et al.*, 2006; Valdez-Taubas and Pelham, 2005), targeting proteins to distinct subcellular membranes or membrane microdomains (El-Husseini *et al.*, 2001; Roy *et al.*, 2005), and regulating the trafficking of proteins between intracellular membranes (Goodwin *et al.*, 2005; Kang *et al.*, 2004; Kinlough *et al.*, 2006; Rocks *et al.*, 2005).

Palmitoylation of CSP could perhaps regulate interactions with other proteins, such as the chaperone protein Hsc70, syntaxin1A, VAMP or synaptotagmin. Although the majority of binding studies used to identify CSP binding partners have utilised recombinant CSP, which is unpalmitoylated, palmitoylation could exert a more subtle regulation on any of these interactions. It is possible that the extensive palmitoylation of CSP is more important in regulating CSP interactions *in vivo* than *in vitro*. For example, palmitoylation may ensure CSP has an optimal membrane topology to facilitate interactions with binding partners.

Another possibility could be that palmitoylation of CSP is directly involved in membrane fusion events. To examine this, correctly sorted but palmitoylation deficient CSP mutants could be employed to assess whether a reduced level of palmitoylation had any effects on exocytosis, assayed, for example, using carbon fibre amperometry (Graham and Burgoyne, 2000). Such functional studies would benefit from a procedure to inactivate endogenous CSP, such as RNA interference.

If palmitoylation were to regulate the correct folding or promote the stability of CSP, it is reasonable to assume that unpalmitoylated CSP would form aggregates when expressed in cells, or would become degraded. Confocal microscopy of fluorescently labelled expressed proteins would allow any protein aggregation to be visualised, and pulse-chase labelling using radioisotopes would allow the half-life of the protein to be determined and compared to that of wild-type CSP: a decrease in half-life would suggest increased protein degradation.

Another possibility is that palmitoylation is required for the correct intracellular sorting of CSP, perhaps due to palmitate anchors preferentially partitioning into specific subcellular membranes or membrane microdomains. In this way, palmitoylation may act as a retention signal, by trapping CSP once it reaches a specific intracellular compartment. Alternatively, palmitoylation may serve to target CSP to the site of vesicle budding, thus facilitating the sorting of CSP onto

vesicle membranes. In support of this idea was the observation that unpalmitoylated CSP truncation mutants are localised almost exclusively to membranes of the ER, and not to the plasma membrane/vesicles where full-length CSP is resident. This suggests that the lack of extensive palmitoylation may interfere with the targeting of CSP to vesicle membranes. Indeed, once CSP truncation mutants become palmitoylated, following the addition of amino acids downstream of the cysteine string domain, they are no longer localised at the ER; instead, they are correctly sorted to post-ER membrane compartments. Thus, the results suggest, at present, that the palmitoylation of CSP functions to sort CSP to its correct intracellular compartment. It would be interesting to determine how many, and which, cysteines within the cysteine string domain are required for the correct intracellular sorting of CSP.

As unpalmitoylated CSP mutants are associated with the ER, an obvious possibility is that CSP binding to ER membranes precedes palmitoylation, and that the enzyme(s) that palmitoylate CSP are ER-resident. However, since palmitoylating enzymes are localised to various intracellular membranes in addition to the ER, including the Golgi apparatus, the plasma membrane and endosomes, it will be important to identify CSP palmitoylating enzymes to more fully understand why unpalmitoylated CSP mutants are localised to the ER. For example, it could be that unpalmitoylated CSP accumulates at the ER if it cannot be trapped at other membranes by palmitoylation. Indeed, one possibility that needs to be considered is that the loss of the C-terminal domain may inadvertently force CSP truncation mutants to bind to inappropriate membranes (such as the ER) and become physically separated from their partner PAT.

The proposed role of palmitoylation in regulating CSP traffic out of the ER is similar to the previously reported palmitoylation-dependent sorting of Ras proteins from the ER/Golgi to the PM (Goodwin *et al.*, 2005; Rocks *et al.*, 2005). However, it is not clear how palmitoylation facilitates sorting to post-ER compartments. Palmitoylation has been proposed to increase the affinity of proteins for specific subdomains of the plasma membrane (Melkonian *et al.*, 1999), and, by analogy, palmitoylation may therefore also promote the lateral segregation of proteins at the ER into domains that regulate vesicle budding. This could occur, for example, if palmitoylation increased the affinity of CSPs for a specific membrane geometry such as that occurring at ER exit sites. Alternatively, because palmitoylation has previously been suggested to regulate protein–protein interactions (Hayashi *et al.*, 2005; Washbourne *et al.*, 2001), palmitoylation of CSP may enhance its binding to an ER-localised sorting chaperone. Another possibility is that palmitoylation of CSP increases its affinity for cholesterol-rich membrane

domains, and the increasing gradient of cholesterol from the ER-Golgi-plasma membrane may thus regulate the sorting of palmitoylated CSP (Mitra *et al.*, 2004).

Interestingly, the addition of amino acids downstream from the cysteine string domain of CSP truncation mutants, whilst restoring palmitoylation, also led to an increase in the soluble pool of these mutants. The reason for this is not clear, but it will be worthwhile investigating whether the relationship between the increase in palmitoylation and weaker membrane binding of CSP are connected or are simply coincidental. A stronger membrane affinity may inhibit palmitoylation by physically separating the substrate from the enzyme (for example, if the substrate tightly binds to the wrong membrane). Alternatively, tight membrane binding may cause cysteine residues to become deeply embedded in the bilayer thereby being inaccessible to the palmitoyl transferase. One possibility is that the tight membrane association following loss of the C-terminal domain in the truncation mutants is caused by the inadvertent creation of an artificial membrane spanning domain, whereby the cysteine string domain becomes embedded, or even traverses, the lipid bilayer. The mapping of the minimum membrane binding domain of CSP to amino acids 106-136 agrees well with *in silico* analysis, which predicts a membrane domain between residues 108-130 of CSP (Boal *et al.*, 2007). The analysis revealed that this domain would be membrane embedded, but does not have a tendency to traverse the lipid bilayer. Thus, it is unlikely that removal of the C-terminal domain creates an artificial membrane spanning domain, though this possibility cannot be rejected.

The finding that palmitoylation and intracellular sorting of truncated CSP mutants was restored following the addition of residues downstream from the cysteine string domain prompted investigations into the requirement for specific amino acids within this region for palmitoylation of *full-length* CSP. Alanine scanning mutagenesis was employed to determine if individual residues downstream of the cysteine string domain were important for palmitoylation and membrane binding of full-length CSP. Indeed, membrane binding and palmitoylation of full-length CSP is abolished when the conserved lysine (K137) immediately downstream from the cysteine string domain is mutated to an alanine residue. The specific requirement for this lysine in CSP palmitoylation might be to form part of a recognition site for a palmitoyl transferase. If this were the case, then *in vitro* binding between recombinant purified CSP and specific palmitoyl transferases would be predicted to be significantly reduced following mutation of the lysine 137 residue. Alternatively, lysine 137 may be more important in regulating the correct membrane orientation of CSP. Since lysine is a charged amino acid it is likely have an extra-membrane position rather than be embedded in the bilayer; thus, it may help to orientate the cysteine string domain into a position at the membrane interface that facilitates palmitoylation.

If this were the case, by substituting the lysine for any other charged amino acids would be predicted to restore palmitoylation. Indeed, when lysine 137 was substituted for other charged amino acids (for example, arginine or glutamic acid), membrane binding and palmitoylation of CSP were preserved, suggesting that the lysine 137 is not critical for palmitoylation *per se*, and that any charged amino acids downstream of the cysteine string domain could likely fulfil this role. If this hypothesis were true, then substituting the lysine 137 for other charged hydrophilic amino acids, for example histidine or aspartatic acid, would be tolerated, whereas uncharged hydrophobic amino acids (for example alanine, leucine or valine) would change the conformation of the cysteine string domain to an unfavourable position that does not permit palmitoylation of the cysteines. Interestingly, a charged residue at the N-terminus of the minimum membrane binding domain of CSP is also required for membrane binding of CSP: mutation of lysine 107 to alanine significantly reduces membrane binding, while mutation to arginine has no effect. It is tempting to speculate that K107 has a similar role as K137, to facilitate the orientation of the cysteine string domain to a position that is favourable for palmitoylation to proceed. On a similar note, there is also a conserved lysine towards the end of the cysteine string domain (at position 135), which may also regulate membrane orientation.

The alignment of the minimum membrane binding domain of CSP from different species reveals there are many conserved residues within this region (Figure 3.3*E*). One of these conserved residues is leucine at position 109. Though mutation of this leucine to an alanine or glutamic acid had no noticeable effect on membrane binding of CSP, when the L109E mutant was introduced into CSP(K107E), it dramatically potentiated the reduction in membrane association brought about by the K107E, almost abolishing total membrane binding. It would be interesting to assess the importance of other conserved residues in this region for membrane targeting of CSP. Of particular interest would be to look at the conserved phenylalanine at position 110; phenylalanine residues could play an important role in membrane interactions due to the hydrophobicity of their side chain. Amino acid substitutions introduced at position 110 could therefore be used to assess the importance of this residue for membrane targeting.

CHAPTER FOUR: CYSTEINE HYDROPHOBICITY GOVERNS CSP MEMBRANE TARGETING

4.1 INTRODUCTION

The defining characteristic of CSP is its cysteine string domain, which encodes a stretch of twenty-four amino acids containing a contiguous "string" of fourteen cysteines, the majority of which are thought to be palmitoylated *in vivo* (Gundersen *et al.*, 1994). The results presented in chapter three reveal that, in PC12 cells, the cysteine string domain alone is not sufficient for membrane binding or palmitoylation of CSP. Instead, the cysteine string domain acts in concert with amino acids present in the linker domain to promote CSP membrane association.

Interestingly, the results presented in Chapter Three reveal that palmitoylation of CSP truncation mutants is not essential for membrane binding. These results suggest that the intrinsic hydrophobicity of these mutants is sufficient to promote membrane association. In support of this hypothesis, several studies have previously documented that CSP remains membrane associated following chemical depalmitoylation with hydroxylamine (Chamberlain and Burgoyne, 1998; Mastrogiacomo *et al.*, 1998; van de Goor and Kelly, 1996). Furthermore, chemically-depalmitoylated CSP can only be released from membranes by treating with detergent (Mastrogiacomo *et al.*, 1998), suggesting that CSP remains tightly bound to membranes following depalmitoylation. The membrane association of depalmitoylated CSP may be maintained by the ability of hydrophobic amino acids within the cysteine string domain to interact with the lipid bilayer: following deacylation, the cysteine residues within the cysteine string domain remain in a hydrophobic environment (Mastrogiacomo *et al.*, 1998).

Interestingly, a CSP mutant in which the seven central cysteine amino acids were mutated to more hydrophilic serine residues (7CS), was not palmitoylated and was entirely cytosolic in both PC12 and HeLa cells (Chamberlain and Burgoyne, 1998). This prompted the conclusion that although palmitoylation may not be required for stable membrane association of CSP (following depalmitoylation), it is required for *initial* membrane targeting (Chamberlain and Burgoyne, 1998a). However, since this study was published, palmitoyl transferases have been shown to be integral membrane proteins, and thus, *initial* membrane targeting of CSP must precede palmitoylation. The results presented in the previous chapter show that palmitoylation is not required for membrane binding of CSP truncation mutants, suggesting that there may be an alternative reason for the loss of membrane binding of the 7CS mutant. Although cysteine is often classified as a polar amino acid, the SH group in this amino acid is unreactive with water and thus it behaves essentially as a hydrophobic amino acid (Nagano *et al.*, 1999). Replacement of the seven central cysteines with the more polar amino acid serine, which has a hydrophilic hydroxyl group, may lead to the loss of an intrinsically hydrophobic cysteine string domain,

resulting in a more hydrophilic domain that is potentially unable to associate with membranes. Therefore, the 7CS mutant may be cytosolic and unpalmitoylated simply because of a loss of hydrophobicity, rather than a loss of cysteines *per se.*

The requirement of individual cysteines within the cysteine string domain for initial membrane binding and palmitoylation of CSP is not clear. In this chapter, the importance of individual cysteine residues for CSP membrane binding and palmitoylation will be assessed, and at the same time, the hypothesis that the intrinsic hydrophobicity of the cysteine string domain mediates CSP membrane binding prior to palmitoylation will be tested.

4.2 AN INTACT CYSTEINE STRING DOMAIN IS REQUIRED FOR EFFICIENT MEMBRANE ASSOCIATION OF CSP

Results presented in Figures 3.2-3 reveal that the cysteine string domain and the region immediately upstream mediate membrane association of CSP. However, it is not clear whether an intact cysteine string domain is required for membrane association. Previous studies have shown that a CSP mutant with a shortened cysteine string domain is membrane associated in *Drosophila*, suggesting that an intact cysteine string domain is not required for CSP membrane binding (Arnold *et al.*, 2004). To investigate whether regions within the cysteine string domain are dispensable for the membrane binding of mammalian CSP, two C-terminal CSP truncation mutants lacking the C-terminal half (CSP_{1-124}) or third (CSP_{1-128}) of the cysteine string domain were constructed. PC12 cells were transfected with $EGFP-CSP_{1-124}$, $EGFP-CSP_{1-128}$, $EGFP-CSP_{1-136}$ for forty-eight hours, followed by the separation of cells into cytosolic and membrane fractions. Equal volumes of the isolated cytosolic and membrane fractions were subjected to SDS-PAGE, transfer to nitrocellulose and immunoblotting using a monoclonal antibody against GFP. Figure 4.1 shows that, in contrast to $EGFP-CSP_{1-136}$, C-terminal mutants having a truncated cysteine string domain display significantly reduced levels of membrane association. These results reveal that an intact cysteine string domain is required for the efficient membrane association of CSP (in the absence of palmitoylation).

4.3 ROLE OF SPECIFIC CYSTEINES IN THE CYSTEINE STRING DOMAIN FOR MEMBRANE ASSOCIATION AND PALMITOYLATION OF CSP

Results from the previous section revealed that the entire cysteine string domain is required for efficient membrane association of CSP. However, the role that specific cysteine residues within
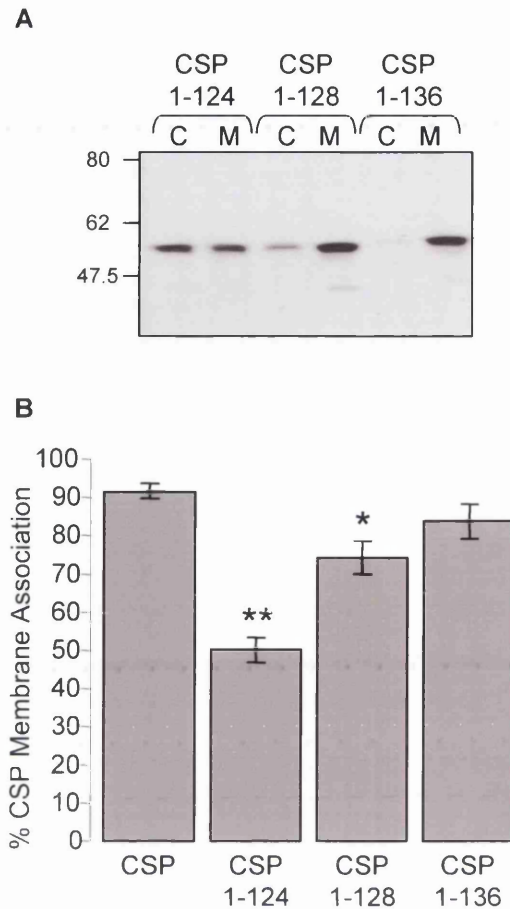
Figure 4.1 An intact cysteine sting domain is required for complete membrane binding of CSP. *A.* PC12 cells transfected with EGFP-CSP cysteine string domain truncation mutants (EGFP-CSP$_{(1-124)}$, EGFP-CSP$_{(1-128)}$ or EGFP-CSP$_{(1-136)}$) for 48 h were fractionated into cytosolic (C) and membrane (M) fractions and analysed following SDS-PAGE and transfer to nitrocellulose membranes by immunoblotting using an anti-GFP monoclonal antibody. The position of molecular weight standards (in kDa) is shown on the left side of the panel. Representative blots are shown. *B.* The percentage CSP membrane association +/- SEM was determined by quantification of immunoblots by densitometry (n = 7 from 5 separate experiments). Statistical significance was determined by a Student's *t*-test, whereby * represents a p value of $< 5 \times 10^{-3}$ and ** represents a p value of $< 5 \times 10^{-7}$, compared to wild-type EGFP-CSP.

the cysteine string domain play in CSP membrane binding is not clear. Although it is likely that most, if not all, of the cysteines in the cysteine string domain become palmitoylated (see Figure 3.1A and Gundersen *et al.*, 1994), the requirement for such an extensive palmitoylation of CSP is not understood. The results presented in chapter three have shown that palmitoylation appears to correlate with the correct intracellular sorting of CSP. However, it is not known if all cysteines within the cysteine string domain require to be palmitoylated for correct sorting to occur. To analyse the importance of individual cysteine residues, a mutational analysis of the cysteine string domain of CSP was performed. The cysteine string domain contains fourteen cysteine residues which have been designated 1-14 (see Figure 4.2A) and a set of four cysteine-to-serine mutants, each containing either three or four mutated cysteines, were constructed within full-length EGFP-CSP, and designated C1-3S, C4-7S, C8-10S and C11-14S (Figure 4.2A). These constructs were transfected into PC12 cells and the distribution of the mutant proteins in recovered cytosol and membrane fractions was examined by immunoblotting using an anti-GFP monoclonal antibody (Figure 4.2A; *Upper panel*). To confirm the faithful partition of proteins into cytosolic and membrane fractions, duplicate nitrocellulose membranes were probed to analyse the distribution of the transferrin receptor (TfR; Figure 4.2A, *Middle panel*) and protein kinase B (PKB; Figure 4.2A, *Lower panel*). Serine substitutions of cysteine residues located in the C-terminal half of the cysteine string domain (C8-10S and C11-14S) were well tolerated, retaining robust membrane binding and palmitoylation at levels that were not significantly different to wild-type EGFP-CSP (Figure 4.2B-D). In contrast, mutations introduced in the N-terminal half of the cysteine string domain (C1-3S and C4-7S) led to the mutant proteins being recovered largely in the cytosolic fraction (Figure 4.2B-D). To investigate the effects of these mutations on the level of palmitoylation, membranes were isolated from transfected cells and treated with 1 M hydroxylamine, pH 7.0, to depalmitoylate proteins (or 1 M Tris, pH 7.0 as a control) for 20 hours at room temperature. Following recovery of the treated membranes, the samples were subjected to SDS-PAGE, transfer to nitrocellulose membranes and immunoblotting using an anti-GFP monoclonal antibody. Figure 4.2E reveals that, as demonstrated in Chapter 3, there is a marked molecular mass shift of ~8 kDa between palmitoylated (Figure 4.2E; *asterisk*) and unpalmitoylated (Figure 4.2E; *arrowhead*) forms of wild-type CSP. Similarly, and in agreement with the quantitative densitometry presented in Figure 4.2D, the C8-10S or C11-14S mutants exhibit a significant band-shift upon HA-induced depalmitoylation indicating that these mutants are modified by palmitoylation (Figure 4.2D). However, the HA-induced band-shift in the C8-10S and C11-14S mutants is smaller than for wild-type EGFP-CSP, suggesting that cysteines are likely to be palmitoylated (and hence to contribute to the mass shift) in wild-type CSP. The HA-induced
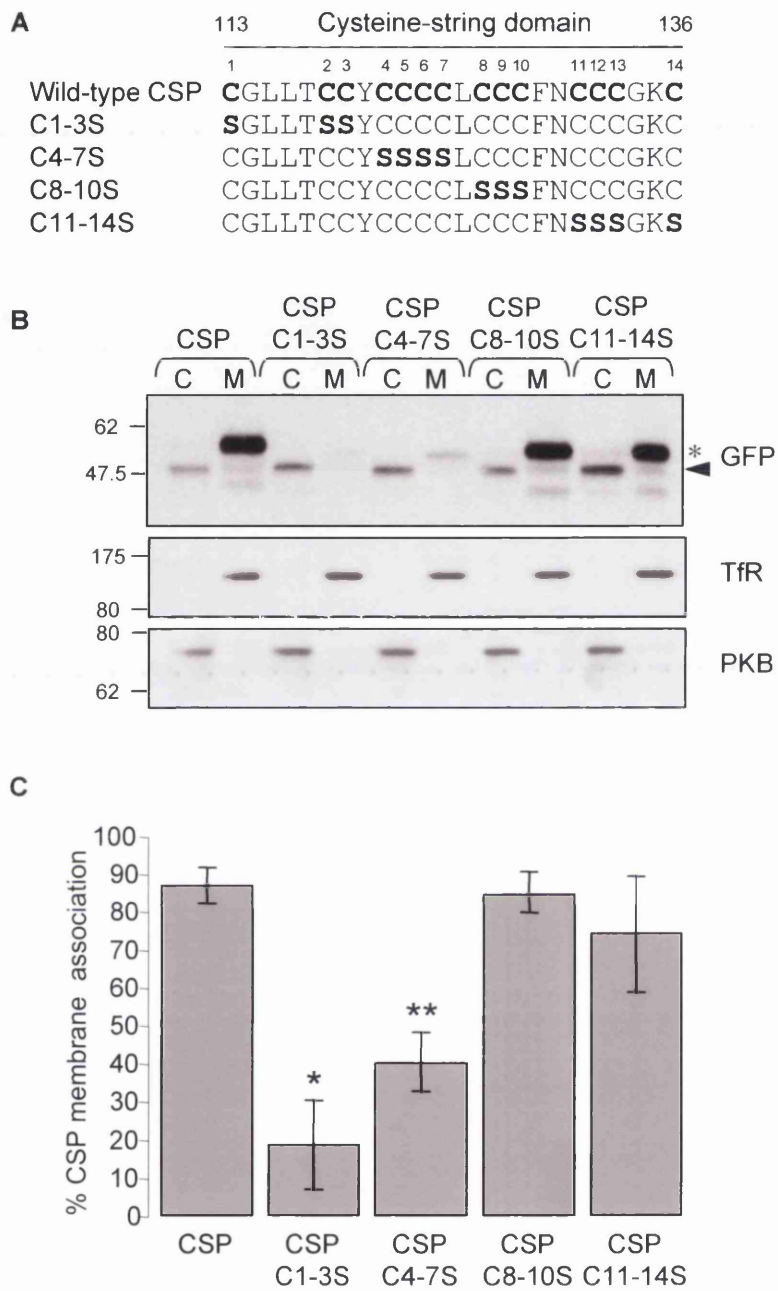
A

113   Cysteine-string domain   136

1	2 3	4 5 6 7	8 9 10	11 12 13	14

Wild-type CSP   **C**GLLT**CC**Y**CCCC**L**CCC**FN**CCC**GK**C**

C1-3S   **S**GLLT**SS**YCCCCLCCCFNCCCGKC

C4-7S   CGLLTCCY**SSSS**LCCCFNCCCGKC

C8-10S   CGLLTCCYCCCCL**SSS**FNCCCGKC

C11-14S   CGLLTCCYCCCCLCCCFN**SSS**GK**S**

B

C

Figure 4.2   Role of the cysteine string domain in CSP membrane binding and palmitoylation: cysteine to serine substitutions (*Continued overleaf*).

D

E

F
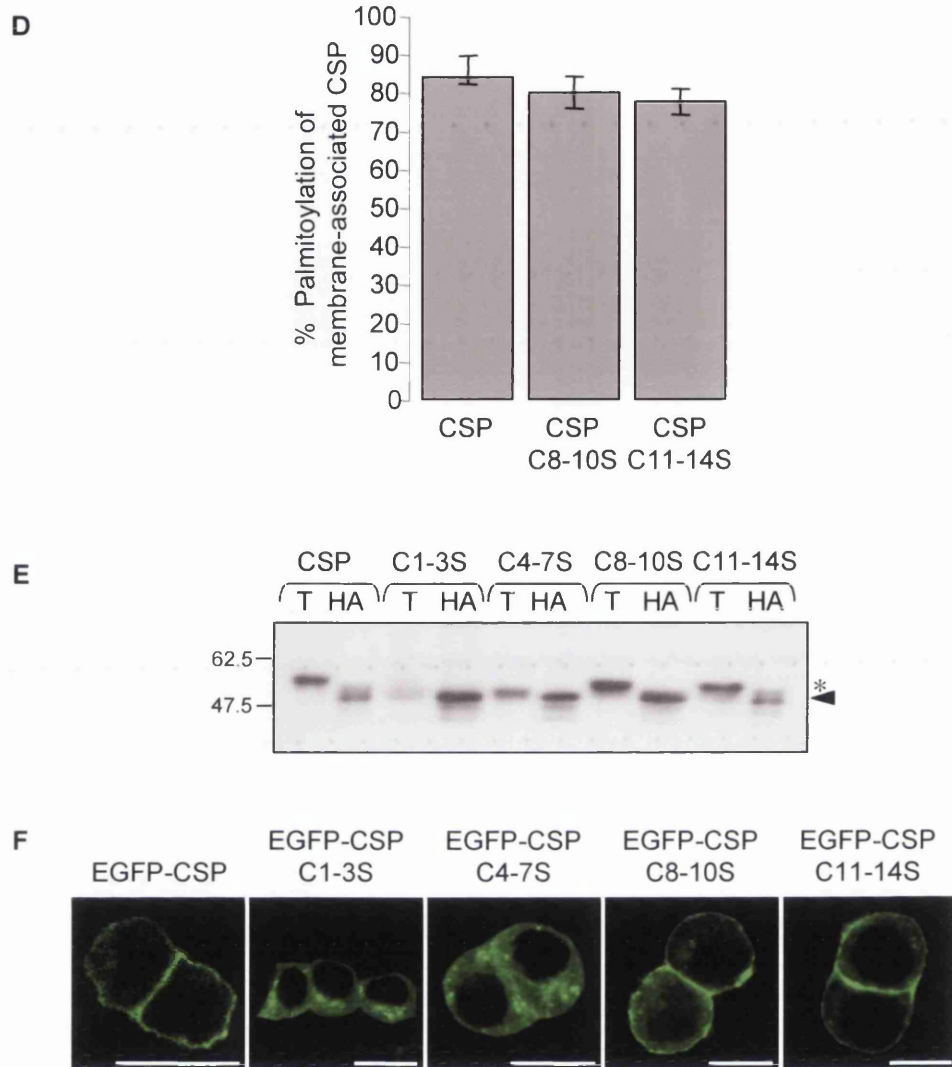
Figure 4.2 *(continued)* Role of the cysteine string domain in CSP membrane binding and palmitoylation: cysteine to serine substitutions.

Figure 4.2 Role of the cysteine string domain in CSP membrane binding and palmitoylation: cysteine to serine substitutions. *A.* Amino acids sequence of the cysteine string domain; cysteine residues are numbered from 1-14. Blocks of 3-4 cysteines were mutated to serines within the cysteine string domain; the names given to these mutants and their position within the cysteine string domain are shown. *B.* PC12 cells transfected with EGFP-CSP cysteine string domain cysteine to serine substitutions (EGFP-CSP(C1-3S), EGFP-CSP(C4-7S), EGFP-CSP(C8-10S), EGFP-CSP(C11-14S)), for 48 h were fractionated into cytosolic (C) and membrane (M) fractions and analysed following SDS-PAGE and transfer to nitrocellulose membranes by immunoblotting using an anti-GFP monoclonal antibody(*Upper panel*). To confirm the faithful partition of proteins into cytosolic and membrane fractions, duplicate nitrocellulose membranes were probed to analyse the distribution of the transferrin receptor (TfR, membrane protein; *Middle panel*) and protein kinase B (PKB, cytosolic protein; *Lower panel*). The position of molecular weight standards (in kDa) is shown on the left side of the panel; on the right side of the panel, *asterisks* identify palmitoylated CSP and *arrowheads* indicate unpalmitoylated CSP. Representative blots are shown. *C.* The percentage CSP membrane association +/- SEM was determined by quantification of immunoblots by densitometry (n = 3 from 3 separate experiments). Statistical significance was determined by a Student's *t*-test, whereby * represents a p value of < 0.02 and ** represents a p value of < 0.006, compared to wild-type EGFP-CSP. *D.* The percentage CSP palmitoylation +/- SEM was determined by quantification of immunoblots by densitometry of the total membrane-bound pool (n = 3 from 3 separate experiments). *E.* PC12 cells were transfected with EGFP-CSP cysteine to serine mutants for 48 h and isolated cell membranes were incubated in 1M Tris, pH 7.0 (T) or 1M hydroxylamine, pH 7.0 (HA) for 20 hours at room temperature. The treated membranes were recovered by centrifugation at 196 000 x *g* for 30 minutes and analysed following SDS-PAGE and transfer to nitrocellulose membranes by immunoblotting using an anti-GFP monoclonal antibody. The position of molecular weight standards (in kDa) is shown on the left; *asterisks* identify palmitoylated CSP and *arrowheads* indicate unpalmitoylated CSP. Representative blots are shown. *F.* PC12 cells growing on glass coverslips and transfected with EGFP-CSP cysteine string domain cysteine to serine substitutions for 48 h were fixed and the localisation of the expressed proteins was determined by confocal microscopy. Images are representative of a single 0.13 μm thick confocal section. Scale bar = 10 μm.

band-shift observed for the C8-10S and C11-14S mutants indicates that mutation of cysteine residues to serines within the C-terminal half of the cysteine string domain does not perturb palmitoylation of the remaining cysteines. To ascertain whether full palmitoylation of the cysteine string domain is required for the correct intracellular sorting of CSP, the subcellular localisation of the cysteine string domain mutants was assessed by confocal microscopy. Figure 4.2*F* illustrates that, in addition to being dispensable for membrane binding and palmitoylation of the remaining cysteines, cysteines within the C-terminal half of the cysteine string domain are not required for membrane sorting of CSP, as the C8-10S and C11-14S mutants showed a strong enrichment at the PM, similar to wild-type EGFP-CSP. In contrast, the C1-3S and C4-7S mutants were dispersed throughout the cytosol of PC12 cells, consistent with their lack of membrane binding (Figure 4.2*F*). These results demonstrate that, despite CSP being extensively palmitoylated, cysteines in the C-terminal half of the cysteine string domain are dispensable for membrane binding, global palmitoylation and intracellular sorting of CSP. In contrast, cysteines in the N-terminal half of the cysteine string domain are important for membrane binding, palmitoylation and subcellular sorting of CSP.

4.4 ROLE OF THE FIRST THREE CYSTEINES IN THE CYSTEINE STRING DOMAIN FOR CSP MEMBRANE BINDING

The finding that mutation of cysteines in the N-terminal half of the cysteine string domain to serine residues inhibited membrane binding, palmitoylation and intracellular sorting, prompted an investigation into the role of individual cysteine residues in this region on CSP membrane association. Since the block replacement of these three cysteine residues with serines resulted in the greatest loss of membrane association of EGFP-CSP (Figure 4.2*B* and *C*; C1-3S), single and double serine substitutions were made to the cysteines in this region of EGFP-CSP (Figure 4.3*A*). Following transfection of these constructs into PC12 cells for 48 hours, expressed proteins were separated into cytosolic and membrane fractions, and subjected to SDS-PAGE, transfer to nitrocellulose membranes, and immunoblotting using an antibody against GFP. Immunoblots presented in the left panel of Figure 4.3*B* indicate that the replacement of any single cysteine residue with serine in the C1-3 region (C113S, C118S, or C119S) of EGFP-CSP is tolerated, with single cysteine mutants partitioning predominantly into the membrane fraction (Figure 4.3*C*). Furthermore, using the band-shift assay, the presence of a more slowly migrating band in the membrane fraction (*asterisk*) compared to the cytosolic fraction (*arrowhead*) suggests that these mutants are efficiently palmitoylated. However, introducing any combination of two cysteine-to-serine mutations in the C1-3 region (C113S/C118S, C113S/C119S or C118S/C119S) of EGFP-CSP promoted a significant reduction in levels
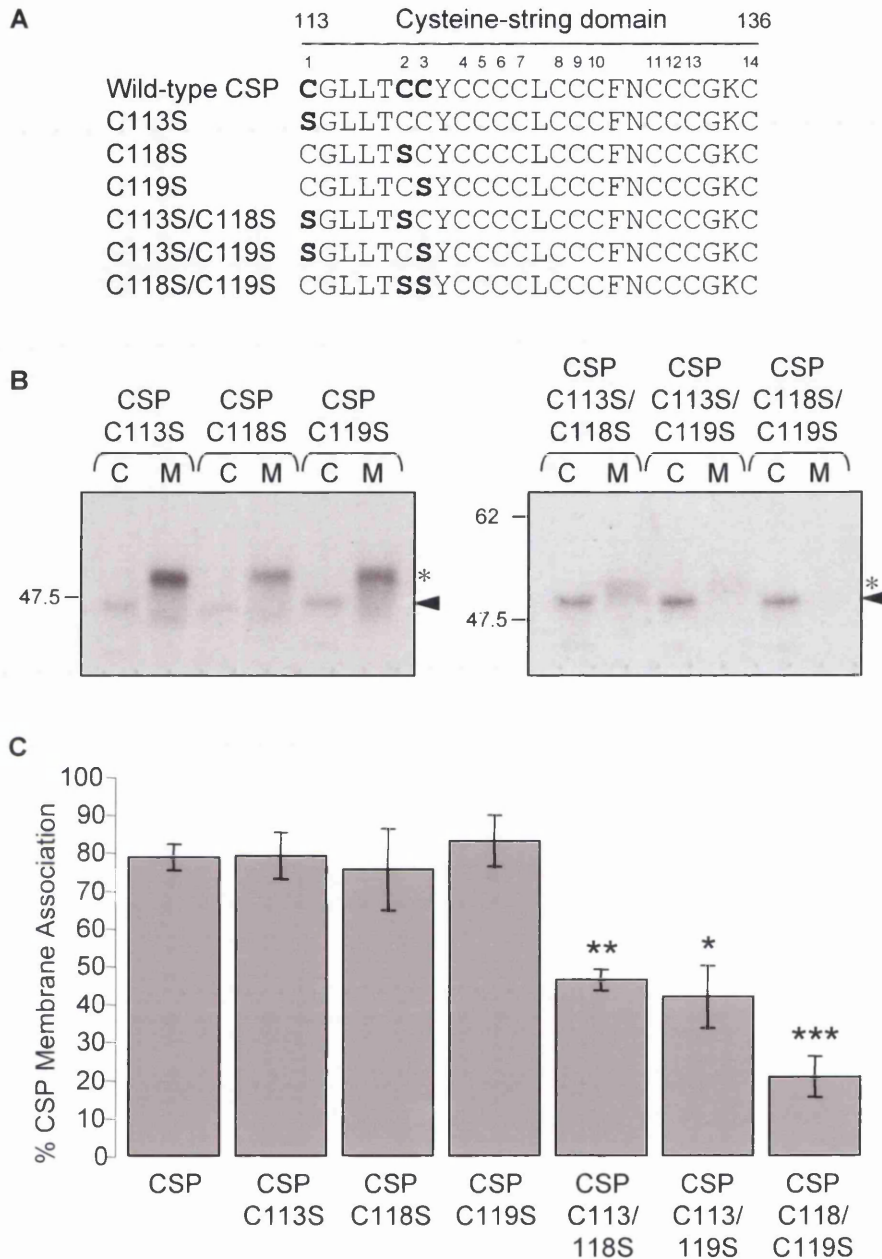
A

113   Cysteine-string domain   136

	1	2 3	4 5 6 7	8 9 10	11 12 13	14

Wild-type CSP **C**GLLT**CC**YCCCCLCCCFNCCCGKC
C113S   **S**GLLTCCYCCCCLCCCFNCCCGKC
C118S   CGLLT**S**CYCCCCLCCCFNCCCGKC
C119S   CGLLTC**S**YCCCCLCCCFNCCCGKC
C113S/C118S **S**GLLT**S**CYCCCCLCCCFNCCCGKC
C113S/C119S **S**GLLTC**S**YCCCCLCCCFNCCCGKC
C118S/C119S CGLLT**SS**YCCCCLCCCFNCCCGKC

B

C

Figure 4.3   **Role of the first three cysteines in the cysteine string domain in CSP membrane binding: single and double serine substitutions.**

Figure 4.3   Role of the first three cysteines in the cysteine string domain in CSP membrane binding: single and double serine substitutions. *A.* The position of the mutated cysteines within the cysteine string domain.   *B.* PC12 cells transfected with EGFP-CSP cysteine to serine single amino acid substitutions (*Left panel*) or double amino acid substitutions (*Right panel*) for 48 h were fractionated into cytosolic (C) and membrane (M) fractions and analysed following SDS-PAGE and transfer to nitrocellulose by immunoblotting using an anti-GFP monoclonal antibody. The position of molecular weight standards (in kDa) is shown on the left side of each panel; on the right side of each panel, *asterisks* identify palmitoylated CSP and *arrowheads* indicate unpalmitoylated CSP. Representative blots are shown. *C.* The percentage CSP membrane association +/- SEM was determined by quantification of immunoblots by densitometry (n = 3 from 3 separate experiments). Statistical significance was determined by a Student's *t*-test, whereby * represents a p value of < 0.02, ** represents a p value of < 0.002 and *** represents a p value of < 0.0009 compared to wild-type EGFP-CSP.

of membrane association, with the mutants partitioning predominantly into the cytosolic fraction (Figure 4.3*B*; *Right panel* and *C*).

4.5 THE IMPORTANCE OF A HYDROPHOBIC CYSTEINE STRING DOMAIN FOR CSP MEMBRANE BINDING

The results presented in chapter three identified that two EGFP-CSP truncation mutants, EGFP-CSP$_{1-136}$ and CSP$_{106-136}$, associate tightly with membranes in the absence of efficient palmitoylation (Figure 3.4*A* and *B*). The finding that CSP mutants are able to associate with membranes through mechanisms other than palmitoylation (most likely through hydrophobic interactions) suggests that the lack of membrane binding of CSP resulting from the replacement of cysteine residues within the N-terminal half of the cysteine string domain with serine residues, may not be caused solely by a loss of palmitoylation. Instead, it is possible that the hydrophobic nature of the cysteine residues provide CSP with an initial membrane affinity. To test this hypothesis, cysteines in the N-terminal half of the cysteine string domain were replaced with residues other than serine. In the first set of experiments, the first three cysteines in the cysteine string domain (C1-3) of EGFP-CSP were replaced with the amino acid alanine (Figure 4.4*A*). Alanine was chosen as a substitute, since it has more hydrophobicity than serine (owing to an apolar methyl side group), but is less hydrophobic than cysteine. This mutant (C1-3A) or C1-3S was transfected into PC12 cells, and forty-eight hours later the level of membrane association of the expressed proteins was assessed by cell fractionation, SDS-PAGE, transfer of proteins to nitrocellulose membranes and immunoblotting using an anti-GFP antibody. To confirm the faithful partition of proteins into cytosolic and membrane fractions, duplicate nitrocellulose membranes were probed to analyse the distribution of the transferrin receptor (TfR; Figure 4.4*B*, *Middle panel*) and protein kinase B (PKB; Figure 4.4*B*, *Lower panel*). Interestingly, and in contrast to the C1-3S mutant, the C1-3A mutant associates with cell membranes and is robustly palmitoylated, as indicated by a band shift in the membrane-associated pool of this mutant (Figure 4.4*B*, *Upper panel*; *asterisk*). Although the level of membrane binding and palmitoylation of C1-3A is significantly reduced when compared to wild-type EGFP-CSP, there is a significant increase in both these parameters compared to C1-3S. These results support the hypothesis that palmitoylation of cysteines 1-3 is not essential for membrane association of CSP, and that polar residues introduced at these positions may directly inhibit membrane binding.

The remaining cysteine residues in the N-terminal half of the cysteine string domain (C4-7) have also been shown to be important for CSP membrane binding and palmitoylation (Figure

A

113   Cysteine-string domain   136

| | 1 | 2 3 | 4 5 6 7 | 8 9 10 | 11 12 13 | 14 |

Wild-type CSP **C**GLLT**CC**YCCCCLCCCFNCCCGKC
C1-3S   **S**GLLT**SS**YCCCCLCCCFNCCCGKC
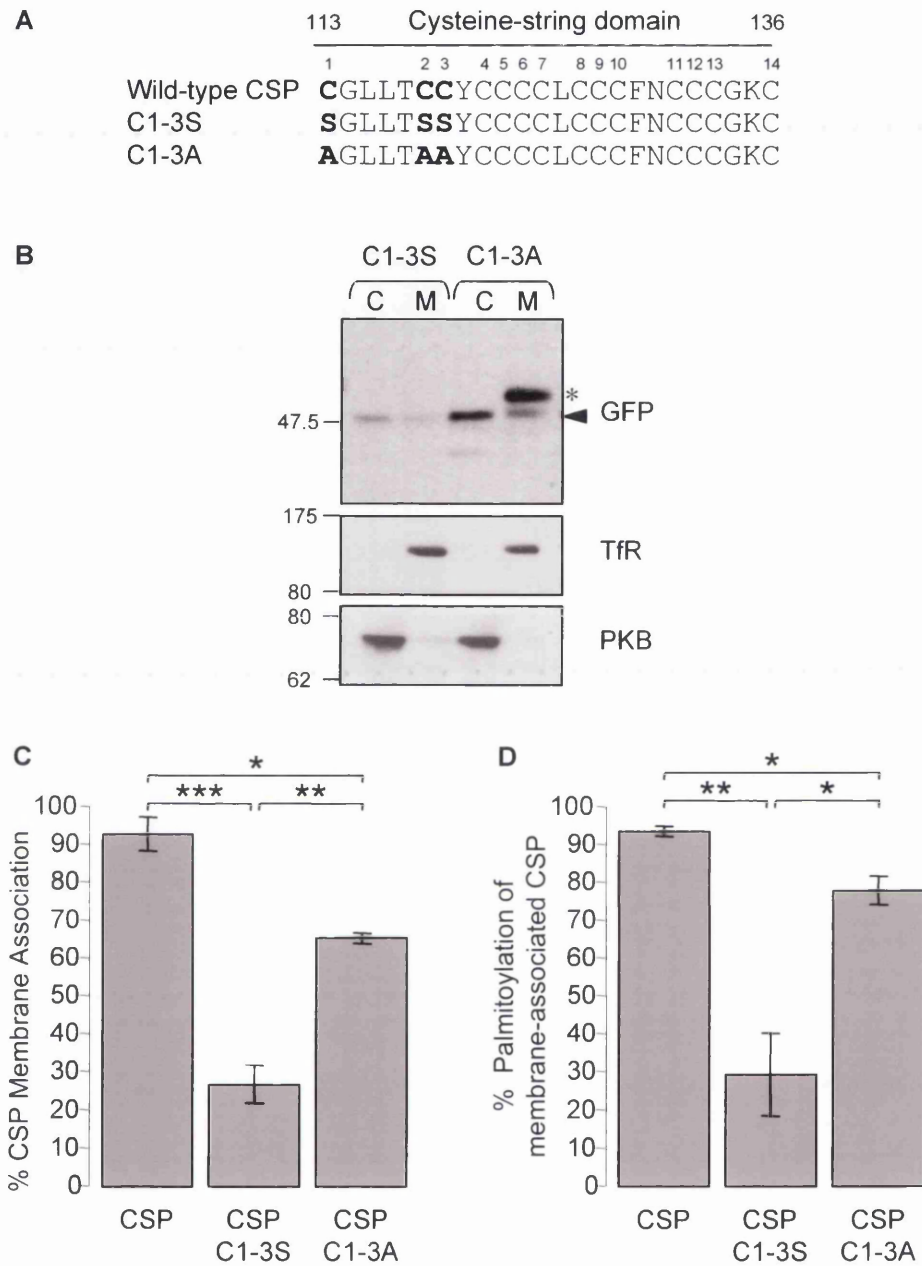C1-3A   **A**GLLT**AA**YCCCCLCCCFNCCCGKC

Figure 4.4 Role of the first three cysteines in the cysteine string domain in CSP membrane binding: comparison of serine and alanine substitutions.

Figure 4.4 Role of the first three cysteines in the cysteine string domain in CSP membrane binding: comparison of serine and alanine substitutions. *A.* The position of the mutated cysteines within the cytsteine string domain. *B.* PC12 cells transfected with EGFP-CSP(C1-3S) or EGFP-CSP(C1-3A) for 48 h were fractionated into cytosolic (C) and membrane (M) fractions and analysed following SDS-PAGE and transfer to nitrocellulose by immunoblotting using an anti-GFP monoclonal antibody (*Upper panel*). To confirm the faithful partition of proteins into cytosolic and membrane fractions, duplicate nitrocellulose membranes were probed to analyse the distribution of the transferrin receptor (TfR, membrane protein; *Middle panel*) and protein kinase B (PKB, cytosolic protein; *Lower panel*). The position of molecular weight standards (in kDa) is shown on the left side of each panel; on the right side of each panel, *asterisks* identify palmitoylated CSP and *arrowheads* indicate unpalmitoylated CSP. Representative blots are shown. *C.* The percentage CSP membrane association +/- SEM was determined by quantification of immunoblots by densitometry (n = 3 from 3 separate experiments). Statistical significance was determined by a Student's *t*-test, whereby * represents a p value of < 0.02 and ** represents a p value of < 3×10^{-4} compared to EGFP-CSP. *D.* The percentage CSP palmitoylation +/- SEM was determined by quantification of immunoblots by densitometry of the total membrane-bound pool (n = 3 from 3 separate experiments). Statistical significance was determined by a Student's *t*-test, whereby * represents a p value of < 0.03 and ** represents a p value of < 0.02 compared to EGFP-CSP.

4.2B-E). Thus, to extend this analysis, these cysteines were also substituted for alanine, or alternatively, for the more hydrophobic amino acid, leucine (Figure 4.5A). PC12 cells expressing these mutants for forty-eight hours were separated into cytosolic and membrane fractions and were analysed by SDS-PAGE, transfer to nitrocellulose membranes and immunoblotting using an anti-GFP monoclonal antibody (Figure 4.5B; Upper panel). To confirm the faithful partition of proteins into cytosolic and membrane fractions, duplicate nitrocellulose membranes were probed to analyse the distribution of the transferrin receptor (TfR; Figure 4.5B, Middle panel) and protein kinase B (PKB; Figure 4.5B, Lower panel). In contrast to the increase in membrane partitioning and palmitoylation displayed by the C1-3A mutant compared to C1-3S (Figure 4.4B-D), a similar substitution of cysteines in the C4-7 region (C4-7A) behaved essentially the same as C4-7S and was only weakly associated with membranes (Figure 4.5B; Upper panel and C). However, replacing the four cysteines in this region with more hydrophobic leucine residues, led to a large pool of the protein associating with cell membranes (Figure 4.5B, Upper panel). The membrane binding of all of the C4-7 mutants was significantly reduced when compared to wild-type EGFP-CSP (Figure 4.5C), but the trend suggests a link between an increase in membrane binding and the hydrophobicity of the amino acids substituted for the cysteine residues (where leucine > alanine > serine). Surprisingly, and in contrast to other cysteine mutants, the membrane-bound pool of C4-7L has a similar molecular mass to the cytosolic pool (arrowhead), and only very small amounts of the protein migrates to the size expected for a palmitoylated pool (asterisk), suggesting that this mutant is unpalmitoylated. The replacement of C4-7 with serine, alanine or leucine residues significantly reduced palmitoylation when compared to wild-type EGFP-CSP (Figure 4.5D). However, the most severe reduction in palmitoylation was observed when the cysteines were replaced with leucine residues, which almost completely abolished the palmitoylation of the remaining cysteines in the cysteine string domain. This suggests that the C4-7L mutation, although preserving membrane binding of CSP, inhibits overall palmitoylation of the cysteine-string domain.

To confirm the observation that the C1-3A mutant was palmitoylated and that the C4-7L mutant was not, [^{3}H] palmitate labelling experiments were performed on PC12 cells expressing these mutant proteins. PC12 cells were transfected in triplicate for 48 hours, and were metabolically labelled with [^{3}H] palmitic acid for 4 hours, followed by immunoprecipitation of EGFP-CSP, SDS-PAGE and analysis by immunoblotting with an anti-GFP monoclonal antibody or fluorography. As shown in the left panel of Figure 4.6A, the labelling pattern of C1-3A was similar to EGFP-CSP (compare to Figure 3.1B), demonstrating that this protein is palmitoylated despite the absence of the first three cysteines in the string domain. The results for C1-3A are

A

113   Cysteine-string domain   136

```
                   1      2 3   4 5 6 7   8 9 10    11 12 13   14
Wild-type CSP  CGLLTCCYCCCCLCCCFNCCCGKC
C4-7S          SGLLTSSYSSSSLCCCFNCCCGKC
C4-7A          AGLLTAAYAAAALCCCFNCCCGKC
C4-7L          AGLLTAAYLLLLLCCCFNCCCGKC
```
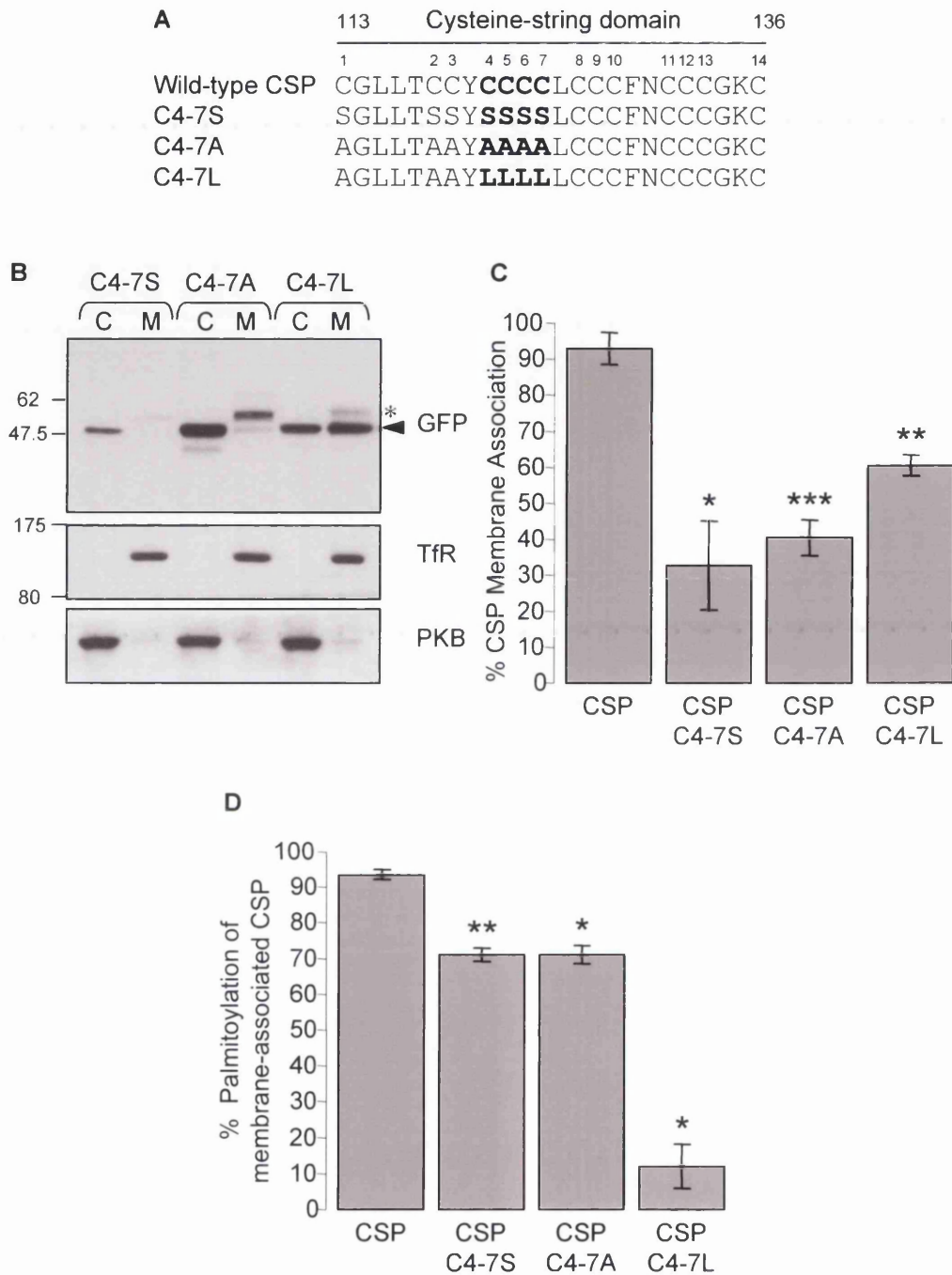
Figure 4.5   Role of cysteines 4-7 in the cysteine string domain in CSP membrane binding: comparison of serine, alanine and leucine substitutions.

Figure 4.5 Role of cysteines 4-7 in the cysteine string domain in CSP membrane binding: comparison of serine, alanine and leucine substitutions. *A.* The position of the mutated cysteines within the cytsteine string domain. *B.* PC12 cells transfected with EGFP-CSP(C4-7S), EGFP-CSP(C4-7A) or EGFP-CSP(C4-7L) for 48 h were fractionated into cytosolic (C) and membrane (M) fractions and analysed following SDS-PAGE and transfer to nitrocellulose membranes by immunoblotting using an anti-GFP monoclonal antibody (*Upper panel*). To confirm the faithful partition of proteins into cytosolic and membrane fractions, duplicate nitrocellulose membranes were probed to analyse the distribution of the transferrin receptor (TfR, membrane protein; *Middle panel*) and protein kinase B (PKB, cytosolic protein; *Lower panel*). The position of molecular weight standards (in kDa) is shown on the left side of each panel; on the right side of each panel, *asterisks* identify palmitoylated CSP and *arrowheads* indicate unpalmitoylated CSP. Representative blots are shown. *B.* The percentage CSP membrane association +/- SEM was determined by quantification of immunoblots by densitometry (n = 3 from 3 separate experiments). Statistical significance was determined by a Student's *t*-test, whereby * represents a p value of < 0.02, ** represents a p value of < 0.003 and *** represents a p value of < 7×10^{-4} compared to EGFP-CSP. *C.* The percentage CSP palmitoylation +/- SEM was determined by quantification of immunoblots by densitometry of the total membrane-bound pool (n = 3 from 3 separate experiments). Statistical significance was determined by a Student's *t*-test, whereby * represents a p value of < 0.003 and ** represents a p value of < 6×10^{-4} compared to EGFP-CSP.
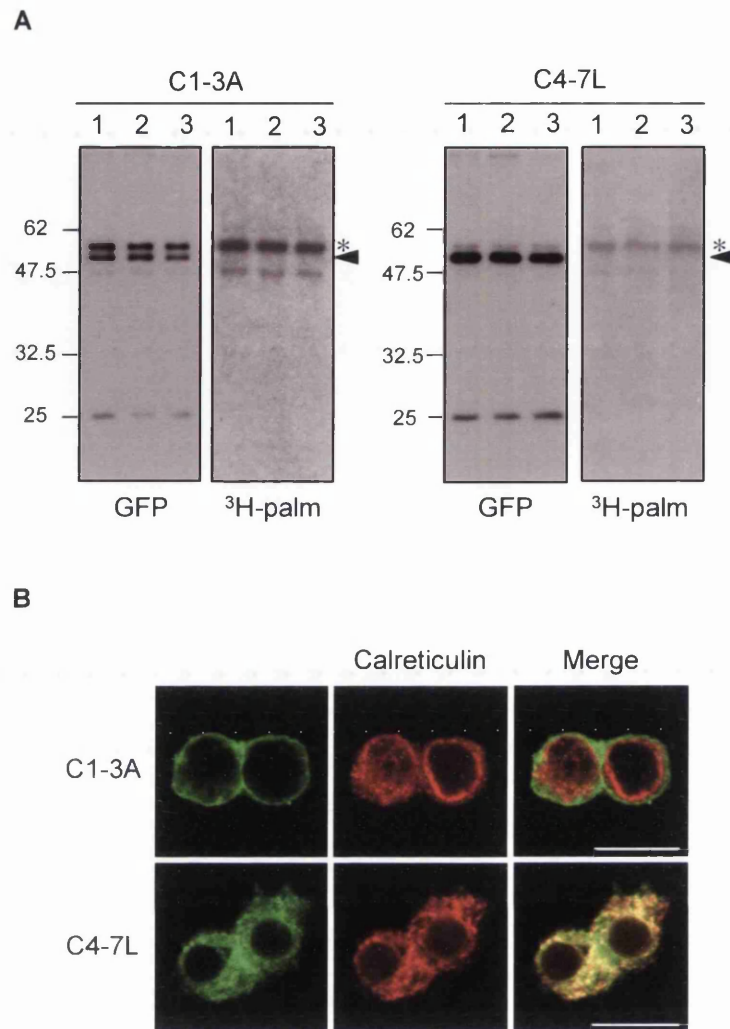
Figure 4.6 Palmitoylation and membrane trafficking of cysteine string domain mutants.
A. PC12 cells were transfected with EGFP-CSP(C1-3A) or EGFP-CSP(C4-7L) in triplicate for 48 h followed by incubation in ^{3}H palmitate for 4 hours. The EGFP tagged expressed proteins were immunoprecipitated from cell lysates and subjected to SDS-PAGE and transfer to nitrocellulose membranes, in duplicate. One membrane was analysed by probing with a monoclonal anti-GFP antibody (left side of each panel; "GFP"), the other was processed for fluorographic detection of incorporated radiolabel (right side of each panel; "^{3}H-palm"). Representative blots are shown. *B*. PC12 cells growing on glass coverslips and transfected with EGFP-CSP(C1-3A) or EGFP-CSP(C4-7L) for 48 h were fixed in 4% (v/v) formaldehyde, permeabilised and probed with a polyclonal anti-calreticulin antibody to label the ER. Calreticulin labelling was detected by probing with a rhodamine-conjugated anti-rabbit IgG (red) and compared with the GFP signal (green). Localisation of the labelled proteins was determined by confocal microscopy and images are representative of a single 0.13 μm thick confocal section. Scale bar = 10 μm.

similar to those seen for wild-type EGFP-CSP, with the higher molecular weight band incorporating [^{3}H] label (*asterisk*), which is clearly distinct from the non-palmitoylated pool of this protein (*arrowhead*). Note that for both C1-3A and wild-type CSP, the lower molecular weight band incorporating the [^{3}H] label is clearly distinct from the non-palmitoylated pool of this protein (*arrowhead*) and likely represents a degraded form of palmitoylated CSP that was visible after longer exposure of the immunoblot. In contrast to C1-3A, the major band detected for the C4-7L mutant (*arrowhead*) does not incorporate [^{3}H] label, although a very minor (~ 5%) higher molecular weight pool of the protein is clearly modified with [^{3}H] palmitate (Figure 4.6*A, right panel; asterisk*). In several experiments, the [^{3}H] signal detected for the C4-7L mutant always overlaid exactly with the minor higher molecular weight band denoted by an arrowhead. Thus, the major pool of membrane-bound C4-7L mutant is unpalmitoylated.

Having shown that mutation of cysteines at position 8-10 and 11-14 could be tolerated without affecting intracellular sorting of CSP (Figure 4.2*F*), the intracellular distribution of the C1-3A and C4-7L mutants (*i.e.* the mutants in the N-terminal half of the cysteine string domain that were membrane-bound) were also examined. PC12 cells were transfected with EGFP-CSP(C1-3A) or C4-7L for forty-eight hours, and the cells were fixed, permeabilised and probed with a polyclonal anti-calreticulin antibody to label the ER. Detection of calreticulin was determined by probing cells with a rhodamine-conjugated anti-rabbit IgG antibody prior to visualization by confocal microscopy. Similar to the C8-10S and C11-14S mutants, the C1-3A mutant was efficiently sorted, showing a strong enrichment at the plasma membrane and little overlap with the marker for the ER, calreticulin (Figure 4.6*B*; *Upper panel*). In contrast, the C4-7L mutant was completely excluded from the plasma membrane and, similar to the unpalmitoylated EGFP-CSP$_{(106-136)}$ and EGFP-CSP$_{(1-136)}$ mutants, exhibited substantial overlap with the ER marker, calreticulin (Figure 4.6*B*; *Lower panel*). Note that cells expressing EGFP-CSP(C4-7L) were permeabilised with digitonin prior to fixation to remove the cytosolic pool of protein (see Chapter 2.6 and (Chamberlain *et al.*, 1996).

4.6 MEMBRANE ASSOCIATION OF EGFP-CSP(C4-7L)

Finally, the membrane interactions of EGFP-CSP(C4-7L) were further examined to determine if the mechanism of membrane binding was the same as that for wild-type EGFP-CSP. This was investigated exactly as for EGFP-CSP$_{(1-136)}$ in Chapter 3.2.4. Figure 4.7 illustrates that, as in Figure 3.6, the peripheral membrane proteins munc18-1 and αSNAP are released to different extents from membranes treated with sodium chloride or sodium carbonate. In contrast, EGFP-CSP(C4-7L) is tightly associated with membranes and can only be released into the supernatant
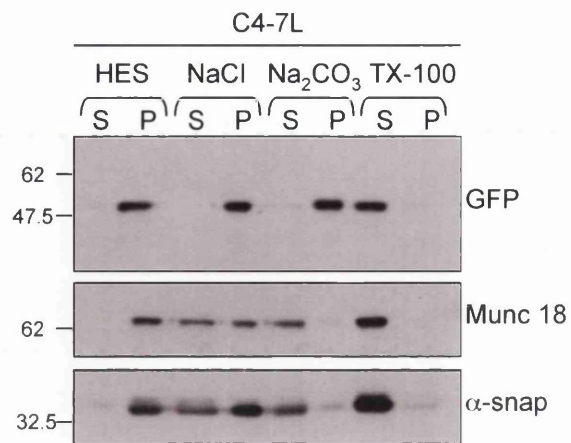
Figure 4.7 Analysis of membrane binding of EGFP-CSP(C4-7L). PC12 cells were transfected with EGFP-CSP(C4-7L) for 48 h and isolated cell membranes were incubated in HES Buffer, 1M NaCl, 0.1 M Na_2CO_3, pH 11.5, or HES Buffer supplemented with 1% (v/v) Triton X-100 for 30 minutes at 4 °C. Supernatant (S) and pelleted membrane (P) fractions were recovered by centrifugation at 196 000 x g for 30 minutes and analysed following SDS-PAGE and transfer to nitrocellulose membranes by immunoblotting using an anti-GFP monoclonal antibody (*Upper panel*). To examine the partition of peripheral membrane proteins into supernatant and pelleted membrane fractions, nitrocellulose membranes were probed using mouse monoclonal antibodies against Munc 18 (*Middle panel*) and α-SNAP (*Lower panel*). Representative blots are shown.

following treatment with Triton® X-100. This result is comparable to that found for both wild-type EGFP-CSP and EGFP-CSP$_{(1-136)}$, and supports the idea that the membrane association of the unpalmitoylated EGFP-CSP(C4-7L) mutant is mediated by hydrophobic interactions between the cysteine string domain and the membrane.

4.7 DISCUSSION

The results presented in Chapter 3 revealed that palmitoylation of CSP truncation mutants is not required for their membrane association, and suggested that the membrane association of CSP prior to palmitoylation may be mediated by hydrophobic interactions between the cysteine string domain and the lipid bilayer. Here, detailed mutagenesis of the cysteine string domain of full length CSP has been used to test this hypothesis, and to examine the role of individual cysteines in membrane binding and palmitoylation.

The results presented in this chapter have shown that cysteine residues in the C-terminal half of the cysteine string domain are dispensable for global palmitoylation and trafficking of CSP. The finding that specific cysteine residues can be mutated without effect on membrane sorting suggests that the extensive palmitoylation of CSP is not a fundamental prerequisite for either membrane binding or intracellular sorting. Although extensive palmitoylation of CSP may be important to maintain the appropriate membrane orientation of the protein, it is also possible that such multiple palmitoylation of CSP is important for some other aspect of CSP function. In support of this, a CSP mutant in which several cysteines in the cysteine string domain had been deleted was correctly targeted to membranes but was unable to rescue the null mutant phenotype when expressed in *Drosophila* (Arnold *et al.*, 2004). The identification of correctly sorted CSP mutants that have reduced levels of palmitoylation (*i.e.* the C8-10S, C11-14S and C1-3A CSP mutants identified in this chapter) will be a valuable tool for future studies investigating the role of palmitoylation in CSP function. Perhaps the proposed function of CSP in exocytosis is dependent on an extensively palmitoylated cysteine string domain, either directly, or through protein-protein interactions. Palmitoylation-deficient CSP mutants that are correctly sorted could be expressed in cells that have a CSP null background (for example, following short interference RNA (siRNA) knockdown); any change in secretion or protein interactions could be measured and attributed to the reduction in palmitoylation.

The finding that membrane binding is preserved following the substitution of cysteines located in the N-terminal half of the cysteine string domain with other hydrophobic amino acids (alanine or leucine), and abolished following substitution with hydrophilic residues (serine)

suggests that the overall hydrophobicity of the cysteine string domain may be important for initial membrane interactions. The hydrophobicity of this domain may therefore act as a membrane targeting motif, that allows CSP to target its partner PAT; alternatively, a hydrophobic motif may form part of a recognition site that allows the PAT to identify its substrate protein. Interestingly, Gundersen's group (Mastrogiacomo et al., 1998) provided evidence that the cysteine string domain is embedded in the bilayer after chemically induced depalmitoylation; however, it was suggested that it was hydroxylamine treatment that promoted a nonphysiological membrane interaction of the cysteine string region. Although the work presented here supports the results of Mastrogiacomo et al., it clearly implies that membrane insertion of the cysteine string domain of CSP may be physiological and may precede palmitoylation. Interestingly, intermediate immunoreactive bands corresponding to partially palmitoylated CSP are never detected by SDS-PAGE (Chapter 3 (Gundersen et al., 1994). Similarly, membrane-associated, unpalmitoylated protein has not consistently been detected for wild-type CSP. These points imply that the full palmitoylation of CSP is a rapid event, is likely enzyme mediated and occurs in the same compartment to which CSP initially binds. It is interesting to note however that *Drosophila* CSP does not associate with membranes and is not palmitoylated when expressed in PC12 cells (Van de Goor and Kelly, 1996). This finding may suggest that membrane integration of the cysteine string domain prior to palmitoylation requires a specific chaperone factor that is not conserved between *Drosophila* and mammalian CSPs.

A mutant has been identified of full-length CSP (C4-7L), which has a robust membrane binding occurring in the absence of palmitoylation. This mutant behaves in a similar way to the C-terminal truncation mutants (introduced in Chapter 3) and indeed, has a similar ER localisation. The discovery that a full length CSP mutant shares the same ER localisation in the absence of palmitoylation as the C-terminal truncation mutants argues against the notion that the loss of the C-terminal domain creates an artificial membrane-spanning domain that forces these mutants to associate with membranes inappropriately.

The results presented in Figure 4.5 suggest that the hydrophobicity of the cysteine string domain also appears to be critical in determining whether CSP becomes palmitoylated: palmitoylation is inhibited if the hydrophobicity of the cysteine string domain is either too high (C4-7L) or too weak (C4-7S). This supports the finding that a weakened membrane binding correlated with the palmitoylation of CSP truncation mutants (Chapter 3). Thus, two different sets of experiments have suggested a link between the strength of membrane binding and the incidence of palmitoylation. One possibility for this link may be explained if the mutants that have an increased level of membrane affinity get "trapped" on the wrong membrane, and so become

physically separated from their partner palmitoyl transferase. Conversely, mutants with membrane affinities that are too weak may simply never encounter membranes, and by association, palmitoyl transferases. Alternatively, the strength of membrane binding may be important for enzyme-substrate recognition, or possibly palmitate transfer onto substrate proteins. Indeed, the strength of initial membrane interaction of substrate proteins may be one way a palmitoyl transferase exhibits a level of substrate specificity.

The membrane interaction of hydrophobic cysteine-rich domains may play a general role in initial membrane binding of palmitoylated proteins. Of interest, El-Husseini *et al.* (2000) identified a hydrophobic sequence, ^{3}Cys-Leu-^{5}Cys-Ile-Val, required for palmitoylation and correct targeting of PSD-95; the cysteines at position 3 and 5 of this sequence are both sites for palmitoylation. Mutation of either cysteine at position 3 or 5 of this sequence to serine almost abolished total palmitoylation of PSD-95; however, single leucine mutations (particularly at position 5) allowed robust incorporation of palmitate (El-Husseini *et al.*, 2000; Topinka and Bredt, 1998). Furthermore, the overall hydrophobic character of the sequence Met-Leu-Cys-Cys-Met was essential for the palmitoylation of GAP-43 (El-Husseini *et al.*, 2000). These results were interpreted to suggest that the PSD-95 and GAP-43 PATs may specifically recognize these hydrophobic sequences. However, based on the results in this chapter, it is possible that this sequence also plays an important role in membrane binding (independently of PAT) before palmitoylation. Thus, hydrophobic cysteine rich domains may represent a common motif that directly associates with membranes before palmitoylation. It would be interesting to determine whether hydrophobic cysteine rich domains present in other proteins, such as SNAP25, also serve this same function. A caveat is that inhibition of PSD-95 palmitoylation increases the soluble pool of this protein (El-Husseini *et al.*, 2000), suggesting that the membrane interaction of this protein in the absence of palmitoylation is weaker than observed for CSP mutants.

The three separate membrane-associated mutants generated so far (EGFP-CSP$_{(106-136)}$, EGFP-CSP$_{(1-136)}$ and EGFP-CSP(C4-7L)), which each display defective palmitoylation, co-localise with ER markers. This finding raises the possibility that CSP may associate initially with the ER, and that subsequent palmitoylation is required for ER exit and correct intracellular sorting of CSP.

CHAPTER FIVE: SPECIFIC DHHC PROTEINS PALMITOYLATE CSP

AND PROMOTE ITS STABLE MEMBRANE ASSOCIATION

5.1 INTRODUCTION

Palmitoylation regulates the membrane interactions of many proteins. In addition to functioning as a simple membrane anchor, palmitoylation can also regulate protein sorting and the micro-localisation of proteins within membranes (El-Husseini *et al.*, 2001; Goodwin *et al.*, 2005; Kang *et al.*, 2004; Rocks *et al.*, 2005; Roy *et al.*, 2005). Despite several attempts to identify palmitoyl transferases over many years, it was only relatively recently that palmitoylating enzymes containing a conserved DHHC cysteine rich domain (CRD) were first identified in yeast (Lobo *et al.*, 2002; Roth *et al.*, 2002), where they mediate the majority of palmitoylation reactions (Roth *et al.*, 2006). Subsequent analyses in mammalian cells identified a family of twenty-three proteins containing a conserved DHHC-CRD, and several of these proteins have since been shown to have palmitoyl transferase activity (Fernandez-Hernando *et al.*, 2006; Fukata *et al.*, 2004; Huang *et al.*, 2004; Keller *et al.*, 2004; Swarthout *et al.*, 2005).

Sequence analyses of DHHC proteins predicts that they are polytopic membrane proteins, with the DHHC region present on the cytosolic face of the membrane (Politis *et al.*, 2005). Two lines of evidence have suggested that the DHHC domain of these proteins may form part of the enzyme active site. First, mutations introduced into the DHHC domain of these enzymes renders them inactive (Ducker *et al.*, 2004; Fernandez-Hernando *et al.*, 2006; Fukata *et al.*, 2004; Hayashi *et al.*, 2005; Huang *et al.*, 2004; Lam *et al.*, 2006; Lobo *et al.*, 2002; Roth *et al.*, 2002; Smotrys *et al.*, 2005; Swarthout *et al.*, 2005; Valdez-Taubas and Pelham, 2005). Second, reports have demonstrated that these enzymes become palmitoylated on the conserved cysteine residue within the DHHC domain, suggesting that they may form an acyl-enzyme intermediate (Ducker *et al.*, 2004; Fukata *et al.*, 2004; Hayashi *et al.*, 2005; Keller *et al.*, 2004; Lobo *et al.*, 2002; Roth *et al.*, 2002; Smotrys *et al.*, 2005; Swarthout *et al.*, 2005).

The localisation of DHHC proteins (or palmitoyl transferase activity) have been identified at the Golgi apparatus, ER, plasma membrane, on endosomes/vesicular compartments and the yeast vacuole (Dunphy *et al.*, 1996; Fukata *et al.*, 2004; Huang *et al.*, 2004; Keller *et al.*, 2004; Roth *et al.*, 2002; Schroeder *et al.*, 1996; Singaraja *et al.*, 2002; Swarthout *et al.*, 2005; Uemura *et al.*, 2002; Valdez-Taubas and Pelham, 2005; Veit *et al.*, 2001). The subcellular localisation of only a subset of the DHHC proteins has been determined so far, however, gaining a complete profile of the localisation of each of the DHHC proteins may help to understand how palmitoylation is spatially regulated.

Cysteine string protein is palmitoylated on up to fourteen cysteine residues present within its cysteine string domain (Gundersen *et al.*, 1994). Although the enzymes that palmitoylate CSP have not been identified, two recent studies have reported a loss of CSP palmitoylation in the nervous system of DHHC17 mutant *Drosophila*, which results in defective presynaptic neurotransmission (Ohyama *et al.*, 2007; Stowers and Isacoff, 2007). However, it is not known whether DHHC17 palmitoylates mammalian CSP *in vivo*, and it is also formally possible that the effects of the DHHC17 mutation in *Drosophila* on CSP palmitoylation are indirect. In addition, CSP has a widespread tissue distribution outside the nervous system of both mammals and *Drosophila* (Chamberlain and Burgoyne, 1996; Coppola and Gundersen, 1996; Eberle *et al.*, 1998), and it is not clear whether the same DHHC protein(s) palmitoylate CSP in every cell type. Furthermore, it is possible that more than one DHHC protein may be active against CSP; indeed, eNOS, SNAP25, $G_{\alpha s}$, GAP43 and Lck have each been shown to be substrates for multiple palmitoyl transferases (Fernandez-Hernando *et al.*, 2006; Fukata *et al.*, 2004; Huang *et al.*, 2004).

Determining the palmitoyl transferases that are active towards CSP, and the intracellular localisations of these enzymes, will provide important information about the intracellular location of CSP palmitoylation.

5.2 LOCALISATION OF DHHC PROTEINS IN PC12 CELLS.

To identify the localisation of all of the twenty-three murine DHHC proteins, PC12 cells growing on duplicate glass coverslips were transfected with HA-tagged versions of each of the twenty-three DHHC proteins for forty-eight hours prior to the cells being fixed and permabilised. To detect expressed DHHC proteins, the cells were probed with a FITC-conjugated anti-HA antibody. The DHHC proteins studied to date have been shown to be predominantly localised to the ER and Golgi apparatus in mammalian cells (Huang *et al.*, 2004; Keller *et al.*, 2004; Singaraja *et al.*, 2002; Swarthout *et al.*, 2005; Uemura *et al.*, 2002). Therefore, cells on one coverslip were probed for a marker of the ER by incubating in a polyclonal anti-calreticulin antibody; on another coverslip, cells were probed for a marker of the Golgi apparatus by incubating with a GRASP55 (Golgi reassembly stacking protein of 55 kDa; Shorter *et al.*, 1999) antibody. Calreticulin and GRASP55 labelling was detected by probing with rhodamine-conjugated anti-rabbit and anti-sheep IgGs, respectively, and the fluorescence was visualised by confocal microscopy. Screening of coverslips by confocal microscopy revealed that overexpressed DHHC proteins in PC12 cells can be broadly classed into three

subcellular localisations: predominantly Golgi-localised, ER-localised, or having a plasma membrane/endosomal localisation (Figure 5.1A). The majority of DHHC proteins are localised at the Golgi apparatus, and this is the case for DHHC3, -7, -8, -9, -11, -12, -15, -16, -17, -21, and -22. Seven DHHC proteins displayed coincidence with the ER marker calreticulin: DHHC1, -4, -6, -13, -18, -19, and -23. The remaining DHHC proteins, DHHC2, -5, -10, -14 and -20, displayed partial localisation at both the plasma membrane and an intracellular location, a distribution that may represent endosomal compartments. Representative images illustrating examples of Golgi-, ER- and plasma membrane/endosomal-localised DHHC proteins against endogenous calreticulin and GRASP55 staining in PC12 cells are presented in Figure 5.1 *B-D*.

5.3 CSP MEMBRANE BINDING AND PALMITOYLATION IS INEFFICIENT IN HEK293 CELLS AND IS ENHANCED BY CO-EXPRESSION OF SPECIFIC GOLGI-LOCALISED DHHC PROTEINS

The identification of the unpalmitoylated CSP mutants, CSP_{1-136} and C4-7L (in Chapters Three and Four), which are localised to ER membranes led to the hypothesis that CSP first associates with ER membranes prior to palmitoylation, and that CSP palmitoylating enzymes (and hence the site of CSP palmitoylation) are also localised to this compartment. This hypothesis would imply that the CSP_{1-136} and C4-7L mutants are somehow "unpalmitoylatable", perhaps due to an altered membrane topology or altered protein folding. However, it is also possible that CSP becomes palmitoylated at a distinct membrane compartment to the ER, and that the CSP_{1-136} and C4-7L mutants associate inappropriately with ER membranes, and thereby remain unpalmitoylated because they are physically separated from their partner palmitoyl transferases. By identifting the palmitoyl transferases that modify CSP, it will be possible to determine the subcellular localisation of CSP palmitoylation, which will illuminate the pathway involved in CSP membrane trafficking. As a first step, a range of cell types were screened in order to identify cells that inefficiently palmitoylate CSP. Chinese hamster ovary (CHO), COS1, HeLa, Human Embryonic Kidney (HEK) 293 and PC12 cells (as a control) were transfected with EGFP-CSP for forty-eight hours, and cells were separated into cytosolic (C) and membrane fractions (M) and analysed following SDS-PAGE and immunoblotting using a polyclonal anti-CSP antibody (Figure 5.2). Of all the cells types examined, endogenous CSP immunoreactivity was only detected in PC12 cells, consistent with CSP being predominantly found in neuronal and neuroendocrine cell types. The transfection efficiency and palmitoylation of CSP (identified by an *asterisk*) varied greatly between cell types, with PC12 and HEK293 cells showing the greatest levels of CSP expression. The presence of immunoreactive bands in the membrane fractions that migrate at different sizes by SDS-PAGE suggests that the efficiency of

A

Golgi		ER	PM/Endosomes
DHHC3	DHHC15	DHHC1	DHHC2
DHHC7	DHHC16	DHHC4	DHHC5
DHHC8	DHHC17	DHHC6	DHHC10
DHHC9	DHHC21	DHHC13	DHHC14
DHHC11	DHHC22	DHHC18	DHHC20
DHHC12		DHHC19	
		DHHC23	
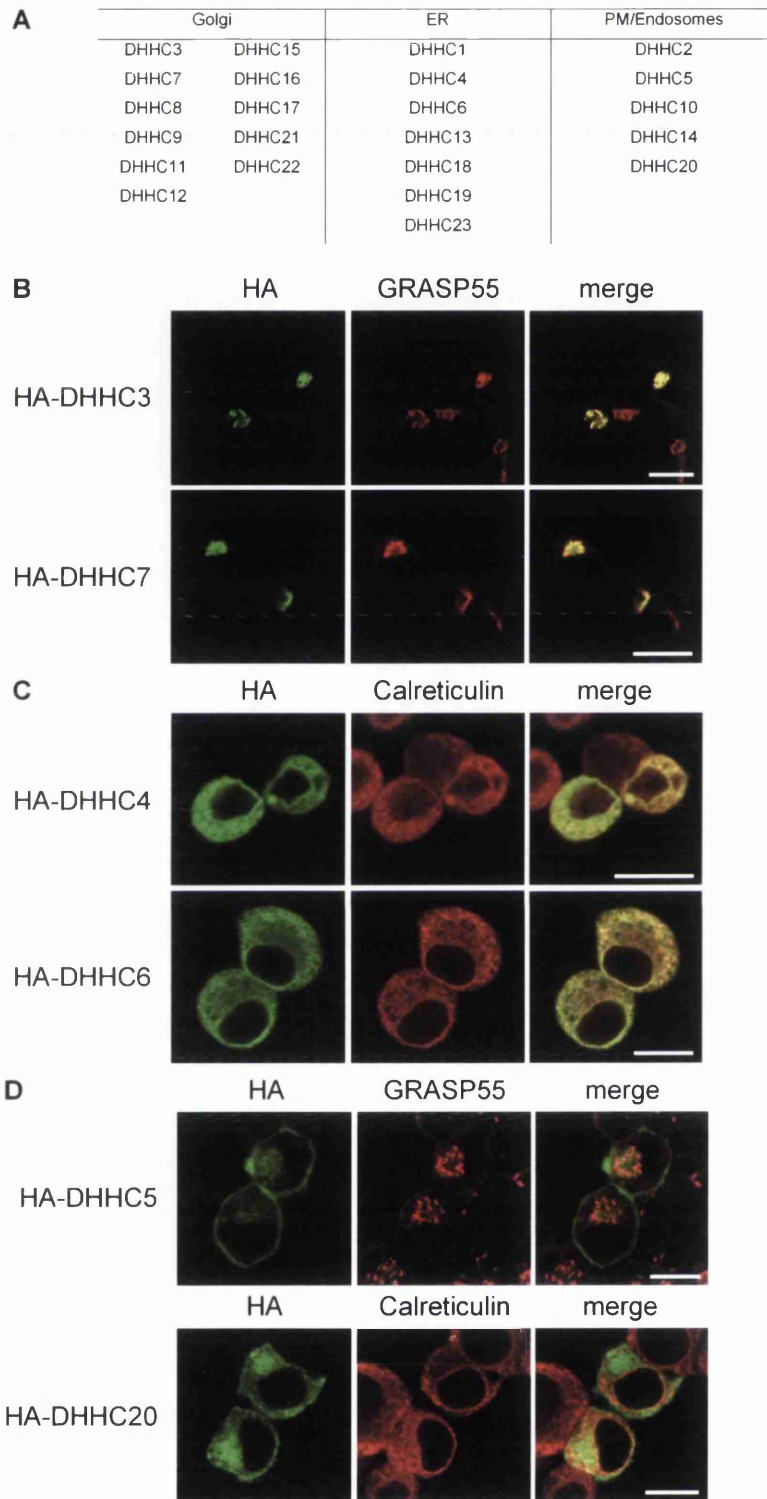
Figure 5.1 Localisation of DHHC clones in PC12 cells

Figure 5.1 Localisation of DHHC clones in PC12 cells. *A.* The localisation of the 23 DHHC clones in PC12 cells was determined by confocal microscopy and can be categorised into the following localisations: ER, Golgi, or PM/endosomal compartment. PC12 cells growing on glass coverslips were transfected with empty vector or each of the 23 DHHC clones for 48 h, in duplicate. Cells were fixed in 4% (v/v) formaldehyde, permeabilised and probed with a FITC-conjugated anti-HA antibody to label overexpressed DHHC. Transfected cells were co-stained with a marker for the ER by probing with a polyclonal anti-calreticulin antibody. Calreticulin labelling was detected by probing with a rhodamine-conjugated anti-rabbit IgG. Alternatively, transfected cells were co-stained with a marker for the Golgi apparatus by probing with a polyclonal anti-GRASP55 antibody. GRASP55 labelling was detected by probing with a rhodamine-conjugated anti-sheep IgG. *B.* Representative images showing examples of DHHC clones that have a Golgi-localisation, DHHC3 and DHHC7 (green). Golgi-localisation was determined by the coincidence of green fluorescence with that of GRASP-55 (red). *C.* Representative images showing examples of DHHC clones that have an ER localisation, DHHC4 and DHHC6 (green). ER-localisation was determined by the coincidence of green fluorescence with that of calreticulin (red). *D.* Representative images showing examples of DHHC clones that have a PM/endosomal localisation, DHHC5 and DHHC20 (green). DHHC5 fluorescence was compared to that of Golgi-localised GRASP55 (red; *Upper panel*); DHHC20 fluorescence was compared to that of ER-localised calreticulin (red; *Lower panel*). Images are representative of a single 0.13 µm thick confocal section. Scale bar = 10 µm.
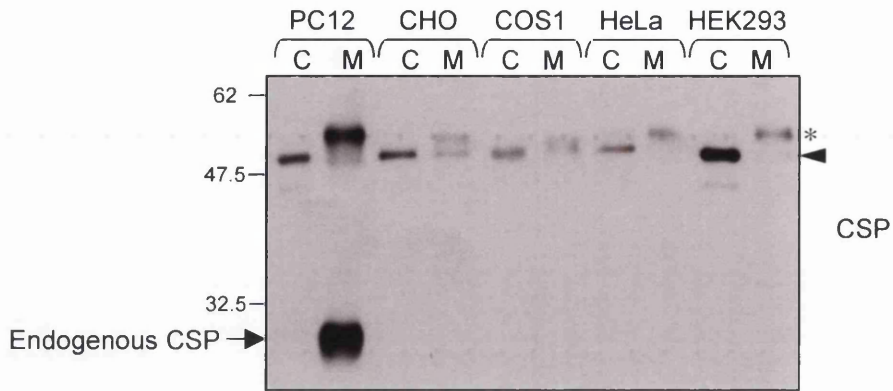
Figure 5.2 Membrane binding and palmitoylation of EGFP-CSP in various cell types. PC12, CHO, COS1 , HeLa and HEK293 cells were transfected with EGFP-CSP. Forty-eight hours post-transfection, the cells were fractionated into cytosolic (C) and membrane (M) fractions and analysed following SDS-PAGE and transfer to nitrocellulose membranes by immunoblotting using an anti-CSP polyclonal antibody. Note the presence of endogenous CSP (at approximately 28 kDa; indicated by an *arrow*) is only detected in PC12 cells. The positions of molecular weight standards (in kDa) are shown on the left side of the panel; *asterisks* identify palmitoylated CSP and *arrowheads* indicate unpalmitoylated CSP. A representative blot is shown.

CSP palmitoylation varies significantly between cell types. Whereas the upper palmitoylated band is the major form of EGFP-CSP in transfected PC12 cells, only a small pool of the protein is palmitoylated when expressed in HEK293 cells (Figure 5.2). This suggests that only a limited amount of palmitoyl transferases active against CSP are expressed in HEK293 cells, and thus, this cell type was employed to characterise CSP palmitoylating enzymes in mammalian cells. To determine whether any of the DHHC proteins are able to palmitoylate CSP in HEK293 cells, cells were cotransfected with EGFP-CSP and HA-tagged versions of each of the twenty-three DHHC proteins. Twenty-four hours post-transfection, the cells were separated into cystosolic and membrane fractions, followed by analysis by SDS-PAGE and immunoblotting using an anti-GFP monoclonal antibody (Figure 5.3A and B). CSP membrane binding was specifically and significantly enhanced by DHHC3, -7, -15 and -17, which was due to the palmitoylation of CSP as determined by the band-shift on SDS-PAGE gels (Figure 5.3A; *asterisk*). Thus, expression of these specific DHHC proteins is sufficient to catalyse the extensive palmitoylation of CSP and to promote its stable membrane attachment. Interestingly, co-expression of EGFP-CSP with DHHC11 consistently and significantly reduced the basal level of CSP membrane interaction in HEK293 cells (Figure 5.3 A and B).

To determine the expression levels of the individual DHHC clones, lysates of HEK293 cells expressing each of the twenty-three HA-tagged DHHC proteins were subjected to SDS-PAGE and immunoblotting using a monoclonal anti-HA antibody (Figure 5.4). The DHHC proteins were expressed at different levels, and the blot shown in Figure 5.4 is highly exposed (and clearly saturated for certain DHHCs) to allow expression of poorly expressed DHHCs to be visualised. Poor expression levels of some of the DHHC proteins is also apparent in other studies (Fernandez-Hernando *et al.*, 2006; Ohno *et al.*, 2006). That some of the DHHC proteins were poorly expressed in HEK293 cells (Figure 5.4) may indicate that the identification of only four enzymes that palmitoylate CSP may be an underestimate; however, repeated attempts to either "normalise" the expression levels of the DHHCs or significantly increase the expression levels of the poorly expressed DHHCs have proved unsuccessful. However, note that several "inactive" DHHC proteins were expressed at greater or similar levels than "active" DHHC proteins, confirming the specificity of the results. The identification of DHHC17 as an enzyme that palmitoylates mammalian CSP agrees well with recent analyses of *Drosophila* mutants (Ohyama *et al.*, 2007; Stowers and Isacoff, 2007).

The finding that the enzymes that are able to palmitoylate CSP in HEK293 cells are Golgi-localised in PC12 cells (Figure 5.1 A and B) was interesting since results presented in the previous chapters have suggested that CSP becomes palmitoylated at the ER in PC12 cells. This proposal was based on the ER localisation of non-palmitoylated CSP mutants. To
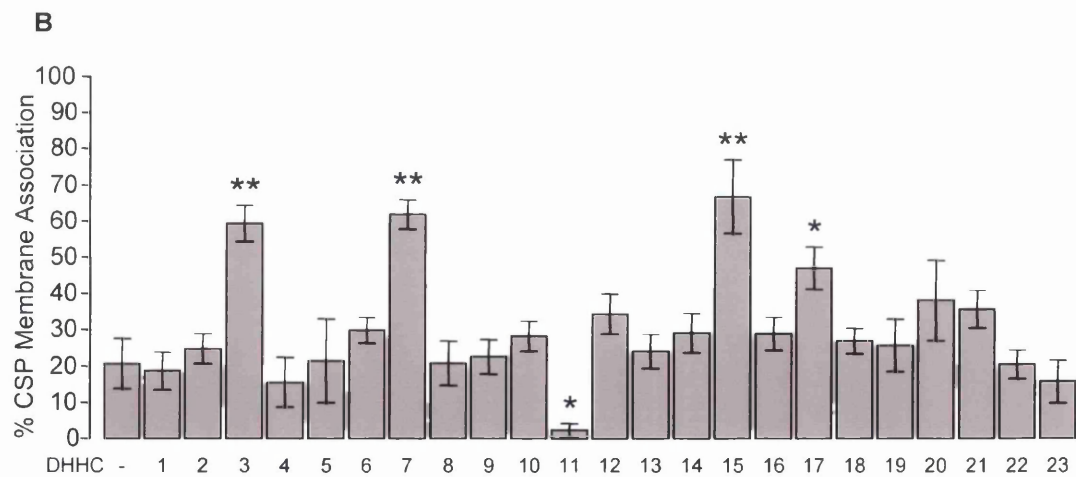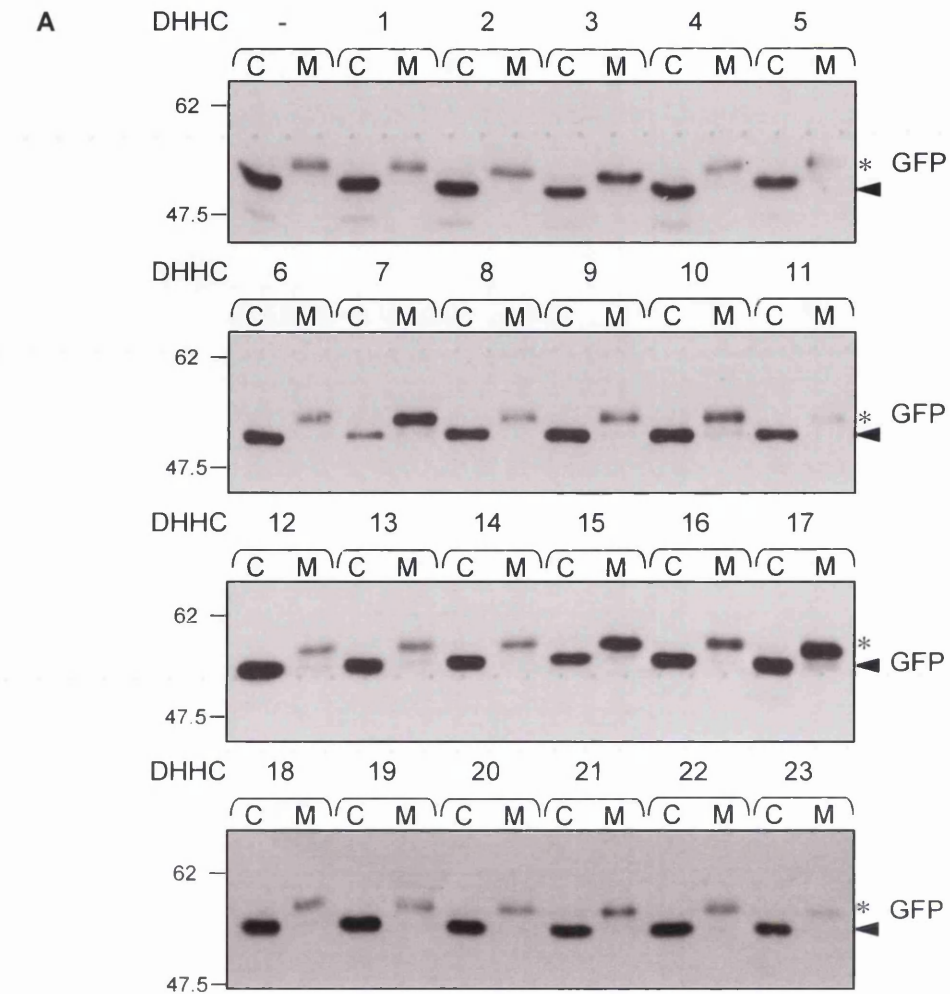
Figure 5.3 Specific DHHC proteins regulate EGFP-CSP membrane binding

Figure 5.3 Specific DHHC proteins regulate EGFP-CSP membrane binding. *A.* HEK293 cells were transfected with 0.8 μg of EGFP-CSP in the absence (-) or presence of 1.6 μg of each of the 23 HA-tagged DHHC consructs (1-23). Forty-eight hours post-transfection, the cells were fractionated into cytosolic (C) and membrane (M) fractions and analysed following SDS-PAGE and transfer to nitrocellulose membranes by immunoblotting using a monoclonal anti-GFP antibody. The positions of molecular weight standards (in kDa) are shown on the left side of the panel; *asterisks* identify palmitoylated CSP and *arrowheads* indicate unpalmitoylated CSP. Representative blots are shown. *B.* The percentage CSP membrane association +/- SEM was determined by quantification of immunoblots by densitometry (n=5 from 5 separate experiments). * represents a p value of < 0.03 and ** represents a p value of < 0.004 compared to EGFP-CSP in the absence of DHHC expression.
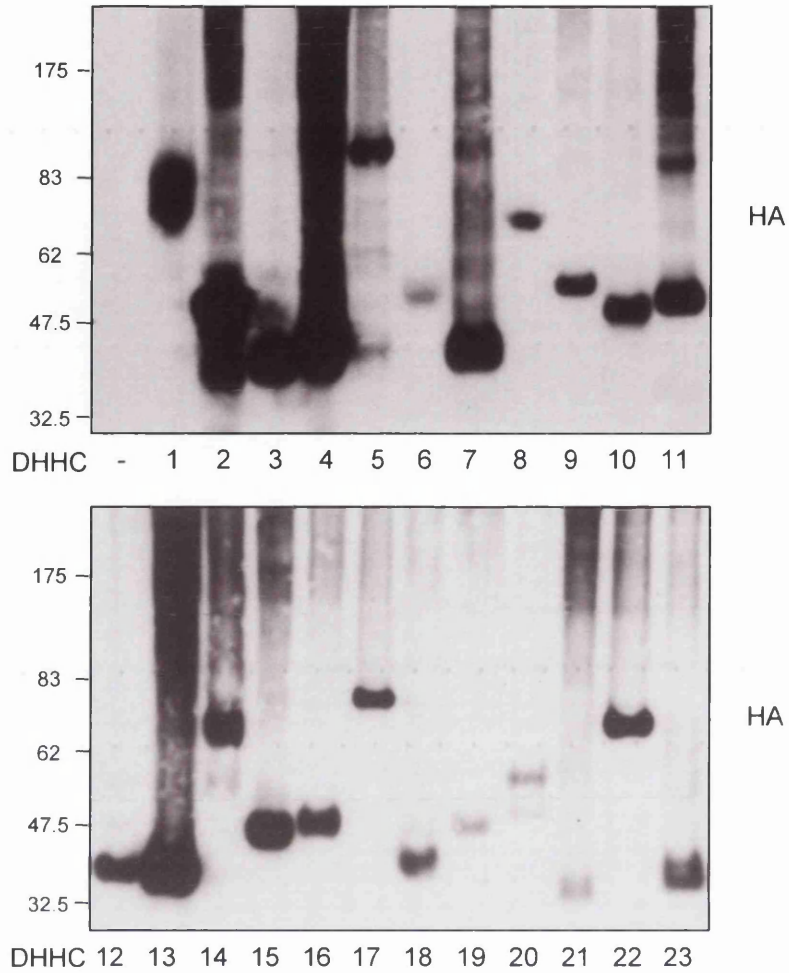
Figure 5.4 Expression of DHHC clones in HEK293 cells. HEK293 cells were transfected with equal amounts of empty vector (-) or each of the 23 murine DHHC clones (DHHC1-23). Forty-eight hours post-transfection, the cells were lysed and analysed following SDS-PAGE and transfer to nitrocellulose membranes by immunoblotting using an anti-HA monoclonal antibody. The positions of molecular weight standards (in kDa) are shown on the left side of the panel. A representative blot is shown.

investigate whether the CSP palmitoylating enzymes are localised to the same compartment when overexpressed in HEK293 cells, cells growing on glass coverslips were transfected with HA-tagged versions of each of DHHC3, -7, -15, and -17 for forty-eight hours. The cells were fixed, permeabilised, and overexpressed DHHC proteins were labelled by probing the cells with a FITC-conjugated anti-HA antibody. Cells were probed with an anti-GRASP55 antibody to label the Golgi apparatus, and GRASP55 staining was detected by probing with a rhodamine-conjugated anti-sheep IgG prior to visualisation by confocal microscopy. Figure 5.5A reveals that, as in PC12 cells, DHHC3, -7, -15, and -17 all overlap with the marker for the Golgi apparatus. To confirm that different DHHC proteins are localised to specific compartments in HEK293 cells, cells were also transfected with DHHC4 and -6 and were probed with anti-calreticulin antibody to label the ER. To detect ER staining, cells were probed with a rhodamine-conjugated anti-rabbit antibody followed by confocal microscopy analysis. As shown in Figure 5.5B DHHC4 and -6 are both localised to the ER when expressed in HEK293 cells and have the same localisation when expressed in PC12 cells. Since several other DHHC proteins are also localised to the Golgi in HEK293 cells (Ohno *et al.*, 2006), there is clearly specificity for CSP within this Golgi subset of DHHC proteins. It will be interesting to determine the factors that regulate this substrate specificity.

To ensure that the changes in membrane binding/palmitoylation of CSP induced by co-transfection of DHHC3, -7, -15 and -17 were mediated by direct palmitoylation of CSP by the transfected enzymes, the effect of catalytically-inactive DHHC mutants on CSP membrane binding and palmitoylation were examined in HEK293 cells. A loss of DHHC protein palmitoylating activity has been reported whenever cysteine mutations have been introduced into the DHHC domain of several DHHC proteins (Ducker *et al.*, 2004; Fernandez-Hernando *et al.*, 2006; Fukata *et al.*, 2004; Hayashi *et al.*, 2005; Huang *et al.*, 2004; Lam *et al.*, 2006; Lobo *et al.*, 2002; Roth *et al.*, 2002; Smotrys *et al.*, 2005; Swarthout *et al.*, 2005; Valdez-Taubas and Pelham, 2005). Cyseine-to-serine substitutions were constructed in the DHHC domains of DHHC3, -7, -15, and -17 (DHHC3(C157S), DHHC7(C160S), DHHC15(C159S) and DHHC17(C457S)), and wild-type or mutant DHHC proteins were transfected along with EGFP-CSP into HEK293 cells. Twenty-four hours later, the transfected cells were separated into cytosolic and membrane fractions to measure the extent of membrane association of the transfected proteins. Equal volumes of the isolated cytosolic and membrane fractions were subjected to SDS-PAGE, transfer to nitrocellulose and immunoblotting using a monoclonal antibody against GFP to detect EGFP-CSP, or HA to detect DHHC expression. EGFP-CSP, when transfected into HEK293 cells alone, partitions predominantly in the cystosolic fraction, with only a minimal pool of the protein palmitoylated and membrane-associated (Figure 5.6A;

A

B
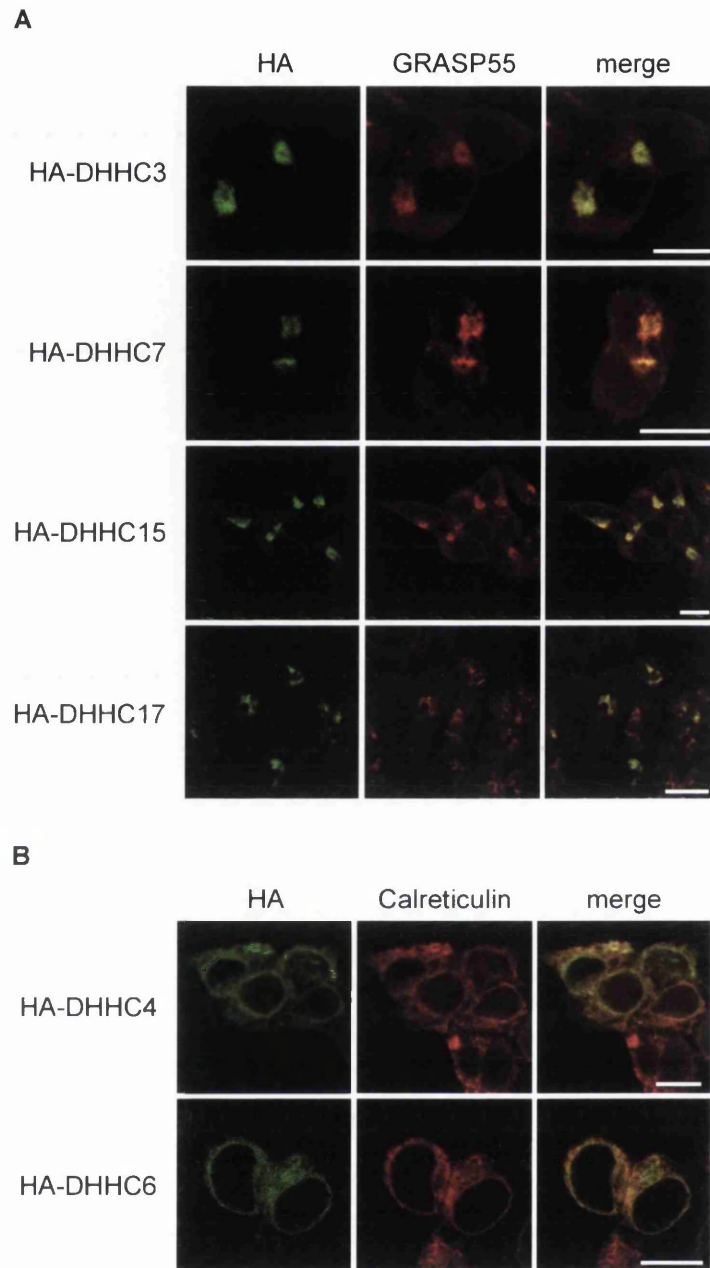
Figure 5.5 CSP palmitoylating enzymes are localised to the Golgi in HEK293 cells. *A.* HEK-293 cells growing on glass coverslips and transfected with HA-DHHC3, HA-DHHC7, HA-DHHC15 or HA-DHHC17 for forty-eight hours were fixed in 4% (v/v) formaldehyde, permeabilised and probed with a FITC-conjugated monoclonal anti-HA antibody. Golgi localisation was determined by probing with an anti-GRASP55 polyclonal antibody. GRASP-55 labelling was detected by probing with an Alexa Fluor® 568 donkey anti-sheep (red) and compared with the FITC signal (green). *B.* HEK-293 cells growing on glass coverslips transfected with HA-DHHC4 or HA-DHHC6 for 48 h were fixed in 4% (v/v) formaldehyde, permeabilised and probed with a FITC-conjugated monoclonal anti-HA antibody. Calreticulin labelling was detected by probing with an Alexa Fluor® 594 goat anti-rabbit antibody (red) and compared with the GFP signal (green). Images are representative of a single 0.13 μm thick confocal section through HEK-293 cells. Scale bar = 10 μm.
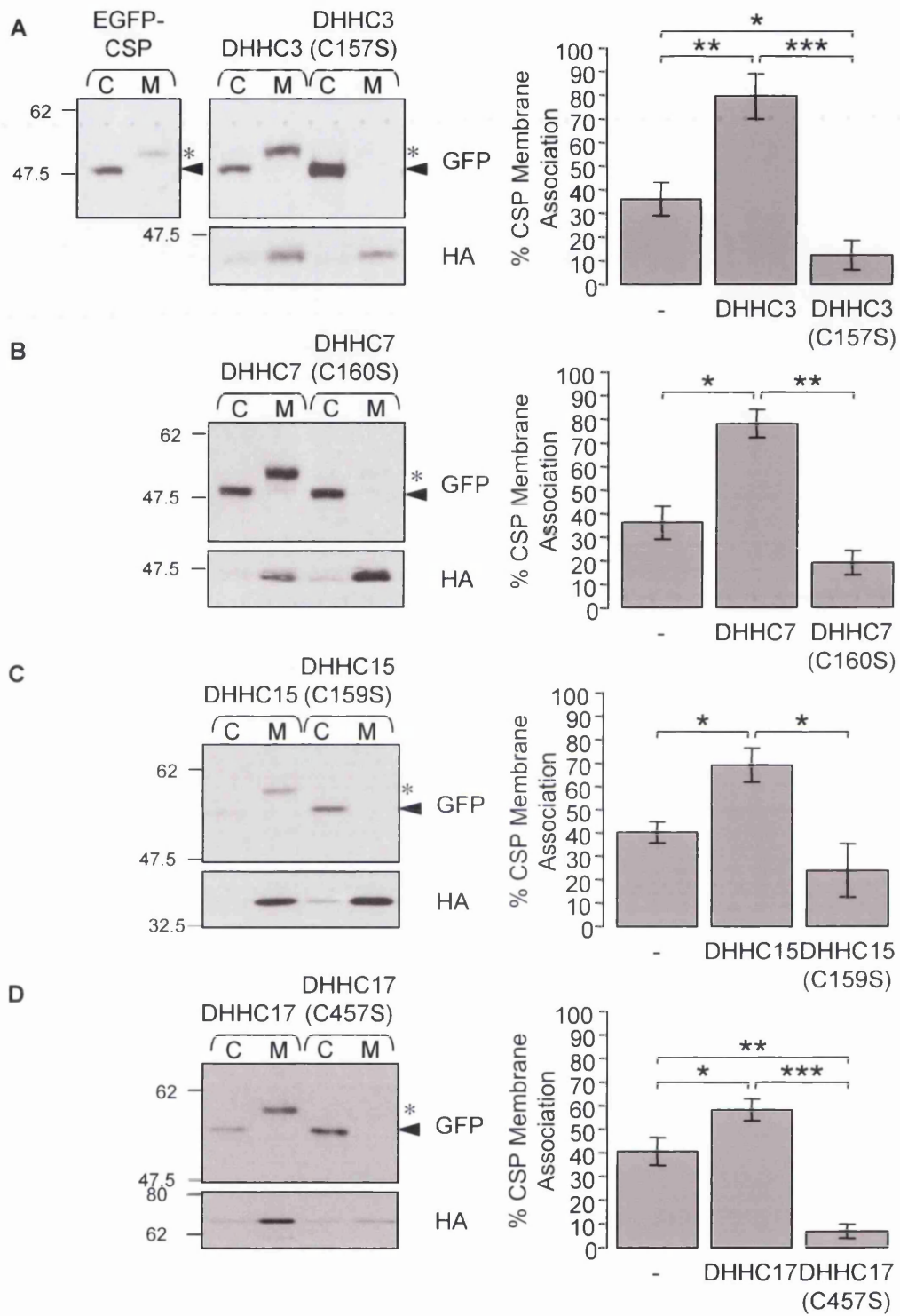
Figure 5.6 Increased membrane binding and palmitoylation of EGFP-CSP by DHHC proteins is prevented by mutations in the DHHC domain.

Figure 5.6 Increased membrane binding and palmitoylation of EGFP-CSP by DHHC proteins is prevented by mutations in the DHHC Domain. HEK-293 cells were transfected with 0.8 µg of EGFP-CSP or co-transfected with 0.8 µg of EGFP-CSP and 1.6 µg of wild-type DHHC3, -7, -15 or -17, or 1.6 µg of the inactive DHHC mutants, DHHC3(C157S), DHHC7(C160S), DHHC15(C159S) or DHHC17(C457S). Forty-eight hours post-transfection, expressed proteins were separated into cytosolic and membrane fractions and analysed following SDS-PAGE and transfer to nitrocellulose membranes by immunoblotting using an anti-GFP monoclonal antibody (*Upper panel*). The co-expression of DHHC proteins was confirmed by probing duplicate nitrocellulose membranes using an anti-HA monoclonal antibody (*Lower panel*). The positions of molecular weight standards (in kDa) are shown on the left side of each panel; *asterisks* identify palmitoylated CSP and *arrowheads* indicate unpalmitoylated CSP. Representative blots are shown. *A.* The membrane profile of EGFP-CSP in HEK-293 cells (*left panel*) and EGFP-CSP following co-transfection with DHHC3 and DHHC3(C157S)(*centre panel*). *Right panel* The percentage CSP membrane association +/- SEM was determined by quantification of immunoblots by densitometry (n=6 from 4 separate experiments). * represents a p value of < 0.03, ** represents a p value of < 0.003, and *** represents a p value of $< 2 \times 10^{-4}$. *B.* The membrane profile of EGFP-CSP in HEK-293 cells following co-transfection with DHHC7 and DHHC7(C160S)(*left panel*). *Right panel* The percentage CSP membrane association +/- SEM was determined by quantification of immunoblots by densitometry (n=6 from 4 separate experiments). * represents a p value of $< 6 \times 10^{-4}$ and ** represents a p value of $< 2 \times 10^{-5}$. *C.* The membrane profile of EGFP-CSP in HEK-293 cells following co-transfection with DHHC15 and DHHC15(C159S)(*left panel*). *Right panel* The percentage CSP membrane association +/- SEM was determined by quantification of immunoblots by densitometry (n=8 from 5 separate experiments). * represents a p value of < 0.004. *D.* The membrane profile of EGFP-CSP in HEK-293 cells following co-transfection with DHHC17 and DHHC17(C457S)(*left panel*). *Right panel* The percentage CSP membrane association +/- SEM was determined by quantification of immunoblots by densitometry (n=5 from 3 separate experiments). * represents a p value of < 0.04, ** represents a p value of < 0.002, and *** represents a p value of $< 2 \times 10^{-5}$.

Left panel). In contrast to the wild-type DHHC proteins, and despite being expressed at similar levels, all of the inactive mutants had no stimulatory effect on CSP palmitoylation or membrane binding in HEK293 cells (Figure 5.6*A-D*). Furthermore, all of the mutant DHHC proteins inhibited CSP palmitoylation, and this was significant for both DHHC3 and -17 (Figure 5.6*A* and *D*; *Right panel*). Thus, the ability of DHHC3, -7, -15 and -17 to increase membrane binding and palmitoylation of CSP is dependent upon the palmitoyl transferase activity of the enzymes.

5.4 LIKE CSP, SNAP25 MEMBRANE BINDING IS ENHANCED BY CO-EXPRESSION OF SPECIFIC GOLGI-LOCALISED DHHC PROTEINS IN HEK293 CELLS

The SNARE protein SNAP25 is similar to CSP in that it is multiply palmitoylated and lacks transmembrane domains or prenylation/myristoylation sites. In addition, the cysteines in SNAP25 are also present in an overall hydrophobic domain. Thus, it was of interest to examine whether DHHC proteins could also enhance membrane binding of SNAP25. SNAP25 is membrane-associated due to palmitoylation on up to four cysteine residues present within its cysteine-rich linker domain (Gonelle-Gispert *et al.*, 2000; Lane and Liu, 1997; Veit *et al.*, 1996). Overexpression of DHHC-3, -7 and -17 have been shown to increase incorporation of radiolabelled palmitate into SNAP25 in HEK293 cells (Fukata *et al.*, 2004). The majority of EGFP-SNAP25 is found in the cytosolic fraction of transfected HEK293 cells, suggesting that palmitoylation is inefficient in these cells (Figure 5.7*A*; *Left panel*). To determine whether the co-expression of DHHC proteins is able to increase the membrane affinity of SNAP25, HEK293 cells transfected with EGFP-SNAP25 and DHHC3, -7, or -17 for forty-eight hours were separated into cytosolic and membrane fractions and the distribution of proteins in these fractions was examined by SDS-PAGE and immunoblotting (Figure 5.7*A-C*). Co-expression of DHHC3, -7, and -17 proteins promoted a significant increase in EGFP-SNAP25 membrane association: this effect was specific as it was abolished by mutations within the DHHC domain, and indeed mutant DHHC7 and -15 significantly decreased the level of EGFP-SNAP25 membrane binding (Figure 5.7*A-C*). These results demonstrate that specific DHHC proteins are also able to promote the stable membrane binding of SNAP25 in HEK293 cells, suggesting that the mechanisms of palmitoylation and membrane binding of CSP and SNAP25 are similar.

5.5 CSP CO-LOCALISES AT THE GOLGI WITH CO-EXPRESSED DHHC PROTEINS

To extend the observation that co-expression of DHHC3, -7, -15, and -17 promote membrane association of CSP, confocal imaging analysis was used to compare the subcellular localisations of EGFP-CSP and HA-tagged DHHC proteins following their co-transfection into HEK293
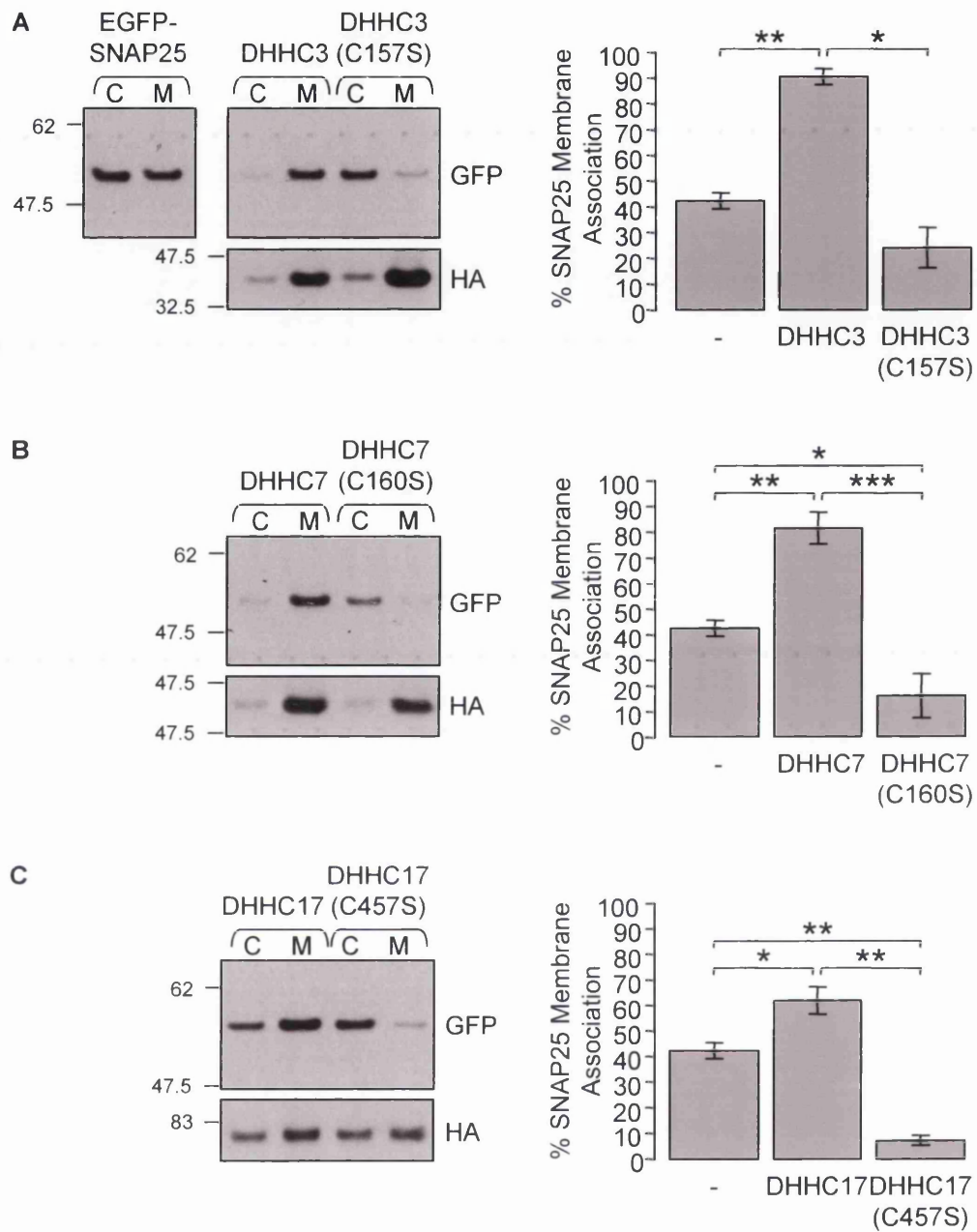
Figure 5.7 Membrane binding of EGFP-SNAP25 is increased by co-expression of DHHC proteins.

Figure 5.7 Membrane binding of EGFP-SNAP25 is increased by co-expression of DHHC proteins. HEK-293 cells were transfected with 0.8 μg of EGFP-SNAP25 or co-transfected with 0.8 μg of EGFP-SNAP25 and 1.6 μg of wild-type DHHC3, -7, or -17, or 1.6 μg of the inactive DHHC mutants, DHHC3(C157S), DHHC7(C160S), or DHHC17(C457S). Forty-eight hours post-transfection, expressed proteins were separated into cytosolic and membrane fractions and analysed following SDS-PAGE and transfer to nitrocellulose membranes by immunoblotting using an anti-GFP monoclonal antibody (*Upper panel*). The co-expression of DHHC proteins was confirmed by probing duplicate nitrocellulose membranes using an anti-HA monoclonal antibody (*Lower panel*). The positions of molecular weight standards (in kDa) are shown on the left side of each panel. Representative blots are shown. *A.* The membrane profile of EGFP-SNAP25 in HEK-293 cells (*left panel*) and EGFP-SNAP25 following co-transfection with DHHC3 and DHHC3(C157S)(*centre panel*). *Right panel* The percentage SNAP25 membrane association +/- SEM was determined by quantification of immunoblots by densitometry (n=4 from 2 separate experiments). * represents a p value of < 0.002 and ** represents a p value of $< 4 \times 10^{-5}$. *B.* The membrane profile of EGFP-SNAP25 in HEK-293 cells following co-transfection with DHHC7 and DHHC7(C160S)(*left panel*). *Right panel* The percentage SNAP25 membrane association +/- SEM was determined by quantification of immunoblots by densitometry (n=4 from 2 separate experiments). * represents a p value of < 0.05, ** represents a p value of < 0.004, and *** represents a p value of < 0.002. *C.* The membrane profile of EGFP-CSP in HEK-293 cells following co-transfection with DHHC17 and DHHC17(C457S)(*left panel*). *Right panel* The percentage CSP membrane association +/- SEM was determined by quantification of immunoblots by densitometry (n=4 from 2 separate experiments). * represents a p value of < 0.03 and ** represents a p value of $< 9 \times 10^{-4}$.

cells. When EGFP-CSP was co-transfected into HEK293 cells with empty pEFBOS-HA vector, expressed CSP displayed a dispersed localisation throughout the cytosol, consistent with the results of subcellular fractionation (Figure 5.8*A*; *Upper panel*). In contrast, co-expression of EGFP-CSP with DHHC3, -7, -15 or -17 lead to the redistribution of EGFP-CSP from the cytosol to a perinuclear compartment that coincides with the localisation of the DHHC protein (Figure 5.8*A*). Thus, CSP co-localises at the Golgi with DHHC3, -7, -15 and -17. Mutations in the DHHC domain of DHHC3, -7, -15 and -17 inhibits the palmitoylating activity of these enzymes towards CSP (Figure 5.6). To investigate the localisation of inactive DHHC proteins in HEK293 cells, and determine whether the co-expression of the mutants has any effect on CSP localisation, HEK293 cells were co-transfected with EGFP-CSP and HA-tagged DHHC3(C157S) or DHHC7(C160S) and the localisation of the proteins was determined by confocal microscopy (Figure 5.8*B*). Although the DHHC-to-DHHS mutations in DHHC3 or -7 did not appear to change the intracellular distribution (*i.e.* Golgi localisation) of these enzymes compared to wild-type, there was no obvious co-localisation of EGFP-CSP with mutant DHHC protein, and indeed, the localisation of EGFP-CSP was similar to that observed in HEK293 cells co-expressing EGFP-CSP and the empty pEFBOS-HA vector (Figure 5.8*A*; *Upper panel*, and Figure 5.8*B*). Together, these results demonstrate that the co-expression of CSP palmitoylating enzymes promotes the interaction of CSP with Golgi membranes, and that this interaction is dependent on the catalytic activity of the palmitoyl transferase.

5.6 OVEREXPRESSION OF CATALYTICALLY INACTIVE DHHC PROTEINS DOES NOT PREVENT CSP MEMBRANE BINDING, PALMITOYLATION OR TRAFFICKING IN PC12 CELLS

DHHC-to-DHHS mutation leads to a loss of CSP palmitoylating activity of DHHC proteins in HEK293 cells, and indeed, these mutants appear to have a dominant-negative activity in this cell type by suppressing the basal level of CSP palmitoylation and membrane binding. Thus, it was examined whether the inactive DHHC mutants could act as dominant negative mutants of CSP palmitoylation in a cell type where CSP is endogenously expressed and efficiently palmitoylated. In PC12 cells, the majority of overexpressed EGFP-CSP is predominantly found in the membrane fraction and, as highlighted by the change in migration following SDS-PAGE, is fully palmitoylated (Figure 3.1*B* and *C*; Figure 5.9*A*: *Left panel*). EGFP-CSP and the inactive DHHC mutants DHHC3(C157S), DHHC7(C160S), DHHC15(C159S) or DHHC17(C457S) were co-transected into PC12 cells and, forty-eight hours later, cystoslic and membrane fractions were isolated and examined by SDS-PAGE and immunblotting using an anti-GFP monoclonal antibody (Figure 5.9*A*; *Right panel*). No detectable change in either the level of EGFP-CSP membrane association or palmitoylation could be observed following co-expression
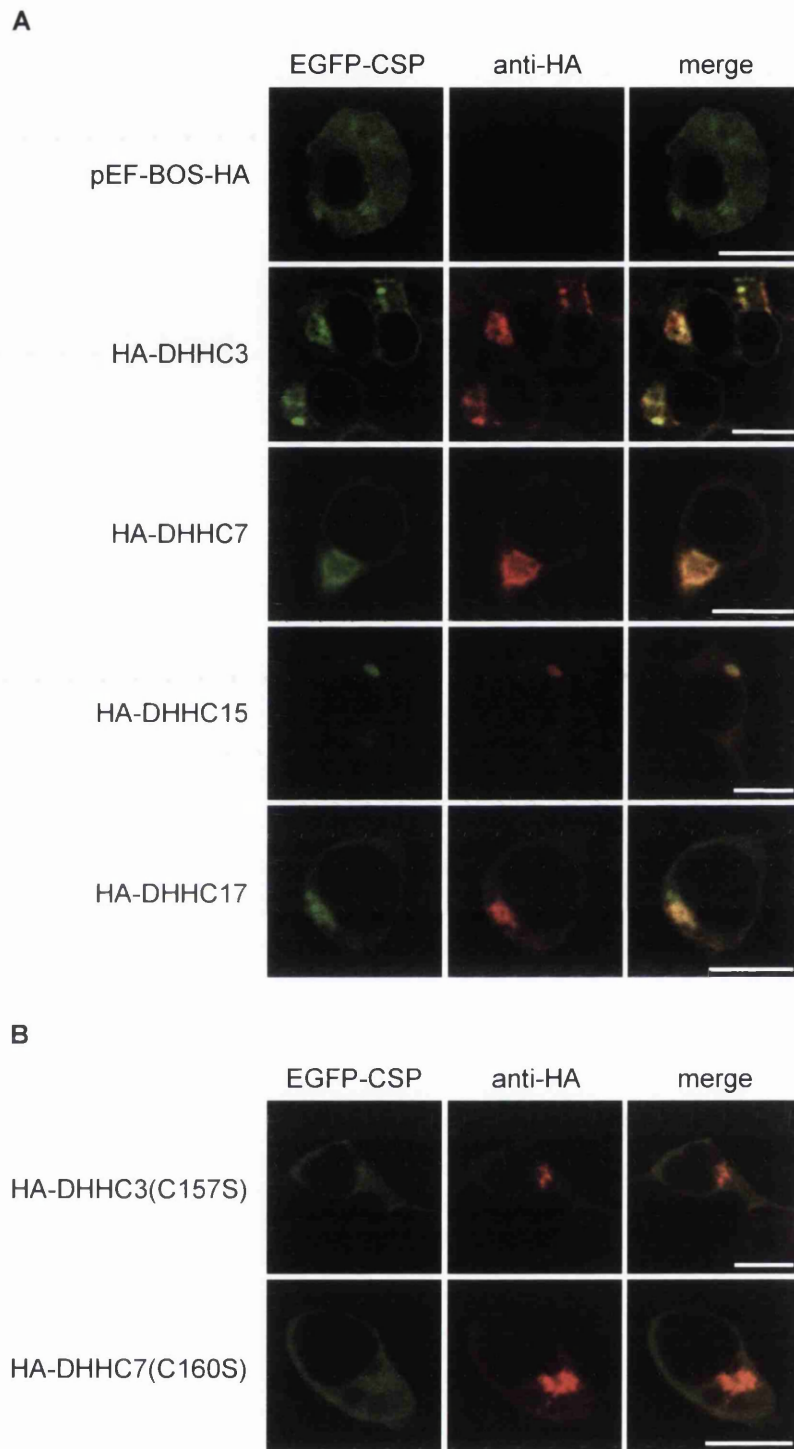
Figure 5.8 Localisation of EGFP-CSP in HEK-293 cells following co-expression of DHHC proteins.

Figure 5.8 Localisation of EGFP-CSP in HEK-293 cells following co-expression of DHHC proteins. HEK-293 cells growing on glass coverslips were co-transfected with EGFP-CSP and empty vector (pEF-BOS-HA), HA-DHHC3, HA-DHHC7, HA-DHHC15 or HA-DHHC17 (*A*) or the inactive mutants HA-DHHC3(C157S) or HA-DHHC7(C160S)(*B*). Forty-eight hours later, the cells were fixed in 4% (v/v) formaldehyde, permeabilised and probed with a rhodamine-conjugated mouse monoclonal anti-HA antibody to label expressed DHHC proteins (red) and compared with the GFP signal (green). Localisations of the labelled proteins were determined by confocal microscopy and images are representative of a single 0.13 μm thick confocal section through HEK-293 cells. Scale bar = 10 μm.
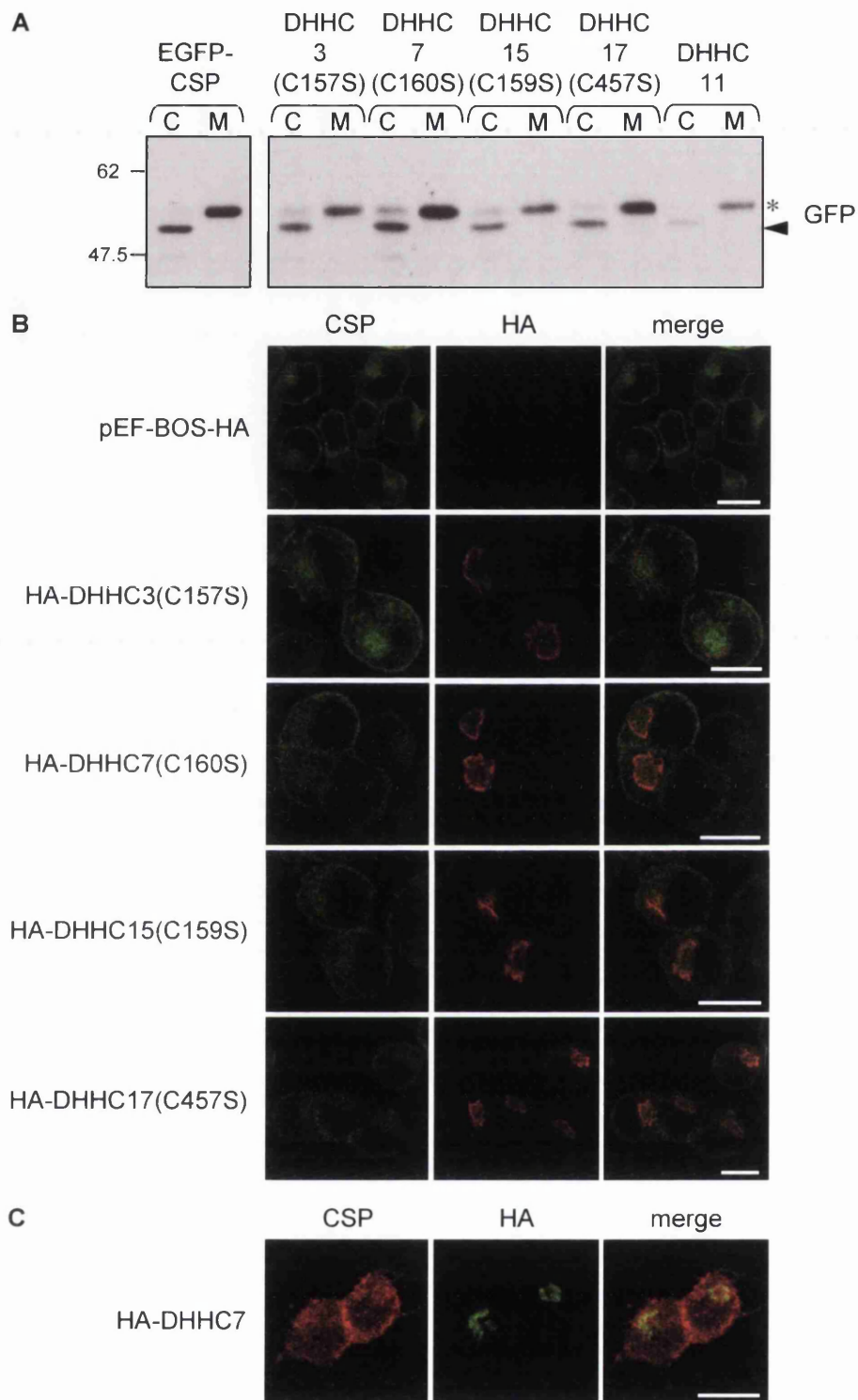
Figure 5.9 Inactive DHHC mutants do not affect CSP membrane association, palmitoylation or localisation in PC12 cells.

Figure 5.9 Inactive DHHC mutants do not affect CSP membrane association, palmitoylation or localisation in PC12 cells. *A.* PC12 cells were transfected with 0.8 μg of EGFP-CSP or co-transfected with 0.8 μg of EGFP-CSP and 1.6 μg of the inactive DHHC mutants DHHC3(C157S), DHHC7(C160S), DHHC15(C159S) or DHHC17(C457S), or 1.6 μg of DHHC11. Forty-eight hours post-transfection, expressed proteins were separated into cytosolic and membrane fractions and analysed following SDS-PAGE and transfer to nitrocellulose membranes by immunoblotting using an anti-GFP monoclonal antibody. The positions of molecular weight standards (in kDa) are shown on the left side of each panel; *asterisks* identify palmitoylated CSP and *arrowheads* indicate unpalmitoylated CSP. Representative blots are shown. *B.* PC12 cells growing on glass coverslips were transfected with empty vector (pEF-BOS-HA) or the inactive DHHC mutants, DHHC3(C157S), DHHC7(C160S), DHHC15(C159S) or DHHC17(C457S). Forty-eight hours later, the cells were fixed in 4% (v/v) formaldehyde, permeabilised and probed with a rhodamine-conjugated mouse monoclonal anti-HA antibody to label expressed DHHC proteins (red). To label endogenous CSP, the cells were probed with a polyclonal anti-CSP antibody. CSP labelling was detected by probing with an Alexa Fluor® 488 goat anti-rabbit IgG (green) and compared with the DHHC signal. *C.* PC12 cells growing on glass coverslips were transfected with HA-DHHC7. Forty-eight hours later, the cells were fixed and permeabilised. DHHC7 was detected by probing cells with a FITC-conjugated anti-HA mouse monoclonal antibody (green). Endogenous CSP was labelled by probing cells with a polyclonal anti-CSP antibody. CSP labelling was detected by probing with an Alexa Fluor® 494 goat anti-rabbit IgG (red) and compared with the DHHC signal. Localisation of the labelled proteins were determined by confocal microscopy and images are representative of a single 0.13 μm thick confocal section through PC12 cells. Scale bar = 10 μm.

of the inactive DHHC mutants in PC12 cells. Since DHHC11 consistently and statistically reduced the basal level of EGFP-CSP membrane binding following co-transfection in HEK293 cells (Figure 5.3), this protein was also co-expressed with EGFP-CSP in PC12 cells to investigate whether DHHC11 could prevent CSP membrane binding or palmitoylation. As shown in Figure 5.9A (*Right panel*) the co-expression of DHHC11 also had no effect on EGFP-CSP membrane binding or palmitoylation. To determine whether the expression of the inactive DHHC mutants had any effect on the distribution of *endogenous* CSP, PC12 cells were transfected with the HA-tagged DHHC C-S mutants (or empty pEFBOS-HA vector as a control), and the localisation of endogenous CSP in DHHC transfected cells was determined by immunofluorescence and confocal microscopy (Figure 5.9B). There was no detectable change in the localisation or trafficking of CSP in PC12 cells transfected with the C-S DHHC mutant proteins compared to empty pEFBOS-HA vector (Figure 5.9B), consistent with the previous finding that the inactive DHHC mutants have no effect on CSP membrane binding or palmitoylation (Figure 5.9A). Interestingly, and in contrast to the effects of DHHC overexpression on CSP localisation in HEK293 cells (Figure 5.8A), no change in subcellular localisation was observed for endogenous CSP following the overexpresion of DHHC7 in PC12 cellls (Figure 5.9C).

There are a number of possibilities to explain why DHHC C-to-S mutants have no effect on CSP membrane binding and palmitoylation in PC12 cells. One aspect that may be particularly relevant is whether the mutants have strong or weak dominant-negative activity. For example, expression of the mutants in HEK293 cells may be sufficient to out-compete the limiting amount of DHHC proteins active against CSP in these cells, but may be inefficient at blocking palmitoylation in PC12 cells if these cells contain excess DHHC protein. To determine the efficiency with which the individual inactive DHHC-DHHS mutants are able to suppress the catalytic activity of wild-type DHHC protein, HEK293 cells were transfected with EGFP-CSP alone, co-transfected with EGFP-CSP and DHHC3, or co-transfected with EGFP-CSP, DHHC3 and DHHC3(C157S), DHHC7(C160S), DHHC15(C159S) or DHHC17(C457S). Cells were separated into cytosolic and membrane fractions, and the partitioning of EGFP-CSP into these fractions was determined by subjecting equal volumes of each fraction to SDS-PAGE, transfer to nitrocellulose and immunoblotting using a monoclonal anti-GFP antibody. Figure 5.10 (*Left panel*) demonstrates that, as previously shown, EGFP-CSP membrane binding and palmitoylation is inefficient in HEK293 cells, but is promoted following co-expression with DHHC3. Interestingly, the efficient membrane binding and palmitoylation of EGFP-CSP following co-expression of DHHC3 is not perturbed by the co-expression of the inactive DHHC-DHHS mutants (Figure 5.10). This result clearly shows that these mutants are not able
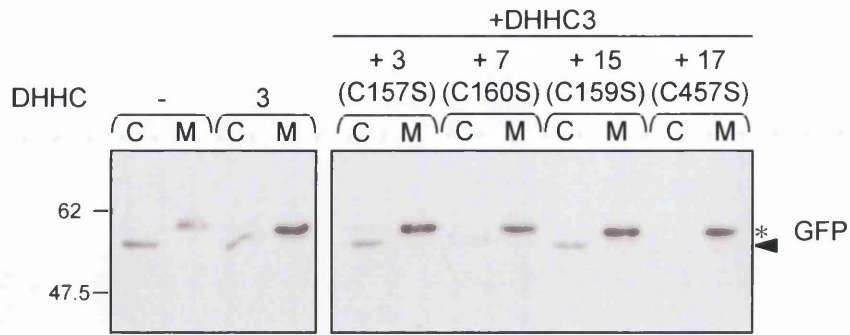
Figure 5.10 Inactive DHHC mutants do not act as dominant negative against wild-type protein. HEK 293 cells were transfected with 0.8 µg of EGFP-CSP or co-transfected with 0.8 µg of EGFP-CSP and 1.6 µg of DHHC3 (*Left panel*) or co-transfected with 0.8 µg of EGFP-CSP, 1.6 µg of DHHC3 and 1.6 µg of either DHHC3(C157S), DHHC7(C160S), DHHC15(C159S) or DHHC17(C457S) (*Right panel*). Forty-eight hours post-transfection, expressed proteins were separated into cytosolic and membrane fractions and analysed following SDS-PAGE and transfer to nitrocellulose membranes by immunoblotting using an anti-GFP monoclonal antibody. The positions of molecular weight standards (in kDa) are shown on the left side of each panel; *asterisks* identify palmitoylated CSP and *arrowheads* indicate unpalmitoylated CSP. Representative blots are shown.

to act as strong dominant negative inhibitors of DHHC enzymic activity, and provides an explanation as to why these mutants do not affect CSP palmitoylation in PC12 cells.

5.7 DISCUSSION

The twenty-three murine DHHC clones have been expressed in PC12 cells and their localisation, as determined by confocal microscopy, can been broadly categorised into three groups: ER, Golgi apparatus, and plasma membrane/endosomal (Figure 5.1). The localisation of the DHHC proteins to these subcellular organelles fits well with published data in which the localisation of a subset of the DHHC proteins and/or palmitoyl transferase activity has been identified (Dunphy *et al.*, 1996; Fukata *et al.*, 2004; Huang *et al.*, 2004; Keller *et al.*, 2004; Roth *et al.*, 2002; Schroeder *et al.*, 1996; Singaraja *et al.*, 2002; Swarthout *et al.*, 2005; Uemura *et al.*, 2002; Valdez-Taubas and Pelham, 2005; Veit *et al.*, 2001). Recently, the intracellular localisation of the twenty-two human DHHC proteins in HEK293 cells has been published (Ohno *et al.*, 2006). While the subcellular localisation of the murine DHHC clones determined in this study agrees well with published data for the human DHHCs, a few discrepancies have arisen. The notable differences include the different localisations of DHHC4, -11 and -12; however, this may reflect the different localisation of DHHC proteins between species. However, Swf1, the yeast homologue of DHHC4, is ER-localised (Valdez-Taubas and Pelham, 2005), supporting the observations of an ER localisation of murine DHHC4 in mammalian cells (Figure 5.1*C*; *Upper panel*; Figure 5.5*B*; *Upper panel*). In contrast, Ohno *et al* reports human DHHC4 at the Golgi (Ohno *et al.*, 2006). The lack of readily available antibodies specific for the DHHC proteins has hindered the characterisation of endogenous DHHC proteins in various cell types or tissues, and the generation of such antibodies will be an important development. In addition, techniques such as quantitative PCR could be employed to detect DHHC mRNA in individual cell types and tissues.

The results presented in Chapter Four suggest that the hydrophobic cysteine-rich domain of CSP facilitates membrane anchoring prior to palmitoylation. However, it was not clear whether this interaction is stable or weak/transient. The inefficient palmitoylation of EGFP-CSP in HEK293 cells allowed this question to be addressed. Indeed, despite the large fraction of unpalmitoylated EGFP-CSP in HEK293 cells, no significant quantity of this unpalmitoylated protein can be detected in the membrane fraction (Figure 5.2). This suggests that the cysteine-rich domain is not able to mediate stable membrane binding of full-length CSP in the absence of palmitoylation. Confocal imaging also revealed a dispersed, mainly cytosolic localisation of EGFP-CSP in HEK293 cells (Figure 5.8*A*; *Upper panel*).

Results in this chapter have identified four palmitoyl transferases, DHHC3, -7, -15 and -17, that are able to palmitoylate CSP and lead to its stable membrane binding (Figure 5.3). These CSP palmitoylating enzymes are localised to the Golgi apparatus, based on their coincidence with the medial Golgi protein GRASP55 as observed by confocal microscopy in both HEK293 and PC12 cells (Figures 5.1 and 5.5A), and this implies that CSP palmitoylation also occurs in the Golgi. This finding was surprising, as the unpalmitoylated CSP mutants identified in Chapters Three and Four were localised to the ER, prompting the suggestion that CSP is targeted to the ER for palmitoylation to occur. However, the identification of the Golgi apparatus as the site of CSP palmitoylation suggests that the CSP mutants may instead be mislocalised at the ER, and perhaps be unpalmitoylated because they are physically separated from their partner palmitoyl transferases. Now that the intracellular site of CSP palmitoylation has been highlighted, it is important to establish the mechanisms that enable CSP to target its cognate palmitoyl transferase on Golgi membranes.

The identification of four DHHC proteins that palmitoylate CSP may be an underestimate, since many of the DHHC proteins were only poorly expressed in HEK293 cells (Figure 5.4). However, many non-active DHHC proteins were expressed at similar or higher levels than DHHC3, -7, -15 and -17. For example, DHHC2 and -4 were expressed at higher levels than DHHC3 and -7, and DHHC11 was expressed at similar levels, yet these proteins had no stimulatory effect on CSP palmitoylation. Similarly, DHHC12, -14, -16 and -22 were all expressed at similar levels to DHHC17 (and DHHC13 was more highly expressed), yet these enzymes also failed to palmitoylate CSP. This demonstrates that the ability of DHHC3, -7, -15 and -17 to modify CSP are not simply related to expression levels, and confirms the specificity of the results. As four enzymes were able to palmitoylate CSP in HEK293 cells, there may be some redundancy in palmitoylation of DHHC substrates. Indeed, several other proteins have also been found to be substrates for multiple DHHC proteins, and thus the finding that four palmitoyl transferases are active towards CSP is not surprising in the context of a cellular screening assay. However, it is worth noting that genetic studies carried out in yeast have demonstrated that specific enzyme-substrate pairing, whereby the substrate protein is only able to be palmitoylated by a single enzyme, does occasionally occur (Kihara et al., 2005; Lobo et al., 2002; Roth et al., 2002; Smotrys et al., 2005; Valdez-Taubas and Pelham, 2005). Perhaps enzyme-substrate specificity is regulated in mammalian cells partly through different expression profiles of DHHC isoforms, in distinct cell types and tissues. For example, perhaps one of the DHHC proteins active against CSP is expressed at significantly higher levels than the others in PC12 cells. It is important to note that all the enzymes identified as CSP palmitoyl transferases do display some degree of substrate specificity. For example, DHHC17 did not palmitoylate

PSD-95, GAP-43, G_α or the γ2 subunit of $GABA_A$ (Fang *et al.*, 2006; Fukata *et al.*, 2004). Similarly, DHHC15 was inactive against Lck, H-ras and G_α, and was only marginally active against the γ2 subunit of $GABA_A$ (Fang *et al.*, 2006; Fukata *et al.*, 2004). DHHC7 did not enhance palmitoylation of Lck or H-ras, whereas DHHC3 was not active against Lck (Fukata *et al.*, 2004). Furthermore, many of the DHHC proteins that tested negative against CSP have previously been shown to palmitoylate specific substrates (Fernandez-Hernando *et al.*, 2006; Fukata *et al.*, 2004; Swarthout *et al.*, 2005). Thus, there appears to be a good degree of specificity exhibited by the DHHC proteins that palmitoylate CSP. At present it is not known how CSP/DHHC specificity is regulated, but possibilities may include specific structural features within the DHHC region and/or other domains of DHHC3, -7, -15 and -17 that regulate the interaction with CSP. Alternatively, these DHHC proteins may associate with specific sub-domains of the Golgi, which facilitates the interaction with CSP. That other DHHC proteins are also localised to the Golgi yet are inactive towards CSP further strengthens the specificity of the reaction between CSP and DHHC3, -7, -15 and -17.

The expression of CSP palmitoylating enzymes in HEK293 cells leads to co-localisation of CSP with the DHHC proteins at the Golgi apparatus (Figure 5.8*A*). The localisation of CSP at the Golgi may occur due to an absence of important factors in HEK293 cells that are required for the forward transport of CSP out of the Golgi. However, it is important to note that several studies have found that when DHHC proteins are co-expressed with their substrate proteins, the substrate protein becomes trapped with the partner palmitoyl transferase at the intracellular compartment where the palmitoyl transferase normally resides (Fernandez-Hernando *et al.*, 2006; Fukata *et al.*, 2004; Hayashi *et al.*, 2005; Huang *et al.*, 2004; Keller *et al.*, 2004; Uemura *et al.*, 2002). Why substrate proteins become trapped in this way is not known, however one possibility could be due to the lack of DHHC auxiliary proteins, which could serve to control the cycle of enzyme-substrate binding and release. Indeed, the DHHC proteins that palmitoylate yeast and mammalian Ras, Erf2p and DHHC9, require accessory proteins for their activity (Lobo *et al.*, 2002; Swarthout *et al.*, 2005). Trapping may not reflect direct CSP-DHHC binding as attempts to isolate CSP-DHHC interaction by co-immunoprecipitations were unsuccessful.

The overexpression of inactive CSP palmitoylating enzymes in PC12 cells had no effect on CSP membrane binding, palmitoylation or trafficking (Figure 5.9), suggesting that they are not able to act as dominant negative proteins. Another possibility is that PC12 cells express more than one enzyme that is active against CSP, and that this may be able to compensate following the over-expression of an inactive mutant. However, as the overexpression of inactive DHHC

mutants in HEK293 cells was not able to suppress the palmitoylating activity of DHHC3 over-expression towards CSP (Figure 5.10), it is likely that inactive DHHC proteins are only weakly dominant negative. An alternative method to study the DHHC proteins that palmitoylate CSP in PC12 cells is RNAi, and efforts are currently ongoing to optimise protocols for siRNA-induced knockdown of proteins in this cell line. Once these protocols are established, siRNA molecules could be designed against DHHC3, -7, -15 and -17, and their effects on CSP palmitoylation can be investigated.

CHAPTER SIX: PALMITOYLATION AND MEMBRANE INTERACTIONS

OF CSP

6.1 INTRODUCTION

Previous attempts to identify the enzymes responsible for protein palmitoylation were hindered due to difficulties in preserving enzymic activity following purification and the appearance of false positives (Liu *et al.*, 1996), and so the discovery of the DHHC-family of palmitoyl transferases was only made relatively recently (Fukata *et al.*, 2004; Lobo *et al.*, 2002; Roth *et al.*, 2002). Sequence analysis of members of the DHHC family predict that they are polytopic membrane proteins, with the DHHC domain present on the cytosolic face of the membrane (Politis *et al.*, 2005). The discovery that palmitoylating enzymes are membrane-associated was interesting, as previously palmitoylation was regarded as being a prerequisite for the membrane targeting of palmitoylated proteins (Chamberlain and Burgoyne, 1998). As DHHC proteins are integral membrane proteins, substrates must therefore contain additional membrane targeting signals to mediate membrane association prior to palmitoylation. This sets palmitoylation apart from isoprenylation and myristoylation, which occur in the cytosol, and indeed these modifications often facilitate membrane association of proteins prior to palmitoylation (for example, H- and N-Ras (Goodwin *et al.*, 2005; Rocks *et al.*, 2005). The primary membrane targeting information contained within many palmitoylated proteins is easily identifiable (for example, myristoyl and isoprenyl attachment sites, or transmembrane domains). However, the mechanisms employed by other palmitoylated proteins for initial membrane targeting are less well understood.

Two unpalmitoylated CSP mutants were identified in Chapters Three and Four and were found to be localised predominantly to the ER in PC12 cells; these mutants either contain a truncation of the C-terminus immediately after the cysteine-rich domain (CSP_{1-136}) or have four cysteines in the cysteine string domain replaced with leucine residues (CSP(C4-7L)). The identification of two unpalmitoylated CSP mutants that are both localised to ER membranes led to the hypothesis that CSP might interact initially with ER membranes through its hydrophobic cysteine string domain, with palmitoylation being required to allow ER exit and subsequent sorting. The results presented in Chapter Five, however, have identified four CSP-palmitoylating DHHC proteins, DHHC3, -7, -15 and -17, which are all localised to Golgi membranes. The finding that CSP is palmitoylated at the Golgi was surprising; however, the lack of palmitoylation of CSP_{1-136} and CSPC4-7L might be explained if the *initial* membrane interaction of these mutants is altered, resulting in these mutants accumulating on 'inappropriate' intracellular membranes. In this way, the mutant proteins would be physically separated from their partner palmitoyl transferase, and would remain unpalmitoylated.

Results presented in Chapter Three identified a correlation between the strength of membrane association of CSP C-terminal truncation mutants and the probability of palmitoylation (Figure 3.8D). Mutants displaying increased levels of membrane binding were associated with an inhibition of palmitoylation (for example, in the CSP_{1-136} mutant), whereas mutants that had weaker membrane binding were found to promote palmitoylation (for example, CSP_{1-146}). Thus, it appears that for CSP truncation mutants (at least), the strength of membrane binding inversely correlates with palmitoylation. Furthermore, the coincidence of palmitoylation of C-terminal truncation mutants is associated with the onward sorting of CSP (Figure 3.8E); however, it is not known what factors, other than palmitoylation, regulate CSP trafficking.

6.2 CORRELATION BETWEEN CSP MEMBRANE AFFINITY AND PALMITOYLATION

As CSP palmitoylating enzymes are localised to the Golgi, it was reasoned that perhaps the ER localisation of the CSP_{1-136} and CSP(C4-7L) mutants reflects a perturbation of initial membrane interactions. It is not easy to determine if CSP_{1-136} and CSP(C4-7L) have an altered membrane affinity relative to wild-type CSP in PC12 cells due to efficient palmitoylation of the wild-type protein in this cell type. Thus, the membrane binding of CSP_{1-136} and CSP(C4-7L) were analysed in HEK293 cells, which express only limited amounts of the DHHC proteins that are active against CSP (Figure 5.2). EGFP-CSP, EGFP-CSP_{1-136} and EGFP-CSP(C4-7L) were transfected into HEK293 cells for twenty-four hours, and the distribution of these proteins in recovered cytosol and membrane fractions was examined by immunoblotting using an anti-GFP monoclonal antibody (Figure 6.1A). This analysis clearly revealed that both EGFP-CSP_{1-136} and CSP(C4-7L) significantly associated more tightly with membranes than wild-type CSP (Figure 6.1A and B). Note that the membrane-associated fraction of wild-type CSP that was quantified in Figure 6.1A corresponds to the small amount of protein that is palmitoylated in HEK293 cells. Thus, the membrane affinity of CSP_{1-136} and CSP(C4-7L) compared to *unpalmitoylated* wild-type CSP will be substantially greater than suggested by the quantification. Co-expression of EGFP-CSP and active DHHC proteins in HEK293 cells redistributes CSP from the cytosol to a perinuclear localisation, which coincides with the localisation of the co-expressed DHHC protein (Figure 5.8A). EGFP-CSP_{1-136} and EGFP-CSP(C4-7L) are both localised to the ER in PC12 cells (Figures 3.5 and 4.6B), and the intracellular localisations of the two mutants with HA-DHHC3 were compared in HEK293 cells using confocal microscopy by Dr. Luke Chamberlain. This analysis revealed a clear physical separation of both CSP mutants from the Golgi-localised DHHC protein (Figure 6.1C; *Upper and middle panels*). Furthermore, both CSP mutants exhibit an ER-like distribution, which is similar to the localisation observed following their overexpression in PC12 cells (Figures 3.5 and 4.6B), and was confirmed by
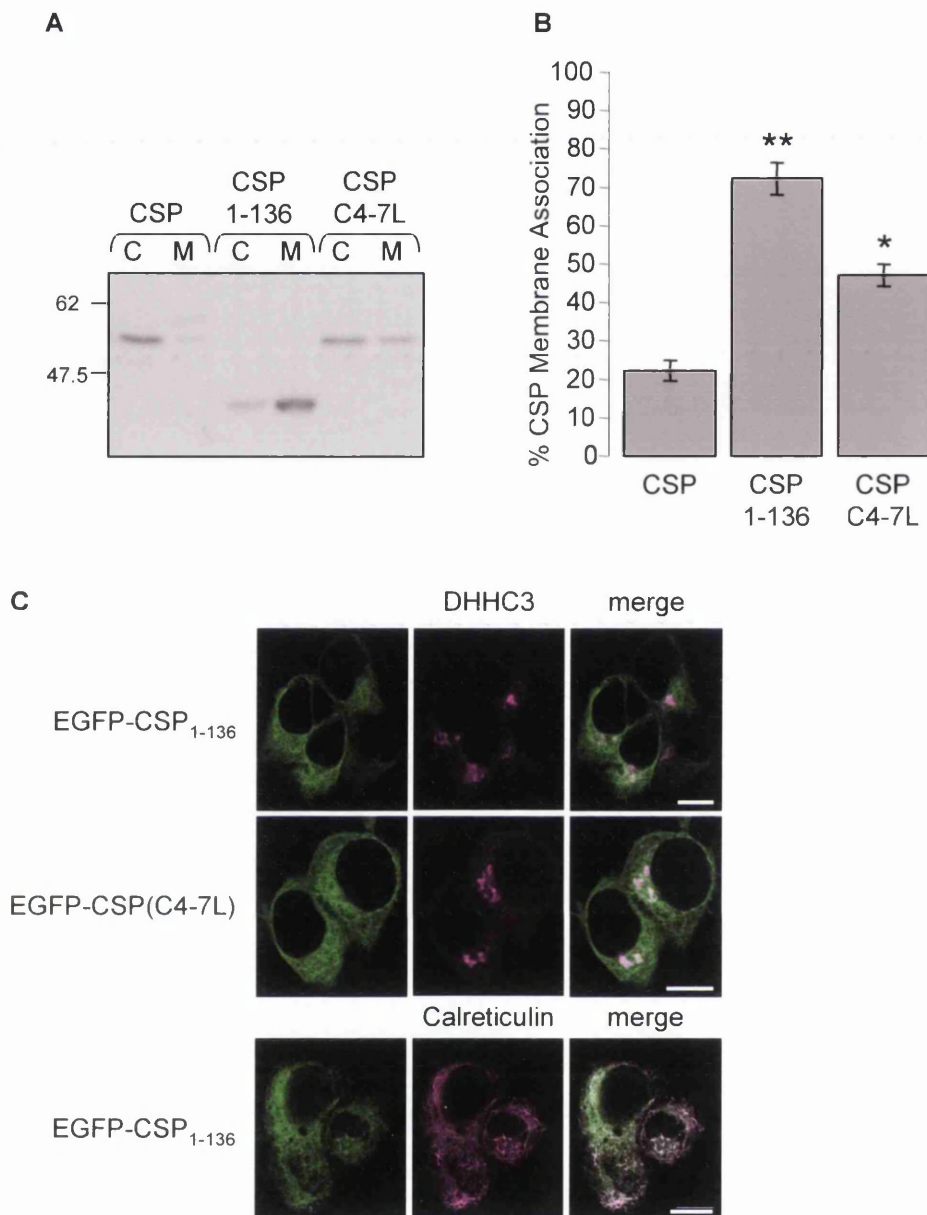
Figure 6.1 Membrane binding of CSP mutants in HEK293 cells. *A*. HEK293 cells transfected with EGFP-CSP, EGFP-CSP$_{1-136}$ and EGFP-CSP(C4-7L) mutants for 24 h were fractionated into cytosolic (C) and membrane (M) fractions and analysed following SDS-PAGE and transfer to nitrocellulose membranes by immunoblotting using an anti-GFP monoclonal antibody. The position of molecular weight standards (in kDa) is shown on the left side of the panel. Representative blots are shown. *B*. The percentage CSP membrane association +/- SEM was determined by quantification of immunoblots by densitometry (n = 6 from 3 separate experiments). Statistical significance was determined by a Student's *t*-test, whereby * represents a p value of < 5 x 10^{-5} and ** represents a p value of < 3 x 10^{-6}, compared to wild-type EGFP-CSP. *C*. HEK293 cells were transfected with EGFP-CSP$_{1-136}$ and HA-DHHC3 (*Upper panel*), EGFP-CSP(C4-7L) and HA-DHHC3 (*Centre panel*), or with EGFP-CSP$_{1-136}$ alone (*Lower panel*). Cells were fixed, permeabilised, and incubated with rhodamine-conjugated anti-HA (*Upper and Centre panels*) or with anti-calreticulin antibody followed by Alexa Fluor 543-conjugated rabbit secondary antibody (*Lower panel*). Images are representative of a single 0.13 µm thick confocal section. Scale bar = 10 µm. Panel *C* was kindly provided by Dr. Luke Chamberlain.

immunofluorecence of HEK293 cells that were expressing EGFP-CSP$_{1-136}$ and were probed for the ER resident protein calreticulin (Figure 6.1C; *Lower panel*). Thus, CSP mutants that enhance membrane affinity promote association with 'inappropriate' cell membranes, offering an explanation for the finding that these mutants are not efficiently palmitoylated in PC12 cells (See Figures 3.4B and 4.6A; *Right panel*).

The addition of amino acids downstream from the cysteine string domain of EGFP-CSP$_{1-136}$ weakened CSP membrane interactions, which simultaneously promoted its palmitoylation in PC12 cells (Figure 3.8A-D). To determine whether the addition of residues downstream from the cysteine string domain similarly weakens the membrane binding of CSP in HEK293 cells, CSP C-terminal truncation mutants were expressed in HEK293 cells for twenty-four hours, and the level of membrane affinity was assessed by separating the cells into cytosolic and membrane fractions and immunoblotting using a monoclonal anti-GFP antibody (Figure 6.2A). Interestingly, the level of membrane affinity of CSP truncation mutants expressed in HEK293 cells decreased as amino acids were added to the C-terminus of the cysteine string domain, and the presence of K137-P138-K139 in the CSP$_{1-139}$ mutant weakened membrane binding significantly (Figure 6.2). Strikingly, this loss of membrane binding correlated near perfectly with the appearance of a palmitoylated fraction of EGFP-CSP, which became apparent following a longer exposure of the blot (Figure 6.2A; *Lower panel*; *asterisk*). These findings in HEK293 cells further highlight the inverse correlation between membrane affinity of CSP mutants and palmitoylation.

These analyses in HEK293 cells clearly show that the level of membrane binding of CSP mutants decreases as successive amino acids are added to the end of the cysteine string domain. However, these experiments do not provide direct data on *initial* membrane binding of CSP, which directly follows protein synthesis. Thus, to extend this analysis, [^{35}S] cysteine/methionine pulse-chase studies were employed to study the membrane binding and palmitoylation of newly synthesised wild-type and mutant CSP in PC12 cells. To determine the time-course of membrane binding and palmitoylation of full-length CSP, PC12 cells transfected with EGFP-CSP (or EGFP as a control) for forty-eight hours were incubated with radiolabelled cysteine/methionine mix for 15 minutes. Radiolabel was then removed by washing the cells in fresh media, and the cells were separated into cystosolic and membrane fractions following a chase period of 15-60 minutes. GFP-tagged proteins were recovered from isolated cytosol and membrane fractions by immunoprecipitation using anti-GFP magnetic beads. The immunoprecipitated samples were analysed by SDS-PAGE, transfer to duplicate nitrocellulose membranes, and immunoblotting using a monoclonal anti-GFP antibody or by autoradiography
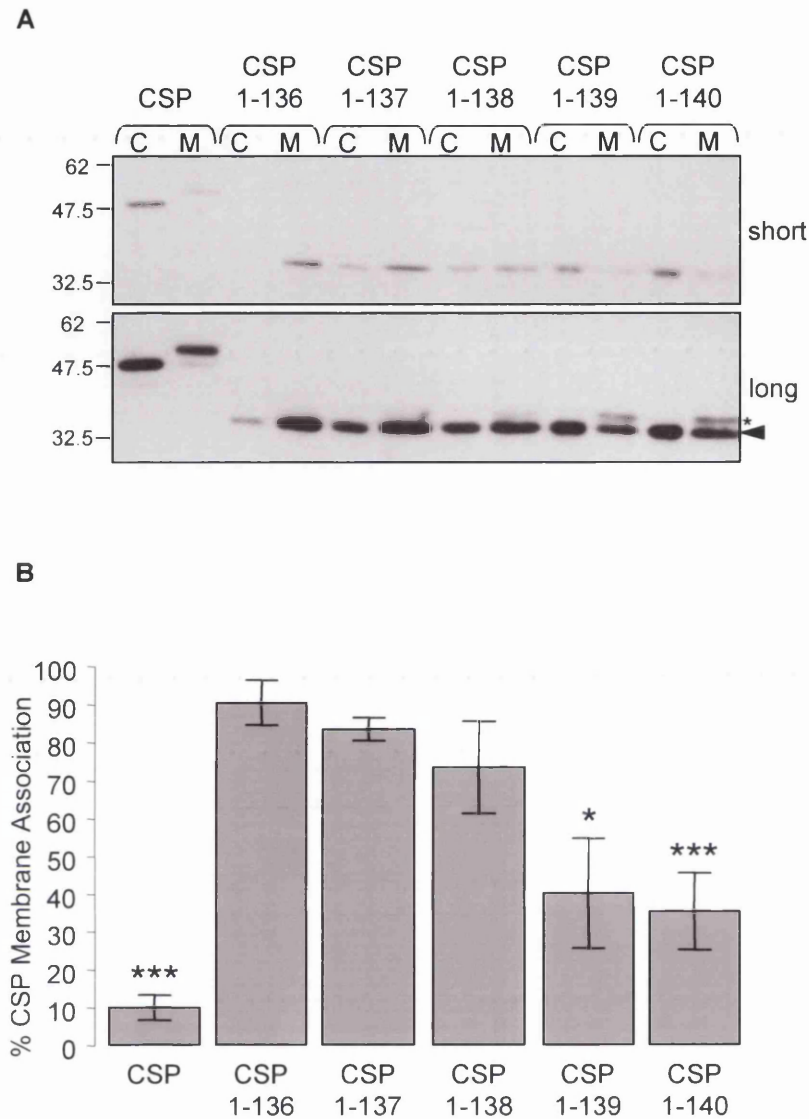
Figure 6.2 Membrane binding of CSP C-terminal truncation mutants in HEK293 cells. *A*. HEK293 cells were transfected with wild-type EGFP-CSP and the indicated C-terminal truncation mutants. Cells were then fractionated into cytosol (C) and membrane (M) fractions, which were examined by immunoblotting with an anti-GFP monoclonal antibody. Shown is a short and long exposure of the same blot. The position of molecular weight standards (in kDa) is shown on the left side of the panel; *arrowheads* indicate unpalmitoylated CSP, whereas *asterisks* highlight palmitoylated CSP. Representative blots are shown. *B*. The percentage CSP membrane association +/- SEM was determined by quantification of immunoblots by densitometry (n = 5 from 3 separate experiments). Statistical significance was determined by a Student's *t*-test, whereby * represents a p value of < 0.02, ** represents a p value of < 2×10^{-3}, and *** represents a p value of < 8×10^{-6} compared to EGFP-CSP$_{1-136}$.

(Figure 6.3*A*). Two significant observations can be made from results presented in the *Upper panel* of Figure 6.3*A*. First, there was a time-dependent appearance of palmitoylated CSP on membranes (*asterisk*). Second, although unpalmitoylated CSP (*arrowhead*) was clearly associated with membranes, the level of membrane association of unpalmitoylated CSP was relatively constant over time. This would be expected if a protein with a weak membrane affinity were transiently associating to cell membranes. Note that in the *Upper panel* of Figure 6.3*A*, the faint band present in the control cytosol lane (pEGFP) is a non-specific band that was occasionally detected in control samples; this band migrates more slowly than the CSP cytosolic band. The initial membrane interaction of CSP C-terminal truncation mutants in PC12 cells was determined using [^{35}S] cysteine/methionine pulse-chase studies, as before and with a 60 minute chase period. C-terminal truncation of CSP causes a marked increase in the level of initial membrane binding of CSP$_{1-136}$ (Figure 6.3*B* and *C*). Consistent with the HEK293 experiments, the addition of three extra residues (K137-P138-K139) downstream of the cysteine string domain significantly reduced the initial membrane binding of CSP (Figure 6.3*B* and *C*), highlighting a clear inverse correlation between the strength of initial membrane tethering and palmitoylation. Note that although a palmitoylated band is present for the CSP$_{1-139}$ and CSP$_{1-140}$ mutants in the immunoblots presented in Figure 6.3*B*, a corresponding band is not readily detectable for these proteins in the ^{35}S-labelled samples. The difficulty detecting a palmitoylated ^{35}S-labelled band for these mutants most likely reflects their decreased efficiency of palmitoylation compared with wild-type CSP (Figure 3.8*A* and *B*).

6.3 MEMBRANE BINDING AND PALMITOYLATION OF CSP ARE INSENSITIVE TO BREFELDIN A TREATMENT

The results presented thus far are consistent with the notion that wild-type CSP likely has a weak membrane affinity (mediated by the cysteine string domain), which is enhanced either by C-terminal truncation (CSP$_{1-136}$) or by the introduction of more hydrophobic amino acids (C4-7L). CSP palmitoylation occurs at the Golgi apparatus, but the mechanism by which CSP targets Golgi membranes for palmitylation to occur is not known. To determine whether wild-type CSP has a specific affinity for Golgi membranes, or whether it has a more general membrane affinity, the effects of Brefeldin A (BFA) on CSP membrane binding and palmitoylation were examined. BFA inhibits the function of ARF1 (ADP-ribosylation factor 1; (Donaldson *et al.*, 1991; Lippincott-Schwartz *et al.*, 1989), a protein essential for vesicle budding from the ER. BFA treatment thus blocks ER-to-Golgi transport and promotes a loss of Golgi integrity and the fusion of Golgi membranes with the ER. HEK293 cells were transfected with EGFP-CSP alone, or co-transfected with EGFP-CSP and DHHC3 or DHHC7, for four
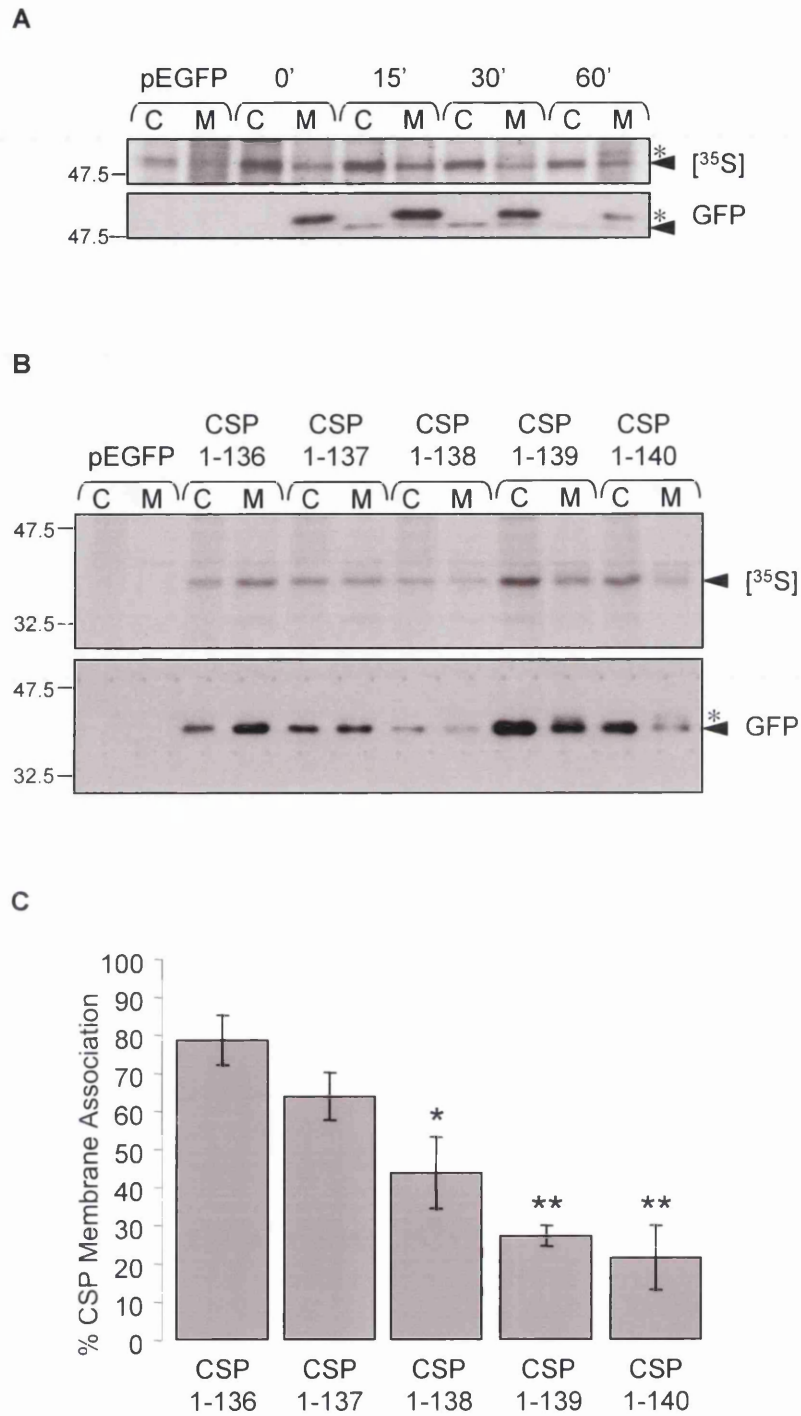
Figure 6.3 Membrane binding of newly synthesised CSP in PC12 cells.

Figure 6.3 Membrane binding of newly synthesised CSP in PC12 cells. *A.* PC12 cells transfected with wild-type EGFP-CSP or empty vector (pEGFP) for 48 h were incubated with [^{35}S]-labelled cysteine/methionine for 15 min, washed and chased for various times as indicated, ranging from 0-60 min. The labelled cells were fractionated into cytosol (C) and membrane (M) fractions, from which GFP-tagged proteins were recovered by immunoprecipitation and subsequently analysed by immunoblotting using an anti-GFP monoclonal antibody *(Upper panel; GFP)*. Duplicate gels were developed using autoradiography (*Lower panel; [^{35}S]*). Note that the ^{35}S-labelled band detected in the EGFP cytosol fraction is a non-specific band that migrates more slowly than cytosolic EGFP-CSP. *B.* PC12 cells transfected with the indicated EGFP-CSP C-terminal truncation mutants or empty vector (pEGFP) for 48 h were incubated with [^{35}S]-labelled cysteine/methionine for 15 min, washed and chased for 60 min. The labelled cells were fractionated into cytosol (C) and membrane (M) fractions. GFP-tagged proteins were recovered by immunoprecipitation and subsequently analysed by immunoblotting using an anti-GFP monoclonal antibody *(Upper panel; GFP)*. Duplicate gels were developed using autoradiography (*Lower panel; [^{35}S]*). The positions of molecular weight standards (in kDa) are shown on the left side of each panel; on the right side of each panel, *asterisks* identify palmitoylated CSP and *arrowheads* indicate unpalmitoylated CSP. Representative blots are shown. *C.* The percentage membrane association of newly-synthesised CSP +/- SEM was determined by quantification of autoradiographs by densitometry (n = 5 from 3 separate experiments). Statistical significance was determined by a Student's *t*-test, whereby * represents a p value of < 0.02 and ** represents a p value of < 2×10^{-3} compared to EGFP-CSP$_{1-136}$.

hours and the cells were then incubated in the presence or absence of 30 μg/ml BFA for a further four hours. In this experimental set-up, BFA will prevent the trafficking of co-transfected DHHC3 and DHHC7 from the ER. Cells were separated into cytosolic and membrane fractions, and the partitioning of EGFP-CSP was analysed by immunoblotting using a monoclonal anti-GFP antibody (Figure 6.4*A*). Figures 6.4*A* and *C* show that BFA treatment did not significantly inhibit membrane binding or palmitoylation of EGFP-CSP either in the absence or presence of DHHC co-transfection. A parallel experiment in which HEK293 cells were transfected with EGFP-SNAP25 demonstrated an almost complete inhibition of membrane binding following BFA treatment (Figure 6.4*B*) in agreement with previous work (Gonzalo and Linder, 1998), and confirms the action of BFA under similar experimental conditions. The results presented in Figure 6.4*A* and *C* imply that CSP palmitoylation does not require a specific intracellular localisation of partner DHHC proteins, but only sufficient cellular expression levels of the enzymes. These results are thus consistent with the notion that CSP has a general membrane affinity rather than recognising specific features inherent to intact Golgi membranes.

To extend these observations and to determine whether CSP membrane association and palmitoylation is also BFA-resistant in a cell type that expresses endogenous CSP, membrane binding and palmitoylation of EGFP-CSP was examined in PC12 cells. Due to lower transfection efficiencies in PC12 cells compared to HEK293 cells, protein expression could not be detected by immunoblotting following an eight-hour transfection period. Thus, [^{35}S] cysteine/methionine pulse-chase experiments were employed to follow membrane binding and palmitoylation specifically of newly synthesised EGFP-CSP. PC12 cells were transfected with pEGFP, EGFP-SNAP25 or EGFP-CSP for forty-eight hours, and were incubated in the presence or absence of 30 μg/ml BFA for 15 minutes. The cells were then incubated in radiolabel in the presence or absence of BFA for 15 min, and, having established that CSP palmitoylation was readily detectable following a 60 minute 'chase' period (Figure 6.3*A*), the cells were washed and incubated for a further 60 minutes in the presence or absence of BFA. In this assay, CSP palmitoylation is dependent upon endogenous DHHC proteins; BFA treatment will promote redistribution of Golgi DHHC proteins to a fused ER-Golgi compartment. Following ^{35}S-labelling, GFP-tagged proteins were then recovered from isolated cytosol and membrane fractions by immunoprecipitation using anti-GFP magnetic beads. The immunoprecipitated samples were resolved by SDS-PAGE, transferred to duplicate nitrocellulose membranes, and immunoblotted using a monoclonal anti-GFP antibody, or were developed by autoradiography. As shown in Figure 6.5*A* and *B*, the initial membrane binding of EGFP-SNAP25 was significantly reduced in the presence of BFA, consistent with previous results (Gonzalo and Linder, 1998) and the results presented in Figure 6.4*B* for HEK293 cells. In contrast, BFA had
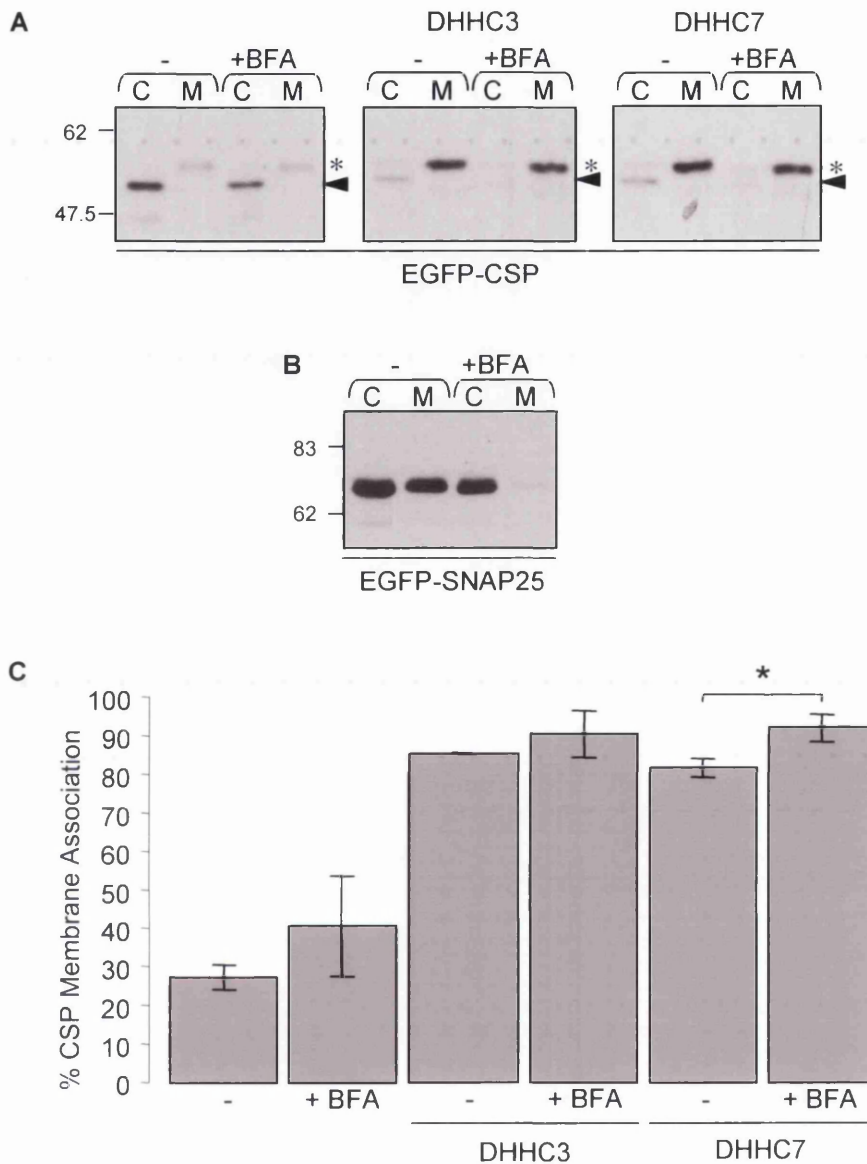
Figure 6.4 Effect of Brefeldin A on EGFP-CSP palmitoylation and membrane association in HEK293 cells. *A*. HEK293 cells were transfected with EGFP-CSP in the presence/absence of DHHC3 or DHHC7. Four hours after transfection, fresh media was added either with or without 30 µg/ml BFA and, after an additional four hours, the cells were fractionated into cytosol (C) and membrane (M) fractions. Equal volumes of the fractions were probed using a monoclonal antibody against GFP. *B*. HEK293 cells transfected with EGFP-SNAP25B were processed as in *A*. The positions of molecular weight standards (in kDa) are shown on the left side of each panel; on the right side of each panel, *asterisks* identify palmitoylated CSP and *arrowheads* indicate unpalmitoylated CSP. Representative blots are shown. *C*. The percentage membrane association of EGFP-CSP +/- SEM in the absence or presence of DHHC3 and -7 co-expression +/- BFA treatment was determined by quantification of immunoblots by densitometry (n = 3 from 2 separate experiments). Statistical significance was determined by a Student's *t*-test, whereby * represents a p value of < 0.05.
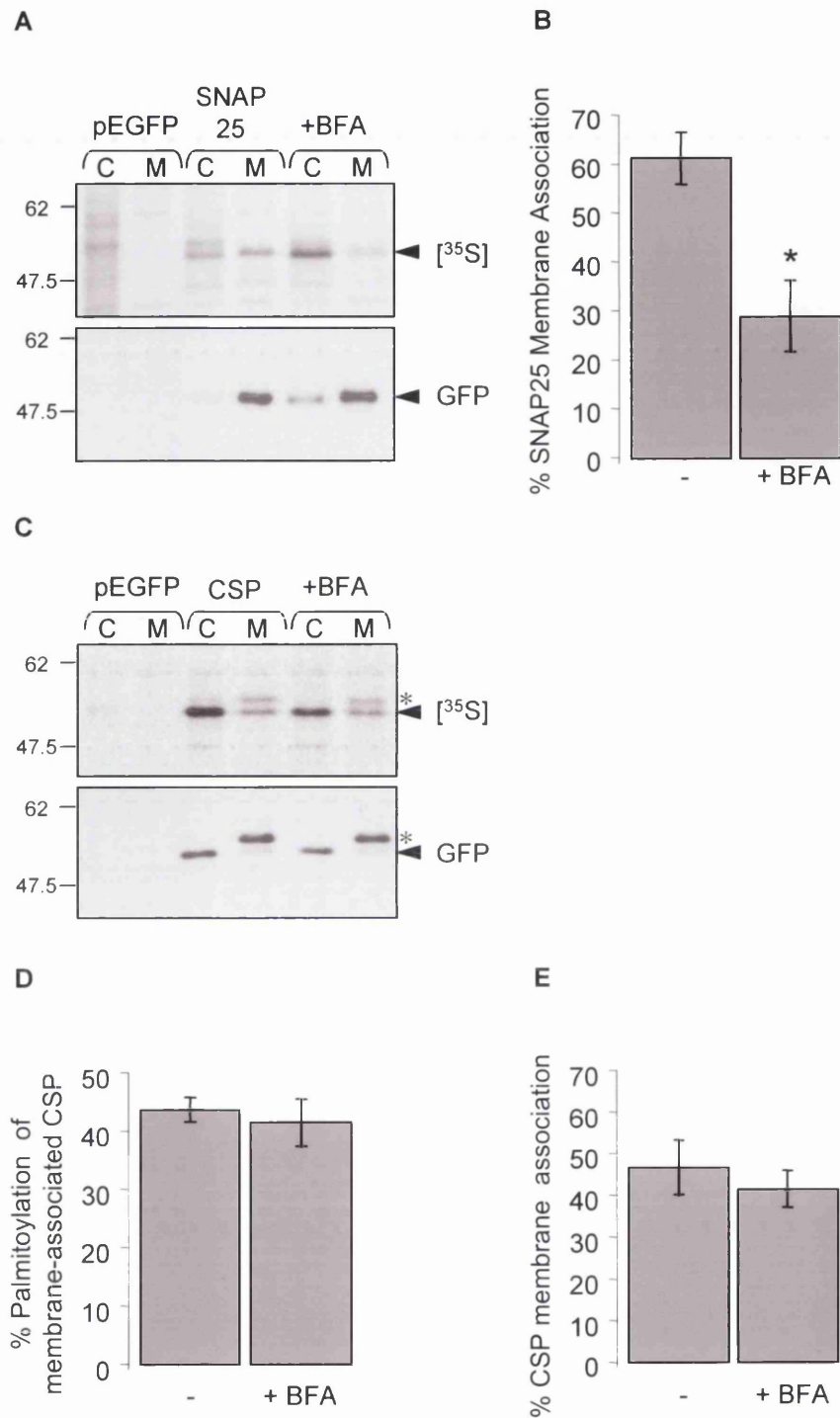
Figure 6.5 Membrane association of newly-synthesised CSP is resistant to Brefeldin A treatment in PC12 cells.

Figure 6.5 Membrane association of newly-synthesised CSP is resistant to Brefeldin A treatment in PC12 cells. PC12 cells were transfected with EGFP-SNAP25B (A) or EGFP-CSP (C) or empty vector (pEGFP; *A* and *C*) for forty-eight hours. Transfected cells were incubated with [^{35}S]-labelled cysteine/methionine for 15 min, washed and chased for a further 60 min. The labelled cells were fractionated into cytosol (C) and membrane (M) fractions, from which GFP-tagged proteins were recovered by immunoprecipitation, subjected to SDS-PAGE and developed using autoradiography *(Upper panel* of *A* and *C; [^{35}S])*. Duplicate gels were analysed by immunoblotting using an anti-GFP monoclonal antibody (*Lower panel* of *A* and *C; GFP*). The positions of molecular weight standards (in kDa) are shown on the left side of panels *A* and *C*; on the right side of panel *C*, *asterisks* identify palmitoylated CSP and *arrowheads* indicate unpalmitoylated CSP. Representative blots are shown. *B.* The percentage membrane association of newly-synthesised SNAP25B in the presence or absence of BFA +/- SEM was determined by quantification of autoradiographs by densitometry (n = 3 from 2 separate experiments). Statistical significance was determined by a Student's *t*-test, whereby * represents a p value of < 0.04 between BFA-treated and untreated cells. *D.* The percentage palmitoylation of membrane-associated newly-synthesised CSP in the presence or absence of BFA +/- SEM was determined by quantification of autoradiographs by densitometry (n = 3 from 2 separate experiments). *E.* The percentage membrane association (sum of unpalmitoylated and palmitoylated membrane bands) of newly-synthesised CSP in the presence or absence of BFA +/- SEM was determined by quantification of autoradiographs by densitometry (n = 3 from 2 separate experiments).

no significant effect on either palmitoylation or membrane association of radiolabelled EGFP-CSP (Figure 6.5C-E). Thus, in both HEK293 cells and PC12 cells, membrane binding and palmitoylation of EGFP-CSP is independent of Golgi integrity or intracellular distribution of DHHC proteins. These results support the notion that CSP has a general (and weak) membrane affinity and that stable membrane attachment requires only sufficient cellular expression of appropriate DHHC proteins.

6.4 BREFELDIN A TREATMENT PROMOTES THE PALMITOYLATION OF CSP(C4-7L) BUT NOT CSP$_{1-136}$

As CSP-palmitoylating DHHC proteins retain activity following BFA treatment, it is possible that the BFA-mediated redistribution of Golgi-localised DHHC proteins to the ER could facilitate the palmitoylation of the ER-localised CSP mutants. Thus, the effects of BFA treatment on palmitoylation of CSP$_{1-136}$ and CSP(C4-7L) were examined in PC12 cells. These experiments are important as they will determine whether CSP(C4-7L) and CSP$_{1-136}$ are unpalmitoylated because they are physically separated from their partner DHHC proteins, or because structural changes in the mutant proteins prevent their palmitoylation. PC12 cells, transfected with EGFP-CSP$_{1-136}$ and EGFP-CSP(C4-7L) for forty-eight hours, were incubated with or without 30 μg/ml BFA in the presence of 10 μg/ml cycloheximide. The use of cycloheximide to block protein synthesis ensures that the effects of BFA are attributable to redistribution of Golgi enzymes to the ER rather than the 'trapping' of newly synthesised DHHC proteins at the ER. As an additional control, transfected cells were also incubated in 10 μg/ml nocodazole. This drug prevents the assembly of microtubules, which are required for retrograde transport of Golgi-derived vesicles to the ER, and BFA treatment in the presence of nocodazole results in Golgi dispersal but no fusion at the Golgi and ER (Lippincott-Schwartz *et al.*, 1990). The cells were separated into cytosolic and membrane fractions, and protein distribution was determined following SDS-PAGE and immunoblotting using a monoclonal anti-GFP antibody. Interestingly, BFA treatment promoted the robust palmitoylation of EGFP-CSP(C4-7L) and significantly enhanced its level of membrane association (Figure 6.6A-C). This observation suggests that BFA-induced mixing of ER and Golgi membranes allows access of Golgi DHHC proteins to EGFP-CSP(C4-7L), facilitating the palmitoylation of this mutant. Furthermore, the presence of nocodazole significantly reduced the level of BFA-induced palmitoylation of EGFP-CSP(C4-7L) (Figure 6.6A; $p<0.03$; n = 4), implying that ER-Golgi fusion is essential for the effects observed. In contrast to EGFP-CSP(C4-7L), BFA treatment had no effect on the palmitoylation status of EGFP-CSP$_{1-136}$. Overall, these results in PC12 cells
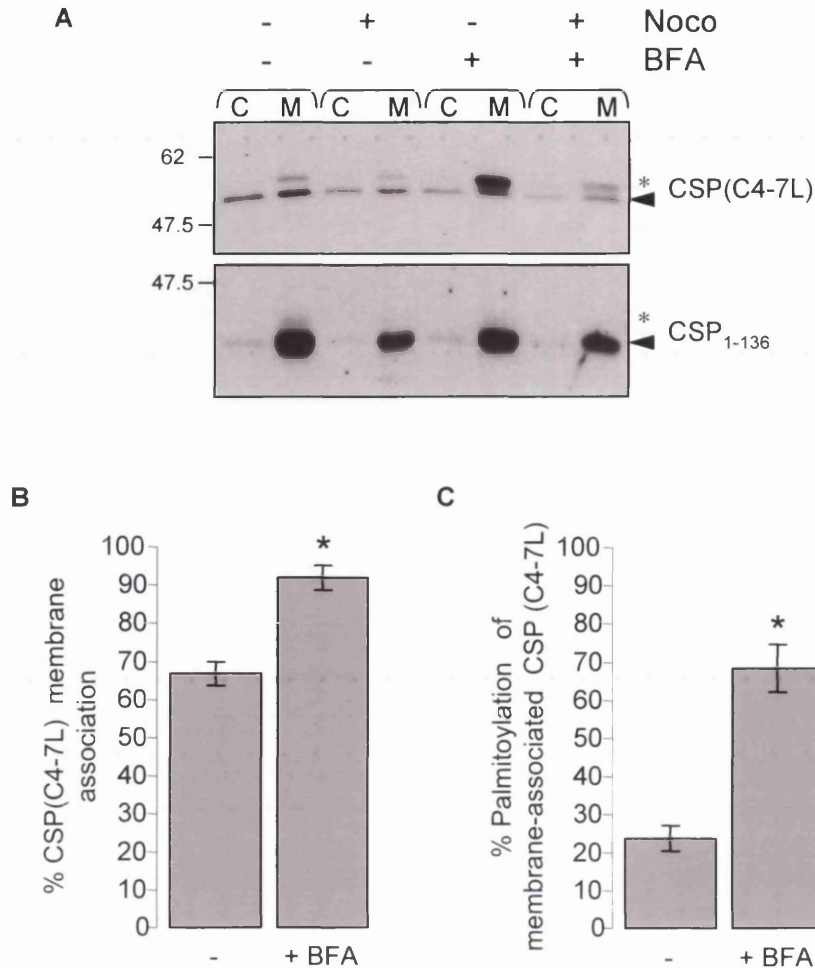
Figure 6.6 Effect of Brefeldin A on CSP mutant proteins in PC12 cells. *A*. PC12 cells were transfected with EGFP-CSP(C4-7L) or EGFP-CSP$_{1-136}$. Forty-eight hours following transfection, cells were incubated for four hours with or without 30 µg/ml BFA in the presence or absence of 10 µg/ml nocodazole. When cells were incubated in both BFA and nocodazole, the nocodazole was added two hours prior to BFA treatment, and maintained throughout the BFA treatment. Cycloheximide (10 µg/ml) was present in all samples. Cells were fractionated into cytosolic (C) and membrane (M) fractions and analysed following SDS-PAGE and transfer to nitrocellulose by immunoblotting using an anti-GFP monoclonal antibody. The positions of molecular weight standards (in kDa) are shown on the left side of the panel; on the right side of each panel, *asterisks* identify palmitoylated CSP and *arrowheads* indicate unpalmitoylated CSP. Representative blots are shown. *B*. The percentage C4-7L membrane association in the presence or absence of BFA +/- SEM was determined by quantification of immunoblots by densitometry (n = 4). Statistical significance was determined by a Student's *t*-test, whereby * represents a p value of < 7 x 10^{-4}. *C*. The percentage C4-7L palmitoylation in the presence or absence of BFA +/- SEM was determined by quantification of immunoblots by densitometry of the total membrane-bound pool (n = 4). Statistical significance was determined by a Student's *t*-test, whereby * represents a p value of < 2 x 10^{-3}.

are particularly relevant as they strongly support the conclusion that DHHC proteins active against CSP are localised predominantly to the Golgi. Furthermore, they support the notion that lack of EGFP-CSP(C4-7L) palmitoylation results from a physical separation of this mutant from its partner Golgi-localised DHHC proteins. These experiments were performed forty-eight hours post-transfection and therefore following the extensive intracellular accumulation of unpalmitoylated EGFP-CSP(C4-7L), yet the majority of expressed EGFP-CSP(C4-7L) is palmitoylated following BFA treatment for four hours (Figure 6.6A). In comparison, only around 20 % of wild-type CSP produced during a 15 minute labelling period was palmitoylated after an hour (Figure 6.5C). These findings suggest that the BFA-induced palmitoylation of CSP(C4-7L) is more efficient than palmitoylation of wild-type CSP. The most likely explanation for these findings is that whereas palmitoylation of CSP is limited by its weak membrane affinity, the tighter membrane binding of CSP(C4-7L) ensures a faster rate of palmitoylation when Golgi enzymes are re-localised to the ER.

As approximately 20% of EGFP-CSP is found palmitoylated and in the membrane fraction when expressed in HEK293 cells (Figure 5.3B), a limited amount of DHHC proteins active against CSP must be present in HEK293 cells, albeit at low expression levels. If the extent of CSP palmitoylation is regulated by a combination of the membrane affinity of unpalmitoylated CSP and the cellular expression levels of DHHC proteins, then the enhanced membrane affinity of CSP(C4-7L) would be predicted to facilitate a more efficient palmitoylation of this mutant in BFA-treated HEK293 cells than observed for wild-type CSP. To test this idea, BFA experiments were performed on HEK293 cells expressing EGFP-CSP$_{1-136}$ and EGFP-CSP(C4-7L). HEK293 cells were cells transfected with EGFP-CSP$_{1-136}$ or EGFP-CSP(C4-7L) alone, or co-transfected with these plasmids and DHHC3 or DHHC7. Four hours post-transfection, the cells were incubated in the presence or absence of 30 μg/ml BFA for a further four hours to promote the mixing of Golgi and ER membranes. Cells were separated into cytosolic and membrane fractions, and the partitioning of EGFP-CSP$_{1-136}$ and EGFP-CSP(C4-7L) was analysed by immunoblotting using a monoclonal anti-GFP antibody (Figure 6.7A). As predicted, BFA treatment of HEK293 cells promoted an ~ 7-fold increase in the extent of EGFP-CSP(C4-7L) palmitoylation in the absence of DHHC co-expression, with around 70% of the protein palmitoylated following BFA treatment (Figure 6.7B). This is in contrast to the almost complete lack of EGFP-CSP(C4-7L) palmitoylation when transfected either in the absence or presence of DHHC3 or -7, but without BFA-induced mixing of ER and Golgi membranes (Figure 6.7A; *Upper panel*). These findings support the notion that, when localised to the same intracellular compartment as partner DHHC proteins, the enhanced membrane affinity of EGFP-CSP(C4-7L) facilitates a faster rate of palmitoylation.
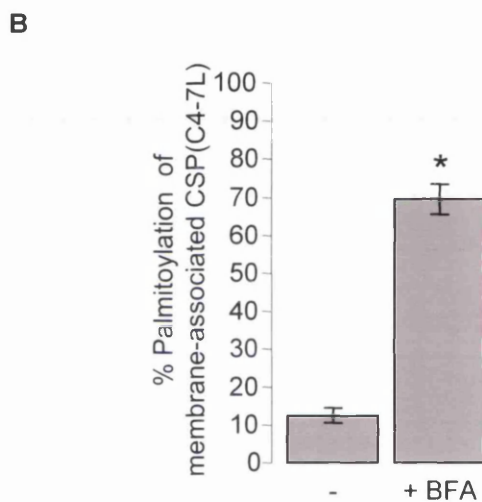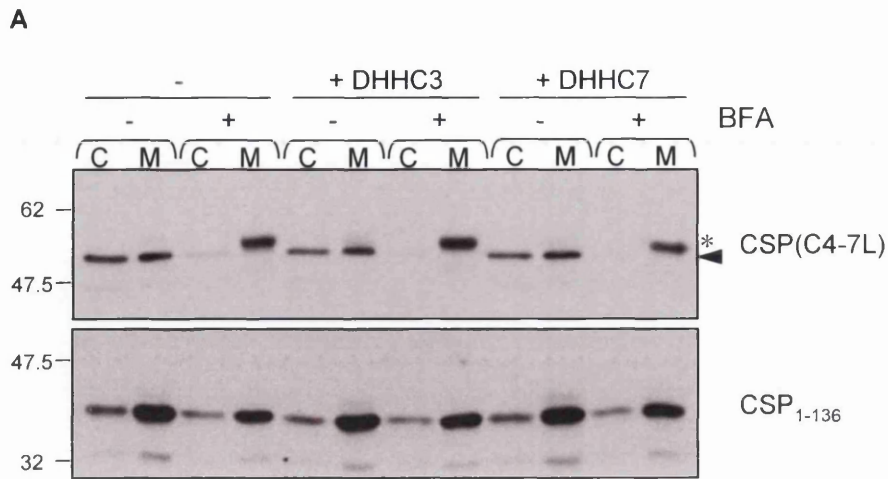
Figure 6.7 Effect of Brefeldin A on palmitoylation of CSP mutant proteins in HEK293 cells. *A.* HEK293 cells were transfected with EGFP-CSP(C4-7L) or EGFP-CSP$_{1-136}$ in the presence or absence of HA-DHHC3 or -7. Four hours post-transfection, the cells were incubated in the absence or presence of 30 µg/ml BFA for a further 4 hours. The cells were then fractionated into cytosol (C) and membrane (M) fractions, equal volumes of which were resolved by SDS-PAGE and probed by immunoblotting using a monoclonal anti-GFP antibody. The positions of molecular weight standards (in kDa) are shown on the left side of each panel; on the right side of each panel, *asterisks* identify palmitoylated CSP and *arrowheads* indicate unpalmitoylated CSP. Representative blots are shown. *B.* The percentage palmitoylation +/- SEM of membrane associated EGFP-CSP(C4-7L) (without co-expression of DHHCs) in the absence or presence of BFA treatment (n=7 from 3 separate experiments). Statistical significance was determined by a Student's *t*-test, whereby * denotes a p value of $< 3 \times 10^{-7}$.

As in PC12 cells, EGFP-CSP$_{1-136}$ was not detectably palmitoylated following BFA-treatment of HEK293 cells, either in the presence or absence of DHHC co-expression (Figure 6.7A; *Lower panel*). The inability of BFA treatment to promote palmitoylation of EGFP-CSP$_{1-136}$ may be because residues in the C-terminus (such as K137-P138-K139) are important for palmitoylation. Indeed, results presented in Chapter Three demonstrated that palmitoylation of full-length CSP was inhibited following mutation of the conserved lysine (K137) immediately downstream from the cysteine string domain to alanine in PC12 cells (Figure 3.9A and B). The CSP$_{1-136}$ mutant might also adopt a membrane orientation that indirectly prevents palmitoylation. For example, it is possible that the lack of a significant amount of charged residues at the C-terminal end of CSP$_{1-136}$ results in the protein 'slipping' into the membrane interior, thus preventing interaction with DHHC proteins.

6.5 CSP(C4-7L) DOES NOT NOTICEABLY REDISTRIBUTE FOLLOWING BREFELDIN A WASHOUT

Palmitoylation plays an important role in the trafficking of many proteins (El-Husseini *et al.*, 2001; Goodwin *et al.*, 2005; Kang *et al.*, 2004; Kinlough *et al.*, 2006; Rocks *et al.*, 2005; Roy *et al.*, 2005). Indeed, results presented in Chapter Three demonstrated that palmitoylation of CSP C-terminal truncation mutants is coupled to efficient intracellular sorting (Figure 3.8E). To determine if CSP palmitoylation is always coupled to forward transport in the secretory pathway, BFA washout experiments were performed by Dr Luke Chamberlain, in order to analyse whether palmitoylated CSP(C4-7L) protein is able to traffic from the ER. PC12 cells growing on glass coverslips were transfected with EGFP-CSP(C4-7L) or EGFP-tagged DHHC-17 as a control for a Golgi protein. Forty-eight hours post-transfection, the cells were treated with 30 μg/ml BFA for 2 hours in the presence of 10 μg/ml cycloheximide. The cells were then either fixed in 4% (v/v) formaldehyde, or were washed five times in fresh media containing cycloheximide but without BFA, and allowed to recover for 4 hours prior to fixing. The distributions of EGFP-tagged proteins were then examined by confocal imaging. As shown in the *lower panel* of Figure 6.8A, DHHC17 showed the expected distributions: Golgi in control cells, dispersed after BFA treatment and Golgi following BFA washout. To quantify these changes, EGFP-DHHC17 distribution was examined by scoring cells for either Golgi localisation or dispersed (ER) distribution (Figure 6.8B). Interestingly, and in contrast to EGFP-DHHC17, no changes in the distribution of EGFP-CSP(C4-7L) following BFA washout could be detected (Figure 6.8A; *Upper panel*). This finding suggests that palmitoylation is not sufficient to direct the exit of EGFP-CSP(C4-7L) from the ER. The amino acid

A
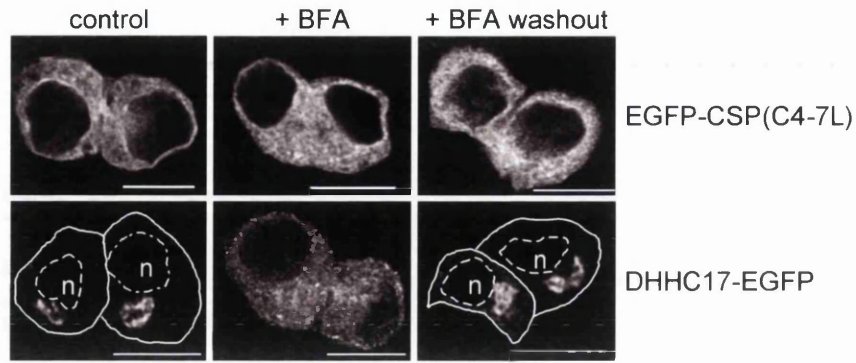
B
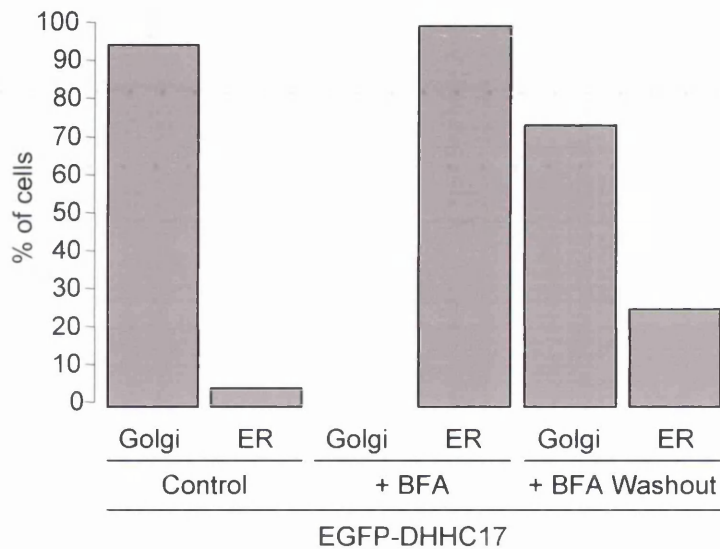
Figure 6.8 Intracellular localisation of EGFP-CSP(C4-7L) following BFA treatment and washout. *A*. PC12 cells transfected with EGFP-CSP(C4-7L) or EGFP-DHHC17 were either untreated (*control*), incubated in 30 μg/ml BFA and 10μg/ml cycloheximide for 2 hours ('+BFA'), or BFA/cycloheximide treated and then washed and incubated in the presence of cycloheximide for 4 hours ('BFA washout'). Cells were examined using a Zeiss LSM510 axiovert laser scanning confocal microscope. For clarity, a rough outline of the cell membrane (solid line) and nuclei (dashed line, *n*) is shown for DHHC17-EGFP-expressing cells that were untreated or subjected to BFA washout. Scale bars represent 10 μm. *B*. DHHC17-EGFP-expressing cells under all treatments were scored for a Golgi localisation or an ER (dispersed) localisation. The total number of cells counted was 61 for the control condition, 50 for BFA treatment and 74 for BFA washout. This figure was kindly provided by Dr. Luke Chamberlain.

sequence/structure of palmitoylated CSP may thus facilitate the movement into budding vesicle at the Golgi but not at the ER. Thus, the specific intracellular compartment at which CSP is palmitoylated, and hence stably anchored to, is likely to play a major role in determining targeting specificity.

6.6 DISCUSSION

The finding that unpalmitoylated CSP mutants are localised to the ER (Chapter Four), but that CSP palmitoylating enzymes are localised to the Golgi apparatus (Chapter Five) was somewhat of a paradox. The apparent inverse correlation between the strength of membrane binding of CSP mutants and the incidence of palmitoylation suggested that the *initial* membranes interactions of CSP might somehow regulate palmitoylation, and that the ER localisations of CSP_{1-136} and CSP(C4-7L) might reflect perturbations of membrane binding prior to palmitoylation.

It is difficult to assess the membrane affinity of wild-type and mutant CSP in PC12 cells, since CSP is so efficiently palmitoylated in this cell type. Therefore, HEK293 cells, which express only limited amounts of the DHHC proteins that are active against CSP (Figure 5.2), were used to examine the relative affinities of wild-type and mutant CSP for membranes in the absence of palmitoylation. In HEK293 cells, unpalmitoylated CSP is largely cytosolic (Figure 6.1A), and membrane binding can be enhanced following the removal of the C-terminal domain (CSP_{1-136}) or through mutations within the cysteine string domain (CSP(C4-7L)). As in PC12 cells, these CSP mutants are localised to the ER, where they are physically separated from the Golgi-localised CSP palmitoylating enzymes (Figure 6.1C). The physical separation of CSP mutants from their partner DHHC proteins offers an explanation why these mutants are unable to be palmitoylated in PC12 cells, and points to perturbations in initial membrane interactions being responsible for a loss of palmitoylation. Further experiments to compare membrane affinities could compare binding of CSP, CSP_{1-136} and CSP(C4-7L) to liposomes, either employing ultracentrifugation or sucrose plasmon resonance measurements.

Pulse-chase labelling was used to analyse the membrane interactions of newly-synthesised wild-type CSP in PC12 cells. CSP has an underlying weak membrane affinity in PC12 cells, based on the finding that there is little change in the amount of unpalmitoylated CSP found in the membrane fraction over time (Figure 6.3A). In contrast, there was an increase in the palmitoylated pool of CSP in the membrane fraction (Figure 6.3A). This phenotype would be expected of a protein that has an underlying weak membrane affinity, and that only becomes

stably membrane associated following palmitoylation. The addition of residues downstream from the cysteine string domain was found to weaken the membrane affinity of CSP C-terminal truncation mutants in PC12 cells (Figure 3.8*A* and *C*). To investigate whether the decrease in membrane binding of these mutants was due to a decrease in *initial* membrane interactions, the membrane binding of these mutants was assessed in HEK293 cells (Figure 6.2), and pulse-chase studies were employed in PC12 cells (Figure 6.3*B* and *C*). Both sets of experiments showed that the addition of specific amino acids downstream from the cysteine string domain, in particular K137A-P138A-K139A, weakened CSP membrane affinity and promoted palmitoylation in both cell types.

That CSP has such a weak membrane affinity implies that CSP may cycle on and off membranes until it becomes "trapped" by palmitoylation by a Golgi-localised DHHC protein. To determine whether CSP recognises a specific factor associated with the Golgi, the fungal metabolite Brefeldin A was utilised. BFA inhibits vesicle budding from the ER (Donaldson *et al.*, 1991; Lippincott-Schwartz *et al.*, 1989), blocking ER-to-Golgi transport and inducing the fusion of Golgi membranes with the ER, thereby promoting the loss of Golgi integrity. Treatment of both PC12 and HEK293 cells with BFA had no effect on CSP palmitoylation, suggesting that an intact Golgi apparatus is not essential for CSP to locate its partner DHHC protein and that CSP does not recognise a specific factor associated with the Golgi. Furthermore, these findings highlight the fact that the subcellular localisation of CSP palmitoylating enzymes is not important for CSP palmitoylation. It is not known why CSP palmitolating enzymes are only localised to the Golgi; however, it is possible that factors associated with the Golgi are important for the sorting of CSP to secretory vesicles. In support of this notion, is the finding that following BFA treatment, the unpalmitoylated and ER-localised mutant, CSP(C4-7L) was palmitoylated in both PC12 and HEK293 cells, however, palmitoylation of CSP(C4-7L) did not allow its exit from the ER (Figure 6.8).

Palmitoylation is clearly essential for the sorting of CSP, but it is not clear whether palmitoylation plays an active role in this process (for example, by driving association of CSP with budding vesicles) or an indirect role (by promoting stable membrane attachment and thus allowing other domains of CSP to facilitate sorting). Whatever the mechanism, the experiments examining CSP(C4-7L) localisation following BFA washout (Figure 6.8) suggest that palmitoylation of CSP can be uncoupled from forward transport in the secretory pathway. It is possible that loss of specific palmitoylated cysteines in the CSP(C4-7L) mutant directly inhibits traffic from the ER (that is, that CSP needs to be fully palmitoylated to traffic). However, this is unlikely as other CSP mutants, which lack 3-4 cysteines residues, and hence palmitoylation

sites, were identified in Chapter Four, and these traffic similarly to wild-type protein (Figure 4.2*F* and Figure 4.6*B*; *Upper panel*). Thus, the view that forward traffic of palmitoylated CSP is linked to palmitoylation at a specific cell location (the Golgi) and that factors required for CSP sorting are not present at the ER following BFA washout is favoured.

CSP(C4-7L) is palmitoylated in HEK293 cells following BFA treatment in the *absence* of DHHC co-expression (Figure 6.7), suggesting that the limited level of endogenous DHHC protein present in HEK293 cells is sufficient to palmitoylate CSP(C4-7L) but not wild-type CSP. CSP(C4-7L) has a stronger membrane affinity than wild-type CSP (Figure 6.1), and thus it is possible that palmitoylation of CSP(C4-7L) is more efficient compared to wild-type CSP following BFA treatment due to a longer-lived membrane association increasing the probability of encountering a DHHC protein. Future work to test this notion might include experiments that allow the rate of CSP palmitoylation to be measured against the rate of CSP(C4-7L) palmitoylation following BFA treatment of HEK293 cells. In this experimental set-up, cells expressing CSP or CSP(C4-7L) would be treated with BFA (in the presence of cycloheximide) for different time-points prior to fractionation. This analysis may also be performed in the PC12 cells transfected with CSP and CSP(C4-7L) in the presence of a palmitoylation inhibitor (such as 2-bromopalmitate). Palmitoylation of CSP and the CSP(C4-7L) mutant could then be compared at different time-points following the removal of the palmitoylation block and addition of BFA.

Further work will be needed to determine the factors that specify the sorting of palmitoylated proteins, such as CSP, into Golgi-derived secretory vesicles. It is possible that the specific lipid composition of the Golgi is well suited to accommodate lipid anchors such as palmitate groups. One hypothesis would be that palmitoylation increases the affinity of CSP for cholesterol-rich membrane domains, and that the increasing gradient of cholesterol from the ER-Golgi-plasma membrane may facilitate the onward trafficking of palmitoylated CSP onto vesicle membranes (Mitra *et al.*, 2004).

CHAPTER SEVEN: CONCLUSIONS AND DISCUSSION

7.1 SUMMARY

The study of protein palmitoylation has been fuelled in recent years by the identification of the DHHC family of palmitoyl transferases (Fukata *et al.*, 2004; Linder and Deschenes, 2007). These enzymes are predicted to be polytopic membrane proteins encoding 4-6 transmembrane domains, which contain a conserved DHHC cysteine rich domain located cytoplasmically, which likely forms the enzyme's active site (Bartels *et al.*, 1999; Ducker *et al.*, 2004; Fernandez-Hernando *et al.*, 2006; Fukata *et al.*, 2004; Hayashi *et al.*, 2005; Huang *et al.*, 2004; Keller *et al.*, 2004; Lam *et al.*, 2006; Lobo *et al.*, 2002; Politis *et al.*, 2005; Roth *et al.*, 2002; Smotrys *et al.*, 2005; Swarthout *et al.*, 2005; Valdez-Taubas and Pelham, 2005). Since their identification, DHHC proteins have been shown to be localised to many intracellular compartments, including the ER, Golgi apparatus, plasma membrane, endosomal compartments and the yeast vacuole (Dunphy *et al.*, 1996; Fukata *et al.*, 2004; Huang *et al.*, 2004; Keller *et al.*, 2004; Roth *et al.*, 2002; Schroeder *et al.*, 1996; Singaraja *et al.*, 2002; Swarthout *et al.*, 2005; Uemura *et al.*, 2002; Valdez-Taubas and Pelham, 2005; Veit *et al.*, 2001).

Since DHHC proteins are membrane-associated, all substrate proteins must contain additional membrane targeting signals to mediate membrane association prior to palmitoylation. There are several mechanisms that substrate proteins use to reach the membrane that houses their partner DHHC protein. A majority of palmitoylated proteins are associated with membranes prior to palmitoylation because they are transmembrane proteins (Roth *et al.*, 2006), and their membrane-spanning domains are inserted into the ER membrane co-translationally, allowing them to traffic through the secretory pathway until they reach their partner DHHC protein. Other palmitoylated proteins first become modified by another lipid moiety, such as isoprenyl or myristoyl groups, which confers sufficient hydrophobicity to allow the protein to interact transiently with membranes.

However, a subset of palmitoylated proteins are synthesised on free ribosomes and do not undergo any known type of lipid modification other than palmitoylation. Examples of such proteins include the enzyme GAD-65, the SNARE protein SNAP-25, the scaffolding protein PSD-95 and the exocytotic chaperone protein CSP. The mechanisms employed by this class of palmitoylated proteins for initial membrane targeting are not well understood.

The aim of this study was to identify the mechanisms that govern the initial membrane binding, palmitoylation and subsequent trafficking of CSP. It was hoped that these analyses, as well as providing essential information on CSP, would also serve as a paradigm to understand the

pathway of palmitoylation utilised by other palmitoylated proteins. In this study, the intrinsic elements that target CSP to the membranes where palmitoyl transferases are localised has been determined and the enzymes that palmitoylate CSP identified.

The results of this study present evidence that:

1. The minimum membrane-binding domain of CSP is composed of residues 106-136, which include the cysteine string domain (113-136) and a short stretch of amino acids immediately upstream in the linker domain.

2. Mutations that enhance CSP membrane affinity promote mislocalisation and inhibit palmitoylation.

3. Membrane association prior to palmitoylation relies on the intrinsic hydrophobicity of cysteine residues present in the cysteine string domain; mutation of the cysteines to more hydrophilic amino acids (for example, serine residues) abolishes membrane binding of full-length CSP.

4. Palmitoylation of CSP is dependent upon amino acids downstream of the cysteine string domain, which are important to weaken membrane affinity of the unpalmitoylated protein.

5. The affinity of CSP for membranes regulates palmitoylation, and these two factors are inversely correlated.

6. The Golgi-localised enzymes DHHC3, -7, -15 and -17 palmitoylate CSP.

7. Palmitoylation of CSP specifically on Golgi membranes may be important for the subsequent sorting of CSP.

7.2 A MODEL OF CSP MEMBRANE INTERACTIONS, PALMITOYLATION AND TRAFFICKING

Based upon these results, a model for CSP membrane binding and palmitoylation is proposed. In this model, CSP utilises a weak membrane affinity to bind transiently to cell membranes and 'sample' them for DHHC content. This weak membrane affinity requires interplay between the hydrophobic cysteine-rich domain and downstream residues. Upon association with Golgi membranes, CSP is recognised by DHHC3, -7, -15, or -17, which catalyse the palmitoylation and stable membrane anchoring of CSP, facilitating forward transport (Figure 7.1A). CSP mutants that have an enhanced membrane affinity rapidly and irreversibly bind to the most abundant cellular membranes, such as the ER, where they become physically separated from their palmitoylating enzymes (Figure 7.1B). BFA treatment induces the fusion of ER and Golgi membranes and puts CSP(C4-7L) and DHHC proteins on the same membrane compartment.
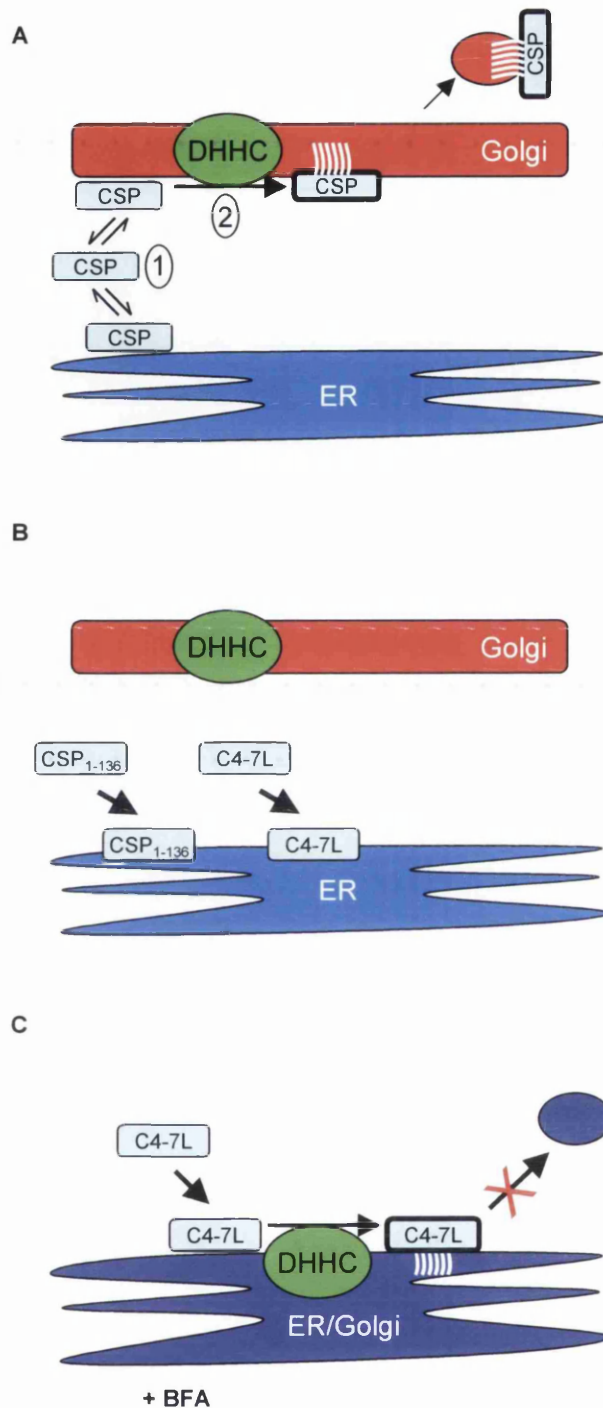
Figure 7.1 Membrane binding and palmitoylation of CSP. *A*.   CSP utilises a weak membrane affinity to sample intracellular membranes (1). Upon binding to Golgi membranes, CSP is recognised and palmitoylated by its partner DHHC proteins (2). Palmitoylation leads to stable membrane binding of CSP, and may facilitate forward transport. *B*. The enhanced membrane affinity of CSP_{1-136} and CSP(C4-7L) leads to tight binding to the most abundant cellular membranes, such as the ER, and physical separation from Golgi-localised DHHC proteins. *C*. Brefeldin A (BFA) treatment induces the fusion of ER and Golgi membranes and puts CSP(C4-7L) and DHHC proteins on the same membrane compartment. This membrane mixing allows palmitoylation of CSP(C4-7L) but is not sufficient to allow transport out of the ER.

This membrane mixing allows palmitoylation of CSP(C4-7L) but is not sufficient to allow transport out of the ER, suggesting that the membrane integrity of the Golgi apparatus is required for the subsequent sorting and transport of CSP onto secretory vesicles (Figure 7.1C).

At the heart of this model is the proposed transient membrane association of CSP. Although direct data to show reversible association of CSP with membranes has not been demonstrated, the following points support this idea:

1. Specific mutations around or within the cysteine string domain lead to stable membrane binding, consistent with the wild-type protein having an underlying membrane affinity.

2. *In silico* analysis identified a region in CSP including the cysteine string domain having a propensity to move to the membrane interface but not traverse the bilayer, and experiments *in vitro* showed an association of recombinant CSP with isolated cellular membranes (Boal *et al.*, 2007).

3. Pulse-chase experiments in PC12 cells reveal a time-dependent increase in palmitoylated CSP on membranes but very little change in the extent of unpalmitoylated CSP in the membrane fraction (Figure 6.3A). These observations would be predicted if CSP was rapidly associating/dissociating from membranes and required palmitoylation for stable membrane binding.

Future work might employ the use of FRAP (fluorescence recovery after photobleaching) techniques to directly demonstrate the association/dissociation of CSP with intracellular membranes (Goodwin *et al.*, 2005; Rocks *et al.*, 2005). Another approach would be to use surface plasmon resonance to measure CSP binding to immobilised lipids (Besenicar *et al.*, 2006).

The model for CSP membrane binding and palmitoylation presented in this study is reminiscent of the kinetic trapping model proposed by Shahinian and Silvius (Shahinian and Silvius, 1995) for prenylated or myristoylated proteins, as exemplified by recent work studying palmitoylation and trafficking of H- and N-Ras (Goodwin *et al.*, 2005; Rocks *et al.*, 2005). Farnesylation of these proteins provides a weak membrane affinity (Magee *et al.*, 1987; Shahinian and Silvius, 1995), which is presumed to allow Ras to cycle on and off membranes, where it can "sample" the different intracellular membranes, until it eventually encounters a membrane housing its partner PAT. Because the Ras palmitoyl transferase, DHHC9, is localised to ER/Golgi membranes (Swarthout *et al.*, 2005), palmitoylation only occurs on these membranes. Palmitoylation confers a stronger membrane affinity to a protein than does prenylation or

myristoylation (Peitzsch and McLaughlin, 1993; Shahinian and Silvius, 1995; Silvius and l'Heureux, 1994), and may ensure that a protein does not dissociate from membranes during vesicle budding and trafficking. Palmitoylation of Ras at the ER/Golgi probably allows Ras to access the secretory pathway, thus facilitating its forward transport to the plasma membrane (Goodwin *et al.*, 2005; Rocks *et al.*, 2005). The results presented in this thesis suggest that membrane 'sampling' through transient membrane interactions is not restricted to lipidated (prenylated or myristoylated) proteins, but may also occur through specialised protein domains, such as the cysteine string domain of CSP.

7.3 CONCLUDING REMARKS

It is clear that palmitoylation can be a more intricate signal than simply providing a hydrophobic membrane anchor. The multiple functions of palmitoylation are diverse and wide: palmitoylation targets both soluble and transmembrane proteins to distinct membrane compartments and membrane microdomains (El-Husseini *et al.*, 2001; Roy *et al.*, 2005; Salaün *et al.*, 2005); it is responsible for the trafficking of proteins between various intracellular organelles (Goodwin *et al.*, 2005; Kang *et al.*, 2004; Kinlough *et al.*, 2006; Rocks *et al.*, 2005); it promotes protein stability (Lam *et al.*, 2006; Linder and Deschenes, 2007; Valdez-Taubas and Pelham, 2005); and regulates protein-protein interaction (Hayashi *et al.*, 2005). In addition, palmitoylation is unique in that it is a reversible modification; indeed, many of the varied functions of palmitoylation rely on this fact (Rocks *et al.*, 2005). Furthermore, the reversibility of palmitoylation means that it can be viewed as a process that must be under regulation. The identification of twenty-three mammalian DHHC proteins has been critical towards understanding the diverse functions of palmitoylation. Importantly, the discovery that DHHC proteins and/or palmitoyl transferase activity is localised to multiple subcellular membranes raises an important question: what regulates the specificity of palmitoylation reactions? For example, is specificity encoded by the DHHC proteins, the subcellular localisation of the DHHC proteins, or a combination of these factors? This question could be addressed by studying palmitoylation of CSP *in vitro* using purified enzymes. Under these conditions, is CSP still only palmitoylated by DHHC3, -7, -15 and -17, or does the removal of cell constraints now allow other DHHC enzymes to palmitoylate CSP?

A CSP mutant protein that associates with ER membranes can effectively be palmitoylated once the Golgi-localised palmitoyl transferases are redistributed following BFA treatment of cells. Thus it is likely that one form of regulation is brought about by the specific subcellular localisation of the different DHHC proteins. Determining the factors that target the individual

DHHC proteins to their resident membrane compartment would help in understanding how DHHC protein localisation is spatially regulated. Interestingly, the length of a protein's membrane-spanning domain has been found to be an important factor in determining the subcellular localisation of membrane proteins (Bretscher and Munro, 1993). Site-directed mutagenesis could be used to artificially change the length of membrane-spanning domains in DHHC proteins. Mutating the hydrophobic amino acids that are positioned at the border of the membrane-spanning domain to hydrophilic amino acids would artificially shorten the length of the membrane-spanning domain; in contrast, the residues that flank membrane-spanning domains could be mutated to hydrophobic amino acids to artificially lengthen membrane-spanning domains. Such studies may reveal factors that govern the various subcellular localisations of different DHHC proteins. However, comparison of predicted membrane-spanning length in DHHC proteins present at distinct intracellular locations does not reveal any obvious differences. Another intriguing possibility is that palmitoylation regulates the sorting of specific DHHC proteins. It is well established that DHHC proteins are palmitoylated in their DHHC domain (Fukata *et al.*, 2004); interestingly, removal of the DHHC domain of DHHC17 led to a loss of Golgi targeting (Huang *et al.*, 2004).

The mechanism by which DHHC proteins transfer palmitoyl groups onto substrate proteins is also unknown. Several studies, including this one, have shown that mutating the conserved cysteine within the DHHC motif renders DHHC proteins catalytically inactive (Ducker *et al.*, 2004; Fernandez-Hernando *et al.*, 2006; Fukata *et al.*, 2004; Hayashi *et al.*, 2005; Huang *et al.*, 2004; Lam *et al.*, 2006; Lobo *et al.*, 2002; Roth *et al.*, 2002; Smotrys *et al.*, 2005; Swarthout *et al.*, 2005; Valdez-Taubas and Pelham, 2005). In addition, many studies have reported that the conserved cysteine residue within the DHHC motif become palmitoylated itself, with the suggestion that DHHC proteins form acyl-enzyme intermediates (Ducker *et al.*, 2004; Fukata *et al.*, 2004; Hayashi *et al.*, 2005; Keller *et al.*, 2004; Lobo *et al.*, 2002; Roth *et al.*, 2002; Smotrys *et al.*, 2005; Swarthout *et al.*, 2005). Understanding how DHHC proteins are able to palmitoylate substrate proteins is key to determining how palmitoylation reactions are regulated.

Another useful method to analyse how DHHC substrate specificity is regulated would be the creation of chimeric DHHC proteins. For example, the DHHC-CRD of a Golgi-localised enzyme inactive against CSP (for example, DHHC11) could be replaced with the cysteine-rich domain of DHHC3, -7, -15 or -17, and this chimeric DHHC protein could be assessed for its ability to palmitoylate CSP. This type of experiment would determine whether the DHHC-CRD of a PAT is responsible for substrate recognition. Furthermore, creating a chimeric ER-localised DHHC protein that has the DHHC-CRD of a CSP-palmitoylating PAT could extend

this type of experiment. If such chimeras were active towards CSP, then it would be possible to conclude that the subcellular localisation of the PAT is not a factor determining either substrate specificity or enzymic acitivity.

In addition to the questions detailed above, many other important aspects about DHHC proteins and CSP palmitoylation should be addressed, including: (i) What DHHC proteins are expressed in PC12 cells? The generation of antibodies against specific DHHC proteins would be a valuable tool to investigate this; additionally, quantitative PCR would be a useful approach to determine the relative levels of DHHC mRNA *in vivo*; (ii) What effect does RNAi knockdown of DHHC expression have on CSP palmitoylation?; (iii) How does palmitoylation of CSP at the Golgi facilitate sorting into budding vesicles? The specific lipid composition of the Golgi may be one factor, and this could be analysed for example following cholesterol depletion of cells or by disrupting the synthesis of specific phospholipids; (iv) As CSP mutants with reduced palmitoylation are efficiently sorted, what function does multiple palmitoylation of CSP play? In this regard it would be interesting to deplete cells of endogenous CSP using siRNA and compare the abilities of transfected (siRNA-resistant) CSP palmitoylation mutants to support exocytosis. These experiments should strengthen our understanding of the mechanisms involved in CSP membrane binding, palmitoylation and trafficking, and the role that palmitoylation plays in CSP function.

APPENDICES

APPENDIX ONE: OLIGONUCLEOTIDE PRIMERS USED TO GENERATE CSP N-TERMINAL TRUNCATION MUTANTS

CSP$_{83\text{-}136}$ Fwd	5'-GCTC**AAGCTT**CTTGCTCTACGTGGCCGAGCAG-3'
CSP$_{84\text{-}136}$ Fwd	5'-GCTC**AAGCTT**GTACGTGGCCGAGCAGTTC-3'
CSP$_{87\text{-}136}$ Fwd	5'-GCTC**AAGCTT**GGCCGAGCAGTTCGGGGAG-3'
CSP$_{89\text{-}136}$ Fwd	5'-GCTC**AAGCTT**GCAGTTCGGGGAGGAGAAC-3'
CSP$_{91\text{-}136}$ Fwd	5'-GCTC**AAGCTT**GGGGGAGGAGAACGTGAAC-3'
CSP$_{92\text{-}136}$ Fwd	5'-GCTC**AAGCTT**GGAGGAGAACGTGAACACC-3'
CSP$_{93\text{-}198}$ Fwd	5'-GCTC**AAGCTT**GGAGAACGTGAACACCTAC-3'
CSP$_{94\text{-}136}$ Fwd	5'-GCTC**AAGCTT**GAACGTGAACACCTACTTTG-3'
CSP$_{95\text{-}136}$ Fwd	5'-GCTC**AAGCTT**GGTGAACACCTACTTTGTG-3'
CSP$_{97\text{-}136}$ Fwd	5'-GCTC**AAGCTT**GACCTACTTTGTGCTCTCC-3'
CSP$_{100\text{-}136}$ Fwd	5'-CAC**AAGCTT**GGTGCTCTCCAGCTGGTGG-3'
CSP$_{103\text{-}136}$ Fwd	5'-TGT**AAGCTT**GAGCTGGTGGGCCAAGGCC-3'
CSP$_{106\text{-}136}$ Fwd	5'-GG**AAGCTT**GGCCGAAGGCCCTGTTCATCTTC-3'
CSP$_{107\text{-}136}$ Fwd	5'-GG**AAGCTT**GAAGGCCCTGTTCATCTTCTGTG-3'
CSP$_{109\text{-}136}$ Fwd	5'-GG**AAGCTT**GCTGTTCATCTTCTGTGGG-3'
CSP$_{110\text{-}136}$ Fwd	5'-GG**AAGCTT**GTTCATCTTCTGTGGGCTG-3'
CSP$_{111\text{-}136}$ Fwd	5'-GG**AAGCTT**GATCTTCTGTGGGCTCCTC-3'
CSP$_{112\text{-}136}$ Fwd	5'-GG**AAGCTT**GTTCTGTGGGCTCCTCACC-3'
CSP$_{113\text{-}136}$ Fwd	5'-GG**AAGCTT**GTGTGGGCTCCTCACCTGCTGC-3'
CSP$_{X\text{-}136}$ Rev	5'-CGC**GGATCC**TTAGCACTTGCCACAGCAGCA-3'
CSP$_{X\text{-}198}$ Rev	5'-**GGATCC**TTAGTTGAACCCGTCGGTGTG-3'

APPENDIX TWO: OLIGONUCLEOTIDE PRIMERS USED TO GENERATE CSP C-TERMINAL TRUNCATION MUTANTS

CSP_{1-112}
Fwd	5'-CAAGGCCCTGTTCATCTTC**TAA**TGTGGGCTCCTCACCTGCTG-3'
Rev	5'-CAGCAGGTGAGGAGCCCACA**TTA**GAAGATGAACAGGGCCTTG-3'

CSP_{1-137}
Fwd	5'-CTGCTGTGGCAAGTGCAAG**TAA**CCCAAGGCGCCTGAGGGG-3'
Rev	5'-CCCCTCAGGCGCCTTGGG**TTA**CTTGCACTTGCCACAGCAG-3'

CSP_{1-138}
Fwd	5'-GTGGCAAGTGCAAGCCC**TAA**AAGGCGCCTGAGGGGGAGGAG-3'
Rev	5'-CTCCTCCCCCTCAGGCGCCTT**TTA**GGGCTTGCACTTGCCAC-3'

CSP_{1-139}
Fwd	5'-GGCAAGTGCAAGCCCAAG**TAA**GCGCCTGAGGGGGAGGAG-3'
Rev	5'-CTCCTCCCCCTCAGGCGC**TTA**CTTGGGCTTGCACTTGCC-3'

CSP_{1-140}
Fwd	5'- CAAGTGCAAGCCCAAGGCG**TAA**CCTGAGGGGGAGGAGACG-3'
Rev	5'- CGTCTCCTCCCCCTCAGG**TTA**CGCCTTGGGCTTGCACTTG-3'

CSP_{1-141}
Fwd	5'- GTGCAAGCCCAAGGCGCCT**TAA**GAGGGGGAGGAGACGGAG-3'
Rev	5'- CTCCGTCTCCTCCCCCTC**TTA**AGGCGCCTTGGGCTTGCAC-3'

CSP_{1-142}
Fwd	5'- CAAGCCCAAGGCGCCTGAG**TAA**GGGGAGGAGACGGAGTTC-3'
Rev	5'- GAACTCCGTCTCCTCCCC**TTA**CTCAGGCGCCTTGGGCTTG-3'

CSP_{1-143}
Fwd	5'- GCCCAAGGCGCCTGAGGGG**TAA**GAGGAGACGGAGTTCTATG-3'
Rev	5'- CATAGAACTCCGTCTCCTC**TTA**CCCCTCAGGCGCCTTGGGC-3'

CSP_{1-144}
Fwd	5'-CCCAAGGCGCCTGAGGGGGAG**TAA**GAGACGGAGTTCTATGTGTC-3'
Rev	5'- GACACATAGAACTCCGTCTC**TTA**CTCCCCCTCAGGCGCCTTGGG-3'

CSP_{1-145}
Fwd	5'- GGCGCCTGAGGGGGAGGAG**TAA**ACGGAGTTCTATGTGTCCC-3'
Rev	5'- GGGACACATAGAACTCCGT**TTA**CTCCTCCCCCTCAGGCGCC-3'

CSP_{1-146}
Fwd	5'- GCGCCTGAGGGGGAGGAGACG**TAA**GAGTTCTATGTGTCCCCCG-3'
Rev	5'- CGGGGGACACATAGAACTC**TTA**CGTCTCCTCCCCCTCAGGCGC-3'

CSP_{1-156}
Fwd	5'- GTCCCCCGAGGACCTGGAG**TAA**GCGCAGCTGCAGTCCGATG-3'
Rev	5'- CATCGGACTGCAGCTGCGC**TTA**CTCCAGGTCCTCGGGGGAC-3'

CSP_{1-166}
Fwd	5'- GTCCGATGAGAGGGAGGCC**TAA**GCAGACACGCCGATCGTC-3'
Rev	5'- GACGATCGGCGTGTCTGC**TTA**GGCCTCCCTCTCATCGGAC-3'

APPENDIX THREE: OLIGONUCLEOTIDE PRIMERS USED TO GENERATE CSP SITE-DIRECTED MUTANTS

K107A
Fwd   5'-CTCTCCAGCTGGTGGGCC**GC**GGCCCTGTTCATCTTCTG-3'
Rev   5'-CAGAAGATGAACAGGGCC**GC**GGCCCACCAGCTGGAGAG-3'

K107E
Fwd   5'-GCTCTCCAGCTGGTGGGCC**GA**GGCCCTGTTCATCTTCTG-3'
Rev   5'-CAGAAGATGAACAGGGC**CT**CGGCCCACCAGCTGGAGAGC-3'

K107R
Fwd   5'-CTCTCCAGCTGGTGGGCC**CG**GGCCCTGTTCATCTTCTG-3'
Rev   5'-CAGAAGATGAACAGGGCC**CG**GGCCCACCAGCTGGAGAG-3'

L109A
Fwd   5'-CAGCTGGTGGGCCAAGGCC**GC**GTTCATCTTCTGTGGGCTC-3'
Rev   5'-GAGCCCACAGAAGATGAACG**CG**GCCTTGGCCCACCAGCTG-3'

L109E
Fwd   5'-GCTGGTGGGCCAAGGCC**GA**GTTCATCTTCTGTGGGCTC-3'
Rev   5'-GAGCCCACAGAAGATGAAC**TC**GGCCTTGGCCCACCAGC-3'

K107A/L109A
Fwd   5'-CTCCAGCTGGTGGGCC**GC**GGCC**GC**GTTCATCTTCTGTGGG-3'
Rev   5'-CCCACAGAAGATGAAC**GC**GGCC**GC**GGCCCACCAGCTGGAG-3'

K107E/L109E
Fwd   5'-CTCCAGCTGGTGGGCC**G**AGGCC**GA**GTTCATCTTCTGTGGG-3'
Rev   5'-CCCACAGAAGATGAAC**TC**GGCCT**C**GGCCCACCAGCTGGAG-3'

K137A
Fwd   5'-GCTGCTGTGGCAAGTGC**GC**GCCCAAGGCGCCTGAGG-3'
Rev   5'-CCTCAGGCGCCTTGGGC**GC**GCACTTGCCACAGCAGC-3'

K137E
Fwd   5'- GCTGCTGTGGCAAGTGC**G**AGCCCAAGGCGCCTGAGG-3'
Rev   5'- CCTCAGGCGCCTTGGGCT**C**GCACTTGCCACAGCAGC-3'

K137R
Fwd   5'- GCTGCTGTGGCAAGTGC**CG**GCCCAAGGCGCCTGAGG-3'
Rev   5'- CCTCAGGCGCCTTGGGC**CG**GCACTTGCCACAGCAGC-3'

P138A
Fwd   5'-GCTGTGGCAAGTGCAAG**G**CCAAGGCGCCTGAGGGGG-3'
Rev   5'-CCCCCTCAGGCGCCTTGG**C**CTTGCACTTGCCACAGC-3'

K139A
Fwd   5'-GTGGCAAGTGCAAGCCC**GC**GGCGCCTGAGGGGGAGG-3'
Rev   5'-CCTCCCCCTCAGGCGCC**GC**GGGCTTGCACTTGCCAC-3'

A140L
Fwd   5'-GGCAAGTGCAAGCCCAAG**CT**GCCTGAGGGGGAGGAGAC-3'
Rev   5'-GTCTCCTCCCCCTCAGGC**AG**CTTGGGCTTGCACTTGCC-3'

P141A
Fwd   5'-CAAGTGCAAGCCCAAGGCG**G**CTGAGGGGGAGGAGACGGAG-3'
Rev   5'-CTCCGTCTCCTCCCCCTCAG**C**CGCCTTGGGCTTGCACTTG-3'

E142A
Fwd   5'-GTGCAAGCCCAAGGCGCCTG**C**GGGGGAGGAGACGGAGTTC-3'
Rev   5'-GAACTCCGTCTCCTCCCCC**G**CAGGCGCCTTGGGCTTGCAC-3'

G143A
Fwd   5'-GCCCAAGGCGCCTGAGG**C**GGAGGAGACGGAGTTCTATGTG-3'
Rev   5'-CACATAGAACTCCGTCTCCTCC**G**CCTCAGGCGCCTTGGGC-3'

C1-3A
Fwd   5'-GTTCATCTTC**G**CTGGGCTCCTCACC**G**CC**G**CCTACTGTTGC-3'
Rev   5'-GCAACAGTAGG**C**GG**C**GGTGAGGAGCCCAG**C**GAAGATGAAC-3'

C4-7A
Fwd   5'-CACCTGCTGCTAC**GCT**GCC**GCC**GC**CCTCTGCTGCTGCTTC-3'
Rev   5'-GAAGCAGCAGCAGAGG**GCGGCGGCAGC**GTAGCAGCAGGTG-3'

C4-7L
Fwd   5'-
        GCCTCCTCACCTGCTGCTAC**CTTCTCCTTCTC**TTATGCTGTTGCTT
        TAACTG-3'
Rev   5'-
        CAGTTAAAGCAACAGCATAA**GAGAAGGAGAAG**GTAGCAGCAGGT
        GAGGAGGC -3'

APPENDIX FOUR: OLIGONUCLEOTIDE PRIMERS USED TO GENERATE INACTIVE DHHC15

DHHC15(C159S)
Fwd   5'-GTTTTAAAAATGGACCATCATT<u>C</u>CCCATGGGTTAATAACTGCATTG-3'
Rev   5'-CAATGCAGTTATTAACCCATGGG<u>G</u>AATGATGGTCCATTTTTAAAAC-3'

BIBLIOGRAPHY

Abrami, L., Kunz, B., Iacovache, I., and van der Goot, F. G. (2008). Palmitoylation and ubiquitination regulate exit of the Wnt signaling protein LRP6 from the endoplasmic reticulum. Proc Natl Acad Sci U.S.A. 105, 5384-5389.

Adamson, P., Marshall, C. J., Hall, A., and Tilbrook, P. A. (1992). Post-translational modifications of p21rho proteins. J Biol Chem 267, 20033-20038.

Advani, R. J., Bae, H. R., Bock, J. B., Chao, D. S., Doung, Y. C., Prekeris, R., Yoo, J. S., and Scheller, R. H. (1998). Seven novel mammalian SNARE proteins localize to distinct membrane compartments. J Biol Chem 273, 10317-10324.

Araki, S., Kikuchi, A., Hata, Y., Isomura, M., and Takai, Y. (1990). Regulation of reversible binding of smg p25A, a ras p21-like GTP-binding protein, to synaptic plasma membranes and vesicles by its specific regulatory protein, GDP dissociation inhibitor. J Biol Chem 265, 13007-13015.

Archer, D. A., Graham, M. E., and Burgoyne, R. D. (2002). Complexin regulates the closure of the fusion pore during regulated vesicle exocytosis. J Biol Chem 277, 18249-18252.

Arnold, C., Reisch, N., Leibold, C., Becker, S., Prufert, K., Sautter, K., Palm, D., Jatzke, S., Buchner, S., and Buchner, E. (2004). Structure-function analysis of the cysteine string protein in *Drosophila*: cysteine string, linker and C terminus. J Exp Biol 207, 1323-1334.

Arunachalam, L., Han, L., Tassew, N. G., He, Y., Wang, L., Xie, L., Fujita, Y., Kwan, E., Davletov, B., Monnier, P. P., Gaisano, H. Y., and Sugita, S. (2007). Munc18-1 Is Critical for Plasma Membrane Localization of Syntaxin1 but Not of SNAP-25 in PC12 Cells. Mol Biol Cell.

Ashery, U., Varoqueaux, F., Voets, T., Betz, A., Thakur, P., Koch, H., Neher, E., Brose, N., and Rettig, J. (2000). Munc13-1 acts as a priming factor for large dense-core vesicles in bovine chromaffin cells. EMBO J 19, 3586-3596.

Augustin, I., Rosenmund, C., Sudhof, T. C., and Brose, N. (1999). Munc13-1 is essential for fusion competence of glutamatergic synaptic vesicles. Nature 400, 457-461.

Baldini, G., Scherer, P. E., and Lodish, H. F. (1995). Nonneuronal expression of Rab3A: induction during adipogenesis and association with different intracellular membranes than Rab3D. Proc Natl Acad Sci U.S.A. 92, 4284-4288.

Bano, M. C., Jackson, C. S., and Magee, A. I. (1998). Pseudo-enzymatic S-acylation of a myristoylated yes protein tyrosine kinase peptide *in vitro* may reflect non-enzymatic S-acylation *in vivo*. Biochem J 330, 723-731.

Barclay, J. W., Craig, T. J., Fisher, R. J., Ciufo, L. F., Evans, G. J. O., Morgan, A., and Burgoyne, R. D. (2003). Phosphorylation of Munc18 by protein kiase C regulates the kinetics of exocytosis. J Biol Chem 278, 10538-10545.

Bark, I. C., and Wilson, M. C. (1994). Human cDNA clones encoding two different isoforms of the nerve terminal protein SNAP-25. Gene 139, 291-292.

Barnard, R. J., Morgan, A., and Burgoyne, R. D. (1997). Stimulation of NSF ATPase activity by alpha-SNAP is required for SNARE complex disassembly and exocytosis. J Cell Biol 139, 875-883.

Barnstable, C. J., Hofstein, R., and Akagawa, K. (1985). A marker of early amacrine cell development in rat retina. Brain Res 352, 286-290.

Bartels, D. J., Mitchell, D. A., Dong, X., and Deschenes, R. J. (1999). Erf2, a novel gene product that affects the localisation and palmitoylation of Ras2 in *Saccharomyces cerevisiae*. Mol Cell Biol 19, 6775-6787.

Baumert, M., Maycox, P. R., Navone, F., De Camilli, P., and Jahn, R. (1989). Synaptobrevin: an integral membrane protein of 18,000 daltons present in small synaptic vesicles of rat brain. EMBO J 8, 379-384.

Bellizzi, J. J., 3rd, Widom, J., Kemp, C., Lu, J. Y., Das, A. K., Hofmann, S. L., and Clardy, J. (2000). The crystal structure of palmitoyl protein thioesterase 1 and the molecular basis of infantile neuronal ceroid lipofuscinosis. Proc Natl Acad Sci U.S.A. 97, 4573-4578.

Bennett, M. K., Calakos, N., and Scheller, R. H. (1992). Syntaxin: a synaptic protein implicated in docking of synaptic vesicles at presynaptic active zones. Science 257, 255-259.

Bennett, M. K., Garcia-Arraras, J. E., Elferink, L. A., Peterson, K., Fleming, A. M., Hazuka, C. D., and Scheller, R. H. (1993). The syntaxin family of vesicular transport receptors. Cell 74, 863-873.

Bennett, M. K., and Scheller, R. H. (1993). The molecular machinery for secretion is conserved from yeast to neurons. Proc Natl Acad Sci U.S.A. 90, 2559-2563.

Besenicar, M., Macek, P., Lakey, J. H., and Anderluh, G. (2006). Surface plasmon resonance in protein-membrane interactions. Chem Phys Lipids 141, 169-178.

Betz, A., Okamoto, M., Benseler, F., and Brose, N. (1997). Direct interaction of the rat unc-13 homologue Munc13-1 with the N-terminus of syntaxin. J Biol Chem 272, 2520-2526.

Bezprozvanny, I., Scheller, R. H., and Tsien, R. W. (1995). Functional impact of syntaxin on gating of N-type and Q-type calcium channels. Nature 378, 623-626.

Bharadwaj, M., and Bizzozero, O. A. (1995). Myelin P0 glycoprotein and a synthetic peptide containing the palmitoylation site are both autoacylated. J Neurochem 65, 1805-1815.

Bijlmakers, M. J., and Marsh, M. (2003). The on-off story of protein palmitoylation. Trends Cell Biol 13, 32-42.

Birnboim, H. C., and Doly, J. (1979). A rapid alkaline extraction procedure for screening recombinant plasmid DNA. Nucleic Acids Res 7, 1513-1523.

Bizzozero, O. A., Bixler, H. A., and Pastuszyn, A. (2001). Structural determinants influencing the reaction of cysteine-containing peptides with palmitoyl-coenzyme A and other thioesters. Biochim Biophys Acta 1545, 278-288.

Blasi, J., Chapman, E. R., Link, E., Binz, T., Yamasaki, S., De Camilli, P., Sudhof, T. C., Niemann, H., and Jahn, R. (1993). Botulinum neurotoxin A selectively cleaves the synaptic protein SNAP-25. Nature 365, 160-163.

Blobel, G. (1980). Intracellular protein topogenesis. Proc Natl Acad Sci U.S.A. 77, 1496-1500.

Boal, F., Zhang, H., Tessier, C., Scotti, P., and Lang, J. (2004). The variable C-terminus of cysteine string proteins modulates exocytosis and protein-protein interactions. Biochemistry 43, 16212-16223.

Boal, F., Le Pevelen, S., Cziepluch, C., Scotti, P., and Lang, J. (2007). Cysteine-string protein isoform beta (Cspbeta) is targeted to the trans-Golgi network as a non-palmitoylated CSP in clonal beta-cells. Biochim Biophys Acta 1773, 109-119.

Bock, J. B., Matern, H. T., Peden, A. A., and Scheller, R. H. (2001). A genomic perspective on membrane compartment organization. Nature 409, 839-841.

Bohm, S., Frishman, D., and Mewes, H. W. (1997). Variations of the C2H2 zinc finger motif in the yeast genome and classification of yeast zinc finger proteins. Nucleic Acids Res 25, 2464.

Bonifacino, J. S., and Glick, B. S. (2004). The mechanisms of vesicle budding and fusion. Cell 116, 153-166.

Braun, J. E., and Scheller, R. H. (1995). Cysteine string protein, a DnaJ family member, is present on diverse secretory vesicles. Neuropharmacology 34, 1361-1369.

Braun, J. E., Wilbanks, S. M., and Scheller, R. H. (1996). The cysteine string secretory vesicle protein activates Hsc70 ATPase. J Biol Chem 271, 25989-25993.

Brenner, S. (1974). The genetics of *Caenorhabditis elegans*. Genetics 77, 71-94.

Bretscher, M. S., and Munro, S. (1993). Cholesterol and the Golgi apparatus. Science 261, 1280-1281.

Bronk, P., Wenniger, J. J., Dawson-Scully, K., Guo, X., Hong, S., Atwood, H. L., and Zinsmaier, K. E. (2001). Drosophila Hsc70-4 is critical for neurotransmitter exocytosis *in vivo*. Neuron 30, 475-488.

Bronk, P., Nie, Z., Klose, M. K., Dawson-Scully, K., Zhang, J., Robertson, R. M., Atwood, H. L., and Zinsmaier, K. E. (2005). The multiple functions of cysteine-string protein analyzed at *Drosophila* nerve terminals. J Neurosci 25, 2204-2214.

Brose, N., Hofmann, K., Hata, Y., and Sudhof, T. C. (1995). Mammalian homologues of *Caenorhabditis elegans* unc-13 gene define novel family of C2-domain proteins. J Biol Chem 270, 25273-25280.

Brose, N., Rosenmund, C., and Rettig, J. (2000). Regulation of transmitter release by Unc-13 and its homologues. Curr Opin Neurobiol 10, 303-311.

Brown, H., Larsson, O., Branstrom, R., Yang, S. N., Leibiger, B., Leibiger, I., Fried, G., Moede, T., Deeney, J. T., Brown, G. R., Jacobsson, G., Rhodes, C. J., Braun, J. E., Scheller, R. H., Corkey, B. E., Berggren, P. O., and Meister, B. (1998). Cysteine string protein (CSP) is an insulin secretory granule-associated protein regulating beta-cell exocytosis. EMBO J 17, 5048-5058.

Bruns, D., and Jahn, R. (2002). Molecular determinants of exocytosis. Pflugers Arch 443, 333-338.

Bukau, B., and Horwich, A. L. (1998). The Hsp70 and Hsp60 chaperone machines. Cell 92, 351-366.

Calakos, N., Bennett, M. K., Peterson, K. E., and Scheller, R. H. (1994). Protein-protein interactions contributing to the specificity of intracellular vesicular trafficking. Science 263, 1146-1149.

Camp, L. A., and Hofmann, S. L. (1993). Purification and properties of a palmitoyl-protein thioesterase that cleaves palmitate from H-Ras. J Biol Chem 268, 22566-22574.

Camp, L. A., Verkruyse, L. A., Afendis, S. J., Slaughter, C. A., and Hofmann, S. L. (1994). Molecular cloning and expression of palmitoyl-protein thioesterase. J Biol Chem 269, 23212-23219.

Casey, P. J., and Seabra, M. C. (1996). Protein prenyltransferases. J Biol Chem 271, 5289-5292.

Chalfie, M., Tu, Y., Euskirchen, G., Ward, W. W., and Prasher, D. C. (1994). Green fluorescent protein as a marker for gene expression. Science 263, 802-805.

Chamberlain, L. H., and Burgoyne, R. D. (1996). Identification of a novel cysteine string protein variant and expression of cysteine string proteins in non-neuronal cells. J Biol Chem 271, 7320-7323.

Chamberlain, L. H., Henry, J., and Burgoyne, R. D. (1996). Cysteine string proteins are associated with chromaffin granules. J Biol Chem 271, 19514-19517.

Chamberlain, L. H., and Burgoyne, R. D. (1997a). The molecular chaperone function of the secretory vesicle cysteine string proteins. J Biol Chem 272, 31420-31426.

Chamberlain, L. H., and Burgoyne, R. D. (1997b). Activation of the ATPase activity of heat-shock proteins Hsc70/Hsp70 by cysteine-string protein. Biochem J 322, 853-858.

Chamberlain, L. H., and Burgoyne, R. D. (1998a). The cysteine-string domain of the secretory vesicle cysteine-string protein is required for membrane targeting. Biochem J 335, 205-209.

Chamberlain, L. H., and Burgoyne, R. D. (1998b). Cysteine string protein functions directly in regulated exocytosis. Mol Biol Cell 9, 2259-2267.

Chamberlain, L. H., Graham, M. E., Kane, S., Jackson, J. L., Maier, V. H., Burgoyne, R. D., and Gould, G. W. (2001). The synaptic vesicle protein, cysteine-string protein, is associated with the plasma membrane in 3T3-L1 adipocytes and interacts with syntaxin 4. J Cell Sci 114, 445-455.

Chamoun, Z., Mann, R. K., Nellen, D., von Kessler, D. P., Bellotto, M., Beachy, P. A., and Basler, K. (2001). Skinny hedgehog, an acyltransferase required for palmitoylation and activity of the hedgehog signal. Science 293, 2080-2084.

Chandra, S., Gallardo, G., Fernandez-Chacon, R., Schluter, O. M., and Sudhof, T. C. (2005). Alpha-synuclein cooperates with CSPalpha in preventing neurodegeneration. Cell 123, 383-396.

Chapman, E. R., Blasi, J., An, S., Brose, N., Johnston, P. A., Sudhof, T. C., and Jahn, R. (1996). Fatty acylation of synaptotagmin in PC12 cells and synaptosomes. Biochem Biophys Res Commun 225, 326-332.

Chapman, E. R. (2002). Synaptotagmin: a Ca^{2+} sensor that triggers exocytosis? Nat Rev Mol Cell Biol 3, 498-508.

Chow, M., Newman, J. F., Filman, D., Hogle, J. M., Rowlands, D. J., and Brown, F. (1987). Myristylation of picornavirus capsid protein VP4 and its structural significance. Nature 327, 482-486.

Christgau, S., Schierbeck, H., Aanstoot, H. J., Aagaard, L., Begley, K., Kofod, H., Hejnaes, K., and Baekkeskov, S. (1991). Pancreatic beta cells express two autoantigenic forms of glutamic acid decarboxylase, a 65-kDa hydrophilic form and a 64-kDa amphiphilic form which can be both membrane-bound and soluble. J Biol Chem 266, 21257-21264.

Christgau, S., Aanstoot, H. J., Schierbeck, H., Begley, K., Tullin, S., Hejnaes, K., and Baekkeskov, S. (1992). Membrane anchoring of the autoantigen GAD65 to microvesicles in pancreatic beta-cells by palmitoylation in the NH2-terminal domain. J Cell Biol 118, 309-320.

Clarke, S., Vogel, J. P., Deschenes, R. J., and Stock, J. (1988). Posttranslational modification of the Ha-ras oncogene protein: evidence for a third class of protein carboxyl methyltransferases. Proc Natl Acad Sci U.S.A. 85, 4643-4647.

Clarke, S. (1992). Protein isoprenylation and methylation at carboxyl-terminal cysteine residues. Annu Rev Biochem 61, 355-386.

Collins, R. N. (2003). Rab and ARF GTPase regulation of exocytosis. Mol Membr Biol 20, 105-115.

Coppola, T., and Gundersen, C. (1996). Widespread expression of human cysteine string proteins. FEBS Lett 391, 269-272.

Couve, A., Protopopov, V., and Gerst, J. E. (1995). Yeast synaptobrevin homologs are modified posttranslationally by the addition of palmitate. Proc Natl Acad Sci U.S.A. 92, 5987-5991.

Craven, S. E., El-Husseini, A. E., and Bredt, D. S. (1999). Synaptic targeting of the postsynaptic density protein PSD-95 mediated by lipid and protein motifs. Neuron 22, 497-509.

Craxton, M. (2001). Genomic analysis of synaptotagmin genes. Genomics 77, 43-49.

Cubitt, A. B., Heim, R., Adams, S. R., Boyd, A. E., Gross, L. A., and Tsien, R. Y. (1995). Understanding, improving and using green fluorescent proteins. Trends Biochem Sci 20, 448-455.

Darchen, F., and Goud, B. (2000). Multiple aspects of Rab protein action in the secretory pathway: focus on Rab3 and Rab6. Biochimie 82, 375-384.

Darios, F., and Davletov, B. (2006). Omega-3 and omega-6 fatty acids stimulate cell membrane expansion by acting on syntaxin 3. Nature 440, 813-817.

Davis, A. F., Bai, J., Fasshauer, D., Wolowick, M. J., Lewis, J. L., and Chapman, E. R. (1999). Kinetics of synaptotagmin responses to Ca^{2+} and assembly with the core SNARE complex onto membranes. Neuron 24, 363-376.

Davletov, B. A., and Sudhof, T. C. (1993). A single C2 domain from synaptotagmin I is sufficient for high- affinity Ca^{2+}/phospholipid binding. J Biol Chem 268, 26386-26390.

Dawson-Scully, K., Bronk, P., Atwood, H. L., and Zinsmaier, K. E. (2000). Cysteine-string protein increases the calcium sensitivity of neurotransmitter exocytosis in *Drosophila*. J Neurosci 20, 6039-6047.

Dawson-Scully, K., Lin, Y., Imad, M., Zhang, J., Marin, L., Horne, J. A., Meinertzhagen, I. A., Karunanithi, S., Zinsmaier, K. E., and Atwood, H. L. (2007). Morphological and functional effects of altered cysteine string protein at the *Drosophila* larval neuromuscular junction. Synapse 61, 1-16.

Deak, F., Schoch, S., Liu, X., Sudhof, T. C., and Kavalali, E. T. (2004). Synaptobrevin is essential for fast synaptic-vesicle endocytosis. Nat Cell Biol 6, 1102-1108.

Devedjiev, Y., Dauter, Z., Kuznetsov, S. R., Jones, T. L., and Derewenda, Z. S. (2000). Crystal structure of the human acyl protein thioesterase I from a single X-ray data set to 1.5 A. Structure 8, 1137-1146.

Dietrich, L. E., and Ungermann, C. (2004). On the mechanism of protein palmitoylation. EMBO Rep 5, 1053-1057.

Donaldson, J. G., Kahn, R. A., Lippincott-Schwartz, J., and Klausner, R. D. (1991). Binding of ARF and beta-COP to Golgi membranes: possible regulation by a trimeric G protein. Science 254, 1197-1199.

Doyle, A., Griffiths, J. B., and Newell, D. G. (1994). Cell and Tissue Culture: Laboratory Procedures. (Chichester, UK., Wiley and Sons).

Drisdel, R. C., and Green, W. N. (2004). Labeling and quantifying sites of protein palmitoylation. Biotechniques 36, 276-285.

Ducker, C. E., Stettler, E. M., French, K. J., Upson, J. J., and Smith, C. D. (2004). Huntingtin interacting protein 14 is an oncogenic human protein: palmitoyl acyltransferase. Oncogene 23, 9230-9237.

Dulubova, I., Sugita, S., Hill, S., Hosaka, M., Fernandez, I., Sudhof, T. C., and Rizo, J. (1999). A conformational switch in syntaxin during exocytosis: role of munc18. EMBO J 18, 4372-4382.

Duncan, J. A., and Gilman, A. G. (1996). Autoacylation of G protein alpha subunits. J Biol Chem 271, 23594-23600.

Duncan, J. A., and Gilman, A. G. (1998). A cytoplasmic acyl-protein thioesterase that removes palmitate from G protein alpha subunits and p21(RAS). J Biol Chem 273, 15830-15837.

Duncan, J. A., and Gilman, A. G. (2002). Characterization of *Saccharomyces cerevisiae* acyl-protein thioesterase 1, the enzyme responsible for G protein alpha subunit deacylation *in vivo*. J Biol Chem 277, 31740-31752.

Dunphy, J. T., Greentree, W. K., Manahan, C. L., and Linder, M. E. (1996). G-protein palmitoyltransferase activity is enriched in plasma membranes. J Biol Chem 271, 7154-7159.

Dunphy, J. T., Schroeder, H., Leventis, R., Greentree, W. K., Knudsen, J. K., Silvius, J. R., and Linder, M. E. (2000). Differential effects of acyl-CoA binding protein on enzymatic and non-enzymatic thioacylation of protein and peptide substrates. Biochim Biophys Acta 1485, 185-198.

Earles, C. A., Bai, J., Wang, P., and Chapman, E. R. (2001). The tandem C2 domains of synaptotagmin contain redundant Ca²⁺ binding sites that cooperate to engage t-SNAREs and trigger exocytosis. J Cell Biol 154, 1117-1123.

Eberle, K. K., Zinsmaier, K. E., Buchner, S., Gruhn, M., Jenni, M., Arnold, C., Leibold, C., Reisch, D., Walter, N., Hafen, E., Hofbauer, A., Pflugfelder, G. O., and Buchner, E. (1998). Wide distribution of the cysteine string proteins in *Drosophila* tissues revealed by targeted mutagenesis. Cell Tissue Res 294, 203-217.

El-Husseini, A. E., Craven, S. E., Chetkovich, D. M., Firestein, B. L., Schnell, E., Aoki, C., and Bredt, D. S. (2000). Dual palmitoylation of PSD-95 mediates its vesiculotubular sorting, postsynaptic targeting, and ion channel clustering. J Cell Biol 148, 159-172.

El-Husseini, A. E., Craven, S. E., Brock, S. C., and Bredt, D. S. (2001). Polarized targeting of peripheral membrane proteins in neurons. J Biol Chem 276, 44984-44992.

Elferink, L. A., Trimble, W. S., and Scheller, R. H. (1989). Two vesicle-associated membrane protein genes are differentially expressed in the rat central nervous system. J Biol Chem 264, 11061-11064.

Englund, P. T. (1993). The structure and biosynthesis of glycosyl phosphatidylinositol protein anchors. Annu Rev Biochem 62, 121-138.

Essrich, C., Lorez, M., Benson, J. A., Fritschy, J. M., and Luscher, B. (1998). Postsynaptic clustering of major GABAA receptor subtypes requires the gamma 2 subunit and gephyrin. Nat Neurosci 1, 563-571.

Evans, G. J., Wilkinson, M. C., Graham, M. E., Turner, K. M., Chamberlain, L. H., Burgoyne, R. D., and Morgan, A. (2001). Phosphorylation of cysteine string protein by protein kinase A. Implications for the modulation of exocytosis. J Biol Chem 276, 47877-47885.

Evans, G. J., and Morgan, A. (2002). Phosphorylation-dependent interaction of the synaptic vesicle proteins cysteine string protein and synaptotagmin I. Biochem J 364, 343-347.

Evans, G. J., Morgan, A., and Burgoyne, R. D. (2003). Tying everything together: the multiple roles of cysteine string protein (CSP) in regulated exocytosis. Traffic 4, 653-659.

Evans, G. J., and Morgan, A. (2005). Phosphorylation of cysteine string protein in the brain: developmental, regional and synaptic specificity. Eur J Neurosci 21, 2671-2680.

Faergeman, N. J., Sigurskjold, B. W., Kragelund, B. B., Andersen, K. V., and Knudsen, J. (1996). Thermodynamics of ligand binding to acyl-coenzyme A binding protein studied by titration calorimetry. Biochemistry 35, 14118-14126.

Faergeman, N. J., and Knudsen, J. (1997). Role of long-chain fatty acyl-CoA esters in the regulation of metabolism and in cell signalling. Biochem J 323 (Pt 1), 1-12.

Fang, C., Deng, L., Keller, C. A., Fukata, M., Fukata, Y., Chen, G., and Luscher, B. (2006). GODZ-mediated palmitoylation of GABA(A) receptors is required for normal assembly and function of GABAergic inhibitory synapses. J Neurosci 26, 12758-12768.

Farazi, T. A., Waksman, G., and Gordon, J. I. (2001). The biology and enzymology of protein N-myristoylation. J Biol Chem 276, 39501-39504.

Farnsworth, C. C., Seabra, M. C., Ericsson, L. H., Gelb, M. H., and Glomset, J. A. (1994). Rab geranylgeranyl transferase catalyzes the geranylgeranylation of adjacent cysteines in the small GTPases Rab1A, Rab3A, and Rab5A. Proc Natl Acad Sci U.S.A. 91, 11963-11967.

Fasshauer, D., Bruns, D., Shen, B., Jahn, R., and Brunger, A. T. (1997). A structural change occurs upon binding of syntaxin to SNAP-25. J Biol Chem 272, 4582-4590.

Fasshauer, D., Eliason, W. K., Brunger, A. T., and Jahn, R. (1998a). Identification of a minimal core of the synaptic SNARE complex sufficient for reversible assembly and disassembly. Biochemistry 37, 10354-10362.

Fasshauer, D., Sutton, R. B., Brunger, A. T., and Jahn, R. (1998b). Conserved structural features of the synaptic fusion complex: SNARE proteins reclassified as Q- and R-SNAREs. Proc Natl Acad Sci U.S.A. 95, 15781-15786.

Fernandez, I., Ubach, J., Dulubova, I., Zhang, X., Sudhof, T. C., and Rizo, J. (1998). Three-dimensional structure of an evolutionarily conserved N-terminal domain of syntaxin 1A. Cell 94, 841-849.

Fernandez, I., Arac, D., Ubach, J., Gerber, S. H., Shin, O., Gao, Y., Anderson, R. G., Sudhof, T. C., and Rizo, J. (2001). Three-dimensional structure of the synaptotagmin 1 C2B-domain: synaptotagmin 1 as a phospholipid binding machine. Neuron 32, 1057-1069.

Fernandez-Chacon, R., Konigstorfer, A., Gerber, S. H., Garcia, J., Matos, M. F., Stevens, C. F., Brose, N., Rizo, J., Rosenmund, C., and Sudhof, T. C. (2001). Synaptotagmin I functions as a calcium regulator of release probability. Nature 410, 41-49.

Fernandez-Chacon, R., Wolfel, M., Nishimune, H., Tabares, L., Schmitz, F., Castellano-Munoz, M., Rosenmund, C., Montesinos, M. L., Sanes, J. R., Schneggenburger, R., and Sudhof, T. C. (2004). The synaptic vesicle protein CSP alpha prevents presynaptic degeneration. Neuron 42, 237-251.

Fernandez-Hernando, C., Fukata, M., Bernatchez, P. N., Fukata, Y., Lin, M. I., Bredt, D. S., and Sessa, W. C. (2006). Identification of Golgi-localized acyl transferases that palmitoylate and regulate endothelial nitric oxide synthase. J Cell Biol 174, 369-377.

Fili, O., Michaelevski, I., Bledi, Y., Chikvashvili, D., Singer-Lahat, D., Boshwitz, H., Linial, M., and Lotan, I. (2001). Direct interaction of a brain voltage-gated K^+ channel with syntaxin 1A: functional impact on channel gating. J Neurosci 21, 1964-1974.

Fischer von Mollard, G., Sudhof, T. C., and Jahn, R. (1991). A small GTP-binding protein dissociates from synaptic vesicles during exocytosis. Nature 349, 79-81.

Fischer von Mollard, G., Stahl, B., Khokhlatchev, A., Sudhof, T. C., and Jahn, R. (1994). Rab3C is a synaptic vesicle protein that dissociates from synaptic vesicles after stimulation of exocytosis. J Biol Chem 269, 10971-10974.

Fisher, R. J., Pevsner, J., and Burgoyne, R. D. (2001). Control of Fusion Pore Dynamics During Exocytosis by Munc18. Science 291, 875-878.

Frolov, A., and Schroeder, F. (1998). Acyl coenzyme A binding protein. Conformational sensitivity to long chain fatty acyl-CoA. J Biol Chem 273, 11049-11055.

Fujita, Y., Shirataki, H., Sakisaka, T., Asakura, T., Ohya, T., Kotani, H., Yokoyama, S., Nishioka, H., Matsuura, Y., Mizoguchi, A., Scheller, R. H., and Takai, Y. (1998). Tomosyn: a syntaxin-1-binding protein that forms a novel complex in the neurotransmitter release process. Neuron 20, 905-915.

Fukata, M., Fukata, Y., Adesnik, H., Nicoll, R. A., and Bredt, D. S. (2004). Identification of PSD-95 palmitoylating enzymes. Neuron 44, 987-996.

Fukushima, Y., Saitoh, T., Anai, M., Ogihara, T., Inukai, K., Funaki, M., Sakoda, H., Onishi, Y., Ono, H., Fujishiro, M., Ishikawa, T., Takata, K., Nagai, R., Omata, M., and Asano, T. (2001). Palmitoylation of the canine histamine H2 receptor occurs at Cys(305) and is important for cell surface targeting. Biochim Biophys Acta 1539, 181-191.

Galli, T., Zahraoui, A., Vaidyanathan, V. V., Raposo, G., Tian, J. M., Karin, M., Niemann, H., and Louvard, D. (1998). A novel tetanus neurotoxin-insensitive vesicle-associated membrane protein in SNARE complexes of the apical plasma membrane of epithelial cells. Mol Biol Cell 9, 1437-1448.

Geppert, M., Goda, Y., Hammer, R. E., Li, C., Rosahl, T. W., Stevens, C. F., and Sudhof, T. C. (1994). Synaptotagmin I: a major Ca^{2+} sensor for transmitter release at a central synapse. Cell 79, 717-727.

Goldberg, J. (1998). Structural basis for activation of ARF GTPase: mechanisms of guanine nucleotide exchange and GTP-myristoyl switching. Cell 95, 237-248.

Gonelle-Gispert, C., Molinete, M., Halban, P. A., and Sadoul, K. (2000). Membrane localization and biological activity of SNAP-25 cysteine mutants in insulin-secreting cells. J Cell Sci 113, 3197-3205.

Gonzalo, S., and Linder, M. E. (1998). SNAP-25 palmitoylation and plasma membrane targeting require a functional secretory pathway. Mol Biol Cell 9, 585-597.

Gonzalo, S., Greentree, W. K., and Linder, M. E. (1999). SNAP-25 is targeted to the plasma membrane through a novel membrane-binding domain. J Biol Chem 274, 21313-21318.

Goodwin, J. S., Drake, K. R., Rogers, C., Wright, L., Lippincott-Schwartz, J., Philips, M. R., and Kenworthy, A. K. (2005). Depalmitoylated Ras traffics to and from the Golgi complex via a nonvesicular pathway. J Cell Biol 170, 261-272.

Graham, M. E., Sudlow, A. W., and Burgoyne, R. D. (1997). Evidence against an acute inhibitory role of nSec-1 (munc-18) in late steps of regulated exocytosis in chromaffin and PC12 cells. J Neurochem 69, 2369-2377.

Graham, M. E., and Burgoyne, R. D. (2000). Comparison of cysteine string protein (Csp) and mutant alpha-SNAP overexpression reveals a role for csp in late steps of membrane fusion in dense-core granule exocytosis in adrenal chromaffin cells. J Neurosci 20, 1281-1289.

Grosshans, B. L., Ortiz, D., and Novick, P. (2006). Rabs and their effectors: achieving specificity in membrane traffic. Proc Natl Acad Sci U.S.A. 103, 11821-11827.

Grote, E., Hao, J. C., Bennett, M. K., and Kelly, R. B. (1995). A targeting signal in VAMP regulating transport to synaptic vesicles. Cell 81, 581-589.

Gulyas-Kovacs, A., de Wit, H., Milosevic, I., Kochubey, O., Toonen, R., Klingauf, J., Verhage, M., and Sorensen, J. B. (2007). Munc18-1: sequential interactions with the fusion machinery stimulate vesicle docking and priming. J Neurosci 27, 8676-8686.

Gundersen, C. B., and Umbach, J. A. (1992). Suppression cloning of the cDNA for a candidate subunit of a presynaptic calcium channel. Neuron 9, 527-537.

Gundersen, C. B., Mastrogiacomo, A., Faull, K., and Umbach, J. A. (1994). Extensive lipidation of a *Torpedo* cysteine string protein. J Biol Chem 269, 19197-19199.

Gundersen, C. B., Umbach, J. A., and Mastrogiacomo, A. (1996). Cysteine-string proteins: a cycle of acylation and deacylation? Life Sci 58, 2037-2040.

Gundersen, C. B., Aguado, F., Sou, S., Mastrogiacomo, A., Coppola, T., Kornblum, H. I., and Umbach, J. A. (2001). Cysteine string proteins are associated with cortical granules of *Xenopus laevis* oocytes. Cell Tissue Res 303, 211-219.

Gutierrez, L., Magee, A. I., Marshall, C. J., and Hancock, J. F. (1989). Post-translational processing of p21ras is two-step and involves carboxyl-methylation and carboxy-terminal proteolysis. EMBO J 8, 1093-1098.

Halachmi, N., and Lev, Z. (1996). The Sec1 family: a novel family of proteins involved in synaptic transmission and general secretion. J Neurochem 66, 889-897.

Hallak, H., Muszbek, L., Laposata, M., Belmonte, E., Brass, L. F., and Manning, D. R. (1994). Covalent binding of arachidonate to G protein alpha subunits of human platelets. J Biol Chem 269, 4713-4716.

Han, W., Rhee, J. S., Maximov, A., Lao, Y., Mashimo, T., Rosenmund, C., and Sudhof, T. C. (2004). N-glycosylation is essential for vesicular targeting of synaptotagmin 1. Neuron 41, 85-99.

Hanahan, D. (1983). Studies on transformation of *Escherichia coli* with plasmids. J Mol Biol 166, 557-580.

Hancock, J. F., Magee, A. I., Childs, J. E., and Marshall, C. J. (1989). All ras proteins are polyisoprenylated but only some are palmitoylated. Cell 57, 1167-1177.

Hancock, J. F., Paterson, H., and Marshall, C. J. (1990). A polybasic domain or palmitoylation is required in addition to the CAAX motif to localize p21ras to the plasma membrane. Cell 63, 133-139.

Hao, J. C., Salem, N., Peng, X. R., Kelly, R. B., and Bennett, M. K. (1997). Effect of mutations in vesicle-associated membrane protein (VAMP) on the assembly of multimeric protein complexes. J Neurosci 17, 1596-1603.

Harrison, S. D., Broadie, K., van de Goor, J., and Rubin, G. M. (1994). Mutations in the *Drosophila Rop* gene suggest a function in general secretion and synaptic transmission. Neuron 13, 555-566.

Hata, Y., Slaughter, C. A., and Sudhof, T. C. (1993). Synaptic vesicle fusion complex contains unc-18 homologue bound to syntaxin. Nature 366, 347-351.

Hata, Y., and Sudhof, T. C. (1995). A novel ubiquitous form of Munc-18 interacts with multiple syntaxins. Use of the yeast two-hybrid system to study interactions between proteins involved in membrane traffic. J Biol Chem 270, 13022-13028.

Hayashi, T., McMahon, H., Yamasaki, S., Binz, T., Hata, Y., Sudhof, T. C., and Niemann, H. (1994). Synaptic vesicle membrane fusion complex: action of clostridial neurotoxins on assembly. EMBO J 13, 5051-5061.

Hayashi, T., Rumbaugh, G., and Huganir, R. L. (2005). Differential regulation of AMPA receptor subunit trafficking by palmitoylation of two distinct sites. Neuron 47, 709-723.

Heckmann, M., Adelsberger, H., and Dudel, J. (1997). Evoked transmitter release at neuromuscular junctions in wild type and cysteine string protein null mutant larvae of *Drosophila*. Neurosci Lett 228, 167-170.

Heindel, U., Schmidt, M. F., and Veit, M. (2003). Palmitoylation sites and processing of synaptotagmin I, the putative calcium sensor for neurosecretion. FEBS Lett 544, 57-62.

Hellsten, E., Vesa, J., Olkkonen, V. M., Jalanko, A., and Peltonen, L. (1996). Human palmitoyl protein thioesterase: evidence for lysosomal targeting of the enzyme and disturbed cellular routing in infantile neuronal ceroid lipofuscinosis. EMBO J 15, 5240-5245.

Hofmann, K. (2000). A superfamily of membrane-bound O-acyltransferases with implications for wnt signaling. Trends Biochem Sci 25, 111-112.

Honsho, M., Mitoma, J. Y., and Ito, A. (1998). Retention of cytochrome b5 in the endoplasmic reticulum is transmembrane and luminal domain-dependent. J Biol Chem 273, 20860-20866.

Hosono, R., Sassa, T., and Kuno, S. (1987). Mutations affecting acetylcholine levels in the nematode *Caenorhabditis elegans*. J Neurochem 49, 1820-1823.

Hou, H., Subramanian, K., LaGrassa, T. J., Markgraf, D., Dietrich, L. E., Urban, J., Decker, N., and Ungermann, C. (2005). The DHHC protein Pfa3 affects vacuole-associated palmitoylation of the fusion factor Vac8. Proc Natl Acad Sci U.S.A. 102, 17366-17371.

Hsu, C. C., Thomas, C., Chen, W., Davis, K. M., Foos, T., Chen, J. L., Wu, E., Floor, E., Schloss, J. V., and Wu, J. Y. (1999). Role of synaptic vesicle proton gradient and protein phosphorylation on ATP-mediated activation of membrane-associated brain glutamate decarboxylase. J Biol Chem 274, 24366-24371.

Hsu, C. C., Davis, K. M., Jin, H., Foos, T., Floor, E., Chen, W., Tyburski, J. B., Yang, C. Y., Schloss, J. V., and Wu, J. Y. (2000). Association of L-glutamic acid decarboxylase to the 70-kDa heat shock protein as a potential anchoring mechanism to synaptic vesicles. J Biol Chem 275, 20822-20828.

Hsu, S. C., Ting, A. E., Hazuka, C. D., Davanger, S., Kenny, J. W., Kee, Y., and Scheller, R. H. (1996). The mammalian brain rsec6/8 complex. Neuron 17, 1209-1219.

Huang, K., Yanai, A., Kang, R., Arstikaitis, P., Singaraja, R. R., Metzler, M., Mullard, A., Haigh, B., Gauthier-Campbell, C., Gutekunst, C. A., Hayden, M. R., and El-Husseini, A. (2004). Huntingtin-interacting protein HIP14 is a palmitoyl transferase involved in palmitoylation and trafficking of multiple neuronal proteins. Neuron 44, 977-986.

Hunt, J. M., Bommert, K., Charlton, M. P., Kistner, A., Habermann, E., Augustine, G. J., and Betz, H. (1994). A post-docking role for synaptobrevin in synaptic vesicle fusion. Neuron 12, 1269-1279.

Inoue, A., Obata, K., and Akagawa, K. (1992). Cloning and sequence analysis of cDNA for a neuronal cell membrane antigen, HPC-1. J Biol Chem 267, 10613-10619.

Jahn, R., and Sudhof, T. C. (1999). Membrane fusion and exocytosis. Annu Rev Biochem 68, 863-911.

Jahn, R. (2000). Sec1/Munc18 proteins: mediators of membrane fusion moving to center stage. Neuron 27, 201-204.

Jahn, R., Lang, T., and Sudhof, T. C. (2003). Membrane fusion. Cell 112, 519-533.

Kanaani, J., el-Husseini Ael, D., Aguilera-Moreno, A., Diacovo, J. M., Bredt, D. S., and Baekkeskov, S. (2002). A combination of three distinct trafficking signals mediates axonal targeting and presynaptic clustering of GAD65. J Cell Biol 158, 1229-1238.

Kang, R., Swayze, R., Lise, M. F., Gerrow, K., Mullard, A., Honer, W. G., and El-Husseini, A. (2004). Presynaptic trafficking of synaptotagmin I is regulated by protein palmitoylation. J Biol Chem 279, 50524-50536.

Kanno, E., and Fukuda, M. (2007). Increased plasma membrane localization of O-glycosylation-deficient mutant of synaptotagmin I in PC12 cells. J Neurosci Res 86, 1036-1043.

Katagiri, H., Terasaki, J., Murata, T., Ishihara, H., Ogihara, T., Inukai, K., Fukushima, Y., Anai, M., Kikuchi, M., Miyazaki, J., and et al. (1995). A novel isoform of syntaxin-binding protein homologous to yeast Sec1 expressed ubiquitously in mammalian cells. J Biol Chem 270, 4963-4966.

Keller, C. A., Yuan, X., Panzanelli, P., Martin, M. L., Alldred, M., Sassoe-Pognetto, M., and Luscher, B. (2004). The gamma2 subunit of GABA(A) receptors is a substrate for palmitoylation by GODZ. J Neurosci 24, 5881-5891.

Khvotchev, M., Dulubova, I., Sun, J., Dai, H., Rizo, J., and Sudhof, T. C. (2007). Dual modes of Munc18-1/SNARE interactions are coupled by functionally critical binding to syntaxin-1 N terminus. J Neurosci 27, 12147-12155.

Kihara, A., Kurotsu, F., Sano, T., Iwaki, S., and Igarashi, Y. (2005). Long-chain base kinase Lcb4 is anchored to the membrane through its palmitoylation by Akr1. Mol Cell Biol 25, 9189-9197.

Kim, P. K., Hollerbach, C., Trimble, W. S., Leber, B., and Andrews, D. W. (1999). Identification of the endoplasmic reticulum targeting signal in vesicle-associated membrane proteins. J Biol Chem 274, 36876-36882.

Kinlough, C. L., McMahan, R. J., Poland, P. A., Bruns, J. B., Harkleroad, K. L., Stremple, R. J., Kashlan, O. B., Weixel, K. M., Weisz, O. A., and Hughey, R. P. (2006). Recycling of MUC1 is dependent on its palmitoylation. J Biol Chem 281, 12112-12122.

Klenchin, V. A., and Martin, T. F. (2000). Priming in exocytosis: attaining fusion-competence after vesicle docking. Biochimie 82, 399-407.

Kleuss, C., and Krause, E. (2003). Galpha(s) is palmitoylated at the N-terminal glycine. EMBO J 22, 826-832.

Knight, D. E. (1999). Secretion from bovine chromaffin cells acutely expressing exogenous proteins using a recombinant Semliki Forest virus containing an EGFP reporter. Mol Cell Neurosci 14, 486-505.

Koegl, M., Zlatkine, P., Ley, S. C., Courtneidge, S. A., and Magee, A. I. (1994). Palmitoylation of multiple Src-family kinases at a homologous N-terminal motif. Biochem J 303, 749-753.

Kohan, S. A., Pescatori, M., Brecha, N. C., Mastrogiacomo, A., Umbach, J. A., and Gundersen, C. B. (1995). Cysteine string protein immunoreactivity in the nervous system and adrenal gland of rat. J Neurosci 15, 6230-6238.

Krasnoperov, V. G., Bittner, M. A., Beavis, R., Kuang, Y., Salnikow, K. V., Chepurny, O. G., Little, A. R., Plotnikov, A. N., Wu, D., Holz, R. W., and Petrenko, A. G. (1997). alpha-Latrotoxin stimulates exocytosis by the interaction with a neuronal G-protein-coupled receptor. Neuron 18, 925-937.

Kutay, U., Hartmann, E., and Rapoport, T. A. (1993). A class of membrane proteins with a C-terminal anchor. Trends Cell Biol 3, 72-75.

Kutay, U., Ahnert-Hilger, G., Hartmann, E., Wiedenmann, B., and Rapoport, T. A. (1995). Transport route for synaptobrevin via a novel pathway of insertion into the endoplasmic reticulum membrane. EMBO J 14, 217-223.

Laemmli, U. K. (1970). Cleavage of structural proteins during the assembly of the head of bacteriophage T4. Nature 227, 680-685.

Lam, K. K. Y., Davey, M., Sun, B., Roth, A. F., Davis, N. G., and Conibear, E. (2006). Palmitoylation by the DHHC protein Pfa4 regulates the ER exit of Chs3. J Cell Biol 174, 19-25.

Lane, S. R., and Liu, Y. (1997). Characterization of the palmitoylation domain of SNAP-25. J Neurochem 69, 1864-1869.

Leung, S. M., Chen, D., DasGupta, B. R., Whiteheart, S. W., and Apodaca, G. (1998). SNAP-23 requirement for transferrin recycling in Streptolysin-O-permeabilized Madin-Darby canine kidney cells. J Biol Chem 273, 17732-17741.

Leventis, R., Juel, G., Knudsen, J. K., and Silvius, J. R. (1997). Acyl-CoA binding proteins inhibit the nonenzymic S-acylation of cysteinyl-containing peptide sequences by long-chain acyl-CoAs. Biochemistry 36, 5546-5553.

Leveque, C., Pupier, S., Marqueze, B., Geslin, L., Kataoka, M., Takahashi, M., De Waard, M., and Seagar, M. (1998). Interaction of cysteine string proteins with the alpha1A subunit of the P/Q-type calcium channel. J Biol Chem 273, 13488-13492.

Liang, X., Lu, Y., Neubert, T. A., and Resh, M. D. (2002). Mass spectrometric analysis of GAP-43/neuromodulin reveals the presence of a variety of fatty acylated species. J Biol Chem 277, 33032-33040.

Liberek, K., Georgopoulos, C., and Zylicz, M. (1988). Role of the *Escherichia coli* DnaK and DnaJ heat shock proteins in the initiation of bacteriophage lambda DNA replication. Proc Natl Acad Sci U.S.A. 85, 6632-6636.

Liberek, K., Marszalek, J., Ang, D., Georgopoulos, C., and Zylicz, M. (1991). *Escherichia coli* DnaJ and GrpE heat shock proteins jointly stimulate ATPase activity of DnaK. Proc Natl Acad Sci U.S.A. 88, 2874-2878.

Lin, R. C., and Scheller, R. H. (2000). Mechanisms of Synaptic Vesicle Exocytosis. Annu Rev Cell Dev Biol 16, 19-49.

Linder, M. E., and Deschenes, R. J. (2007). Palmitoylation: policing protein stability and traffic. Nat Rev Mol Cell Biol 8, 74-84.

Lippincott-Schwartz, J., Yuan, L. C., Bonifacino, J. S., and Klausner, R. D. (1989). Rapid redistribution of Golgi proteins into the ER in cells treated with brefeldin A: evidence for membrane cycling from Golgi to ER. Cell 56, 801-813.

Lippincott-Schwartz, J., Donaldson, J. G., Schweizer, A., Berger, E. G., Hauri, H. P., Yuan, L. C., and Klausner, R. D. (1990). Microtubule-dependent retrograde transport of proteins into the ER in the presence of brefeldin A suggests an ER recycling pathway. Cell 60, 821-836.

Littleton, J. T., Barnard, R. J., Titus, S. A., Slind, J., Chapman, E. R., and Ganetzky, B. (2001). SNARE-complex disassembly by NSF follows synaptic-vesicle fusion. Proc Natl Acad Sci U.S.A. 98, 12233-12238.

Liu, L., Dudler, T., and Gelb, M. H. (1996). Purification of a protein palmitoyltransferase that acts on H-Ras protein and on a C-terminal N-Ras peptide. J Biol Chem 271, 23269-23276.

Liu, T., Tucker, W. C., Bhalla, A., Chapman, E. R., and Weisshaar, J. C. (2005). SNARE-driven, 25-millisecond vesicle fusion *in vitro*. Biophys J 89, 2458-2472.

Lobo, S., Greentree, W. K., Linder, M. E., and Deschenes, R. J. (2002). Identification of Ras Palmitoyltransferase in *Saccharomyces cerevisiae*. J Biol Chem 277, 41268-41273.

Loranger, S. S., and Linder, M. E. (2002). SNAP-25 traffics to the plasma membrane by a syntaxin-independent mechanism. J Biol Chem 277, 34303-34309.

Luan, P., Balch, W. E., Emr, S. D., and Burd, C. G. (1999). Molecular dissection of guanine nucleotide dissociation inhibitor function *in vivo*. Rab-independent binding to membranes and role of Rab recycling factors. J Biol Chem 274, 14806-14817.

Magee, A. I., Gutierrez, L., McKay, I. A., Marshall, C. J., and Hall, A. (1987). Dynamic fatty acylation of p21N-ras. EMBO J 6, 3353-3357.

Magee, T., and Marshall, C. (1999). New insights into the interaction of Ras with the plasma membrane. Cell 98, 9-12.

Mann, R. K., and Beachy, P. A. (2004). Novel lipid modifications of secreted protein signals. Annu Rev Biochem 73, 891-923.

Martens, S., Kozlov, M. M., and McMahon, H. T. (2007). How synaptotagmin promotes membrane fusion. Science 316, 1205-1208.

Martin-Moutot, N., Charvin, N., Leveque, C., Sato, K., Nishiki, T., Kozaki, S., Takahashi, M., and Seagar, M. (1996). Interaction of SNARE complexes with P/Q-type calcium channels in rat cerebellar synaptosomes. J Biol Chem 271, 6567-6570.

Mastrogiacomo, A., Evans, C. J., and Gundersen, C. B. (1994a). Antipeptide antibodies against a *Torpedo* cysteine-string protein. J Neurochem 62, 873-880.

Mastrogiacomo, A., Parsons, S. M., Zampighi, G. A., Jenden, D. J., Umbach, J. A., and Gundersen, C. B. (1994b). Cysteine string proteins: a potential link between synaptic vesicles and presynaptic Ca^{2+} channels. Science 263, 981-982.

Mastrogiacomo, A., and Gundersen, C. B. (1995). The nucleotide and deduced amino acid sequence of a rat cysteine string protein. Brain Res Mol Brain Res 28, 12-18.

Mastrogiacomo, A., Kohan, S. A., Whitelegge, J. P., and Gundersen, C. B. (1998a). Intrinsic membrane association of Drosophila cysteine string proteins. FEBS Lett 436, 85-91.

Mastrogiacomo, A., Kornblum, H. I., Umbach, J. A., and Gundersen, C. B. (1998b). A *Xenopus* cysteine string protein with a cysteine residue in the J domain. Biochim Biophys Acta 1401, 239-241.

Matthew, W. D., Tsavaler, L., and Reichardt, L. F. (1981). Identification of a synaptic vesicle-specific membrane protein with a wide distribution in neuronal and neurosecretory tissue. J Cell Biol 91, 257-269.

Mayer, M. P., and Bukau, B. (2005). Hsp70 chaperones: cellular functions and molecular mechanism. Cell Mol Life Sci 62, 670-684.

McLaughlin, S., and Aderem, A. (1995). The myristoyl-electrostatic switch: a modulator of reversible protein-membrane interactions. Trends Biochem Sci 20, 272-276.

McMahon, H. T., Ushkaryov, Y. A., Edelmann, L., Link, E., Binz, T., Niemann, H., Jahn, R., and Sudhof, T. C. (1993). Cellubrevin is a ubiquitous tetanus-toxin substrate homologous to a putative synaptic vesicle fusion protein. Nature 364, 346-349.

McMahon, H. T., Missler, M., Li, C., and Sudhof, T. C. (1995). Complexins: cytosolic proteins that regulate SNAP receptor function. Cell 83, 111-119.

McNew, J. A., Parlati, F., Fukuda, R., Johnston, R. J., Paz, K., Paumet, F., Sollner, T. H., and Rothman, J. E. (2000). Compartmental specificity of cellular membrane fusion encoded in SNARE proteins. Nature 407, 153-159.

Medine, C. N., Rickman, C., Chamberlain, L. H., and Duncan, R. R. (2007). Munc18-1 prevents the formation of ectopic SNARE complexes in living cells. J Cell Sci 120, 4407-4415.

Melkonian, K. A., Ostermeyer, A. G., Chen, J. Z., Roth, M. G., and Brown, D. A. (1999). Role of lipid modifications in targeting proteins to detergent-resistant membrane rafts. Many raft proteins are acylated, while few are prenylated. J Biol Chem 274, 3910-3917.

Minami, Y., Hohfeld, J., Ohtsuka, K., and Hartl, F. U. (1996). Regulation of the heat-shock protein 70 reaction cycle by the mammalian DnaJ homolog, Hsp40. J Biol Chem 271, 19617-19624.

Mitchell, D. A., Farh, L., Marshall, T. K., and Deschenes, R. J. (1994). A polybasic domain allows nonprenylated Ras proteins to function in *Saccharmocyces cervevisiae*. J Biol Chem 269, 21540-21546.

Mitchell, D. A., Vasudevan, A., Linder, M. E., and Deschenes, R. J. (2006). Protein palmitoylation by a family of DHHC protein *S*-acyltransferases. J Lipid Res 47, 1118-1127.

Mitra, K., Ubarretxena-Belandia, I., Taguchi, T., Warren, G., and Engelman, D. M. (2004). Modulation of the bilayer thickness of exocytic pathway membranes by membrane proteins rather than cholesterol. Proc Natl Acad Sci U.S.A. 101, 4083-4088.

Miura, G. I., Buglino, J., Alvarado, D., Lemmon, M. A., Resh, M. D., and Treisman, J. E. (2006). Palmitoylation of the EGFR ligand Spitz by Rasp increases Spitz activity by restricting its diffusion. Dev Cell 10, 167-176.

Morales, J., Fishburn, C. S., Wilson, P. T., and Bourne, H. R. (1998). Plasma membrane localization of G alpha z requires two signals. Mol Biol Cell 9, 1-14.

Morales, M., Ferrus, A., and Martinez-Padron, M. (1999). Presynaptic calcium-channel currents in normal and csp mutant *Drosophila* peptidergic terminals. Eur J Neurosci 11, 1818-1826.

Morgan, A., and Burgoyne, R. D. (1997). Common mechanisms for regulated exocytosis in the chromaffin cell and the synapse. In Seminars in Cell and Developmental Biology, R. D. Burgoyne, and P. Mombaerts, eds. (Cambridge, Academic Press), pp. 141-149.

Nadler, M. J., Hu, X. E., Cassady, J. M., and Geahlen, R. L. (1994). Posttranslational acylation of the transferrin receptor in LSTRA cells with myristate, palmitate and stearate: evidence for distinct acyltransferases. Biochim Biophys Acta 1213, 100-106.

Nagano, N., Ota, M., and Nishikawa, K. (1999). Strong hydrophobic nature of cysteine residues in proteins. FEBS Lett 458, 69-71.

Naren, A. P., Nelson, D. J., Xie, W., Jovov, B., Pevsner, J., Bennett, M. K., Benos, D. J., Quick, M. W., and Kirk, K. L. (1997). Regulation of CFTR chloride channels by syntaxin and Munc18 isoforms. Nature 390, 302-305.

Natochin, M., Campbell, T. N., Barren, B., Miller, L. C., Hameed, S., Artemyev, N. O., and Braun, J. E. (2005). Characterization of the G alpha(s) regulator cysteine string protein. J Biol Chem 280, 30236-30241.

Nie, Z., Ranjan, R., Wenniger, J. J., Hong, S. N., Bronk, P., and Zinsmaier, K. E. (1999). Overexpression of cysteine-string proteins in Drosophila reveals interactions with syntaxin. J Neurosci 19, 10270-10279.

Novick, P., Field, C., and Schekman, R. (1980). Identification of 23 complementation groups required for post-translational events in the yeast secretory pathway. Cell 21, 205-215.

Novick, P., and Zerial, M. (1997). The diversity of Rab proteins in vesicle transport. Curr Opin Cell Biol 9, 496-504.

O'Connor, V., Heuss, C., De Bello, W. M., Dresbach, T., Charlton, M. P., Hunt, J. H., Pellegrini, L. L., Hodel, A., Burger, M. M., Betz, H., Augustine, G. J., and Schafer, T. (1997). Disruption of syntaxin-mediated protein interactions blocks neurotransmitter secretion. Proc Natl Acad Sci U.S.A. 94, 12186-12191.

Ohki, R., Kawamata, T., Katoh, Y., Hosoda, F., and Ohki, M. (1992). *Escherichia coli* dnaJ deletion mutation results in loss of stability of a positive regulator, CRP. J Biol Chem 267, 13180-13184.

Ohno, Y., Kihara, A., Sano, T., and Igarashi, Y. (2006). Intracellular localization and tissue-specific distribution of human and yeast DHHC cysteine-rich domain-containing proteins. Biochim Biophys Acta 1761, 474-483.

Ohyama, T., Verstreken, P., Ly, C. V., Rosenmund, T., Rajan, A., Tien, A. C., Haueter, C., Schulze, K. L., and Bellen, H. J. (2007). Huntingtin-interacting protein 14, a palmitoyl transferase required for exocytosis and targeting of CSP to synaptic vesicles. J Cell Biol 179, 1481-1496.

Oyler, G. A., Higgins, G. A., Hart, R. A., Battenberg, E., Billingsley, M., Bloom, F. E., and Wilson, M. C. (1989). The identification of a novel synaptosomal-associated protein, SNAP-25, differentially expressed by neuronal subpopulations. J Cell Biol 109, 3039-3052.

Palade, G. (1975). Intracellular aspects of the process of protein synthesis. Science 189, 347-358.

Parlati, F., McNew, J. A., Fukuda, R., Miller, R., Sollner, T. H., and Rothman, J. E. (2000). Topological restriction of SNARE-dependent membrane fusion. Nature 407, 194-198.

Pechlivanis, M., and Kuhlmann, J. (2006). Hydrophobic modifications of Ras proteins by isoprenoid groups and fatty acids - More than just membrane anchoring. Biochim Biophys Acta 1764, 1914-1931.

Peitzsch, R. M., and McLaughlin, S. (1993). Binding of acylated peptides and fatty acids to phospholipid vesicles: pertinence to myristoylated proteins. Biochemistry 32, 10436-10443.

Pennuto, M., Bonanomi, D., Benfenati, F., and Valtorta, F. (2003). Synaptophysin I controls the targeting of VAMP2/synaptobrevin II to synaptic vesicles. Mol Biol Cell 14, 4909-4919.

Pepinsky, R. B., Zeng, C., Wen, D., Rayhorn, P., Baker, D. P., Williams, K. P., Bixler, S. A., Ambrose, C. M., Garber, E. A., Miatkowski, K., Taylor, F. R., Wang, E. A., and Galdes, A. (1998). Identification of a palmitic acid-modified form of human Sonic hedgehog. J Biol Chem 273, 14037-14045.

Pereira-Leal, J. B., and Seabra, M. C. (2000). The mammalian Rab family of small GTPases: definition of family and subfamily sequence motifs suggests a mechanism for functional specificity in the Ras superfamily. J Mol Biol 301, 1077-1087.

Pereira-Leal, J. B., Hume, A. N., and Seabra, M. C. (2001). Prenylation of Rab GTPases: molecular mechanisms and involvement in genetic disease. FEBS Lett 498, 197-200.

Pereira-Leal, J. B., and Seabra, M. C. (2001). Evolution of the Rab family of small GTP-binding proteins. J Mol Biol 313, 889-901.

Perin, M. S., Fried, V. A., Mignery, G. A., Jahn, R., and Sudhof, T. C. (1990). Phospholipid binding by a synaptic vesicle protein homologous to the regulatory region of protein kinase C. Nature 345, 260-263.

Perin, M. S., Brose, N., Jahn, R., and Sudhof, T. C. (1991). Domain structure of synaptotagmin (p65). J Biol Chem 266, 623-629.

Petaja-Repo, U. E., Hogue, M., Leskela, T. T., Markkanen, P. M., Tuusa, J. T., and Bouvier, M. (2006). Distinct subcellular localization for constitutive and agonist-modulated palmitoylation of the human delta opioid receptor. J Biol Chem 281, 15780-15789.

Peters, C., Bayer, M. J., Buhler, S., Andersen, J. S., Mann, M., and Mayer, A. (2001). Trans-complex formation by proteolipid channels in the terminal phase of membrane fusion. Nature 409, 581-588.

Pevsner, J., Hsu, S. C., Braun, J. E., Calakos, N., Ting, A. E., Bennett, M. K., and Scheller, R. H. (1994a). Specificity and regulation of a synaptic vesicle docking complex. Neuron 13, 353-361.

Pevsner, J., Hsu, S. C., and Scheller, R. H. (1994b). n-Sec1: a neural-specific syntaxin-binding protein. Proc Natl Acad Sci U.S.A. 91, 1445-1449.

Pfeffer, S. R. (2001). Rab GTPases: specifying and deciphering organelle identity and function. Trends Cell Biol 11, 487-491.

Pobbati, A. V., Stein, A., and Fasshauer, D. (2006). N- to C-terminal SNARE complex assembly promotes rapid membrane fusion. Science 313, 673-676.

Poirier, M. A., Xiao, W., Macosko, J. C., Chan, C., Shin, Y. K., and Bennett, M. K. (1998). The synaptic SNARE complex is a parallel four-stranded helical bundle. Nat Struct Biol 5, 765-769.

Politis, E. G., Roth, A. F., and Davis, N. G. (2005). Transmembrane Topology of the Protein Palmitoyl Transferase Akr1. J Biol Chem 280, 10156-10163.

Porter, J. A., Ekker, S. C., Park, W. J., von Kessler, D. P., Young, K. E., Chen, C. H., Ma, Y., Woods, A. S., Cotter, R. J., Koonin, E. V., and Beachy, P. A. (1996a). Hedgehog patterning activity: role of a lipophilic modification mediated by the carboxy-terminal autoprocessing domain. Cell 86, 21-34.

Porter, J. A., Young, K. E., and Beachy, P. A. (1996b). Cholesterol modification of hedgehog signaling proteins in animal development. Science 274, 255-259.

Pupier, S., Leveque, C., Marqueze, B., Kataoka, M., Takahashi, M., and Seagar, M. J. (1997). Cysteine string proteins associated with secretory granules of the rat neurohypophysis. J Neurosci 17, 2722-2727.

Putilina, T., Wong, P., and Gentleman, S. (1999). The DHHC domain: a new highly conserved cysteine-rich motif. Mol Cell Biochem 195, 219-226.

Qi, J., Peters, K. W., Liu, C., Wang, J. M., Edinger, R. S., Johnson, J. P., Watkins, S. C., and Frizzell, R. A. (1999). Regulation of the amiloride-sensitive epithelial sodium channel by syntaxin 1A. J Biol Chem 274, 30345-30348.

Qian, Y. Q., Patel, D., Hartl, F. U., and McColl, D. J. (1996). Nuclear magnetic resonance solution structure of the human Hsp40 (HDJ-1) J-domain. J Mol Biol 260, 224-235.

Ravichandran, V., Chawla, A., and Roche, P. A. (1996). Identification of a novel syntaxin- and synaptobrevin/VAMP-binding protein, SNAP-23, expressed in non-neuronal tissues. J Biol Chem 271, 13300-13303.

Rea, S., and James, D. E. (1997). Moving GLUT4: the biogenesis and trafficking of GLUT4 storage vesicles. Diabetes 46, 1667-1677.

Rea, S., Martin, L. B., McIntosh, S., Macaulay, S. L., Ramsdale, T., Baldini, G., and James, D. E. (1998). Syndet, an adipocyte target SNARE involved in the insulin-induced translocation of GLUT4 to the cell surface. J Biol Chem 273, 18784-18792.

Redecker, P., Pabst, H., and Grube, D. (1998). Munc-18-1 and cysteine string protein (csp) in pinealocytes of the gerbil pineal gland. Cell Tissue Res 293, 245-252.

Resh, M. D. (1999). Fatty acylation of proteins: new insights into membrane targeting of myristoylated and palmitoylated proteins. Biochim Biophys Acta 1451, 1-16.

Resh, M. D. (2006). Trafficking and signaling by fatty-acylated and prenylated proteins. Nat Chem Biol 2, 584-590.

Rhee, J. S., Li, L. Y., Shin, O. H., Rah, J. C., Rizo, J., Sudhof, T. C., and Rosenmund, C. (2005). Augmenting neurotransmitter release by enhancing the apparent Ca^{2+} affinity of synaptotagmin 1. Proc Natl Acad Sci U.S.A. 102, 18664-18669.

Richmond, J. E., Weimer, R. M., and Jorgensen, E. M. (2001). An open form of syntaxin bypasses the requirement for UNC-13 in vesicle priming. Nature 412, 338-341.

Rickman, C., Meunier, F. A., Binz, T., and Davletov, B. (2004). High affinity interaction of syntaxin and SNAP-25 on the plasma membrane is abolished by botulinum toxin E. J Biol Chem 279, 644-651.

Rickman, C., Medine, C. N., Bergmann, A., and Duncan, R. R. (2007). Functionally and spatially distinct modes of munc18-syntaxin 1 interaction. J Biol Chem 282, 12097-12103.

Roberts, E., and Kuriyama, K. (1968). Biochemical-physiological correlations in studies of the gamma-aminobutyric acid system. Brain Res 8, 1-35.

Robinson, L. J., Busconi, L., and Michel, T. (1995). Agonist-modulated palmitoylation of endothelial nitric oxide synthase. J Biol Chem 270, 995-998.

Rocks, O., Peyker, A., Kahms, M., Verveer, P. J., Koerner, C., Lumbierres, M., Kuhlmann, J., Waldmann, H., Wittinghofer, A., and Bastiaens, P. I. (2005). An acylation cycle regulates localization and activity of palmitoylated Ras isoforms. Science 307, 1746-1752.

Rosendal, J., Ertbjerg, P., and Knudsen, J. (1993). Characterization of ligand binding to acyl-CoA-binding protein. Biochem J 290, 321-326.

Roth, A. F., Feng, Y., Chen, L., and Davis, N. G. (2002). The yeast DHHC cysteine-rich domain protein Akr1p is a palmitoyl transferase. J Cell Biol 159, 23-28.

Roth, A. F., Wan, J., Bailey, A. O., Sun, B., Kuchar, J. A., Green, W. N., Phinney, B. S., Yates, J. R., 3rd, and Davis, N. G. (2006). Global analysis of protein palmitoylation in yeast. Cell 125, 1003-1013.

Rowe, J., Calegari, F., Taverna, E., Longhi, R., and Rosa, P. (2001). Syntaxin 1A is delivered to the apical and basolateral domains of epithelial cells: the role of munc-18 proteins. J Cell Sci 114, 3323-3332.

Roy, S., Plowman, S., Rotblat, B., Prior, I. A., Muncke, C., Grainger, S., Parton, R. G., Henis, Y. I., Kloog, Y., and Hancock, J. F. (2005). Individual palmitoyl residues serve distinct roles in H-ras trafficking, microlocalization, and signaling. Mol Cell Biol 25, 6722-6733.

Sabatini, B. L., and Regehr, W. G. (1996). Timing of neurotransmission at fast synapses in the mammalian brain. Nature 384, 170-172.

Sakisaka, T., Meerlo, T., Matteson, J., Plutner, H., and Balch, W. E. (2002). Rab-alphaGDI activity is regulated by a Hsp90 chaperone complex. EMBO J 21, 6125-6135.

Salaün, C., Gould, G. W., and Chamberlain, L. H. (2005). The SNARE proteins SNAP-25 and SNAP-23 display different affinities for lipid rafts in PC12 cells. Regulation by distinct cysteine-rich domains. J Biol Chem 280, 1236-1240.

Salminen, A., and Novick, P. J. (1987). A ras-like protein is required for a post-Golgi event in yeast secretion. Cell 49, 527-538.

Sambrook, J., Fritsch, E. F., and Maniatis, T. (1989). Molecular Cloning: A Laboratory Manual. (NJ, Cold Spring Harbour Laboratory Press.).

Schiavo, G., Benfenati, F., Poulain, B., Rossetto, O., Polverino de Laureto, P., DasGupta, B. R., and Montecucco, C. (1992a). Tetanus and botulinum-B neurotoxins block neurotransmitter release by proteolytic cleavage of synaptobrevin. Nature 359, 832-835.

Schiavo, G., Poulain, B., Rossetto, O., Benfenati, F., Tauc, L., and Montecucco, C. (1992b). Tetanus toxin is a zinc protein and its inhibition of neurotransmitter release and protease activity depend on zinc. EMBO J 11, 3577-3583.

Schiavo, G., Rossetto, O., Catsicas, S., Polverino de Laureto, P., DasGupta, B. R., Benfenati, F., and Montecucco, C. (1993a). Identification of the nerve terminal targets of botulinum neurotoxin serotypes A, D, and E. J Biol Chem 268, 23784-23787.

Schiavo, G., Santucci, A., Dasgupta, B. R., Mehta, P. P., Jontes, J., Benfenati, F., Wilson, M. C., and Montecucco, C. (1993b). Botulinum neurotoxins serotypes A and E cleave SNAP-25 at distinct COOH-terminal peptide bonds. FEBS Lett 335, 99-103.

Schiavo, G., Shone, C. C., Rossetto, O., Alexander, F. C., and Montecucco, C. (1993c). Botulinum neurotoxin serotype F is a zinc endopeptidase specific for VAMP/synaptobrevin. J Biol Chem 268, 11516-11519.

Schiavo, G., Malizio, C., Trimble, W. S., Polverino de Laureto, P., Milan, G., Sugiyama, H., Johnson, E. A., and Montecucco, C. (1994). Botulinum G neurotoxin cleaves VAMP/synaptobrevin at a single Ala-Ala peptide bond. J Biol Chem 269, 20213-20216.

Schiavo, G., Stenbeck, G., Rothman, J. E., and Sollner, T. H. (1997). Binding of the synaptic vesicle v-SNARE, synaptotagmin, to the plasma membrane t-SNARE, SNAP-25, can explain docked vesicles at neurotoxin-treated synapses. Proc Natl Acad Sci U.S.A. 94, 997-1001.

Schluter, O. M., Khvotchev, M., Jahn, R., and Sudhof, T. C. (2002). Localization versus function of Rab3 proteins. Evidence for a common regulatory role in controlling fusion. J Biol Chem 277, 40919-40929.

Schluter, O. M., Schmitz, F., Jahn, R., Rosenmund, C., and Sudhof, T. C. (2004). A complete genetic analysis of neuronal Rab3 function. J Neurosci 24, 6629-6637.

Schmitz, F., Tabares, L., Khimich, D., Strenzke, N., de la Villa-Polo, P., Castellano-Muñoz, M., Bulankina, A., Moser, T., Fernandez-Chacon, R., and Sudhof, T.C. (2006). CSP alpha-deficiency causes massive and rapid photoreceptor degeneration. Proc Natl Acad Sci U.S.A. 103, 2926-2931.

Schoch, S., Deak, F., Konigstorfer, A., Mozhayeva, M., Sara, Y., Sudhof, T. C., and Kavalali, E. T. (2001). SNARE function analyzed in synaptobrevin/VAMP knockout mice. Science 294, 1117-1122.

Schroeder, H., Leventis, R., Shahinian, S., Walton, P. A., and Silvius, J. R. (1996). Lipid-modified, cysteinyl-containing peptides of diverse structures are efficiently S-acylated at the plasma membrane of mammalian cells. J Cell Biol 134, 647-660.

Schulze, K. L., Littleton, J. T., Salzberg, A., Halachmi, N., Stern, M., Lev, Z., and Bellen, H. J. (1994). rop, a *Drosophila* homolog of yeast Sec1 and vertebrate n-Sec1/Munc-18 proteins, is a negative regulator of neurotransmitter release *in vivo*. Neuron 13, 1099-1108.

Seabra, M. C., Goldstein, J. L., Sudhof, T. C., and Brown, M. S. (1992). Rab geranylgeranyl transferase. A multisubunit enzyme that prenylates GTP-binding proteins terminating in Cys-X-Cys or Cys-Cys. J Biol Chem 267, 14497-14503.

Segev, N., Mulholland, J., and Botstein, D. (1988). The yeast GTP-binding YPT1 protein and a mammalian counterpart are associated with the secretion machinery. Cell 52, 915-924.

Shahin, V., Datta, D., Hui, E., Henderson, R. M., Chapman, E. R., and Edwardson, J. M. (2008). Synaptotagmin perturbs the structure of phospholipid bilayers. Biochemistry 47, 2143-2152.

Shahinian, S., and Silvius, J. R. (1995). Doubly-lipid-modified protein sequence motifs exhibit long-lived anchorage to lipid bilayer membranes. Biochemistry 34, 3813-3822.

Shao, X., Li, C., Fernandez, I., Zhang, X., Sudhof, T. C., and Rizo, J. (1997). Synaptotagmin-syntaxin interaction: the C2 domain as a Ca^{2+}-dependent electrostatic switch. Neuron 18, 133-142.

Shen, J., Tareste, D. C., Paumet, F., Rothman, J. E., and Melia, T. J. (2007). Selective activation of cognate SNAREpins by Sec1/Munc18 proteins. Cell 128, 183-195.

Shen, L., Liang, F., Walensky, L. D., and Huganir, R. L. (2000). Regulation of AMPA receptor GluR1 subunit surface expression by a 4. 1N-linked actin cytoskeletal association. J Neurosci 20, 7932-7940.

Sheng, Z. H., Rettig, J., Takahashi, M., and Catterall, W. A. (1994). Identification of a syntaxin-binding site on N-type calcium channels. Neuron 13, 1303-1313.

Shorter, J., Watson, R., Giannakou, M. E., Clarke, M., Warren, G., and Barr, F. A. (1999). GRASP55, a second mammalian GRASP protein involved in the stacking of Golgi cisternae in a cell-free system. EMBO J 18, 4949-4960.

Sigal, C. T., Zhou, W., Buser, C. A., McLaughlin, S., and Resh, M. D. (1994). Amino-terminal basic residues of Src mediate membrane binding through electrostatic interaction with acidic phospholipids. Proc Natl Acad Sci U.S.A. 91, 12253-12257.

Silvius, J. R., and l'Heureux, F. (1994). Fluorimetric evaluation of the affinities of isoprenylated peptides for lipid bilayers. Biochemistry 33, 3014-3022.

Singaraja, R. R., Hadano, S., Metzler, M., Givan, S., Wellington, C. L., Warby, S., Yanai, A., Gutekunst, C. A., Leavitt, B. R., Yi, H., Fichter, K., Gan, L., McCutcheon, K., Chopra, V., Michel, J., Hersch, S. M., Ikeda, J. E., and Hayden, M. R. (2002). HIP14, a novel ankyrin domain-containing protein, links huntingtin to intracellular trafficking and endocytosis. Hum Mol Genet 11, 2815-2828.

Sleat, D. E., Sohar, I., Lackland, H., Majercak, J., and Lobel, P. (1996). Rat brain contains high levels of mannose-6-phosphorylated glycoproteins including lysosomal enzymes and palmitoyl-protein thioesterase, an enzyme implicated in infantile neuronal lipofuscinosis. J Biol Chem 271, 19191-19198.

Smotrys, J. E., Schoenfish, M. J., Stutz, M. A., and Linder, M. E. (2005). The vacuolar DHHC-CRD protein Pfa3p is a protein acyltransferase for Vac8p. J Cell Biol 170, 1091-1099.

Solimena, M., Aggujaro, D., Muntzel, C., Dirkx, R., Butler, M., De Camilli, P., and Hayday, A. (1993). Association of GAD-65, but not of GAD-67, with the Golgi complex of transfected Chinese hamster ovary cells mediated by the N-terminal region. Proc Natl Acad Sci U.S.A. 90, 3073-3077.

Solimena, M., Dirkx, R., Jr., Radzynski, M., Mundigl, O., and De Camilli, P. (1994). A signal located within amino acids 1-27 of GAD65 is required for its targeting to the Golgi complex region. J Cell Biol 126, 331-341.

Sollner, T., Bennett, M. K., Whiteheart, S. W., Scheller, R. H., and Rothman, J. E. (1993a). A protein assembly-disassembly pathway in vitro that may correspond to sequential steps of synaptic vesicle docking, activation, and fusion. Cell 75, 409-418.

Sollner, T., Whiteheart, S. W., Brunner, M., Erdjument-Bromage, H., Geromanos, S., Tempst, P., and Rothman, J. E. (1993b). SNAP receptors implicated in vesicle targeting and fusion. Nature 362, 318-324.

Soyombo, A. A., and Hofmann, S. L. (1997). Molecular cloning and expression of palmitoyl-protein thioesterase 2 (PPT2), a homolog of lysosomal palmitoyl-protein thioesterase with a distinct substrate specificity. J Biol Chem 272, 27456-27463.

Stevens, D. R., Wu, Z. X., Matti, U., Junge, H. J., Schirra, C., Becherer, U., Wojcik, S. M., Brose, N., and Rettig, J. (2005). Identification of the minimal protein domain required for priming activity of Munc13-1. Curr Biol 15, 2243-2248.

Stowers, R. S., and Isacoff, E. Y. (2007). Drosophila huntingtin-interacting protein 14 is a presynaptic protein required for photoreceptor synaptic transmission and expression of the palmitoylated proteins synaptosome-associated protein 25 and cysteine string protein. J Neurosci 27, 12874-12883.

Sudhof, T. C., Baumert, M., Perin, M. S., and Jahn, R. (1989). A synaptic vesicle membrane protein is conserved from mammals to Drosophila. Neuron 2, 1475-1481.

Sudhof, T. C. (2004). The synaptic vesicle cycle. Annu Rev Neurosci 27, 509-547.

Sugimoto, H., Hayashi, H., and Yamashita, S. (1996). Purification, cDNA cloning, and regulation of lysophospholipase from rat liver. J Biol Chem 271, 7705-7711.

Sutton, K. G., McRory, J. E., Guthrie, H., Murphy, T. H., and Snutch, T. P. (1999). P/Q-type calcium channels mediate the activity-dependent feedback of syntaxin-1A. Nature 401, 800-804.

Sutton, R. B., Fasshauer, D., Jahn, R., and Brunger, A. T. (1998). Crystal structure of a SNARE complex involved in synaptic exocytosis at 2.4 A resolution. Nature 395, 347-353.

Swarthout, J. T., Lobo, S., Farh, L., Croke, M. R., Greentree, W. K., Deschenes, R. J., and Linder, M. E. (2005). DHHC9 and GCP16 constitute a human protein fatty acyltransferase with specificity for H- and N-Ras. J Biol Chem 280, 31141-31148.

Swayne, L. A., Blattler, C., Kay, J. G., and Braun, J. E. (2003). Oligomerization characteristics of cysteine string protein. Biochem Biophys Res Commun 300, 921-926.

Szule, J. A., Jarvis, S. E., Hibbert, J. E., Spafford, J. D., Braun, J. E., Zamponi, G. W., Wessel, G. M., and Coorssen, J. R. (2003). Calcium-triggered membrane fusion proceeds independently of specific presynaptic proteins. J Biol Chem 278, 24251-24254.

Tahara, M., Coorssen, J. R., Timmers, K., Blank, P. S., Whalley, T., Scheller, R., and Zimmerberg, J. (1998). Calcium can disrupt the SNARE protein complex on sea urchin egg secretory vesicles without irreversibly blocking fusion. J Biol Chem 273, 33667-33673.

Tellam, J. T., McIntosh, S., and James, D. E. (1995). Molecular identification of two novel Munc-18 isoforms expressed in non-neuronal tissues. J Biol Chem 270, 5857-5863.

Teng, F. Y., Wang, Y., and Tang, B. L. (2001). The syntaxins. Genome Biol 2, 3012.1-3012.7.

Topinka, J. R., and Bredt, D. S. (1998). N-terminal palmitoylation of PSD-95 regulates association with cell membranes and interaction with K$^+$ channel Kv1.4. Neuron 20, 125-134.

Touchot, N., Chardin, P., and Tavitian, A. (1987). Four additional members of the ras gene superfamily isolated by an oligonucleotide strategy: molecular cloning of YPT-related cDNAs from a rat brain library. Proc Natl Acad Sci U.S.A. 84, 8210-8214.

Towler, D. A., Adams, S. P., Eubanks, S. R., Towery, D. S., Jackson-Machelski, E., Glaser, L., and Gordon, J. I. (1987). Purification and characterization of yeast myristoyl CoA:protein N-myristoyltransferase. Proc Natl Acad Sci U.S.A. 84, 2708-2712.

Toyoda, T., Sugimoto, H., and Yamashita, S. (1999). Sequence, expression in *Escherichia coli*, and characterization of lysophospholipase II. Biochim Biophys Acta 1437, 182-193.

Trimble, W. S., Cowan, D. M., and Scheller, R. H. (1988). VAMP-1: a synaptic vesicle-associated integral membrane protein. Proc Natl Acad Sci U.S.A. 85, 4538-4542.

Ubach, J., Zhang, X., Shao, X., Sudhof, T. C., and Rizo, J. (1998). Ca^{2+} binding to synaptotagmin: how many Ca^{2+} ions bind to the tip of a C2-domain? EMBO J 17, 3921-3930.

Uemura, T., Mori, H., and Mishina, M. (2002). Isolation and characterization of Golgi apparatus-specific GODZ with the DHHC zinc finger domain. Biochem Biophys Res Commun 296, 492-496.

Umbach, J. A., Zinsmaier, K. E., Eberle, K. K., Buchner, E., Benzer, S., and Gundersen, C. B. (1994). Presynaptic dysfunction in *Drosophila* csp mutants. Neuron 13, 899-907.

Umbach, J. A., and Gundersen, C. B. (1997). Evidence that cysteine string proteins regulate an early step in the Ca^{2+}-dependent secretion of neurotransmitter at *Drosophila* neuromuscular junctions. J Neurosci 17, 7203-7209.

Umbach, J. A., Saitoe, M., Kidokoro, Y., and Gundersen, C. B. (1998). Attenuated influx of calcium ions at nerve endings of csp and shibire mutant *Drosophila*. J Neurosci 18, 3233-3240.

Ungermann, C., Nichols, B. J., Pelham, H. R. B., and Wickner, W. (1998). A vacuolar v-t-SNARE complex, the predominant form *in vivo* and on isolated vacuoles, is disassembled and activated for docking and fusion. J Cell Biol 140, 61-69.

Valdez-Taubas, J., and Pelham, H. R. (2005). Swf1-dependent palmitoylation of the SNARE Tlg1 prevents its ubiquitination and degradation. EMBO J 24, 2524-2532.

van de Goor, J., and Kelly, R. B. (1996). Association of *Drosophila* cysteine string proteins with membranes. FEBS Lett 380, 251-256.

Varoqueaux, F., Sigler, A., Rhee, J. S., Brose, N., Enk, C., Reim, K., and Rosenmund, C. (2002). Total arrest of spontaneous and evoked synaptic transmission but normal synaptogenesis in the absence of Munc13-mediated vesicle priming. Proc Natl Acad Sci U.S.A. 99, 9037-9042.

Veit, M., Sollner, T. H., and Rothman, J. E. (1996). Multiple palmitoylation of synaptotagmin and the t-SNARE SNAP-25. FEBS Lett 385, 119-123.

Veit, M. (2000). Palmitoylation of the 25-kDa synaptosomal protein (SNAP-25) *in vitro* occurs in the absence of an enzyme, but is stimulated by binding to syntaxin. Biochem J 345, 145-151.

Veit, M., Becher, A., and Ahnert-Hilger, G. (2000). Synaptobrevin 2 is palmitoylated in synaptic vesicles prepared from adult, but not from embryonic brain. Mol Cell Neurosci 15, 408-416.

Veit, M., Laage, R., Dietrich, L., Wang, L., and Ungermann, C. (2001). Vac8p release from the SNARE complex and its palmitoylation are coupled and essential for vacuole fusion. EMBO J 20, 3145-3155.

Veit, M., and Schmidt, M. F. (2001). Enzymatic depalmitoylation of viral glycoproteins with acyl-protein thioesterase 1 *in vitro*. Virology 288, 89-95.

Verhage, M., Maia, A. S., Plomp, J. J., Brussaard, A. B., Heeroma, J. H., Vermeer, H., Toonen, R. F., Hammer, R. E., van den Berg, T. K., Missler, M., Geuze, H. J., and Sudhof, T. C. (2000). Synaptic assembly of the brain in the absence of neurotransmitter secretion. Science 287, 864-869.

Verkruyse, L. A., and Hofmann, S. L. (1996). Lysosomal targeting of palmitoyl-protein thioesterase. J Biol Chem 271, 15831-15836.

Voets, T., Toonen, R. F., Brian, E. C., de Wit, H., Moser, T., Rettig, J., Sudhof, T. C., Neher, E., and Verhage, M. (2001). Munc18-1 promotes large dense-core vesicle docking. Neuron 31, 581-591.

Vogel, K., Cabaniols, J. P., and Roche, P. A. (2000). Targeting of SNAP-25 to membranes is mediated by its association with the target SNARE syntaxin. J Biol Chem 275, 2959-2965.

von Heijne, G., and Gavel, Y. (1988). Topogenic signals in integral membrane proteins. Eur J Biochem 174, 671-678.

Wang, A., Deems, R. A., and Dennis, E. A. (1997a). Cloning, expression, and catalytic mechanism of murine lysophospholipase I. J Biol Chem 272, 12723-12729.

Wang, A., Loo, R., Chen, Z., and Dennis, E. A. (1997b). Regiospecificity and catalytic triad of lysophospholipase I. J Biol Chem 272, 22030-22036.

Wang, C.-T., Grishanin, R., Earles, C. A., Chang, P. Y., Martin, T. F. J., Chapman, E. R., and Jackson, M. B. (2001). Synaptotagmin modulation of fusion pore kinetics in regulated exocytosis of dense core vesicles. Science 294, 1111-1115.

Wang, G., Witkin, J. W., Hao, G., Bankaitis, V. A., Scherer, P. E., and Baldini, G. (1997c). Syndet is a novel SNAP-25 related protein expressed in many tissues. J Cell Sci 110, 505-513.

Washbourne, P., Cansino, V., Mathews, J. R., Graham, M., Burgoyne, R. D., and Wilson, M. C. (2001). Cysteine residues of SNAP-25 are required for SNARE disassembly and exocytosis, but not for membrane targeting. Biochem J 357, 625-634.

Weber, T., Zemelman, B. V., McNew, J. A., Westermann, B., Gmachl, M., Parlati, F., Sollner, T. H., and Rothman, J. E. (1998). SNAREpins: minimal machinery for membrane fusion. Cell 92, 759-772.

Weimbs, T., Low, S. H., Chapin, S. J., Mostov, K. E., Bucher, P., and Hofmann, K. (1997). A conserved domain is present in different families of vesicular fusion proteins: a new superfamily. Proc Natl Acad Sci U.S.A. 94, 3046-3051.

Weninger, K., Bowen, M. E., Choi, U. B., Chu, S., and Brunger, A. T. (2008). Accessory proteins stabilize the acceptor complex for synaptobrevin, the 1:1 syntaxin/SNAP-25 complex. Structure 16, 308-320.

Whitley, P., Grahn, E., Kutay, U., Rapoport, T. A., and von Heijne, G. (1996). A 12-residue-long polyleucine tail is sufficient to anchor synaptobrevin to the endoplasmic reticulum membrane. J Biol Chem 271, 7583-7586.

Wiser, O., Bennett, M. K., and Atlas, D. (1996). Functional interaction of syntaxin and SNAP-25 with voltage-sensitive L- and N-type Ca^{2+} channels. EMBO J 15, 4100-4110.

Wong, S. H., Zhang, T., Xu, Y., Subramaniam, V. N., Griffiths, G., and Hong, W. (1998). Endobrevin, a novel synaptobrevin/VAMP-like protein preferentially associated with the early endosome. Mol Biol Cell 9, 1549-1563.

Wu, S. K., Zeng, K., Wilson, I. A., and Balch, W. E. (1996). Structural insights into the function of the Rab GDI superfamily. Trends Biochem Sci 21, 472-476.

Xiao, J., Xia, Z., Pradhan, A., Zhou, Q., and Liu, Y. (2004). An immunohistochemical method that distinguishes free from complexed SNAP-25. J Neurosci Res 75, 143-151.

Yamasaki, S., Baumeister, A., Binz, T., Blasi, J., Link, E., Cornille, F., Roques, B., Fykse, E. M., Sudhof, T. C., Jahn, R., and et al. (1994a). Cleavage of members of the synaptobrevin/VAMP family by types D and F botulinal neurotoxins and tetanus toxin. J Biol Chem 269, 12764-12772.

Yamasaki, S., Binz, T., Hayashi, T., Szabo, E., Yamasaki, N., Eklund, M., Jahn, R., and Niemann, H. (1994b). Botulinum neurotoxin type G proteolyses the Ala81-Ala82 bond of rat synaptobrevin 2. Biochem Biophys Res Commun 200, 829-835.

Yang, B., Gonzalez, L. C., Jr., Prekeris, R., Steegmaier, M., Advani, R. J., and Scheller, R. (1999). SNARE interactions are not selective. J Biol Chem 274, 5649-5653.

Yeh, D. C., Duncan, J. A., Yamashita, S., and Michel, T. (1999). Depalmitoylation of endothelial nitric-oxide synthase by acyl-protein thioesterase 1 is potentiated by Ca^{2+}-calmodulin. J Biol Chem 274, 33148-33154.

Yochem, J., Uchida, H., Sunshine, M., Saito, H., Georgopoulos, C. P., and Feiss, M. (1978). Genetic analysis of two genes, dnaJ and dnaK, necessary for *Escherichia coli* and bacteriophage lambda DNA replication. Mol Gen Genet 164, 9-14.

Yoshida, A., Oho, C., Omori, A., Kuwahara, R., Ito, T., and Takahashi, M. (1992). HPC-1 is associated with synaptotagmin and omega-conotoxin receptor. J Biol Chem 267, 24925-24928.

Zeng, Q., Subramaniam, V. N., Wong, S. H., Tang, B. L., Parton, R. G., Rea, S., James, D. E., and Hong, W. (1998). A novel synaptobrevin/VAMP homologous protein (VAMP5) is increased during *in vitro* myogenesis and present in the plasma membrane. Mol Biol Cell 9, 2423-2437.

Zha, J., Weiler, S., Oh, K. J., Wei, M. C., and Korsmeyer, S. J. (2000). Posttranslational N-myristoylation of BID as a molecular switch for targeting mitochondria and apoptosis. Science 290, 1761-1765.

Zhai, L., Chaturvedi, D., and Cumberledge, S. (2004). Drosophila wnt-1 undergoes a hydrophobic modification and is targeted to lipid rafts, a process that requires porcupine. J Biol Chem 279, 33220-33227.

Zhang, F. L., and Casey, P. J. (1996). Protein prenylation: molecular mechanisms and functional consequences. Annu Rev Biochem 65, 241-269.

Zhang, H., Kelley, W. L., Chamberlain, L. H., Burgoyne, R. D., Wollheim, C. B., and Lang, J. (1998). Cysteine-string proteins regulate exocytosis of insulin independent from transmembrane ion fluxes. FEBS Lett 437, 267-272.

Zhang, H., Kelley, W. L., Chamberlain, L. H., Burgoyne, R. D., and Lang, J. (1999). Mutational analysis of cysteine-string protein function in insulin exocytosis. J Cell Sci 112, 1345-1351.

Zhang, H., Peters, K. W., Sun, F., Marino, C. R., Lang, J., Burgoyne, R. D., and Frizzell, R. A. (2002a). Cysteine string protein interacts with and modulates the maturation of the cystic fibrosis transmembrane conductance regulator. J Biol Chem 277, 28948-28958.

Zhang, H., Schmidt, B. Z., Sun, F., Condliffe, S. B., Butterworth, M. B., Youker, R. T., Brodsky, J. L., Aridor, M., and Frizzell, R. A. (2006). Cysteine string protein monitors late steps in cystic fibrosis transmembrane conductance regulator biogenesis. J Biol Chem 281, 11312-11321.

Zhang, X., Kim-Miller, M. J., Fukuda, M., Kowalchyk, J. A., and Martin, T. F. (2002b). Ca^{2+}-dependent synaptotagmin binding to SNAP-25 is essential for Ca^{2+}-triggered exocytosis. Neuron 34, 599-611.

Zheng, J., Knighton, D. R., Xuong, N. H., Taylor, S. S., Sowadski, J. M., and Ten Eyck, L. F. (1993). Crystal structures of the myristylated catalytic subunit of cAMP-dependent protein kinase reveal open and closed conformations. Protein Sci 2, 1559-1573.

Zinsmaier, K. E., Hofbauer, A., Heimbeck, G., Pflugfelder, G. O., Buchner, S., and Buchner, E. (1990). A cysteine-string protein is expressed in retina and brain of *Drosophila*. J Neurogenet 7, 15-29.

Zinsmaier, K. E., Eberle, K. K., Buchner, E., Walter, N., and Benzer, S. (1994). Paralysis and early death in cysteine string protein mutants of *Drosophila*. Science 263, 977-980.